Evaluation of Targeted Selective Inhibitors to Enhance Temozolomide Treatment Sensitivity in Acute Myeloid Leukemia

by

Asmaa Abdullah Basonbul

A thesis submitted in partial fulfillment of the requirements for the degree of

Doctor of Philosophy

Department of Medicine
University of Alberta

Abstract

Temozolomide (TMZ) is an alkylating agent with limited activity in acute myeloid leukemia (AML). The DNA repair enzyme O^6-methylguanine methyltransferase (MGMT) enhances tumor cell resistance to TMZ. B-cell lymphoma-2 (BCL-2) and mouse double minute 2 homology (MDM2) are proteins involved in AML cell survival and chemotherapeutic resistance. BCL-2 is an antiapoptotic protein that prevents cell apoptosis, and MDM2 is a ubiquitin E3 ligase that mediates p53 degradation. Inhibiting BCL-2 and restoring p53 functions may affect AML treatment.

Venetoclax (VEN) is a small molecule that promotes cell apoptosis through inhibition of the BCL-2 protein. Idasanutlin (IDA) is an MDM2-specific inhibitor that disrupts p53:MDM2 interactions and restores p53 functions. This study established the need to enhance TMZ sensitivity in AML cells with high and low MGMT expression levels by incorporating VEN and IDA into TMZ treatment.

AML human cell lines and blast-containing mononuclear cells were used to evaluate MGMT and target proteins for each inhibitor. Cell viability, cell apoptosis, and DNA damage were assessed with TMZ alone and in combination with a pre-selected inhibitory concentration of 50% (IC50) of a VEN or IDA inhibitor. Further, VEN inhibitor was applied *in vivo* using mouse model. Leukemic engrafted mice treated with selected TMZ and VEN concentrations, alone and in combination, were evaluated for survival and $CD45^+$ and $CD33^+$ expression in the bone marrow.

In high and low MGMT-expressing AML cell lines, co-incubation of TMZ with VEN at IC50 resulted in a marked enhancement of TMZ sensitivity. In VEN+TMZ treated cell lines, apoptosis was induced and severe DNA damage was observed compared to TMZ alone. AML patient

samples were resistant to TMZ alone but became sensitized to TMZ+VEN in combination, including those with high MGMT expression levels. The combination-treated mice had the longest survival among the group; however, by the time of death, no difference was seen in $CD45^+$ cells compared to the single drug or untreated groups.

In high and low MGMT-expressing cells, co-incubation of TMZ with IDA at IC50 did not improve TMZ sensitivity, regardless of p53 status. In both high and low MGMT-expressing cells, there was no evidence of DNA damage in the TMZ+IDA combination groups compared to TMZ alone. AML patient samples were resistant to TMZ alone and highly sensitive to IC50 IDA. IDA did not enhance the TMZ sensitivity, as insignificant cell death was observed in IDA alone and TMZ combination.

VEN enhances TMZ cytotoxicity in high and low MGMT cells by decreasing cell viability, increasing cell apoptosis, and inducing DNA damage. The opposite was observed in IDA and TMZ combination-treated cells. Overall, we found VEN and TMZ combination to be promising to pursue further for clinical trails.

Preface

This thesis is an original work by Asmaa Abdullah Basonbul. The research project, of which this thesis is a part, received human research ethics approval from the University of Alberta Health Research Ethics Board (HREB) under the project name "Novel strategy to overcome resistance in leukemia ", No. Pro00043783, 2013-11-18. In addition, the project received animal research ethics approval from the University of Alberta HREB under the project name "Temozolomide plus anti-apoptotic agents in AML", No. AUP00003651, 2021-06-22.

The author completed Part I of the mandatory training requirements for animal users established by the Canadian Council on Animal Care. This allowed the author to dissect mice and extract their femur bone marrow after euthanasia.

A modified version of Chapter 2 of this thesis was submitted as a manuscript for publication in PLOS ONE on August 7, 2023, with the following information: **Asmaa A. Basonbul**, Teresa Fong, Joseph M. Brandwein, **"Venetoclax Enhances Temozolomide-Mediated Cytotoxicity in Acute Myeloid Leukemia Cells"**; its current status is "under review".

I performed the experiments, collected and analyzed data, as well as wrote the manuscript. Teresa Fong monitored and euthanized the mice. Joseph M. Brandwein was the supervisory author, and Teresa Fong assisted with manuscript edits.

The next-generation sequencing for the p53 mutation in patient samples in Chapter 3 was carried out by the Alberta Precision Laboratory at the University of Alberta Hospital. The other experiments and data analysis were performed by myself.

This thesis is dedicated to my parents, Abdallah Basonbul and Fatimah Basonbul, and my family, Mubarak Ba Sunbul (husband), Rateel, Amir and Jood Ba Sunbul (children), who give me strength, love, and support. Thank you all.

Acknowledgments

“Whoever does not thank people has not thanked Allah.”

Prophet Mohammed, Peace Be Upon Him

First of all, my gratitude and thanks to Allah for lighting my path and giving me strength during this journey to end my project successfully. This project would not have been possible without many supportive and collaborative people.

To my supervisor, Dr. Joseph Brandwein, for his unwavering guidance and exceptional support throughout my PhD journey. I appreciate his understanding and thank him for standing with me during difficult times, including political issues between Saudi Arabia and Canada, COVID-19, and pregnancies. Despite his busy schedule and time spent in clinic, he granted me time for constructive feedback that has significantly enriched my research.

To co-supervisor Dr. Luc Berthiaume, who challenges me to show the better side of myself and to do more. I appreciate his support in opening his lab to use the Cytation5 machine to generate significant data for this project.

To the committee member, Dr. Michael Weinfeld, who helped me understand my research from a cytogenetic perspective. His feedback, suggestions, and critiques improved the quality of this research.

To the research assistants in Dr. Brandwein’s lab, Zoulika Zak and Teresa Fong. Zoulika Zak took my hand and taught me the fundamentals of the leukemia field. Teresa Fong supported me during the animal experiments. She has my genuine gratitude for our relationship, the fun times we had together in the lab, and the way she encouraged me to unwind during tough times.

To the patients with leukemia who participated in this project. I appreciate their trust in the process of scientific inquiry. Their willingness to participate and provide valuable samples was fundamental to the success of my research.

To the entire team at Canadian Biosample Repository, Amie Lee, Matthew Klassen, and Tegan Zork, for providing the samples from patients with AML. I appreciate their cooperation and flexibility in providing the samples at specific times based on the experimental procedure.

To Dr. Andrew Masoud at Dr. Murray's and Dr. Laiji Li at Dr. Ballermann's labs for giving me the opportunity to use the fluorescence microscope. To Dr. Faisal Rashed at Dr. Weinfeld's lab for helping me to optimize the alkaline comet assay protocol.

To Umm Al Qura University in the Kingdom of Saudi Arabia, through the Ministry of Higher Education, for sponsoring my graduate studies at the University of Alberta. Their financial support enabled me to pursue and successfully accomplish my graduate studies.

To my parents, brothers, and sister back home for their encouragement, prayers, and belief in my abilities to do this. To my husband and children for their patience, empathy, and ability to create a peaceful and supportive home environment.

To my role model in professional and scientific research, Dr. Jamil Sofie, for his unlimited support personally and academically since my first day here in Canada. His support influenced my aspirations and ambitions, shaping both the academic and personal aspects of my experience.

To my friends and others around me at the University of Alberta and beyond, thank you for your words of encouragement, shared moments of celebration, and for providing me with breaks from research life. You have been a source of strength and I am fortunate to have shared this experience with you.

Table Contents

List of Tables

List of Figures

List of Abbreviations

A	
AIC	Amino imidazole carboxamide
AML	Acute myeloid leukemia
AP	Apurinic/apyrimidinic
AP-1	Activator protein-1
APAF-1	Apoptotic protease activating factor 1
APL	Acute promyelocytic leukemia
ATCC	American type tissue collection
ATP	Adenosine triphosphate
AUC	Area under the curve
B	
BAD	BCL-2 antagonist of cell death
BAK	BCL-2-antagonist/killer
BAX	BCL-2-associated X protein
BCA	Bicinchoninic acid
BCL-2	B-cell lymphoma-2
BCL2L2	BCL-2-Like 2
BCL-XL	BCL-extra-large
BER	Base excision repair
BH	BCL-2 homology
BID	BH3-interacting domain death agonist
BIK	BCL-2-interacting killer
BIM	BCL-2 interacting mediator of cell death
BM	Bone marrow
C	
C	Cytosine
C-PARP	Cleaved-poly (ADP-ribose) polymerases 1
CBC	Complete blood count
CDKs	Cyclin dependent kinases
Chk1 &2	Checkpoint kinases 1 and 2
CLL	Chronic lymphocytic leukemia
CMC-Na	Sodium carboxymethyl cellulose
CpG	Cysteine-phosphate-guanine
CR	Complete response
CRi	Complete response with incomplete recovery of blood counts
CRp	Complete response with incomplete platelet recovery
CYP450	Cytochrome P450
D	
DISC	Death-inducing signalling complex
DMSO	Dimethyl sulfoxide
DNA	Deoxyribonucleic acid
DSBs	Double-stranded breaks
DPBS	Dulbecco's phosphate buffered saline
E	
EAP	Extrinsic apoptotic pathway

EDTA	Ethylenediaminetetraacetic acid
ELN	European LeukemiaNet
Em	Emission
ER	Endoplasmic reticulum
ERK1/2	Extracellular signal-regulated kinase 1/2
ETS	E26 transformation-specific
Ex	Excitation
F	
FADD	Fas-associated death domain
Fas-L	Fas ligand
FISH	Fluorescence *in situ* hybridization
FLAG-IDA	Fludarabine, cytarabine and idarubicin
FLT3	FMS-like tyrosine kinase 3
FLT3-ITD	FLT3-internal tandem duplication
FLT3-TKD	FLT3-tyrosine kinase domain
G	
G-CSF	Granulocyte-colony stimulating factor
GF-AFC	Glycyl-phenylalanyl-aminofluorocoumarin
GO	Gemtuzumab ozogamicin
H	
H_2O	Water
HAUSP	Ubiquitin-specific protease
HSCs	Hematopoietic stem cells
HSCT	Hematopoietic stem cell transplantation
I	
IAP	Intrinsic apoptotic pathway
ICC	International consensus classification
IC50	inhibitory concentration 50%
IDA	Idasanutlin
IDH1	Isocitrate dehydrogenase 1
ITD	Internal tandem duplication
L	
LDAC	Low-dose cytarabine
M	
MCL-1	Myeloid cell leukemia sequence-1
MDM2	Mouse double minute 2 homology
MEK1/2	Mitogen-activated protein kinase kinase 1/2
MGMT	Methylguanine methyltransferase
MLFS	Morphologic leukemia-free state
MMR	Mismatch repair
MOMP	Mitochondrial outer membrane permeabilization
MRD	Minimal residual disease
MTIC	Methyl-(triazen-1-yl) imidazole carboxamide
N	
N^3-MeA	N^3-methyladenine
N^7-MeG	N^7-methylguanine

NAD	Nicotinamide adenine dinucleotide
NADP	Nicotinamide adenine dinucleotide phosphate
NADPH	Nicotinamide adenine dinucleotide phosphate dehydrogenase
NOD/scid IL2Rg^{null}	Nonobese diabetic/severe combined immune deficiency IL2 receptor common gamma chain
O	
O^6-MeG	O^6-methylguanine
ORR	Overall response rate
OS	Overall survival
P	
PARP 1	Poly-(ADP ribose) polymerase 1
PB	Peripheral blood
PCR	Polymerase chain reaction
PI	Propidium iodide
PI3K	Phosphatidylinositol 3 kinase
PMAIP1	Phorbol myristate acetate induced protein 1
PR	Partial response
pRb	Retinoblastoma protein
PUMA	P53-upregulated modulator of apoptosis
R	
RBC	Red blood cell
R/R	Relapsed/refractory
RT-qPCR	Real-time quantitative PCR
S	
SDS	Sodium dodecyl sulphate
SFEM	Serum-free expansion medium
SR1	StemRegenin1
SSBs	Single-strand breaks
STAT	Signal transducer and activator of transcription
T	
T	Thymine
t ½	Half-life
t-BID	Truncated BID
TET2	Ten-eleven translocation
TKD	Tyrosine kinase domain
TMZ	Temozolomide
TNF	Tumour necrosis factor
TP53	Tumor suppressor p53
TRADD	TNFR-associated death domain
TRAIL	TNF-related apoptosis-inducing ligand
V	
VEN	Venetoclax
W	
WBC	White blood cells
WHO	World Health Organization

CHAPTER 1

Introduction

1 Introduction

1.1 Acute Myeloid Leukemia

1.1.1 Background

Acute myeloid leukemia (AML) is an aggressive hematological malignancy arising from genetic mutations in hematopoietic stem cells (HSCs). AML targets the myeloid lineage by accumulating highly proliferative myeloblasts with a lack of differentiation and apoptosis in the bone marrow (BM) [1]. AML is caused by somatic mutations resulting from gene alterations, including chromosomal abnormalities or isolated gene mutations [2, 3]. In addition, AML can be acquired by exposure to smoking, ionizing radiation, or cytotoxic chemotherapy [1, 2].

The non-functional myeloblast is expanded and accumulates in the BM, resulting in BM failure and ineffective hematopoiesis [1, 4]. Myeloblasts fail to undergo differentiation and resist apoptosis are then released into the peripheral blood (PB) causing organ infiltration.

Worldwide, the annual incidence of AML is ~2.5–3 cases per 100 000 population [2]. AML is predominantly a disease of the elderly, with a median age at diagnosis of ~70 years [5]. The early (four-weeks) mortality death rate in this group is 45% compared to adults in general, which is 20% [6]. With older age, the likelihood of adverse risk cytogenetic abnormalities is increased, and the prognosis becomes poor. Patients with AML die due to BM or organ infiltration resulting in infections and bleeding, and most die within one year if left untreated [2, 7].

1.1.2 Classification

Despite the complexity of AML, ongoing research has improved our understanding of the disease. Recently, the World Health Organization (WHO) published the fifth edition AML

classification, which takes into consideration cytogenetic abnormalities, mutational profiles, and patient history. AML is classified into two classes; AML with defining genetic abnormalities and AML defined by differentiation (Table 1.1) [8, 9]. There is also the International Consensus Classification (ICC) of myeloid neoplasms and acute leukemias (Appendix Tables 1). The ICC is intended to provide better treatment prognostic correlations [10].

Table 1.1: WHO 5th AML classification

AML with Defining Genetic Abnormalities
o AML with *RUNX1::RUNX1T1* fusion
o AML with *CBFB::MYH11* fusion
o APL with *PML::RARA* fusion
o AML with *KMT2A* rearrangement
o AML with *DEK::NUP214* fusion
o AML with *MECOM* rearrangement
o AML with *RBM15::MRTFA* fusion
o AML with *BCR::ABL1* fusion*
o AML with *NUP98* rearrangement
o AML with *NPM1* mutation
o AML with *CEBPA* mutation
- Biallelic mutations (bi*CEBPA*)
- Single mutations in Bzip region (smbZIP-*CEBPA*)
o AML, myelodysplasia-related (AML-MR)
o AML with other defined genetic alterations
- AML with *RUNX1T3*(*CBFA2T3*)*::GLIS2*
- AML with *KAT6A::CREBBP*
- AML with *FUS::ERG*
- AML with *MNX1::ETV6*
- AML with *NPM1::MLF1*
AML Defined by Differentiation*

- AML with minimal differentiation
- AML without maturation
- AML with maturation
- Acute myelomonocytic leukemia
- Acute monocytic leukemia
- Acute erythroid leukemia
- Acute megakaryoblastic leukemia
- Acute basophilic leukemia

* Refer to Appendix Table 2 for differentiation markers. AML, Acute myeloid leukemia*; AML-MR,* AML-myelodysplasia-related; APL, Acute promyelocytic leukemia; *BCR::ABL1,* Breakpoint cluster region::ABL proto-oncogene 1; *biCEBPA,* Biallelic CCAAT enhancer binding protein α; *CBFB::MYH11,* Core binding factor beta::myosin heavy chain protein 11; *CEBPA,* CCAAT Enhancer binding protein α; *DEK::NUP214,* DEK-proto-oncogene**::**Nucleoporin 214; *FUS::ERG,* Fused In Sarcoma::ETS related gene; *KAT6A::CREBBP*, Lysine Acetyltransferase 6A::CREB binding protein; *KMT2A,* Lysine (K)-specific methyltransferase 2A; *MECOM,* MDS1 and EVI1 complex locus protein EVI1; *MNX1::ETV6,* Motor Neuron And Pancreas Homeobox 1::ETS variant transcription factor 6; *NPM1,* Nucleophosmin 1; *NPM1::MLF1,* Nucleophosmin 1::myeloid leukemia factor 1; *NUP98***,** Nucleoporin 98; *PML::RARA,* Promyelocytic leukemia::retinoic acid receptor alpha; *RBM15::MRTFA,* RNA binding mortify 15:: myocardin-related transcription factor; *RUNX1::RUNX1T1,* Runt-related transcription factor1::Runt-related transcription factor 1 translocated to 1; *RUNX1T3(CBFA2T3)::GLIS2,* Runt-related transcription factor1 translocated to 3::GLIS family zinc finger 2; *smbZIP-CEBPA,* Single mutations in Bzip region- CCAAT Enhancer binding protein α.

AML prognosis can be classified into three categories, based on cytogenetic and mutational profiles: favorable, intermediate, and adverse. This classification is known as the European LeukemiaNet (ELN) risk classification. Recently this has been reclassified, as described in Table 1.2 [11]. AML is associated with a variety of somatic mutations, some of the most common are

nucleophosmin (*NPM1*) and FMS-like tyrosine kinase 3 – internal tandem duplication (*FLT3 – ITD*), and tumor suppressor p53 gene (*TP53*).

Table 1.2: 2022 European LeukemiaNet (ELN) risk classification by genetics at initial diagnosis

Risk category	Genetic abnormality
Favorable	○ t(8;21)(q22;q22.1)/*RUNX1*::*RUNX1T1* ○ inv(16)(p13.1q22) or t(16;16)(p13.1;q22)/*CBFB*::*MYH11* ○ Mutated *NPM1* without *FLT3*-ITD ○ bZIP in-frame mutated *CEBPA*
Intermediate	○ Mutated *NPM1* with *FLT3*-ITD ○ Wild-type *NPM1* with *FLT3*-ITD ○ t(9;11)(p21.3;q23.3)/*MLLT3*::*KMT2A* ○ Cytogenetic and/or molecular abnormalities not classified as favorable or adverse
Adverse	○ t(6;9)(p23;q34.1)/*DEK*::*NUP214* ○ t(v;11q23.3)/*KMT2A*-rearranged ○ t(9;22)(q34.1;q11.2)/*BCR*::*ABL1* ○ t(8;16)(p11;p13)/*KAT6A*::*CREBBP* ○ inv(3)(q21.3q26.2) or t(3;3)(q21.3;q26.2)/*GATA2*, *MECOM(EVI1)* ○ t(3q26.2;v)/*MECOM(EVI1)*-rearranged ○ −5 or del(5q); −7; −17/abn(17p) ○ Complex karyotype, monosomal karyotype ○ Mutated *ASXL1*, *BCOR*, *EZH2*, *RUNX1*, *SF3B1*, *SRSF2*, *STAG2*, *U2 AF1*, or *ZRSR2* ○ Mutated *TP53*

abn, abnormal; *ASXL1,* Additional sex combs like 1; *BCOR,* BCL-6 corepressor; *BCR::ABL1,* Breakpoint cluster region::ABL proto-oncogene 1; bZIP, basic leucine zipper; *CBFB::MYH11,* Core binding factor beta::myosin heavy chain protein 11; *CEBPA, CCAAT* enhancer binding protein α; *DEK::NUP214,* DEK-proto-oncogene*::*Nucleoporin 214; del, deletion; *EZH2,* Enhancer of zeste homolog 2; *FLT3,* Fms-like tyrosine kinase 3; *GATA2,* GATA- binding factor

2; inv, inversion; KAT6A:: CREBBP, Lysine Acetyltransferase 6A::CREB binding protein; *KMT2A,* Lysine (K)-specific methyltransferase 2A; *MECOM (EVI1), MDS1 and EVI1 complex locus protein EVI1;* MLLT3, mixed lineage leukemia translocated to 3; *NPM1,* Nucleophosmin 1; *RUNX1::RUNX1T1,* Runt-related transcription factor1::Runt-related transcription factor 1 translocated to 1; *SF3B1,* Splicing factor 3b subunit 1; *SRSF2,* serine/arginine-rich splicing factors 2; *STAG2,* STAG2 cohesin complex component; t, translocation; *TP53,* Tumor protein p53; *U2AF1,* U2 small nuclear RNA auxiliary factor 1; *ZRSR2,* zinc finger CCCH-type, RNA binding motif and serine/arginine rich 2.

NPM1 is a nuclear phosphoprotein that shuttles continuously between the nucleus and cytoplasm [12]. Functionally, it is involved in ribosome biogenesis, DNA repair, and apoptosis [13]. It interacts as chaperone with some tumor suppressors, including cyclin dependent kinase 2 A (CDKN2A) /p14ARF and p53. The NPM1 mutation frequency in AML is 25 – 30% and 80% of the mutation occurred in a four-base pair duplication in the coding region of exon 12. Resulting in improper nuclear export signals that sequester NPM1 in the cytoplasm. As mentioned NPM1 is a chaperone of P14ARF, resulting in inhibition of MDM2, which consequently promotes p53 degradation and cell proliferation [12].

FLT3 is a membrane binding receptor with an intrinsic tyrosine kinase domain (*TKD*). *FLT3* is important in normal hematopoiesis and cell growth in the presence of stem cell factor and interleukin 3, which maintains cell proliferation in primitive hematopoietic progenitor cells and early myeloid and lymphoid precursors. *FLT3* is expressed (> 90%) in AML blast cells with various level and considered one of the most common genetic abnormalities. The *FLT3* mutation may occur within *FLT3* receptor compositions either internal tandem duplication (*ITD*) of the juxtamembrane domain (15–25%) or *TKD* (5–10%) and results in signal transduction pathway

stimulation, which enhances hematopoietic progenitor cell proliferation and survival [14]. The *TP53* gene and developing leukemia is discussed in details in Section 1.4.1.

Patients with *NPM1* mutations or *RUNX1::RUNX1T1* and *CBFB::MYH11* fusions are categorized as favorable risk. The intermediate risk category includes patients with *FLT3-ITD* mutation with either wild-type or mutated *NPM1* gene. Patients are classified as adverse risk when they have complex karyotypes, *TP53* mutations and/or certain other cytogenetic abnormalities and myelodysplasia associated mutations.

1.1.3 Symptoms and Diagnosis

The early signs of AML are fever, weakness, fatigue, weight loss and decreased appetite [7]. The impairment of hematopoiesis results in cytopenias, which increases the risk of anemia, bleeding and infection [2]. The primary diagnosis is established by examination of the BM and PB morphology and immunophenotyping by flow cytometry (Table 1.3) [11]. The WHO5th diagnostic criteria include ≥ 20% myeloblasts or equivalents in the PB or BM, although for some genetic subtypes < 20% blasts is sufficient to make a diagnosis [8, 11]. The diagnostic markers for AML classification defined by differentiation are defined in Appendix Table 2.

Table 1.3: AML diagnostic procedures

Test	Procedures
Primary	○ **Complete blood count and differential** ○ **BM aspirate** ○ **BM trephine biopsy** ○ **Immunophenotyping by flowcytometry:** - Precursor marker: CD34, CD117, HLA-DR - Myeloid markers: cytoplasmic myeloperoxidase, CD33, CD13 - Myeloid maturation markers: CD11b, CD15, CD64, CD65 - Monocytic markers: CD14, CD36, CD64, CD4, CD38, CD11c - Megakaryocytic markers: CD41 (glycoprotein IIb/IIIa), CD61 (glycoprotein IIIa), CD36 - Erythroid markers: CD235a (glycophorin A), CD71, CD36
Genetic Analysis	○ **Screening for gene mutations:** - *FLT3, IDH1, IDH2* - *NPM1* - *CEBPA, # DDX41, TP53; ASXL1, BCOR, EZH2, RUNX1, SF3B1, SRSF2, STAG2, U2AF1, ZRSR2* ○ **Screening for gene rearrangements**** - *PML::RARA, CBFB::MYH11, RUNX1::RUNX1T1, KMT2A rearrangements, BCR::ABL1* ○ **Additional genes recommended to test at diagnosis** - *ANKRD26, BCORL1, BRAF, CBL, CSF3R, DNMT3A, ETV6, GATA2, JAK2, KIT, KRAS, NRAS, NF1, PHF6, PPM1D, PTPN11, RAD21, SETBP1, TET2, WT1*

Cytogenetic Analysis	○ t(8;21)(q22;q22.1) ○ inv(16)(p13.1q22) or t(16;16)(p13.1;q22) ○ t(9;11)(p21.3;q23.3) ○ Cytogenetic and/or molecular abnormalities not classified as favorable or adverse ○ t(6;9)(p23;q34.1) ○ t(v;11q23.3) ○ t(9;22)(q34.1;q11.2) ○ t(8;16)(p11;p13) ○ inv(3)(q21.3q26.2) or t(3;3)(q21.3;q26.2) ○ t(3q26.2;v) ○ −5 or del(5q); −7; −17/abn(17p)

DDX41, DEAD-box RNA helicase 41; abn, abnormal; *ANKRD26,* Ankyrin repeat domain containing 26; *ASXL1,* Additional sex combs like 1; *BCOR,* BCL-6 corepressor; *BCORL1,* BCL-6 corepressor like 1; *BCR::ABL1,* Breakpoint cluster region::ABL proto-oncogene 1; BM, Bone marrow; *BRAF,* B-RAF proto-oncogene, serine/threonine kinase; *CBFB::MYH11,* Core binding factor beta*::* myosin heavy chain protein 11; *CBL,* Casitas B lineage lymphoma; CD, common differentiation; *CEBPA, CCAAT* enhancer binding protein α; *CSF3R,* Colony-stimulating factor 3 receptor; del, deletion; *DNMT3A,* DNA methyltansferase 3A; *ETV6,* ETS variant transcription factor 6; *EZH2,* Enhancer of zeste homolog 2; *FLT3,* Fms-like tyrosine kinase 3; *GATA2,* GATA- binding factor 2; HLA-DR, Human leukocyte antigen – DR isotype; *IDH1,* Isocitrate dehydrogenase 1; *IDH2,* Isocitrate dehydrogenase 2; Inv, inversion; *JAK2,* Janus Kinase 2; *KIT,* KIT proto-oncogene, receptor tyrosine kinase; *KMT2A,* Lysine (K)-specific methyltransferase 2A; *KRAS,* Kirsten rat sarcoma virus; *NF1,* Neurofibromatosis type 1; *NPM1,* Nucleophosmin 1; *NRAS,* neuroblastoma RAS viral oncogene homolog; *PHF6,* PHD finger protein 6; *PML::RARA,* Promyelocytic leukemia::retinoic acid receptor alpha; *PPM1D,* Protein phosphatase magnesium-dependent 1D; *PTPN11,* Protein tyrosine phosphatase non-receptor type 11; *RAD21,* Double-strand-break repair protein RAD21; *RUNX1::RUNX1T1,* Runt-related transcription factor1:: Runt-related transcription factor 1 translocated to 1; *SETBP1,* SET binding protein 1; *SF3B1,* Splicing factor 3b subunit 1; *SRSF2,* serine/arginine-rich splicing factors 2; *STAG2,* STAG2 cohesin complex component; t, translocation; *TET2,* Ten–eleven translocation 2; *TP53,* Tumor

protein p53; *U2AF1,* U2 small nuclear RNA auxiliary factor 1; *WT1,* Wilms' tumor 1; *ZRSR2,* zinc finger CCCH-type, RNA binding motif and serine/arginine rich 2.

Complete blood counts (CBC) samples from patients with AML typically demonstrate low RBC and platelet counts as well as low neutrophil counts; there may also be circulating blasts. Table 1.4 provides a normal adult reference range of different types of blood cells [15].

Table 1.4: Adult normal reference range of complete blood count (CBC)

Cell Type	Reference Range
Red Blood Cell	Men $5.0 \pm 0.5 \times 10^{12}$/l Women $4.3 \pm 0.5 \times 10^{12}$/l
White Blood Cell	$4.0–10.0 \times 10^{9}$/l
Differential White Cell	Neutrophils $2.0–7.0 \times 10^{9}$/l (40–80%) Lymphocytes $1.0–3.0 \times 10^{9}$/l (20–40%) Monocytes $0.2–1.0 \times 10^{9}$/l (2–10%) Eosinophils $0.02–0.5 \times 10^{9}$/l (1–6%) Basophils $0.02–0.1 \times 10^{9}$/l (<1–2%)
Platelet	$280 \pm 130 \times 10^{9}$/l

Mean $\pm$ 2 standard division (95% range)

To confirm an AML diagnosis, a BM aspirate and trephine biopsy should be performed for morphologic examination. The BM aspirate can be obtained from a puncture of the ilium, sternum, or the spines of lumbar vertebrae. The aspirate contains the BM fluid and myeloblast cells, which is normally ranged between of 0–3 (95% range) [16]. The trephine biopsy can be obtained from the posterior or anterior iliac spine. It is carried out by measuring the BM cellularity within BM tissue. This determines the proportion of hematopoietic cells in the tissue and their maturation [17]. Both samples typically demonstrate an increase in blast cells, which

may contain Auer rods. The Auer rod is an aggregation of azurophilic granule elongated-needles like shape [4].

Immunophenotyping is used to confirm the diagnosis. This uses a specific monoclonal antibody to detect cell surface markers (antigens) by flow cytometry. Viable or fixed isolated mononuclear cells can be used. The mononuclear cell isolation method is shown in section 2.2.2. Each specific cell type has a unique marker, as shown in Table 1.3 [18]. An AML sample should overexpress at least one of the above-mentioned markers.

Cytogenetic analysis is used to investigate patient karyotype (chromosome) normality. Cells can be obtained from the PB or BM. Samples are cultured with mitogen until they reach the metaphase stage when the cell chromosomes can be observed microscopically [19]. A normal human cell has 23 pairs of chromosomes, that is, 46 chromosomes in total. Patients with AML mostly have abnormal karyotypes, including translocation (t), deletion (del), or inversion (inv) (Table 1.3). Identifying the cytogenetics of a patient helps with treatment options and prognosis.

Fluorescence *in situ* hybridization (FISH) is a sensitive diagnostic technique used to detect translocation in the metaphase or interphase stages [19, 20]. The probe DNA sequence is integrated into the genomic DNA and once this probe binds to the targeted DNA, the conjugated fluorophore can be visualized using a fluorescence microscope [19]. A FISH probe can detect centromeres, oncogenes, tumour suppressor genes, or complex chromosome arrangements; however, it is limited to the specific gene tested and is not used for screening [20].

Further, genetic analysis is needed to define the AML classification [19]. Specific gene panels (Table 1.3) must be screened for mutations or rearrangements, usually via either polymerase chain reaction (PCR) or next generation sequencing (NGS). PCR amplifies a specific DNA

fragment [20] that can be detected quantitatively through real-time quantitative PCR (RT-qPCR). Detection of any of the above-mentioned genes is used to diagnose and classify AML.

Flow cytometry is also used to measure minimal residual disease (MRD) that remains after treatment and can cause patient relapse. MRD is a prognostic biomarker used to determine a patient's response to treatment. Multiparameter flow cytometry and RT-qPCR are used to evaluate MRD [21].

1.1.4 Therapies

1.1.4.1 Intensive Chemotherapy

In AML patients < 70 years of age, intensive induction chemotherapy ("3+7" induction) is considered standard care. Three days of intravenous anthracycline (daunorubicin 60 mg/m^2, idarubicin 10–12 mg/m^2, or mitoxantrone 10–12 mg/m^2) and 7 days of continuous-infusion cytarabine (100–200 mg/m^2) achieves complete response (CR) in 60–85% of cases [7, 22]. The anthracycline induces DNA damage through inhibition of topoisomerase II, resulting DNA DSBs and apoptosis. It also causes cytotoxicity through generating free radical [23]. On the other hand, cytarabine inhibits DNA replication during S phase, ultimately leading to cell death [24]. For AML with *FLT3* mutations, oral midostaurin 50 mg (an FLT3 inhibitor) is added to the 3+7 induction therapy from day 8 to 21, as it has been shown to improve survival in these patients [11, 25].

For favourable and some intermediate cytogenetic risk groups (Refer to 1.1.2 for definitions), gemtuzumab ozogamicin (GO) immunotherapy is added [11]. GO is a humanized anti-CD33 immunoglobulin G4 monoclonal antibody that binds to the CD33 antigen, which is highly

expressed in myeloid leukemia cells [3]. When added to conventional 3+7 induction chemotherapy GO has been shown to improve overall survival (OS) in these subgroups [26].

For adverse risk groups (Refer to 1.1.2 for definition), which includes therapy-related AML and AML with MDS-related changes, CPX-351 is mostly used [3]. CPX-351 is a liposomal formulation of cytarabine and daunorubicin at a fixed molar ratio of 5:1. This has been shown to produce higher remission rates and improved survival compared with standard 3+7 chemotherapy [27].

To prevent relapse post-remission, patients undergoing intensive chemotherapy subsequently receive up to several cycles of conventional consolidation chemotherapy and may undergo allogeneic hematopoietic stem cell transplantation (HSCT) [3, 22]. Post-remission HSCT has curative potential and is the recommended treatment for patients with intermediate and adverse risk AML [11]. However, there are significant risks and toxicities associated with HSCT, including opportunistic infections and graft-versus-host disease.

1.1.4.2 Non-intensive Chemotherapy

Most patients $\geq$70 years, and some younger patients, are ineligible for intensive chemotherapy because of age, frailty and medical comorbidities [28, 29]. For these patient's treatment is given with palliative intent and usually consists of either a hypomethylating agent (azacitidine or decitabine) or low-dose cytarabine (LDAC), usually in combination with the BCL-2 inhibitor venetoclax (VEN) (Refer to 1.3.3.3 for details). Although complete remissions can be obtained in some patients, nearly all patients eventually relapse, with median OS of 7-14 months [30, 31].

1.1.4.3 Relapsed patients

For relapsed patients with *FLT3* mutations gilteritinib, a potent oral FLT3 inhibitor, can produce transient remissions in 30-40% of patients [32]. For relapsed patients with *isocitrate dehydrogenase 1* (*IDH1*) mutation, the oral IDH1 inhibitor ivosidenib can be used [33], while for patients with *IDH2* mutations the oral IDH2 inhibitor enasidenib can be utilized [34]; these 2 drugs are available in the U.S. but not in Canada. The *IDH* enzyme catalyzes the oxidative decarboxylation of isocitrate to α-ketoglutarate and reduces nicotinamide adenine dinucleotide phosphate ($NADP^+$) to NADPH [35]. The *IDH1* mutation is present in 5–15% of AML cases, while IDH2 is present in 10-18% [36]. With *IDH* mutations, α-ketoglutarate is reduced to the oncometabolite 2-hydroxyglutarate and NADPH is converted to $NADP^+$. Accumulation of 2-hydroxyglutarate causes inhibited deoxyribonucleic acid (DNA) methylation by decreasing ten-eleven translocation (*TET2*) enzyme, which blocks cell differentiation [35, 37].

For younger fit patients who have relapsed, intensive re-induction chemotherapy may be given, using regimens such as FLAG-IDA (fludarabine, cytarabine and idarubicin) plus granulocyte-colony stimulating factor (G-CSF) [38]. Although second remission can be obtained in some cases, further relapse is inevitable unless patients undergo subsequent HSCT [39].

1.2 Temozolomide

The potential for alkylating agents to be used in cancer chemotherapy came to the fore during World War II. In one particular bombing raid in 1943, 100 tons of mustard gas (bis-chloroethyl sulphide) were released into the harbor of Bari, Italy. Most of the soldiers died and those who survived suffered from poisoning and severe leukopenia. Therefore, it was explored to treat leukemia patients, but it did not succeed due to vesicant action. The related nitrogen mustard compounds were tested and shown to be effective. As a result of binding the nitrogen mustard to

N^7 nitrogen on the DNA base guanine causes cross-linking of the DNA strands and blocks DNA replication. These compounds represent the first alkylating agents used to treat cancer [40]. The alkylating agent is an antineoplastic drug responsible for adding an alkyl (e.g. methyl) group to DNA, causing cell death.

Temozolomide (TMZ; $C_6H_6N_6O_2$) is an imidazotetrazine classified as alkylating agent prodrug with antitumor activity [41]. It was discovered in 1987 by Professor Malcolm Stevens in a multidisciplinary drug discovery laboratory in the pharmacy department at Aston University in the United Kingdom. TMZ was first used in 1999 as a second-line therapy to treat glioblastoma, which is the most malignant type of glioma [42, 43].

1.2.1 Mechanism of Action

At physiological pH, TMZ easily crosses the intracellular membrane. The C4 atom in the heterocyclic ring of TMZ interacts with H_2O to generate the active metabolite 3-methyl-(triazen-1-yl) imidazole-4-carboxamide (MTIC) and CO_2 [43, 44]. MTIC is unstable and further hydrolyzed to 4-amino-5-imidazolecarboxamide (AIC) and the methyldiazonium ion to methylate DNA (Fig. 1.1) [41]. TMZ methylation occurs at several nucleobases during DNA replication, including the O^6 and N^7 positions of guanine and the N^3 position of adenine. This interferes with DNA synthesis, causing a cell cycle arrest at the G2/M phase [44, 45]. DNA methylation represents 90% at N^7 guanine and N^3 adenine [42]. O^6-guanine undergoes <8% methylation; however, this is considered a lethal step that mediates cytotoxicity [43, 46] because O^6-methylguanine is mis-paired with thymine (T) instead of cytosine (C) (O^6-MeG:T) during DNA replication [47]. O^6-MeG:T is identified and excised by the mismatch repair (MMR) pathway (Refer to 1.2.4.2 for details). Repeatedly adding a methyl group to the O^6 guanine

nucleobase during DNA replication leads to a futile repair cycle and DNA double-stranded breaks (DSBs) that trigger cell apoptosis [48, 49].

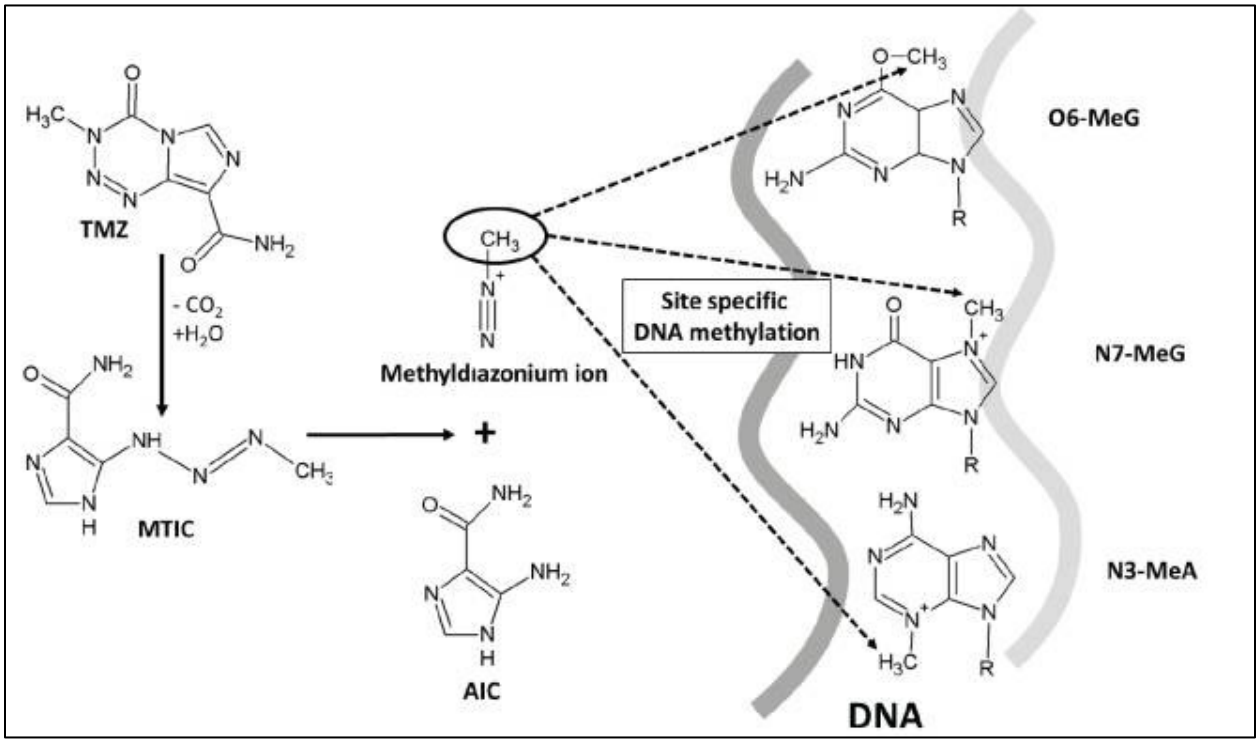

Figure 1.1: The structure and mechanism of action of TMZ. Adapted from Ortiz *et al*., 2018 [43]; Copyright 2021 Bentham Science Publishers. Licensed under a Creative Commons BY-Non-Commercial 4.0. AIC, Amino imidazole carboxamide; DNA, deoxyribonucleic acid; N^3-MeA, N^3-methyladenine; N^7-MeG, N^7-methylguanine; O^6-MeG, O^6-methylguanine; TMZ, temozolomide; MTIC, methyl-(triazen-1-yl) imidazole carboxamide.

This process is executed smoothly, without the use of an intermediate metabolite or supporting cofactor [49]. However, the pH of the environment is crucial for TMZ activity; TMZ is stable under acidic conditions (pH <5) and active under physiological and basic conditions (pH >7) [41].

1.2.2 Pharmacokinetics

TMZ has a low molecular weight (194.154 g/mol) and lipophilic properties [43]. It is an oral or intravenous prescription drug with 100% bioavailability [43, 48]. The oral form is highly absorbed by the intestine, with a high peak plasma concentration after 20 minutes [43]. The half-life (t ½) of TMZ is 1.8 hours and longer for its metabolite [44].

TMZ exhibits high penetration in all tissues, including nervous tissue. It can easily pass through the blood-brain barrier and reach the cerebrospinal fluid at a concentration of up to 40% of the plasma level [41, 48]. It is mostly eliminated by the hepatobiliary system and around 10–15% is excreted through the urine [43].

TMZ is preferred over other alkylating agents, because its function is metabolically independent of cytochrome P450 (CYP450) enzymes and the kidneys. In addition, it has mild-to-moderate and reversible toxic side effects. The hematological side effects are myelosuppression with delayed thrombocytopenia that appears 21–28 days after starting the treatment cycle. However, this effect is limited if the TMZ dose is maintained below 1000 mg/m^2. Thrombocytopenia is a long-term effect of TMZ use. Regarding non-hematological side effects, patients may experience low-recurrence nausea and vomiting, mild headaches, fatigue and occasional skin reactions [43].

1.2.3 Temozolomide Treatment for AML

For decades, the DNA-damaging agent has been used to successfully treat a wide range of cancers [50]. TMZ was used as a double-treating agent for a patient diagnosed with meningeal central nervous system and primary plasma cell leukemia. Primary plasma cell leukemia is an aggressive form of multiple myeloma. TMZ 150 mg/m^2 orally daily for 5 days was added in the third cycle of myeloma chemotherapy, which consisted of bortezomib, lenalidomide and

dexamethasone. Assessing the monoclonal plasma cells in the cerebrospinal fluid before and after TMZ addition demonstrated a complete eradication of leukemic cells after TMZ treatment (34.4% before treatment) [51].

TMZ exhibits anti-leukemic effects as a single agent in AML patients. Four out of 19 patients achieved complete clearance of BM blast cells following a 200 mg/m^2 dose given daily for 7 days [52, 53]. At this dose, TMZ exhibits limited toxicity and most treatments can be administered on an outpatient basis [53].

A case report outlined the unintentional development of chronic lymphocytic leukemia (CLL) in a glioblastoma patient. Treatment with TMZ resulted in the successful eradication of CLL, which indicates the ability of TMZ to inhibit B, T, and natural killer cells [54].

1.2.4 TMZ Resistance

TMZ should generate about 5000 DNA-methylated adducts to cause apoptosis [49]. The efficacy of TMZ depends on the efficacy of DNA repair pathways (Fig. 1.2), either enzymatically, in the presence of O^6-methylguanine methyltransferase (MGMT), or mechanistically, through MMR or base excision repair (BER) [42, 47]. MGMT and MMR are responsible for O^6-MeG nucleotides, while BER is responsible for N^7-MeG and N^3-MeA nucleotides. The following text discusses these repair mechanisms and their impact on TMZ sensitivity.

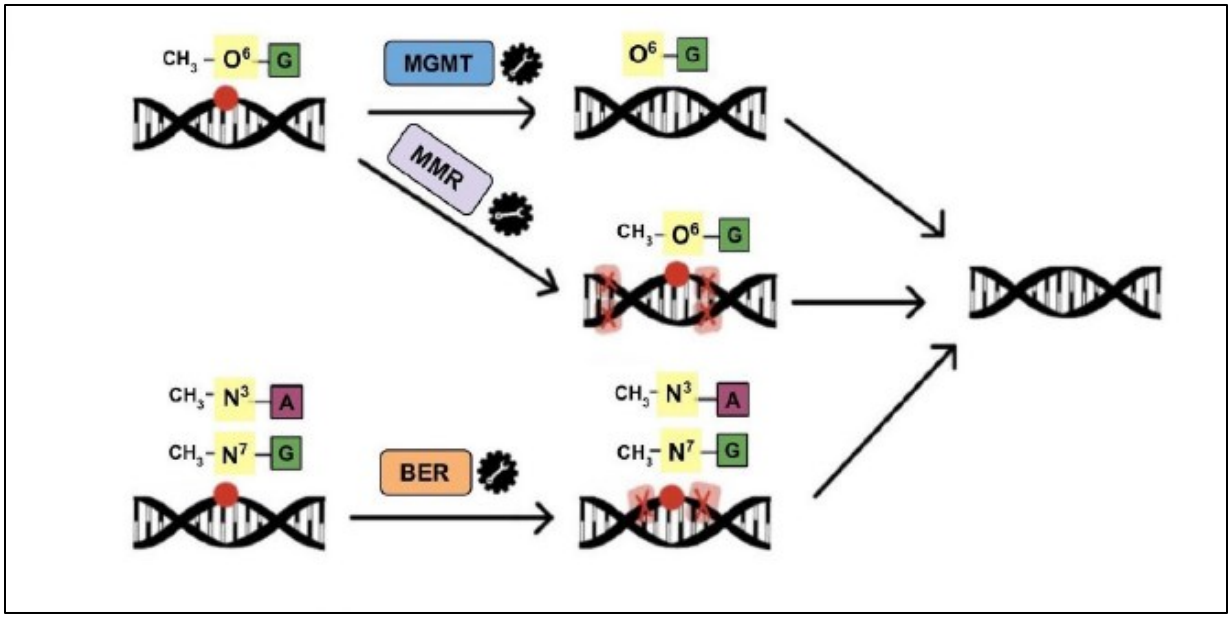

Figure 1.2: DNA repair mechanisms activated following TMZ cytotoxicity. Adapted from Singh *et al*., 2021 [55]; Creative Common BY- 4.0. BER, base excision repair; MGMT, methylguanine methyltransferase; MMR, mismatch repair.

1.2.4.1 O^6-Methylguanine Methyltransferase

The MGMT protein is a "double-edged sword" that is expressed in both normal and abnormal tissues [47, 52]. It is normally most abundant in the liver and least abundant in the pancreas, hematopoietic cells, lymphoid tissues and brain. Its physiological function is to protect normal tissue from cytotoxic and mutagenic effects and cancer cells from methylation that causes cell death [47].

The MGMT gene is located on chromosome 10 [43]. This gene is regulated by the methylation of cytosine-phosphate-guanine (CpG) islands in the MGMT gene promoter located in the -252 to -155 and -90 to +65 regions [41]. The MGMT protein is expressed when the CpG islands of the

MGMT promoter are unmethylated [43]; in contrast, MGMT silencing occurs when the CpG islands of the MGMT promoter are methylated, leading to a lack of MGMT protein expression.

Methylation of the MGMT promoter is directly correlated with the TMZ response [41]. MGMT promoter methylation in glioblastoma patients is associated with longer OS after treatment with TMZ compared with no methylation (methylated: 9.7, unmethylated: 6.8 months) [46].

MGMT is a direct single repair pathway ending with self-inactivation after duty [56, 57]. It maintains genomic integrity by removing the O^6-methyl group added by TMZ to guanine and restoring to normal [47, 58]. Consequently, methylated MGMT becomes inactive and immediately undergoes degradation through ubiquitin proteasome pathway. The cancer cell must maintain the MGMT level to prevent the carcinogenic effect of TMZ [56]. Therefore, TMZ response is directly correlated with MGMT level. Cells that highly express MGMT are likely to be resistance to TMZ and vice versa [43]. Additionally, inhibiting MGMT using small interfering RNA with nanoparticles for protection was successfully achieved in glioblastoma xenograft mice causing an increased TMZ sensitivity and extending the mice's survival [59].

A phase II clinical trial found that the antileukemic activity of TMZ in AML was restricted to cases with very low MGMT expression. AML patients ≥60 years with poor prognosis were treated orally with 200 mg/m^2 TMZ daily for 7 days. Five out of 46 (11%) patients had CR or complete response with incomplete platelet recovery (CRp). Patients with positive MGMT expression in the BM were significantly less likely to respond to TMZ compared with MGMT-negative patients (P= 0.003), with an overall response rate (ORR) of 6% and 60%, respectively. The ORR included CR and partial response (PR), and the response criteria were <5% blasts in a normocellular BM, absolute neutrophil count >1.0 × 10^9/l, and platelets >100 × 10^9/l, with no extramedullary disease [52].

In a follow-up study in which only pre-selected AML patients with low MGMT expression were treated with TMZ, only 28% had complete clearance of blasts in the BM, with 22% CR/CRp, with counts of 50–100 × 10^9/l [60]. This is indicating that other mechanisms mediate TMZ drug resistance. This theory could be true as TMZ and MGMT inhibitor combination was explored previously in a phase I study. Only one out of eight relapsed/refractory (R/R) acute leukemia patients achieved complete remission. The study concluded no benefit of the combination compared with TMZ monotherapy [61].

1.2.4.2 Mismatch Repair

The MMR pathway recognizes and corrects DNA damage that occurs spontaneously during DNA replication in the S phase or following exposure to carcinogenic agents [62]. In addition, the pathway is involved in repairing the mispairing induced by TMZ.

The repair mechanism begins with the formation of the recognition complex, *MutSα* (*MSH2:MSH6*), to identify the damage that occurred in a single base pair. Long mispairing, from 10 to 16 nucleotides, is recognized through *MutSβ* (*MSH2:MSH3*). The complex recruits *MutL homolog 1* (*MLH1*) protein, which comprises *PMS2* (*MutLα*), *PMS1* (*MutLβ*), or *MLH3* (*MutL γ*), for scaffolding and stabilization. *MutLα* is an important protein; as complexed with *MutS*, it functions as an endonuclease (Exo1) and removes the mismatch in newly replicated DNA. Then, the DNA polymerase (Pol*δ*) fills the gap with newly synthesized DNA and ligase I seals the DNA [56].

The MMR system should be activated in response to TMZ [42]. In the absence of MGMT, the MMR system recognizes the mismatch of O^6-MeG with (T) and induces a futile repair cycle causing DNA DSBs [43]. An impaired MMR system is considered a risk factor for TMZ resistance. Defects in MMR genes, such as *PMS2*, *MLH1*, *MSH2*, *MSH3* and *MSH6*, result in

impaired MMR function [41]. Consequently, the unrecognizable methylated nucleobase that is induced by TMZ causes cell resistance [42, 56].

1.2.4.3 Base Excision Repair

BER is a frontline process that corrects single nucleotide modifications caused by single-strand breaks (SSBs), oxidizing agents, ionization radiation, and alkylating agents [42, 55]. The TMZ cytotoxicity caused by N^7 guanine and N^3 adenine is minimal; however, an N^3 lesion is lethal if is left unrepaired [42, 46]. These methyl adducts immediately become substrates of the BER pathway [46]. In this pathway, 90% of TMZ methylation that occurs at N^7 guanine and N^3 adenine is repaired quickly and efficiently [49].

DNA lesion repair is initiated when an altered DNA base is recognized by DNA damage-sensing glycosylases [56]. The DNA glycosylase enzymes cleave the damaged nucleoside(s) at the N-glycosidic bond (uracil DNA glycosylase for uracil base and T:G glycosylase for TG base pair), leaving a basic apurinic/apyrimidinic (AP) site. To ensure the accuracy of the repair, the specific glycosylase enzyme is attached to the AP site until the next step [56, 63]. The damage site is excised by AP endonucleases/redox factor 1. For minor damage, DNA polymerase β synthesizes a single base AP site; for extensive DNA damage, DNA polymerases β, δ and ε with supporting and stabilization of proliferating cell nuclear antigen (PCNA) and replication factor-C proteins can synthesize two to eight nucleotides [56]. Finally, the corrected strand is sealed by DNA ligase III or I for minor and extensive damage, respectively [63]. N^3-MeA and N^7-MeG are substrate for DNA glycosylase. It found glioblastoma tissues have higher DNA glycosylase compared to non-neoplastic brain, which promotes resistance to TMZ [41]. The DNA polymerase β enzyme also inhibits TMZ sensitivity, which protects DNA damage by inhibiting DNA lyase activity [55].

Poly-(ADP ribose) polymerase 1 (PARP1) is a protein involved in the BER pathway [42, 46]. PARP1 recognizes SSBs by synthesizing poly-(ADP-ribose) from nicotinamide adenine dinucleotide (NAD^+) to recruit BER pathway proteins [43]. Excessive activation of PARP1 causes DNA damage and a reduction in the levels of NAD^+ and adenosine triphosphate (ATP), resulting in cell apoptosis [49, 55]. Inhibition of PARP1 and 2 enhances TMZ activity by promoting DNA DSBs and cell apoptosis [42, 46].

This evidence indicates the existence of other methods of TMZ resistance that remain unknown. Therefore, other strategies are needed to overcome TMZ resistance. In this research, we used a combination approach to enhance TMZ sensitivity. We chose the most recent molecular target inhibitors, VEN and idasanutlin (IDA), for combination with TMZ to treat AML cells. The following outline will extensively discuss both inhibitors.

1.3 BCL-2 Targeted Inhibition

1.3.1 Cell Apoptosis

Apoptosis is a physiologically programmed cell death process that removes damaged or infected cells from the body. In humans, approximately 330 billion cells die and are renewed each day [64]. The German scientist and philosopher Carl Vogt first reported the term ‘cell death’ in 1842 [64, 65]. Using a crude microscope, he observed cartilage cells from midwife toads dying and being replaced [64].

There are two distinct apoptotic pathways, the extrinsic apoptotic pathway (EAP) and the intrinsic apoptotic pathway (IAP). The EAP is the death receptor pathway, and the IAP is the mitochondrial pathway. Both pathways lead to cells undergoing morphological changes

including cytoplasmic and nuclear shrinkage (pyknosis), nuclear breakdown (karyorrhexis), and plasma membrane blebbing [66].

1.3.1.1 Extrinsic Apoptotic Pathway

The EAP is initiated when extracellular stimuli target plasma membrane receptors [66]. Extracellular ligands such as tumour necrosis factor (TNF), Fas ligand (Fas-L), and TNF-related apoptosis-inducing ligand (TRAIL) bind to their specific death receptors on the cell membrane, which are type 1 TNF receptor, Fas (also known as CD95/Apo-1) and TRAIL receptor, respectively. Upon ligand binding to the death receptor, a cascade is initiated leading to formation of a death-inducing signalling complex (DISC), which consists of the adaptor proteins Fas-associated death domain (FADD) and TNFR-associated death domain (TRADD). FADD binds to the caspase initiators procaspase-8 and procaspase-10 within DISC, leading to activation of caspase-8 followed by caspase-3 and caspase-7, which trigger cell death (Fig. 1.3) [64, 67].

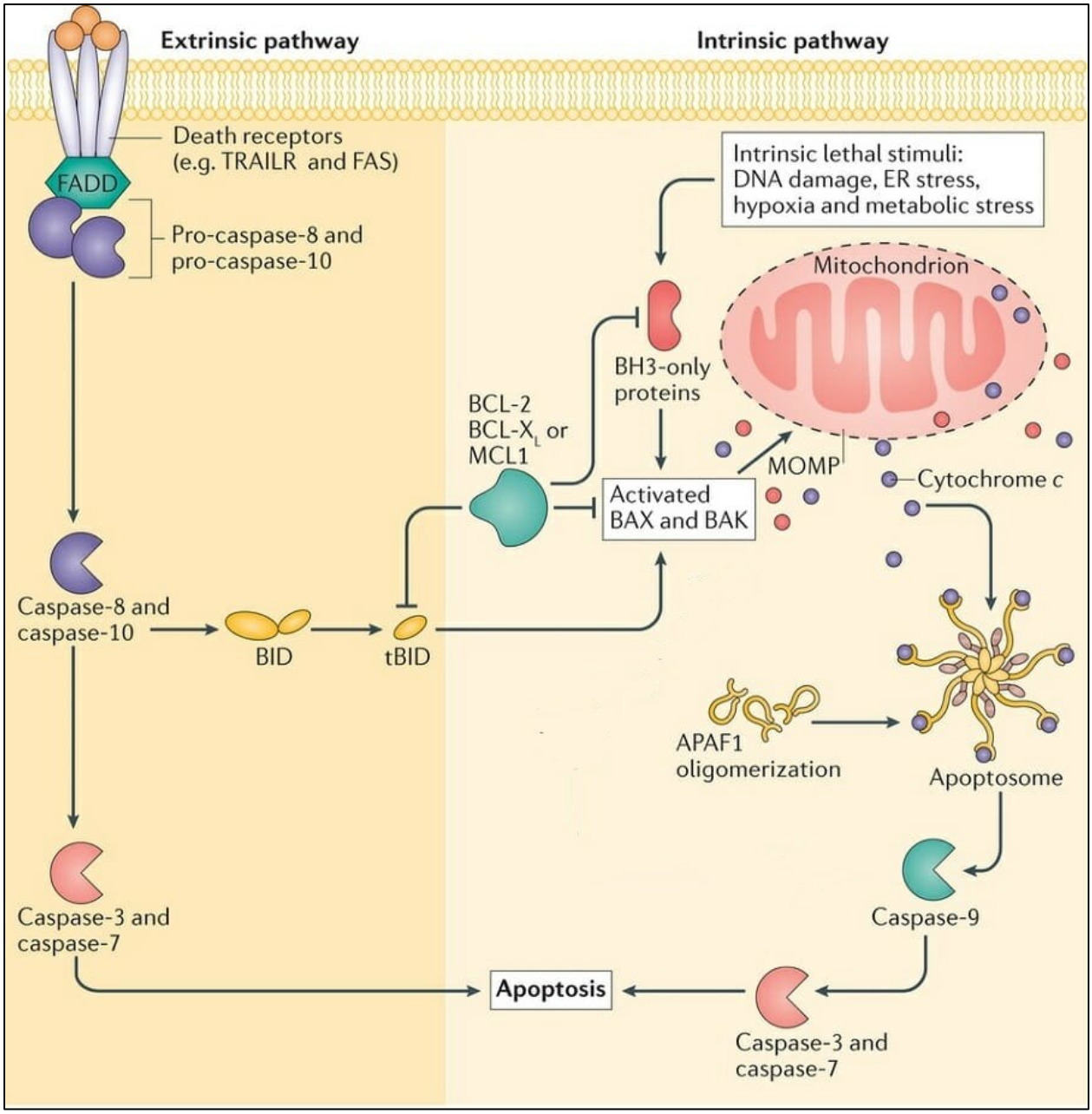

Figure 1.3: Extrinsic and intrinsic apoptotic pathways. Adapted from Apoptosis: Biology dictionary [updated 2017]. Available at https://biologydictionary.net/apoptosis/ [68]; public domain. APAF-1, apoptotic protease activating factor 1; BAK, BCL-2-antagonist/killer; BAX, BCL-2-associated X protein; BCL-2, B-cell lymphoma-2; BH, BCL-2 homology; BID, BH3-interacting domain death agonist; DNA, deoxyribonucleic acid; ER, endoplasmic reticulum; FADD, Fas-associated death domain; MCL1, myeloid cell leukemia sequence 1; MOMP,

mitochondrial outer membrane permeabilization; tBID, truncated BID; TRAILR, TNF-related apoptosis-inducing ligand receptor.

1.3.1.2 Intrinsic Apoptotic Pathway

The IAP is regulated by the B-cell lymphoma-2 (BCL-2) protein family, which is classified into three groups based on structure and function [69]:

1. Anti-apoptotic proteins containing BCL-2 homology (BH) domains BH1-4, including BCL-2, BCL-extra-large (BCL-XL), BCL-W (BCL-2L2), and myeloid cell leukemia sequence 1 (MCL1).

2. Pro-apoptotic effector proteins containing BH1-3, including BCL-2-associated X protein (BAX) and BCL-2-antagonist/killer (BAK).

3. Pro-apoptotic proteins with BH3 only, which are subdivided into the activator proteins BCL-2 interacting mediator of cell death (BIM), BH3-interacting domain death agonist (BID), and p53-upregulated modulator of apoptosis (PUMA); and the sensitizer proteins BCL-2 antagonist of cell death (BAD), BCL-2-interacting killer (BIK), and NOXA (phorbol-12-myristate-13-acetate-induced protein 1 (PMAIP1)).

The IAP is activated through extra- and intra-cellular stresses such as DNA damage, oxidative stress, irradiation and treatment with cytotoxic drugs [67]. The IAP involves cross-talk between anti-apoptotic proteins and pro-apoptotic effectors [69]. BH3-only pro-apoptotic proteins are activated, leading to activation of pro-apoptotic effectors BAX and BAK. The death mediator BAX/BAK forms homo-oligomers and initiates mitochondrial outer membrane permeabilization (MOMP), resulting in the formation of proteinaceous pores and release of cytochrome *c* to the

cytosol. The cytochrome *c* interacts with apoptotic protease activating factor 1 (APAF-1) and pro-caspase-9 in the presence of ATP to form an apoptosome [70, 71]. The apoptosome is a multi-protein complex that functions as a caspase mediator by activating caspase-9 through proteolytic cleavage [67]. Lastly, caspase-9 activates caspase-3 and caspase-7, which are released via proteolysis and induce cell death (Fig. 1.3) [69]. The EAP and IAP are connected at the caspase-8 step, where BID is cleaved to produce truncated BID (t-BID), which activates the death mediator BAX/BAK and induces MOMP [64].

1.3.2 BCL-2 in AML

The gene encoding *BCL-2* is located at chromosome 14q32 [72]. BCL-2 was found to be overexpressed in AML patients with 84% at diagnosis and 95% at relapse, and it is associated with prolonged leukemic cell survival and resistance to apoptosis [73]. Patients with AML, therefore, have a poor prognosis, low complete remission rates, and significantly reduced survival [74]. The anti-apoptotic MCL-1 protein is also involved in AML disease progression but is not as important for myeloblast survival as BCL-2 [75].

1.3.3 BCL-2 Inhibitor Venetoclax

VEN (ABT-199; Venclexta®; $C_{45}H_{50}ClN_7O_7S$) is the first oral, small molecule, highly selective and specific inhibitor of the anti-apoptotic BCL-2 protein to be approved for clinical use [76, 77]. It has been approved by the U.S. Food and Drug Administration since 2016 to treat adult CLL, and in 2018 it was approved for use in newly diagnosed patients with AML who are aged ≥ 75 years, or who are ineligible for intensive chemotherapy in combination with hypomethylating agents or LDAC [77]. It was also approved by Health Canada in 2020, in combination with azacitidine, for the same indication.

1.3.3.1 Mechanism of Action

In cancer cells, BCL-2 binds to BIM to prevent apoptosis. VEN induces dissociation of BIM from BCL-2 and then binds to the BH3-binding groove [78]. The pro-apoptotic activator BIM then activates the pro-apoptotic effectors BAX and BAK. The death mediator BAX/BAK oligomerizes and initiates MOMP, leading to cytochrome *c* release, activation of the caspase cascade and, finally, apoptosis (Fig. 1.4) [70, 71].

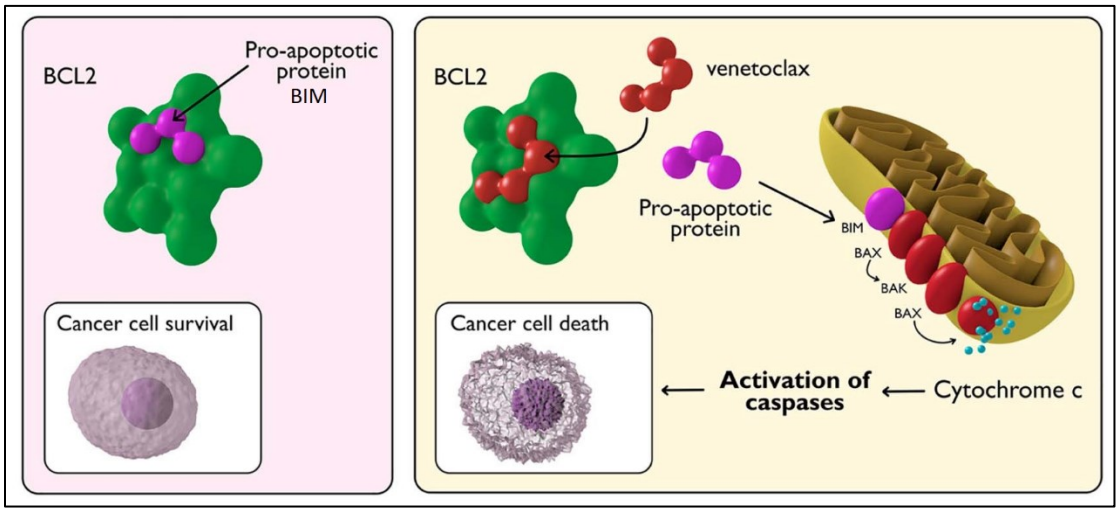

Figure 1.4: Mechanism of action of the BCL-2 inhibitor VEN. Adapted from Mihalyova *et al*., 2018 [79]; Copyright 2018 ISEH – Society for Hematology and Stem Cells. Published by Elsevier Inc. All rights reserved. BAK, BCL-2-antagonist/killer; BAX, BCL-2-associated X protein; BCL-2, B-cell lymphoma-2; BIM, BCL-2 interacting mediator of cell death.

1.3.3.2 Pharmacokinetics

VEN (molecular weight 868.44 g/mol) is orally bioavailable (5.4%) [80] with slow absorption. Peak plasma levels are reached 5 to 8 hours after dose administration [81]. Administration with a high-fat meal increases VEN exposure by approximately 50% compared with a low-fat meal [78, 81]. Lipid in food increases VEN intestinal lymphatic transport by providing a lipoprotein-rich

environment when lipid is converted to triglyceride-rich lipoprotein in enterocytes [82]. It is highly bound to human plasma protein (> 99%) [83].

VEN is metabolized by the CYP450 isoform 3A4 enzyme, which is mainly present in the liver [83]. Metabolism generates the active metabolite M27, which has no pharmacological activity *in vivo* or *in vitro*, with at least 58-fold lower BCL-2 inhibitory activity compared with VEN [84]. The proposed pathway for M27 formation is through mono-oxidation of VEN on the 6 position of the cyclohexenyl moiety to produce M5, followed by enzyme-mediated cyclization at the α-carbon of piperazine (Fig. 1.5) [84].

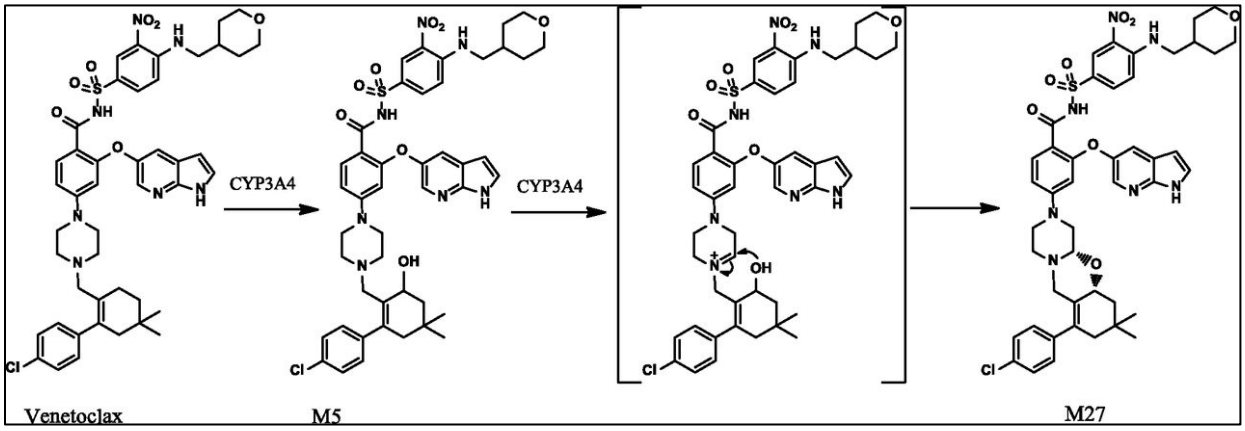

Figure 1.5: Proposed pathway formation of VEN metabolite M27. Adapted from Liu *et al*., 2016 [84]; Copyright 2017 by The American Society for Pharmacology and Experimental Therapeutics. CYP 3A4, cytochrome P450 isoform 3A4.

VEN has a t ½ of 26 hours versus 58.8 hours for M27. VEN is mainly eliminated in the feces (> 99.9 %), with only minimal excretion in the urine (< 0.1%) [78]. M27 is eliminated through the hepatobiliary route [84]. CYP3A4 inhibitors can be administered with VEN to increase exposure, while moderate and strong CYP3A4 inhibitors decrease VEN clearance to 19% and 84%, respectively [83].

Hemolytic anemia, tumour lysis syndrome, myelosuppression with or without infection and bleeding due to neutropenia and thrombocytopenia are the most common hematological side effects associated with VEN use [11, 78]. Non-hematological side effects include diarrhea, nausea, vomiting, fatigue, musculoskeletal pain, cough, dyspnea, edema, abdominal pain, headache, and rash [78].

1.3.3.3 Venetoclax Treatment for AML

An ORR of 6/32 (19%) was obtained when VEN monotherapy was administrated to high-risk patients with R/R AML. In this study, 12 (38%) of patients had *IDH1/2* mutations as a result of disease progression. Among these patients, 4 (33%) achieved a CR or a complete response with incomplete recovery of blood counts (CRi). *IDH1/2* mutations lead to dysregulated mitochondrial function by decreasing cytochrome *c* oxidase activity, which in turn increases BCL-2 expression. However, VEN efficacy is not limited to patients with *IDH1/2* mutations, since patients with wild-type *IDH1/2* also were sensitive to VEN therapy [76].

VEN has also been studied in combination with the hypomethylating agents azacitidine and decitabine. VEN and azacitidine demonstrated a 65% CR/CRi with median OS of 14.2 months, and the addition of VEN to decitabine resulted in a 72% CR/CRi and a median OS of 15.2 months. When VEN was added to LDAC in elderly untreated patients with AML, a synergistic effect was seen with enhanced patient remission of up to 54% [85]. The VIALE A study found that the combination of VEN + azacitidine produced superior OS compared with azacitidine alone in older AML patients unfit for intensive chemotherapy, and has now become the standard of care for these patients [30].

VEN is more widely known than first-generation navitoclax (ABT-263) because VEN has a 200-fold higher affinity binding to BCL-2 over BCL-XL. Navitoclax has more potent inhibition of

BCL-XL, which is known to be a key mediator of platelet survival; as a result, severe thrombocytopenia is associated with navitoclax use [83]. In addition, VEN activity is independent of cytogenetic profiling or genetic mutation status, which makes it suitable for most patients with AML who have a poor prognosis [75].

1.4 MDM2 Targeted Inhibition

1.4.1 P53 Tumour Suppressor Protein

TP53 gene encodes the p53 tumour suppressor protein, which is known as the 'guardian of the genome'[86]. It is located on chromosome 17p13.1 and codes for a 393 amino acid long phosphoprotein [87]. It was first identified in 1979 as an oncogene, then as a potential tumour suppressor in 1989 [86]. P53 is involved in DNA repair, senescence, cell cycle arrest and apoptosis [86, 88]. In the next section p53 functions are discussed in details.

1.4.1.1 P53 Function

P53 can be activated through post-translational chemical modifications such as phosphorylation, acetylation, ubiquitination, and methylation [67, 86]. Depending on the stress signal that cause the DNA damage, p53 promotes specific gene transcription to accomplish one of these cellular functions; DNA repair, cell-cycle arrest, apoptosis and senescence (Fig. 1.6) [86].

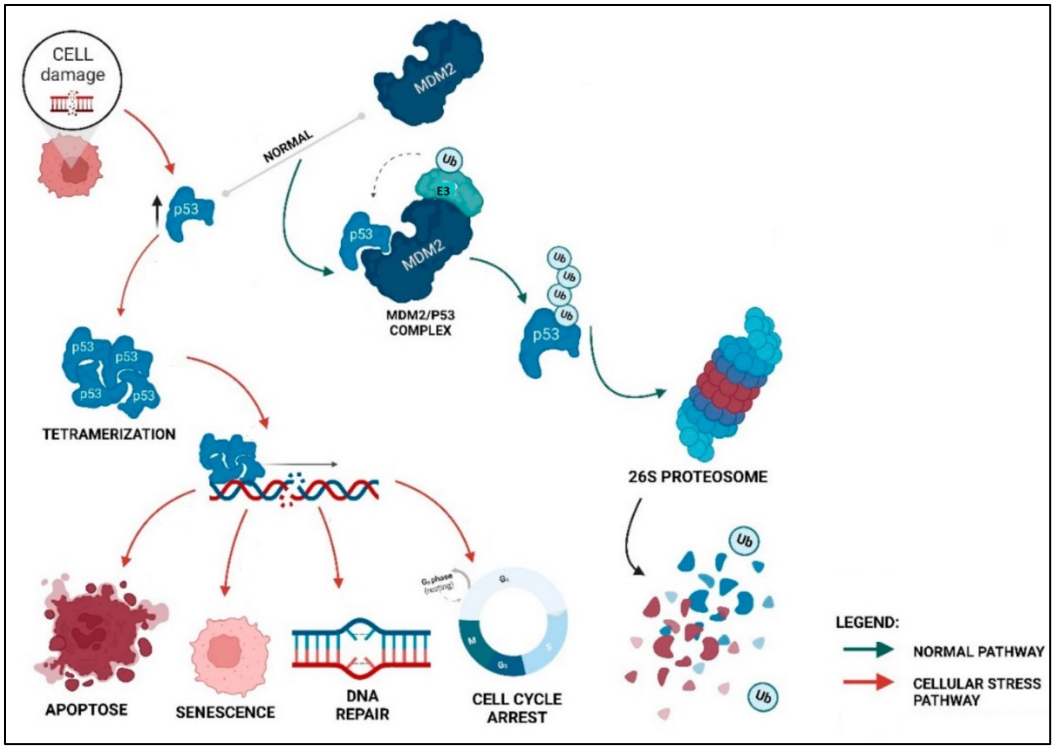

Figure 1.6: P53 functions and MDM2 ubiquitylation mechanism. Adapted from Vicente and Salvador, 2022 [89]; Creative Common BY- license. P53, tumor protein p53; MDM2, mouse double minute 2 homolog; Ub, ubiquitination.

In DNA repair, the DNA damage sensor proteins including ataxia telangiectasia mutated (ATM) and ATM and Rad3-related protein (ATR) are activated in DNA DSBs and SSBs, respectively. Functionally, the ATR and ATM are recruited to the site of the damage to stimulate checkpoint kinases 1 and 2 (Chk1 and Chk2), respectively, resulting in p53 phosphorylation and induction of p21, which inhibits the cyclin E/ CDK2 complex during the cell cycle to arrest the cell and induce DNA repair before cell division [63, 90].

Upregulating of p21 protein causes cell-cycle arrest to enable the DNA repair as mentioned earlier. Interestingly, p21 can interact with multiple CDKs to cause cell-cycle arrest at different

phases, including at the G1/S phase via interaction with cyclin E/CDK2 and cyclin D/CDK4, and at the G2/M phase with cyclin B/CKD1 [86, 90].

The cyclin complex additionally inhibits the cell cycle progression by dephosphorylating retinoblastoma protein (pRb) to become activated and binding to the E2F transcription factor, which prevents cell cycle progression [63].

P53 can induce apoptosis through dual transcription-dependent and -independent pathways in the nucleus and the mitochondria [67, 91]. In the nucleus, it promotes the EAP by increasing expression of the death receptors Fas and TRAIL [86]. In the mitochondria, it induces the IAP by activating pro-apoptotic proteins (PUMA) and suppressing anti-apoptotic proteins (BCL-2), leading to apoptosis. Additionally, p53 can directly interact with BAX leading to homo-oligomerization, induction of MOMP and cytochrome *c* release [67].

Long-term stress exposure maintains p53 phosphorylation and causes p21 overexpression to maintain replication arrest, which is called cell senescence. This irreversible cell arrest causes mitochondrial dysfunction and generates reactive oxygen species (ROS) through a signaling pathway mediated by GADD45-p38 (MAPK14)-GRB2-TGFβ, which sustains the DNA damage response [92].

In normal unstressed cells, p53 is unstable with a short t ½ of only 5–30 minutes and is regulated by mouse double minute 2 homolog (MDM2) protein (Fig. 1.6) [91]. The t ½ increases when cells are exposed to stress signals leading to p53 activation. In the following section MDM2 protein is discussed in details.

1.4.2 MDM2 Protein

MDM2 was first discovered on double-minute chromosomes of spontaneously transformed mouse 3T3 fibroblasts [91]. Human *MDM2* was first known in 1992 and is located on the long arm 13–14 of chromosome 12 [93].

1.4.2.1 MDM2 Function

MDM2 protein controls p53 protein expression through an autoregulatory negative feedback loop. The p53 binds to MDM2 protein at the N-terminal hydrophobic cleft and also binds to the P2 promoter of *MDM2* to upregulate gene expression and later the protein levels [94].

MDM2 is an E3 ligase that promotes p53 degradation through a ubiquitin-dependent pathway on nuclear and cytoplasmic 26S proteasomes [91]. Proteasomes are cylindrical multi-protein complexes that require ATP to unfold p53 protein for degradation into short peptide fragments (oligopeptides) ranging in size from 3 to 25 amino acid residues (Fig. 1.6) [63].

The ubiquitylation mechanism is a rapid, specific, localized and irreversible process for p53 protein destruction [63]. It can involve monoubiquitination or polyubiquitination depending on the MDM2 level. Mono-ubiquitination is dominant at low MDM2 levels and involves p53 export from the nucleus to the cytoplasm for degradation. At high MDM2 levels, polyubiquitination occurs within the nucleus and p53 is degraded by nuclear proteasomes [95]. Polyubiquitation occurs when one ubiquitin molecule is initially linked by its C-terminal glycine to the ε-amino side chain of a lysine present in a target protein; a second ubiquitin molecule is then linked to lysine-48 in the first ubiquitin and this process is repeated a number of times [63].

In the absence of stress, MDM2 maintains p53 at low levels [91]. In contrast, after the p53 DNA damage response is completed, MDM2 levels rise to rapidly remove p53 through polyubiquitination [95].

MDM2 is abnormally expressed as a result of gene amplification, increased transcription and enhanced translation [94]. It is upregulated through phosphorylation of Ser166 and Ser186 residues, [96] which occurs by activation of the protein kinase B (PKB/AKT) survival signal after stimulation of the pathway. Phosphorylated MDM2 is translocated from the cytoplasm to the nucleus to attack p53 [63]. In addition, *MDM2* gene transcription is increased when receptor tyrosine kinases bind to specific growth factors, leading to activation of Ras and then Raf. Subsequent signal transduction via mitogen-activated protein kinase kinase 1/2 (MEK1/2) and extracellular signal-regulated kinase 1/2 (ERK1/2) increases E26 transformation-specific (ETS) and activator protein-1 (AP-1) transcription factors [63]. MDM2 overexpression in highly proliferating cells is thus a consequence of Ras pathway activation, activation of ETS transcription factor and subsequent upregulation of MDM2 expression [96].

MDM2 is downregulated by the tumour suppressor $p14^{ARF}$, which binds to MDM2 in the nucleoplasm and keeps it in the nucleolus. This sequestration of MDM2 elevates p53 levels and thus allows free p53 activity [63].

1.4.2.2 MDM2 in AML

P53 is mutated in more than half of all cancers [86]. Fortunately, p53 is mutated in only 5–8% of newly diagnosed patients with AML [94], although this frequency is higher in patients with secondary AML. However, p53 function is inactivated or dysregulated due to overexpression of

MDM2 protein, which is a negative regulator of p53. MDM2 overexpression is mostly recognized in wild-type p53 cancer, where it inhibits p53 transcriptional activation [96]. Inhibition of p53 leads to the development of highly proliferative leukemic cells and resistance to apoptosis resulting in poor prognosis AML [94, 96].

1.4.3 MDM2 Inhibitor Idasanutlin

Idasanutlin (IDA; RG-7388; RO5503781; $C_{31}H_{29}Cl_2F_2N_3O_4$) is a selective second-generation MDM2 inhibitor [97]. It prevents protein–protein interactions that disrupt p53:MDM2 interaction and restores p53 function [94, 97, 98]. IDA was an advancement of the first-generation MDM2 inhibitor RG7112 [94]. RG7112 was used as monotherapy and combination with cytarabine or doxorubicin to treat patients with solid tumor, hematological neoplasms or sarcoma. A modest response was observed in AML treated patients regardless of p53 status [99]. Moreover, it was observed with signs of gastrointestinal toxicity, myelosuppression and related complications such as sepsis and hemorrhage. Clinical development of RG7112 was halted as a result of inconsistent pharmacokinetic results [94].

1.4.3.1 Mechanism of Action

IDA binds the surface of MDM2 at the p53 binding pocket to block interaction between the MDM2 protein and the transcriptional activation domain of p53 [97, 100]. Consequently, it targets p21, which causes cell-cycle arrest at the G1 phase [92]. In addition, IDA upregulates the apoptotic modulator PUMA, which binds to BCL-2 to initiate the IAP (Fig. 1.7) [101]. IDA has been shown to have a dose-dependent effect on p53 stabilization, apoptosis and cell-cycle arrest [102].

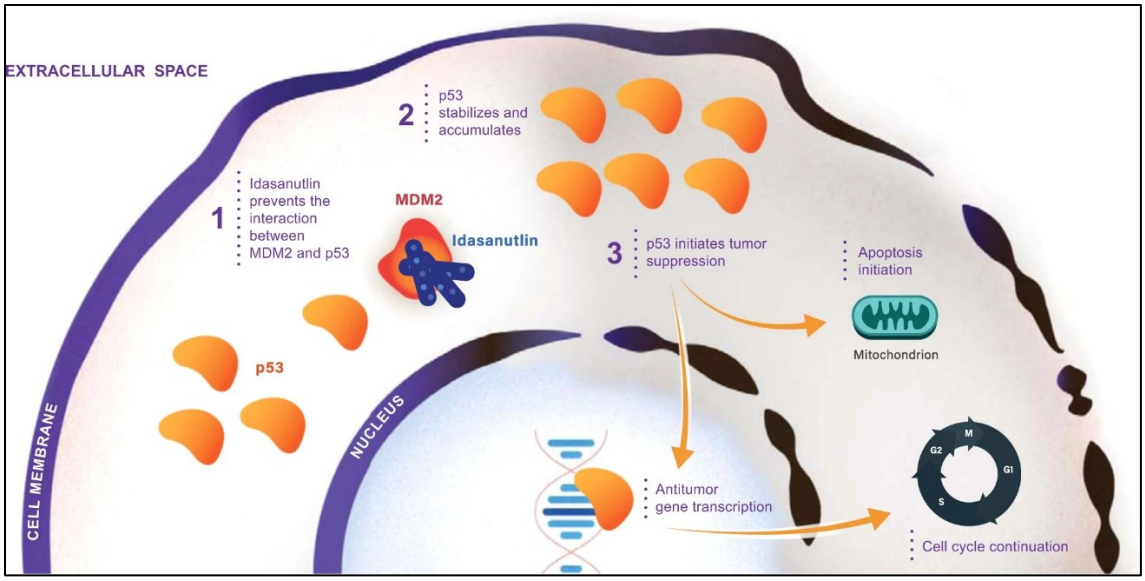

Figure 1.7: Mechanism of action of the MDM2 inhibitor IDA. Adapted from Konopleva *et al.*, 2020 [94] and reproduced with permission from Springer Nature. P53, tumor protein p53; MDM2, mouse double minute 2 homolog.

1.4.3.2 Pharmacokinetics

IDA is a pyrrolidine small molecule (molecular weight 616.5 g/mol) with high potency [94, 97, 103] and bioavailability (40.1%) [100]. It is a safe and well-tolerated drug that can be administrated both orally and intravenously [69, 100]. It is metabolized by CYP3A, CYP2C8, and uridine-5′-diphospho-α-d-glucuronic acid glucuronosyltransferases (UGTs) to produce major (M4) and minor (M2) inactive metabolites (Fig. 1.8). The IDA peak plasma concentration is reached less than 10 hours after oral administration. The t ½ is around 1 day for IDA and 2 days for M4. This is related to the IDA:M4 ratio, which is high in M4 by 15.8% at maximum concentration in plasma and 29% area under the curve (AUC) [100].

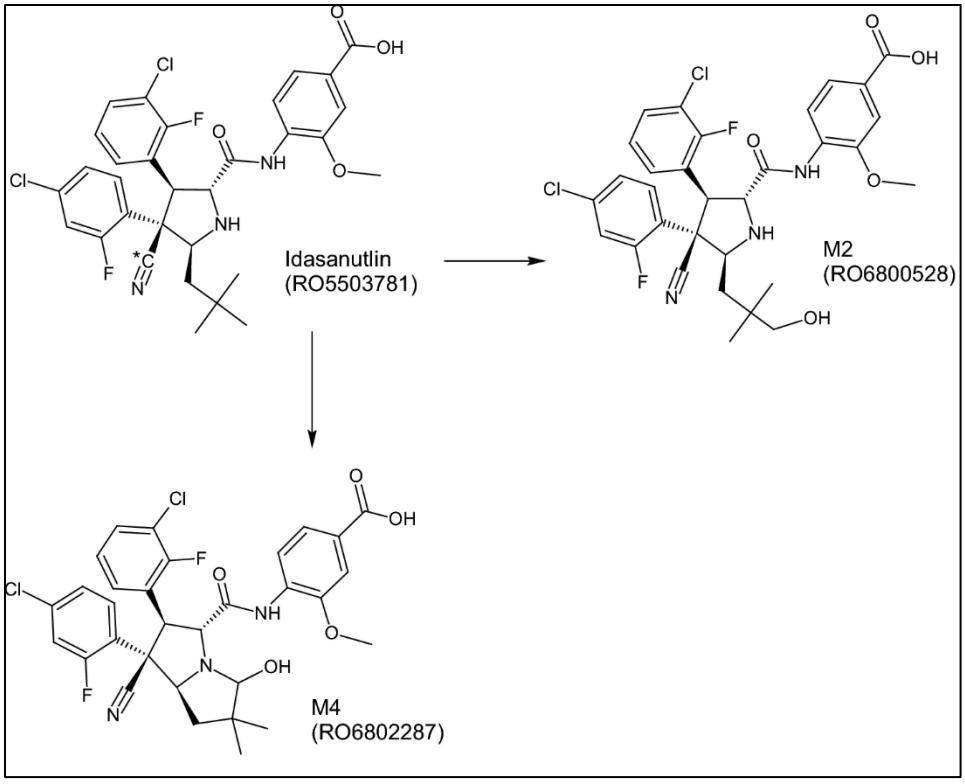

Figure 1.8: Proposed formation pathway for IDA metabolites M2 and M4. Adapted from Papai *et al*., 2019 [100] and reproduced with permission from Springer Nature.

There is not specific food known to increase IDA exposure, but co-administration of CYP3A inhibitors with IDA has a modest effect on exposure by increasing the AUC to 31%. IDA is excreted mainly through the biliary route, with 91.5% present in the feces. Urinary excretion is minimal (< 0.1%) [100]. Adverse events associated with IDA include diarrhea, nausea, vomiting, and myelosuppression resulting in febrile neutropenia and thrombocytopenia [102].

1.4.3.3 Idasanutlin Treatment for AML

Up to 80% of patients with AML express wild-type p53, which should enable cell-cycle arrest and apoptosis [104]. However, this function is disabled due to overexpression of MDM2 [105].

One treatment strategy for AML is to take advantage of functional p53 by inhibiting the MDM2 protein with MDM2 inhibitors such as IDA [96].

When IDA was administered orally and intravenously to AML patients it decreased leukemic cells, with minimum impact on cellular suppression of the BM [69]. Using IDA as monotherapy, 6 of 29 patients (21%) had either a CR (n=2) or CRi/morphologic leukemia-free state (MLFS) (n= 4). When IDA was administered in combination with cytarabine, 11 of 46 patients (24%) had a CR (n=10) or CRi/MLFS (n=1) [69, 106].

The response to IDA, either as monotherapy or in combination with cytarabine, was correlated with MDM2 expression. This observation was confirmed using patient-derived AML blast cells with wild-type p53. Patients achieving CR/CRp/CRi to IDA-containing therapy had significantly higher MDM2 expression in AML blast cells (P=0.0016) compared to those who failed to achieve CR to IDA [98].

IDA was added to cytarabine chemotherapy to treat R/R AML in a Phase 3 randomized study comparing the combination with cytarabine plus placebo. The CR rate and ORR were increased in the IDA + cytarabine group by 3.2% (20.3% vs 17.1%) and 16.8% (38.8% vs 22%), respectively. However, the median OS for the IDA + cytarabine group was not significantly different than the cytarabine + placebo arm (8.3 vs 9.1 months, P= 0.58) [107].

1.5 Thesis Goal and Hypotheses

It is generally recognized that high levels of the DNA repair protein MGMT cause resistance to TMZ. Sensitivity to TMZ in AML is restricted to cases with low MGMT expression; however, the majority of such cases are also resistant to TMZ, for unknown reasons. The purpose of this research is to attempt to enhance TMZ sensitivity in AML cells and thereby overcome drug

resistance, by targeting selected critical leukemic pathways involved in AML cell pathophysiology. The anti-apoptotic protein BCL-2 and MDM2-mediated p53 degradation are involved in cell proliferation, prevention of apoptosis and chemotherapeutic resistance, and have therefore been selected for study.

VEN, as a BCL-2 inhibitor, and IDA, as an MDM2 inhibitor, each has activity in AML and has increased response rates to other antileukemic agents. However, the combination of these inhibitors with TMZ remains uninvestigated. These targeted selective inhibitors have therefore been chosen to investigate whether these agents can enhance sensitivity of AML cells to TMZ.

Main Hypothesis

Enhanced TMZ treatment sensitivity in cells expressing high and low levels of MGMT can be achieved by incorporating a selective targeted inhibitor into the TMZ treatment strategy.

Chapter 2: BCL-2 Targeted Inhibitor Hypothesis

Combining the BCL-2 inhibitor VEN with TMZ can enhance TMZ sensitivity by increasing cell death in AML cells exhibiting both high and low levels of MGMT expression through BCL-2 inhibition and activation of mitochondrial IAP.

Chapter 3: MDM2 Targeted Inhibitor Hypothesis

Combining the MDM2 inhibitor IDA with TMZ can enhance TMZ sensitivity by increasing cell death in AML cells with high and low levels of MGMT expression, through disruption of the p53:MDM2 interaction and restoration of p53 functions.

Overall Objectives

To investigate whether VEN or IDA is able to increase the sensitivity of both high and low MGMT expressing AML cells to TMZ, in cell lines and in patients derived samples. The following will be assessed with each agent:

1. Cell viability.
2. Cell apoptosis.
3. DNA damage.
4. Leukemia cell line engraftment in a mouse model (VEN only).

1.6 References

1. Hoffbrand AV, Moss PAH, Pettit JE. Essential Haematology. 5th ed. Massachustts, USA: Blackwell; 2006.

2. Saxena R, Pati HP. Hematopathology: Advances in Understanding. Singapore: Springer 2019. 1-502 p.

3. Pelcovits A, Niroula R. Acute Myeloid Leukemia: A Review. R I Med J (2013). 2020;103(3):38-40.

4. Vakiti A, Mewawalla P. Acute Myeloid Leukemia. StatPearls [Internet]. Treasure Island (FL): StatPearls; 2022. Available from: www.ncbi.nlm.nih.gov/books/NBK507875/.

5. Ossenkoppele G, Löwenberg B. How I treat the older patient with acute myeloid leukemia. Blood. 2015;125(5):767-74.

6. Sasaki K, Ravandi F, Kadia TM, DiNardo CD, Short NJ, Borthakur G, et al. De novo acute myeloid leukemia: A population-based study of outcome in the United States based on the Surveillance, Epidemiology, and End Results (SEER) database, 1980 to 2017. Cancer. 2021;127(12):2049-61.

7. Kumar CC. Genetic abnormalities and challenges in the treatment of acute myeloid Leukemia. Genes Cancer. 2011;2(2):95-107.

8. Zheng G, Li P, Zhang X, Pan Z. The fifth edition of the World Health Organization Classification and the International Consensus Classification of myeloid neoplasms: evolving guidelines in the molecular era with practical implications. Curr Opin Hematol. 2023;30(2):53-63.

9. Khoury JD, Solary E, Abla O, Akkari Y, Alaggio R, Apperley JF, et al. The 5th edition of the World Health Organization Classification of Haematolymphoid Tumours: Myeloid and Histiocytic/Dendritic Neoplasms. Leukemia. 2022;36(7):1703-19.

10. Arber DA, Orazi A, Hasserjian RP, Borowitz MJ, Calvo KR, Kvasnicka H-M, et al. International Consensus Classification of Myeloid Neoplasms and Acute Leukemias: integrating morphologic, clinical, and genomic data. Blood. 2022;140(11):1200-28.

11. Döhner H, Wei AH, Appelbaum FR, Craddock C, DiNardo CD, Dombret H, et al. Diagnosis and management of AML in adults: 2022 recommendations from an international expert panel on behalf of the ELN. Blood. 2022;140(12):1345-77.

12. Acute myeloid leukemia : methods and protocols: Humana Press; 2017. Available from: https://link-springer-com.login.ezproxy.library.ualberta.ca/book/10.1007/978-1-4939-7142-8.

13. Padmakumar D, Chandraprabha VR, Gopinath P, Vimala Devi ART, Anitha GRJ, Sreelatha MM, et al. A concise review on the molecular genetics of acute myeloid leukemia. Leuk Res. 2021;111:106727.

14. Meshinchi S, Appelbaum FR. Structural and functional alterations of FLT3 in acute myeloid leukemia. Clin Cancer Res. 2009;15(13):4263-9.

15. Lewis SM. Chapter 2 - Reference ranges and normal values. In: Lewis SM, Bain BJ, Bates I, editors. Dacie and Lewis Practical Haematology. 10th ed. Philadelphia: Churchill Livingstone; 2006. p. 11-24.

16. Bates I. Chapter 6 - Bone marrow biopsy. In: Lewis SM, Bain BJ, Bates I, editors. Dacie and Lewis Practical Haematology. 10th ed. Philadelphia: Churchill Livingstone; 2006. p. 115-30.

17. Haferlach T, Schmidts I. The power and potential of integrated diagnostics in acute myeloid leukaemia. Br J Haematol. 2020;188(1):36-48.

18. Matutes E, Morilla R, Catovsky D. Chapter 14 - Immunophenotyping. In: Lewis SM, Bain BJ, Bates I, editors. Dacie and Lewis Practical Haematology. 10th ed. Philadelphia: Churchill Livingstone; 2006. p. 335-55.

19. Qin D. Molecular testing for acute myeloid leukemia. Cancer Biol Med. 2021;19(1):4-13.

20. Vulliamy T, Kaeda J. Chapter 21 - Molecular and cytogenetic analysis. In: Lewis SM, Bain BJ, Bates I, editors. Dacie and Lewis Practical Haematology. 10th ed. Philadelphia: Churchill Livingstone; 2006. p. 555-94.

21. Shimony S, Stahl M, Stone RM. Acute myeloid leukemia: 2023 update on diagnosis, risk-stratification, and management. Am J Hematol. 2023;98(3):502-26.

22. Döhner H, Weisdorf DJ, Bloomfield CD. Acute Myeloid Leukemia. N Engl J Med. 2015;373(12):1136-52.

23. Gewirtz DA. A critical evaluation of the mechanisms of action proposed for the antitumor effects of the anthracycline antibiotics adriamycin and daunorubicin. Biochem Pharmacol. 1999;57(7):727-41.

24. Momparler RL. Optimization of cytarabine (ARA-C) therapy for acute myeloid leukemia. Exp Hematol Oncol. 2013;2:20.

25. Stone RM, Mandrekar SJ, Sanford BL, Laumann K, Geyer S, Bloomfield CD, et al. Midostaurin plus Chemotherapy for Acute Myeloid Leukemia with a FLT3 Mutation. N Engl J Med. 2017;377(5):454-64.

26. Lambert J, Pautas C, Terré C, Raffoux E, Turlure P, Caillot D, et al. Gemtuzumab ozogamicin for de novo acute myeloid leukemia: final efficacy and safety updates from the open-label, phase III ALFA-0701 trial. Haematologica. 2019;104(1):113-9.

27. Lancet JE, Uy GL, Newell LF, Lin TL, Ritchie EK, Stuart RK, et al. Five-year final results of a phase III study of CPX-351 versus 7+3 in older adults with newly diagnosed high-risk/secondary AML. J Clin Oncol. 2020;38(15_suppl):7510-10.

28. Bhansali RS, Pratz KW, Lai C. Recent advances in targeted therapies in acute myeloid leukemia. J Hematol Oncol. 2023;16(1).

29. Brandwein JM, Hallett D, Karkhaneh M, Zhu N, Liew E, Bolster L, et al. An evaluation of no-treatment decisions in patients with newly diagnosed acute myeloid leukemia. Am J Hematol. 2021;96(1):E17-e20.

30. DiNardo CD, Jonas BA, Pullarkat V, Thirman MJ, Garcia JS, Wei AH, et al. Azacitidine and Venetoclax in Previously Untreated Acute Myeloid Leukemia. N Engl J Med. 2020;383(7):617-29.

31. Dombret H, Seymour JF, Butrym A, Wierzbowska A, Selleslag D, Jang JH, et al. International phase 3 study of azacitidine vs conventional care regimens in older patients with newly diagnosed AML with >30% blasts. Blood. 2015;126(3):291-9.

32. Perl AE, Martinelli G, Cortes JE, Neubauer A, Berman E, Paolini S, et al. Gilteritinib or Chemotherapy for Relapsed or Refractory FLT3-Mutated AML. N Engl J Med. 2019;381(18):1728-40.

33. DiNardo CD, Stein EM, de Botton S, Roboz GJ, Altman JK, Mims AS, et al. Durable Remissions with Ivosidenib in IDH1-Mutated Relapsed or Refractory AML. N Engl J Med. 2018;378(25):2386-98.

34. Stein EM, DiNardo CD, Pollyea DA, Fathi AT, Roboz GJ, Altman JK, et al. Enasidenib in mutant IDH2 relapsed or refractory acute myeloid leukemia. Blood. 2017;130(6):722-31.

35. Reitman ZJ, Yan H. Isocitrate dehydrogenase 1 and 2 mutations in cancer: alterations at a crossroads of cellular metabolism. J Natl Cancer Inst. 2010;102(13):932-41.

36. Merchant SL, Culos K, Wyatt H. Ivosidenib: IDH1 Inhibitor for the Treatment of Acute Myeloid Leukemia. J Adv Pract Oncol. 2019;10(5):494-500.

37. Du X, Hu H. The Roles of 2-Hydroxyglutarate. Front Cell Dev Biol. 2021;9:651317.

38. Westhus J, Noppeney R, Dührsen U, Hanoun M. FLAG salvage therapy combined with idarubicin in relapsed/refractory acute myeloid leukemia. Leuk Lymphoma. 2019;60(4):1014-22.

39. Brandwein JM, Saini L, Geddes MN, Yusuf D, Liu F, Schwann K, et al. Outcomes of patients with relapsed or refractory acute myeloid leukemia: a population-based real-world study. Am J Blood Res. 2020;10(4):124-33.

40. Singh RK, Kumar S, Prasad DN, Bhardwaj TR. Therapeutic journery of nitrogen mustard as alkylating anticancer agents: Historic to future perspectives. Eur J Med Chem. 2018;151:401-33.

41. Tomar MS, Kumar A, Srivastava C, Shrivastava A. Elucidating the mechanisms of Temozolomide resistance in gliomas and the strategies to overcome the resistance. Biochim Biophys Acta Rev Cancer. 2021;1876(2):188616.

42. Jiapaer S, Furuta T, Tanaka S, Kitabayashi T, Nakada M. Potential strategies overcoming the temozolomide resistance for glioblastoma. Neurol Med Chir (Tokyo). 2018;58(10):405-21.

43. Ortiz R, Perazzoli G, Cabeza L, Jiménez-Luna C, Luque R, Prados J, Melguizo C. Temozolomide: An updated overview of resistance mechanisms, nanotechnology advances and clinical applications. Curr Neuropharmacol. 2021;19(4):513-37.

44. Wesolowski JR, Rajdev P, Mukherji SK. Temozolomide (Temodar). AJNR Am J Neuroradiol. 2010;31(8):1383-4.

45. Shen W, Hu JA, Zheng JS. Mechanism of temozolomide-induced antitumour effects on glioma cells. J Int Med Res. 2014;42(1):164-72.

46. Fan CH, Liu WL, Cao H, Wen C, Chen L, Jiang G. O6-methylguanine DNA methyltransferase as a promising target for the treatment of temozolomide-resistant gliomas. Cell Death Dis. 2013;4(10):e876-e.

47. Verbeek B, Southgate TD, Gilham DE, Margison GP. O6-Methylguanine-DNA methyltransferase inactivation and chemotherapy. Br Med Bull. 2008;85:17-33.

48. Nagasubramanian R, Dolan ME. Temozolomide: Realizing the promise and potential. Curr Opin Oncol. 2003;15(6):412-8.

49. Kaina B, Christmann M. DNA repair in personalized brain cancer therapy with temozolomide and nitrosoureas. DNA Repair. 2019;78:128-41.

50. Singh R, Mehrotra S, Gopalakrishnan M, Gojo I, Karp JE, Greer JM, et al. Population pharmacokinetics and exposure-response assessment of veliparib co-administered with temozolomide in patients with myeloid leukemias. Cancer Chemother Pharmacol. 2019;83(2):319-28.

51. Zhai Y, Shang J, Yao W, Wu D, Fu C, Yan L. Successful eradication of central nervous system infiltration of primary plasma cell leukemia by temozolomide. Ann Hematol. 2022;101(11):2555-7.

52. Brandwein JM, Yang L, Schimmer AD, Schuh AC, Gupta V, Wells RA, et al. A phase II study of temozolomide therapy for poor-risk patients aged >or=60 years with acute myeloid leukemia: low levels of MGMT predict for response. Leukemia. 2007;21(4):821-4.

53. Seiter K, Liu D, Loughran T, Siddiqui A, Baskind P, Ahmed T. Phase I study of temozolomide in relapsed/refractory acute leukemia. J Clin Oncol. 2002;20(15):3249-53.

54. Rao A, Ramani N, Stoppacher R, Coyle T. Complete response to temozolomide in chronic lymphocytic leukemia. Clin Case Rep. 2017;5(7):1130-1.

55. Singh N, Miner A, Hennis L, Mittal S. Mechanisms of temozolomide resistance in glioblastoma - a comprehensive review. Cancer Drug Resist. 2021;4(1):17-43.

56. Kelley MR, Fishel ML. DNA Repair in Cancer Therapy: Molecular Targets and Clinical Applications. 2nd ed: Elsevier Inc.; 2016. 1-444 p.

57. Sharma S, Salehi F, Scheithauer BW, Rotondo F, Syro LV, Kovacs K. Role of MGMT in tumor development, progression, diagnosis, treatment and prognosis. Anticancer Res. 2009;29(10):3759-68.

58. Ochs K, Kaina B. Apoptosis induced by DNA damage O6-methylguanine is Bcl-2 and caspase-9/3 regulated and Fas/caspase-8 independent. Cancer Res. 2000;60(20):5815-24.

59. Wang K, Kievit FM, Chiarelli PA, Stephen ZR, Lin G, Silber JR, et al. siRNA nanoparticle suppresses drug-resistant gene and prolongs survival in an orthotopic glioblastoma xenograft mouse model. Adv Funct Mater. 2021;31(6).

60. Brandwein JM, Kassis J, Leber B, Hogge D, Howson-Jan K, Minden MD, et al. Phase II study of targeted therapy with temozolomide in acute myeloid leukaemia and high-risk myelodysplastic syndrome patients pre-screened for low O(6) -methylguanine DNA methyltransferase expression. Br J Haematol. 2014;167(5):664-70.

61. Seiter K, Katragadda S, Ponce D, Rasul M, Ahmed N. Temozolomide and cisplatin in relapsed/refractory acute leukemia. J Hematol Oncol. 2009;2:21.

62. Bolufer P, Barragan E, Collado M, Cervera J, López JA, Sanz MA. Influence of genetic polymorphisms on the risk of developing leukemia and on disease progression. Leuk Res. 2006;30(12):1471-91.

63. Weinberg RA. The Biology of Cancer. 1st ed. New York: Garland Science; 2007.

64. Diepstraten ST, Marca JEL, Huang DCS, Kelly GL. Principles for understanding mechanisms of cell death and their role in cancer biology. Precision Cancer Therapies2023. p. 133-50.

65. Vogt KC. Untersuchungen über die Entwicklungsgeschichte der Geburtshelferkrte (Alytes obstetricans): Solothurn : Jent & Gassmann; 1842. Available from: http://hdl.handle.net/10111/UIUCOCA:untersuchungen00vogt.

66. Abeloff's clinical oncology. 6th ed. Niederhuber JE, Armitage JO, Doroshow JH, Kastan MB, Tepper JE, Abeloff MD, editors: Elsevier; 2020.

67. Jan R, Chaudhry GE. Understanding Apoptosis and Apoptotic Pathways Targeted Cancer Therapeutics. Adv Pharm Bull. 2019;9(2):205-18.

68. Apoptosis: Biology dictionary; [updated 2017. Available from: https://biologydictionary.net/apoptosis/.

69. Cassier PA, Castets M, Belhabri A, Vey N. Targeting apoptosis in acute myeloid leukaemia. Br J Cancer. 2017;117(8):1089-98.

70. Zhu H, Almasan A. Development of venetoclax for therapy of lymphoid malignancies. Drug Des Devel Ther. 2017;11:685-94.

71. Korycka-Wolowiec A, Wolowiec D, Kubiak-Mlonka A, Robak T. Venetoclax in the treatment of chronic lymphocytic leukemia. Expert Opin Drug Metab Toxicol. 2019;15(5):353-66.

72. Croce CM, Reed JC. Finally, An Apoptosis-Targeting Therapeutic for Cancer. Cancer Res. 2016;76(20):5914-20.

73. Wei Y, Cao Y, Sun R, Cheng L, Xiong X, Jin X, et al. Targeting Bcl-2 Proteins in Acute Myeloid Leukemia. Front Oncol. 2020;10.

74. Campos EDV, Pinto R. Targeted therapy with a selective BCL-2 inhibitor in older patients with acute myeloid leukemia. Hematol Transfus Cell Ther. 2019;41(2):169-77.

75. Pan R, Hogdal LJ, Benito JM, Bucci D, Han L, Borthakur G, et al. Selective BCL-2 inhibition by ABT-199 causes on-target cell death in acute myeloid Leukemia. Cancer Discov. 2014;4(3):362-675.

76. Konopleva M, Pollyea DA, Potluri J, Chyla B, Hogdal L, Busman T, et al. Efficacy and biological correlates of response in a phase II study of venetoclax monotherapy in patients with acute Myelogenous Leukemia. Cancer Discov. 2016;6(10):1106-17.

77. Yang Y, Shu Y, Chen G, Yin Y, Li F, Li J. A real-world pharmacovigilance study of FDA Adverse Event Reporting System (FAERS) events for venetoclax. PLOS ONE. 2022;17(12):e0278725.

78. Venetoclax: Ontario Health (Cancer Care Ontario); [updated 2022. Available from: https://www.cancercareontario.ca/en/drugformulary/drugs/monograph/44476.

79. Mihalyova J, Jelinek T, Growkova K, Hrdinka M, Simicek M, Hajek R. Venetoclax: A new wave in hematooncology. Exp Hematol. 2018;61:10-25.

80. Kala SG, Chinni S. Development and Characterization of Venetoclax Nanocrystals for Oral Bioavailability Enhancement. AAPS PharmSciTech. 2021;22(3):92.

81. Megías-Vericat JE, Solana-Altabella A, Ballesta-López O, Martínez-Cuadrón D, Montesinos P. Drug-drug interactions of newly approved small molecule inhibitors for acute myeloid leukemia. Ann Hematol. 2020;99(9):1989-2007.

82. Salem AH, Agarwal SK, Dunbar M, Nuthalapati S, Chien D, Freise KJ, Wong SL. Effect of Low- and High-Fat Meals on the Pharmacokinetics of Venetoclax, a Selective First-in-Class BCL-2 Inhibitor. J Clin Pharmacol. 2016;56(11):1355-61.

83. Waldron M, Winter A, Hill BT. Pharmacokinetic and Pharmacodynamic Considerations in the Treatment of Chronic Lymphocytic Leukemia: Ibrutinib, Idelalisib, and Venetoclax. Clin Pharmacokinet. 2017;56(11):1255-66.

84. Liu H, Michmerhuizen MJ, Lao Y, Wan K, Salem AH, Sawicki J, et al. Metabolism and Disposition of a Novel Bcl-2 Inhibitor Venetoclax in Humans and Characterization of its Unusual Metabolites. Drug Metab Dispos. 2016;45(3):294-305.

85. Pollyea DA, Jordan CT. Why are hypomethylating agents or low-dose cytarabine and venetoclax so effective? Curr Opin Hematol. 2019;26(2):71-6.

86. Hernández Borrero LJ, El-Deiry WS. Tumor suppressor p53: Biology, signaling pathways, and therapeutic targeting. Biochim Biophys Acta Rev Cancer. 2021;1876(1):188556.

87. George B, Kantarjian H, Baran N, Krocker JD, Rios A. TP53 in Acute Myeloid Leukemia: Molecular Aspects and Patterns of Mutation. Int J Mol Sci. 2021;22(19).

88. Lee KE. Immunohistochemical Assessment of O(6)-Methylguanine-DNA Methyltransferase (MGMT) and Its Relationship with p53 Expression in Endometrial Cancers. J Cancer Prev. 2013;18(4):351-4.

89. Vicente ATS, Salvador JAR. MDM2-Based Proteolysis-Targeting Chimeras (PROTACs): An Innovative Drug Strategy for Cancer Treatment. Int J Mol Sci. 2022;23(19):11068.

90. Chen J. The Cell-Cycle Arrest and Apoptotic Functions of p53 in Tumor Initiation and Progression. Cold Spring Harb Perspect Med. 2016;6(3):a026104.

91. Moll UM, Petrenko O. The MDM2-p53 interaction. Mol Cancer Res. 2003;1(14):1001-8.

92. Dutto I, Tillhon M, Cazzalini O, Stivala LA, Prosperi E. Biology of the cell cycle inhibitor p21CDKN1A: molecular mechanisms and relevance in chemical toxicology. Archives of Toxicology. 2015;89(2):155-78.

93. Hou H, Sun D, Zhang X. The role of MDM2 amplification and overexpression in therapeutic resistance of malignant tumors. Cancer Cell Int. 2019;19:216.

94. Konopleva M, Martinelli G, Daver N, Papayannidis C, Wei A, Higgins B, et al. MDM2 inhibition: an important step forward in cancer therapy. Leukemia. 2020;34(11):2858-74.

95. Brooks CL, Gu W. Dynamics in the p53-Mdm2 ubiquitination pathway. Cell Cycle. 2004;3(7):895-9.

96. Wade M, Li YC, Wahl GM. MDM2, MDMX and p53 in oncogenesis and cancer therapy. Nat Rev Cancer. 2013;13(2):83-96.

97. PubChem. Compound Summary for CID 53358942, Idasanutlin: National Center for Biotechnology Information; [Available from: https://pubchem.ncbi.nlm.nih.gov/compound/Idasanutlin.

98. Reis B, Jukofsky L, Chen G, Martinelli G, Zhong H, So WV, et al. Acute myeloid leukemia patients' clinical response to idasanutlin (RG7388) is associated with pre-treatment MDM2 protein expression in leukemic blasts. Haematologica. 2016;101(5):e185-e8.

99. Haronikova L, Bonczek O, Zatloukalova P, Kokas-Zavadil F, Kucerikova M, Coates PJ, et al. Resistance mechanisms to inhibitors of p53-MDM2 interactions in cancer therapy: can we overcome them? Cell Mol Biol Lett. 2021;26(1):53.

100. Pápai Z, Chen LC, Da Costa D, Blotner S, Vazvaei F, Gleave M, et al. A single-center, open-label study investigating the excretion balance, pharmacokinetics, metabolism, and

absolute bioavailability of a single oral dose of [(14)C]-labeled idasanutlin and an intravenous tracer dose of [(13)C]-labeled idasanutlin in a single cohort of patients with solid tumors. Cancer Chemother Pharmacol. 2019;84(1):93-103.

101. Nakano K, Vousden KH. PUMA, a Novel Proapoptotic Gene, Is Induced by p53. Molecular Cell. 2001;7(3):683-94.

102. Khurana A, Shafer DA. MDM2 antagonists as a novel treatment option for acute myeloid leukemia: perspectives on the therapeutic potential of idasanutlin (RG7388). Onco Targets Ther. 2019;12:2903-10.

103. Italiano A, Miller WH, Jr., Blay JY, Gietema JA, Bang YJ, Mileshkin LR, et al. Phase I study of daily and weekly regimens of the orally administered MDM2 antagonist idasanutlin in patients with advanced tumors. Invest New Drugs. 2021;39(6):1587-97.

104. Lehmann C, Friess T, Birzele F, Kiialainen A, Dangl M. Superior anti-tumor activity of the MDM2 antagonist idasanutlin and the Bcl-2 inhibitor venetoclax in p53 wild-type acute myeloid leukemia models. J Hematol Oncol. 2016;9(1).

105. Quintás-Cardama A, Hu C, Qutub A, Qiu YH, Zhang X, Post SM, et al. P53 pathway dysfunction is highly prevalent in acute myeloid leukemia independent of TP53 mutational status. Leukemia. 2017;31(6):1296-305.

106. Yee K, Martinelli G, Vey N, Dickinson MJ, Seiter K, Assouline S, et al. Phase 1/1b Study of RG7388, a Potent MDM2 Antagonist, in Acute Myelogenous Leukemia (AML) Patients (Pts). Blood. 2014.

107. Konopleva MY, Röllig C, Cavenagh J, Deeren D, Girshova L, Krauter J, et al. Idasanutlin plus cytarabine in relapsed or refractory acute myeloid leukemia: results of the MIRROS trial. Blood Adv. 2022;6(14):4147-56.

CHAPTER 2*

The Effect of BCL-2 Target Inhibitor Venetoclax on Temozolomide Sensitivity

*A version of this chapter has been sent to PLOS ONE for publish as: Basonbul AA, Fong T, and Brandwein JM. Venetoclax Enhances Temozolomide-Mediated Cytotoxicity in Acute Myeloid Leukemia Cells.

2 The Effect of BCL-2 Target Inhibitor Venetoclax on Temozolomide Sensitivity

2.1 Introduction

Acute myeloid leukemia (AML) is an aggressive hematologic malignancy arising from hematopoietic stem cells. It targets the myeloid lineage by accumulating highly proliferative myeloblast cells in the bone marrow (BM) with a lack of differentiation and apoptosis [1].

AML is predominantly a disease of the elderly, with a median age of 68–70 years [2, 3]. Most of these patients are ineligible for intensive chemotherapy due to age, frailty and medical co-morbidities. Most such patients receive palliative low-dose chemotherapy regimens. Although remissions may be achieved, most patients either fail to respond or subsequently relapse, with median overall survival (OS) ranging from 10–14 months [3, 4].

Temolozomide (TMZ) is an imidazotetrazinone prodrug discovered in 1987, which has antitumor activity [5]. It causes the DNA methylation to a number of nucleobases such as the O^6 and N^7 positions of guanine and the N^3 position of adenine [6]. Methylated O^6 guanine is the most cytotoxic event to the DNA during replication. The O^6-methylguanine (O^6-MeG) mispairs with thymine (T) (O^6-MeG:T) resulting in DNA double strand breaks (DSBs) then cell apoptosis [7].

Resistance to TMZ is largely mediated by the presence of the DNA repair protein methyl guanine methyl transferase (MGMT), which efficiently removes the methyl groups added by TMZ from the O^6 guanine, thereby restoring normal DNA. Therefore, the response to TMZ therapy is dependent on the level of MGMT. Most cells of AML patients have high expression of

MGMT, with only 10–25% of samples having low or absent expression [8, 9]. A previous clinical trial found that antileukemic activity in AML was restricted to those with very low MGMT expression [8]. In a follow-up study, treating AML patients pre-selected for low MGMT expression with TMZ, only 28% had complete clearance of blasts in the marrow, with 22% complete responses (CR) and CR with incomplete platelet recovery [10].

Venetoclax (VEN) is a selective inhibitor targeting the anti-apoptotic protein, B-cell lymphoma gene-2 (BCL-2) [11]. It displaces the pro-apoptotic activator BCL-2 interacting mediator of cell death (BIM), which binds to BCL-2 to prevent apoptosis. This inhibition also activates the death mediator proapoptotic effectors BCL-2-associated X protein (BAX) and BCL-2-antagonist/killer (BAK). BAX/BAK forms homo-oligomers and initiates mitochondrial outer membrane permeabilization (MOMP), forming proteinaceous pores that release cytochrome *c* to the cytosol. Cytochrome *c* then activates the caspase cascade, causing apoptosis [12, 13].

The BCL-2 protein is overexpressed in the vast majority of AML patients (84% at diagnosis and 95% at relapse) [14]. Recently, the combination of VEN with the hypomethylating agent azacitidine was found to produce an improved complete remission rate and OS compared with azacitidine alone [3], and has now been widely adopted as standard frontline therapy in these patients. VEN has also been combined with low-dose cytarabine, resulting in a superior CR rate compared with cytarabine alone [4].

Given the encouraging activity of VEN-based combination regimens, we investigated the potential of VEN to enhance TMZ sensitivity in AML cells with both high and low MGMT expression.

2.2 Materials and Methods

2.2.1 Cell Lines

Human leukemia cell lines; KG1, MV4-11, MOLM13, U937 and HEL were purchased from the American Type Tissue Collection (ATCC). These cells were stored at liquid nitrogen in 10% dimethyl sulfoxide (DMSO) and 90% fetal bovine serum (FBS). When needed the cells were thawed at 37 ºC water bath then washed with Roswell Park Memorial Institute (RPMI) 1640 (Gibco Life Technology), which reconstitutes with 10% FBS and 1% penicillin–streptomycin. These cells were cultured in RPMI 1640 and their growth maintained at 37 ºC with a 5% CO_2 incubator.

2.2.2 AML Patient Samples

Prior ethics approval was obtained from the University of Alberta Health Research Ethics Board (HREB). After obtaining consent, peripheral blood (PB) or BM samples were obtained from newly diagnosed AML patients who were being managed at the University of Alberta Hospital. Samples were drawn in sodium heparin anti-coagulant tubes. The blast-containing mononuclear cells (MNC) were isolated using the Ficoll–Paque (GE Healthcare) method.

Ficoll–Paque media was used to isolate the patient's MNC, which includes monocytes, lymphocytes and granulocytes nucleated cells, from fresh PB or BM samples. This media separates the blood components based on the density gradient. The patient sample was diluted (1:1) with 2% FBS using Dulbecco's phosphate buffered saline (DPBS). Depending on the total volume obtained after dilution, a specific amount (manufacture recommended) of Ficoll reagent was added to the centrifuge tube. The diluted blood sample was carefully layered onto the Ficoll-Paque media solution. The sample was centrifuged at 400x*g* for 40 min. The upper layer

containing plasma and platelets was removed, leaving the MNC layer undisturbed at the interface. The MNC layer was removed and transferred it to a sterile tube to be washed with PBS 350x*g* g for 10 min. Samples were then stored in 10% DMSO and 90% FBS in liquid nitrogen at the Canadian Biosample Repository at the University of Alberta until needed. Sorting for blast cells was not performed; however, only samples with a minimum 70 % blast cells were chosen for analysis. Thawed cells were washed with RPMI 1640 and 2 % DNase I solution (Stem Cell Technologies) to reduce cell clumping after thawing high-concentrated cryopreserved cells prior to performing the desired experiment.

2.2.3 Treatments

The TMZ was purchased from Enzo Life Sciences and VEN (ABT-199) from Selleckchem. Both drugs were dissolved in DMSO then stored at the recommended temperature. A serial dilution of each treatment was prepared freshly in sterile phosphate buffered saline (PBS) to minimize the cytotoxicity effect that could result from the DMSO.

2.2.4 Protein Expression

A total of 10×10^6 cells were collected for protein extraction to be used for Western blot. Radioimmunoprecipitation (RIPA) lysis buffer, in presence of Halt phosphatase and protease inhibitors (Thermo Scientific), was used to quantify the extracted protein using bicinchoninic acid (BCA) assay (Thermo Scientific). The protocol was followed as per manufacturer recommendation. A total of 50 µg of protein was separated on an acrylamide sodium dodecyl sulphate (SDS) gel, 12% for MGMT and BCL-2 detection and 8% for poly (ADP-ribose) polymerases 1 (PARP 1) detection. Nitrocellulose blotting membrane was used for wet-transfer and blocked with Tris-buffer saline in 5% skimmed milk and 0.1% Tween for one hour.

The blot was incubated with MGMT (# 2739), BCL-2 (#15071) and PARP 1 (# 9532) antibodies (Cell Signaling Technology) (1:1,000) overnight at 4˚C. Horse radish peroxidase conjugated secondary antibodies (1:5,000) were chosen based on the primary antibody species. Housekeeping gene β-tubulin (# 2128) or β-actin (# 5125) (Cell Signaling Technology) were used as the loading control.

ImageQuant LAS 500 (GE Healthcare) was used to develop the membrane. The protein of interest and housekeeping gene were quantified using ImageJ. The protein ratio was normalized to the housekeeping gene; a ratio of protein: housekeeping gene < 0.2 was considered negative, between 0.2-0.4 weakly positive and > 0.4 strongly positive [8]. The expression ratio was the average of the protein's expression in multiple blots at various times after normalizing to the housekeeping gene.

2.2.5 Cell Viability

Cells were treated with escalating doses of TMZ; 5, 10, 15, 20, 50 and 100 μM. For VEN, concentrations 2.5, 5, 10, 1000 and 2500 nM were used. The treated cells were incubated at 37°C and 5% CO_2 with a single drug for 72 hours for drug sensitivity screening and determining the 50% inhibitory concentrations (IC50). The incubation time was reduced to 48 hours in the combination experiment to avoid cell death from prolong incubation.

For cell lines, 0.2×10^6 cells were plated in RPMI 1640 then treated and incubated in the above-mentioned condition. The PrestoBlue assay (ThermoFisher Scientific) was used to assess the cell viability. The PrestoBlue is a cell preamble resazurin non-fluorescent solution that can be reduced by dehydrogenase enzyme in metabolic active cells to resorufin fluorescent red color.

The resorufin produce is directly proportional to the number of live cells, which was quantified by Cytation5 (BioTek) at 560 nm Excitation (Ex)/ 590 nm Emission (Em).

For AML patient samples, 2×10^6 cells were plated in serum-free expansion medium (SFEM), containing $CD34^+$ expansion supplement, StemRegenin1 (SR1) and UM729 (pyrimido-[4,5-b]-indole derivative) supplements (Stem Cell Technologies). The cells were treated and incubated at the above-mentioned conditions. CellTiter-Fluor assay (Promega) was used to determine the patients' cell viability. It is depending on the live cell's protease activity. This assay was chosen to increase the sensitivity in low metabolic patient's cell compared to cell lines. The principle is the cell-permeable fluorogenic substrate glycyl-phenylalanyl-aminofluorocoumarin (GF-AFC) is cleaved by cytoplasmic aminopeptidase activity to remove GF amino acids and release AFC. The amount of AFC is directly proportional to the number of live cells. The AFC produced was quantified by Cytation5 (BioTek) at 400 nm Ex /505 nm Em.

Both experimental protocols were followed as per manufacturer's recommendation. All samples were read in a black well plate with a clear bottom to reduce the background noise and improve specificity. The results were normalised to untreated cells to calculate the viability percentage. Low viability percentage indicates the drug efficacy to inhibit the cell proliferation and promote cell death.

2.2.6 Cell Apoptosis

Apoptosis was evaluated using flow cytometry (Beckman Coulter) after treating 2×10^6 cells for 48 hours with TMZ alone or in combination with the IC50 VEN concentrations. The 48 hours' time point was chosen to mimic the cell viability experiment in Section 2.2.5. The treated cells were harvested and washed with 1× binding buffer, then labelled with Annexin V/propidium

iodide (PI) (BD Biosciences) for 30 minutes. When cell loss plasma membrane asymmetry the phosphatidyl serine (PS) is translocated from inner to outer leaflet. Annexin V is fluorochrome-labeled and can bind to PS detecting early apoptosis. As a result of PS translocation, the cell loses the membrane integrity causing late apoptosis or necrosis, which can detect by PI. Therefore, positive Annexin V staining indicates early apoptosis and positive Annexin V and PI indicates late apoptosis. Live cell has intact membrane that shows negative Annexin V and PI. The results were normalised to live cells in untreated sample to calculate the percentage of apoptosis. High early and late apoptotic percentage indicates drug efficacy for causing cell death.

2.2.7 DNA Damage

A total of 0.1×10^6 cells for leukemia cell lines and between $0.1 – 0.3 \times 10^6$ of fresh isolated patient cells were treated with selected doses of TMZ and VEN separately and combined. The cell lines were incubated in RPMI 1640 and patient cells in SFEM for six hours. The Alkaline Comet Assay was used to assess the DNA damage that may occur after treatment. The damaged DNA migrates out of the nucleoid under the influence of an electric current, whereas intact DNA does not. Trevigen kit (Catalog # 4250-050-K**)** was used with minor modifications. After six hours incubation, the cells were washed and suspended in PBS. A 1:10 ratio of treated cell suspension and 1% low-melting agarose was applied on comet microscopic slide. The coated slides were incubated in the dark for 10 min at room temperature then 30 min at 4 °C to solidify the gel. Slides were immersed in lysis solution, cooling for 20 min, and then incubated at 4 °C overnight. The next day, the slides were incubated for one hour in freshly prepared alkaline unwinding solution (pH > 13) at 4 °C.

Slides were subjected to electrophoresis at 25 V using fresh alkaline solution (pH > 13) for 90 min; the slides were washed with dH_2O, then incubated for 5 min in 70% ethanol. Dried slides

were stained with 1x Syber DNA gel stain for 30 min. A fluorescence microscope (Invitrogen EVOS M5000 Imaging System) was used to detect 100 cells per sample. For analysis, CometScore software was used to quantify the comet tail DNA percentage, which is 100 × tail DNA intensity/ cell DNA intensity [15]. A long comet tail seen microscopically indicates DNA damage and will represent a high tail DNA percentage.

2.2.8 Animal Model

Eight to ten-week-old nonobese diabetic/severe combined immune deficiency IL2 receptor common gamma chain (NOD/scid IL2Rg^{null}) mice were used. Each mouse was infused with 10 × 10^6 MOLM13 cells (200 µl) via lateral tail vein injection. TMZ and VEN were evaluated in separate cohorts to determine the ideal dosage for the combination experiment.

TMZ (Enzo Life Sciences) was dissolved in warm DMSO. To prevent DMSO toxicity the stock was diluted with warm PBS to reach 5% DMSO to the desired concentrations. In order to determine the optimal dose for the combination experiments, on day eight following cell infusion TMZ was administered intraperitoneally once daily for five consecutive days at three dose levels in different 5-mouse cohorts: 25, 50 and 100 mg/kg.

VEN (AdooQ BioScience) was dissolved in warm DMSO. To prevent DMSO toxicity the stock was diluted with vehicle 0.5% Sodium carboxymethyl cellulose (CMC-Na) to reach 5% DMSO to the desired concentrations; 50 and 100 mg/kg. On day eight, the dosages were administered orally once daily for five consecutive days in different 5-mouse cohorts.

The optimal TMZ and VEN concentrations were selected from the previous experiments and then used for the combination cohort. On day eight after cell infusion the mice were administered either TMZ and VEN separately or simultaneously depending on the treatment cohort, each

given daily for five days. Each drug was prepared and administrated similarly as previously mentioned. The control groups consisted of mice that received either no cells and drug, or MOLM13 cells but no drug.

The mice were monitored daily for signs of distress. Mice were euthanized at week 18, or sooner if they met prespecified criteria for signs of distress, or if they lost 15 % of their body weight. Flushed BM from the femur of all mice was analyzed for $CD33^+$ and $CD45^+$ expression using flow cytometry. Two mice from each cohort had post-mortem examinations to evaluate for evidence of toxicity and for morphologic evidence of engraftment in spleen and BM. The median OS of each cohort was evaluated.

2.2.9 Statistical Tests

Graphs were represented as means $\pm$ standard deviation. Paired *t*- test and Mann-Whitney were used to calculate the P value for AML cell lines and patient samples, respectively. The test compared the mean of TMZ or VEN alone verses the combination at each TMZ concentration. P values ≤ 0.05 were considered statistically significant; these were annotated in the figures as: * $P \leq 0.05$, ** $P < 0.005$, *** $P < 0.001$ and $P < 0.0001$ and ns as not significant.

2.3 Results

2.3.1 AML Cell Lines

2.3.1.1 Protein Expression

The MGMT protein was highly expressed in KG1 and very low to absent in all other cell lines. BCL-2 was strongly expressed in KG1, MV4-11, and MOLM13 cell lines and absent in U937 and HEL (Figs. 2.1 A-D).

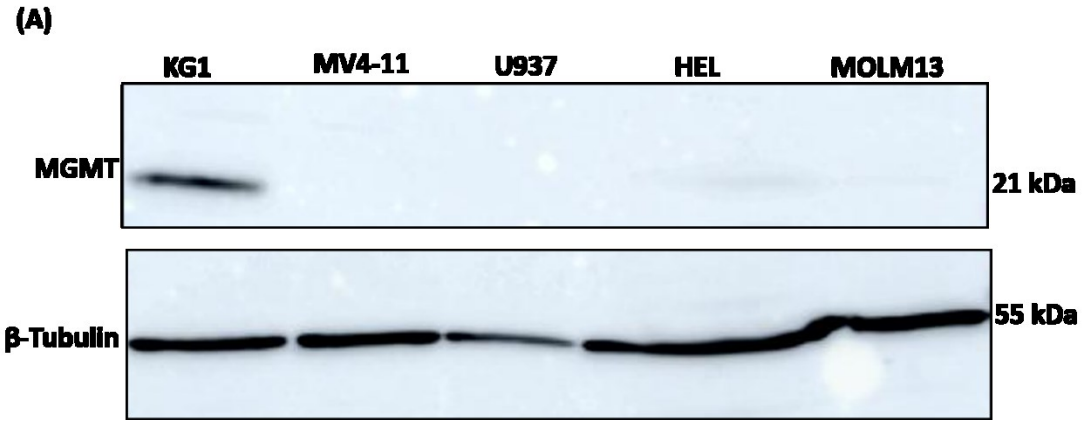
(A)
KG1
MV4-11
U937
HEL
MOLM13
MGMT
21 kDa
β-Tubulin
55 kDa

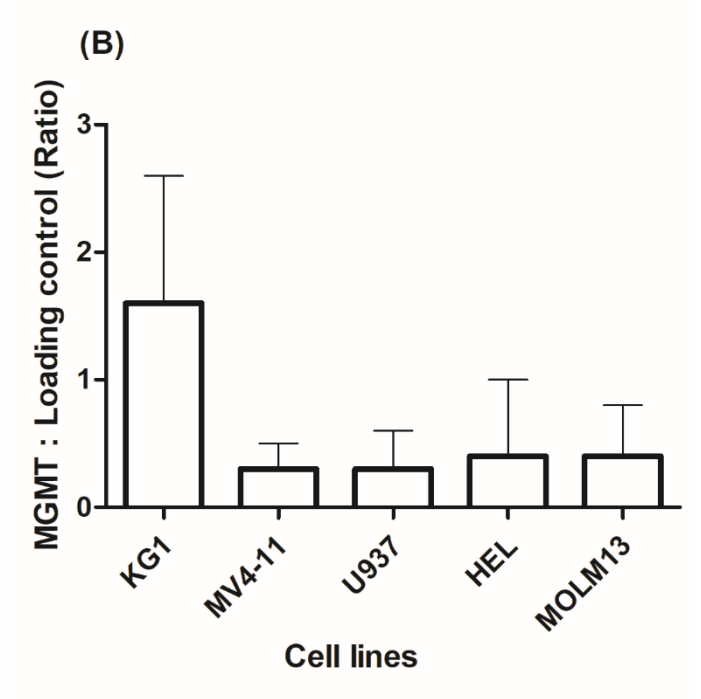
(B)
MGMT : Loading control (Ratio)
3
2
1
0
KG1
MV4-11
U937
HEL
MOLM13
Cell lines

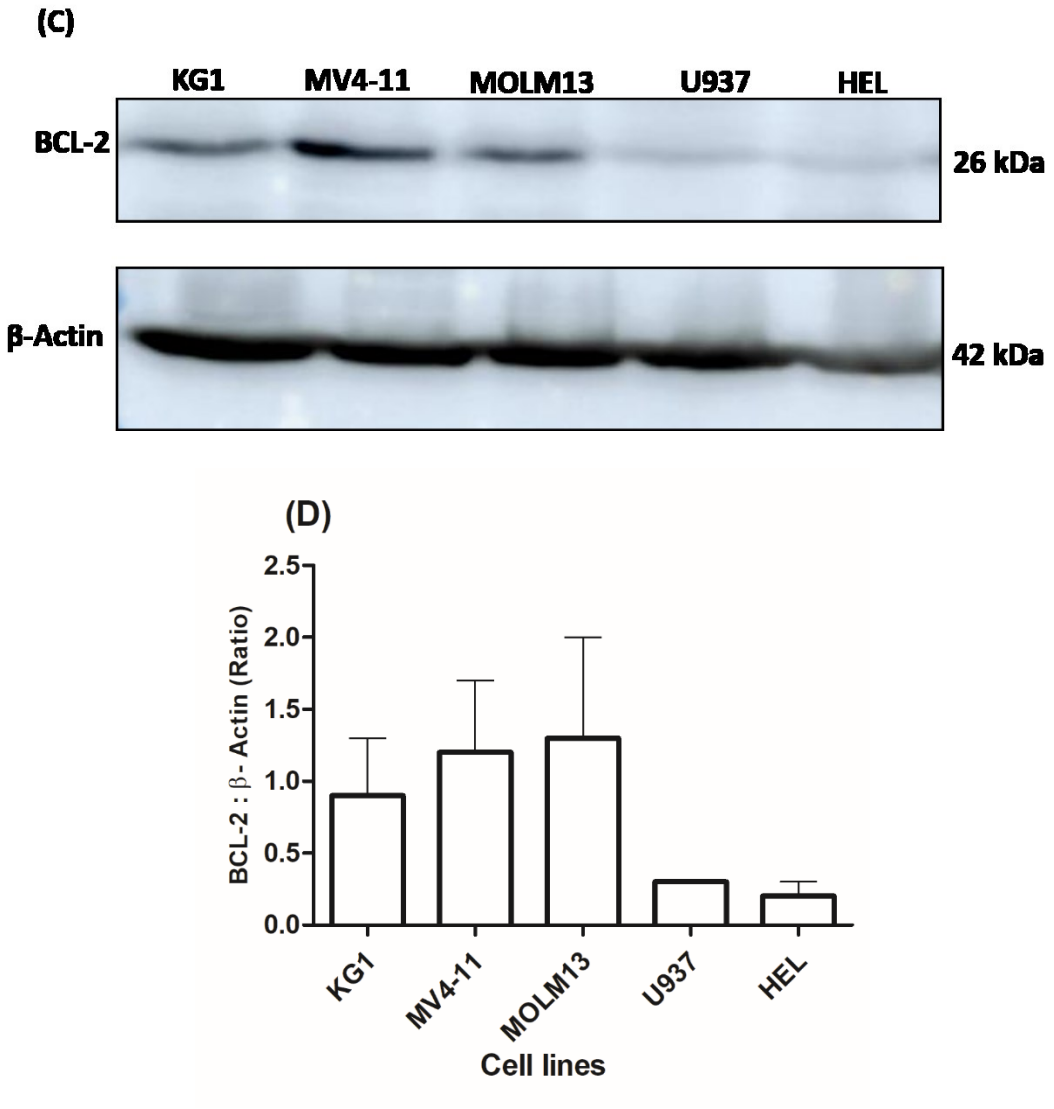

Figure 2.1: Immunoblotting of MGMT and BCL-2 in AML cell lines. (A, B) MGMT (21 kDa), **(C, D)** BCL-2 (26 kDa). A β-Tubulin (55 kDa) and β-Actin (42 kDa) were used as loading controls. The indicated protein expression was determined using whole-cell lysate that was subjected to Western blot and probed with specific antibodies. MGMT: KG1 (n= 18), MV4-11 (n= 16), U937 (n= 4), HEL (n= 5) and MOLM13 (n= 16); BCL-2: KG1 (n= 10), MV4-11 (n= 9), MOLM13 (n= 9), U937 (n= 2) and HEL (n= 2).

2.3.1.2 Cell Viability

Correlating with high MGMT expression (Fig. 1 A), KG1 demonstrated a strong resistance to TMZ (Fig. 2.2 A) after being treated for 72 hours. The MGMT-deficient cell lines MV4-11 and U937 displayed sensitivity to TMZ with > 50% reduction in viability at concentrations of ≥ 5 μM with MV4-11 and ≥ 15 μM with U937. MOLM13 demonstrated reduced sensitivity, with 50% of cell death achieved only at the highest concentration of 30 μM. Despite low MGMT expression, HEL showed resistance to TMZ.

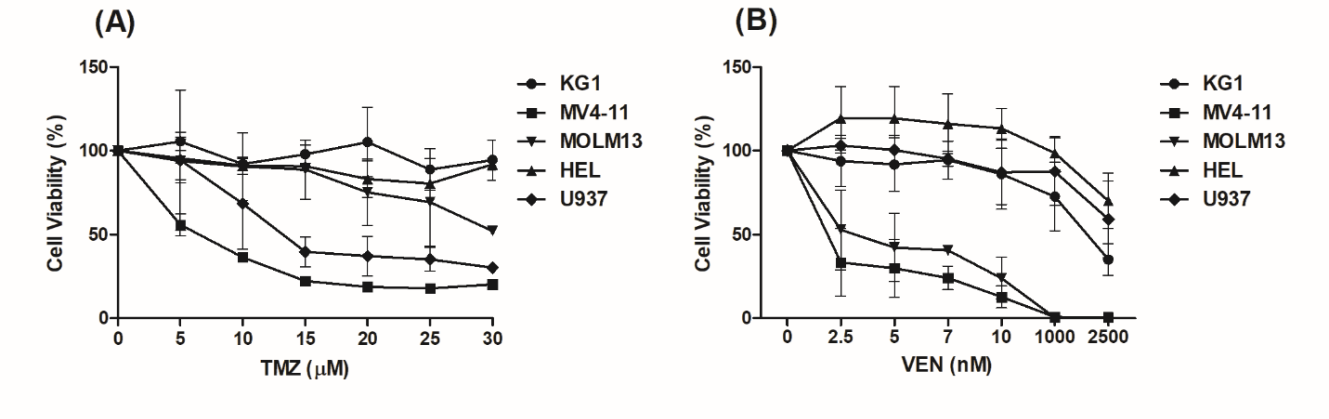

Figure 2.2: Cell line viability after being treated for 72 hours with TMZ and VEN separately. (A) TMZ, and **(B)** VEN. (●) KG1, (■) MV4-11, (▼) MOLM13, (▲) HEL, and (♦) U937. Graphs represent as mean ± standard deviation. TMZ: KG1 (n= 3), MV4-11 (n= 3), MOLM13 (n= 2), HEL (n= 3) and U937 (n= 3); VEN: KG1 (n= 6), MV4-11 (n= 6), MOLM13 (n= 6), HEL (n= 4) and U937 (n= 4).

MV4-11 and MOLM13 were highly sensitive to VEN, correlating with their high BCL-2 expression. A VEN concentration of 2.5 nM resulted in only 33% and 53% residual viability, respectively, with complete inhibition at 1000 nM at 72 hours. In KG1, 50% cell viability was only achieved at ≥ 1000 nM concentrations. The absence of BCL-2 expression in U937 and HEL

corresponded with persistent cell viability after 72 hours of VEN treatment (Fig. 2.2 B). The IC50, 2.5 nM for MV4-11 and MOLM13 and 1000 nM for KG1, were therefore selected for further experiments using VEN.

The KG1, MV4-11 and MOLM13 cells were chosen for TMZ and VEN combination experiments, based on their variable MGMT expression and the high expression of BCL-2 protein. The selected cells were treated with TMZ at escalating doses as a single agent and in combination with the IC50 concentrations of VEN: 1000 nM in KG1 and 2.5 nM in MV4-11 and MOLM13. All the cell lines exposed to the drug combination demonstrated significantly reduced viability compared to TMZ treatment alone (Figs. 2.3 A-C). This included both the low and high-MGMT expressing cells. In KG1 cells there was a trend toward a reduced viability with the combination of VEN and TMZ compared with VEN alone, but this difference did not reach statistical significance (Fig. 2.3 A). In MV4-11 and MOLM13 there was an additive effect seen with the combination as compared with either drug alone, particularly at lower TMZ concentrations (Figs. 2.3 B and C).

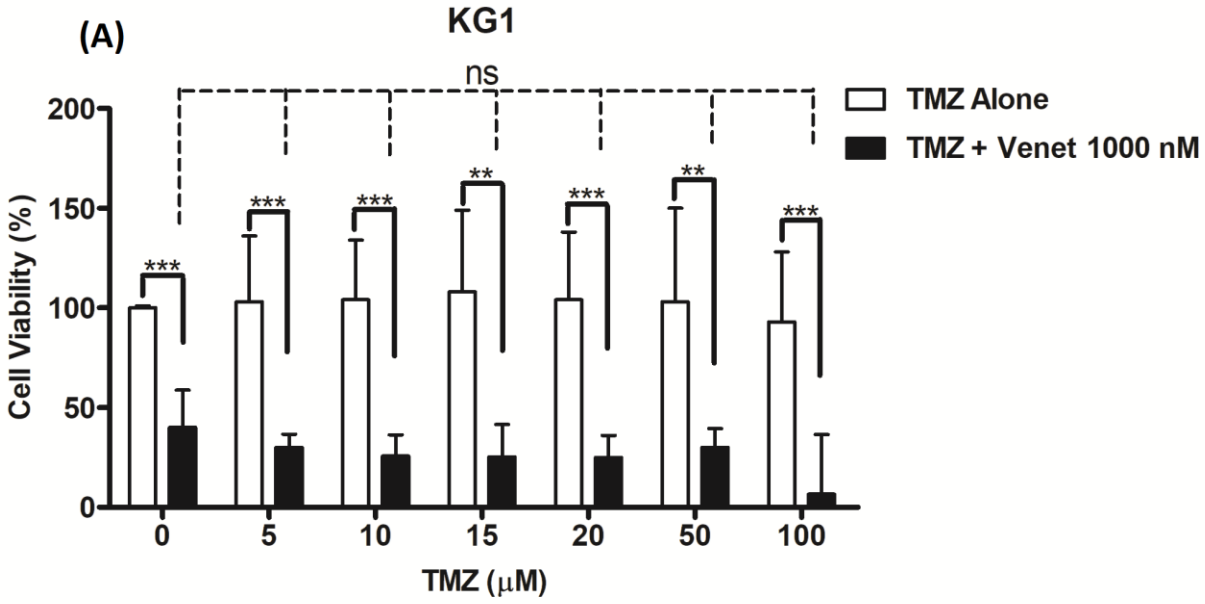

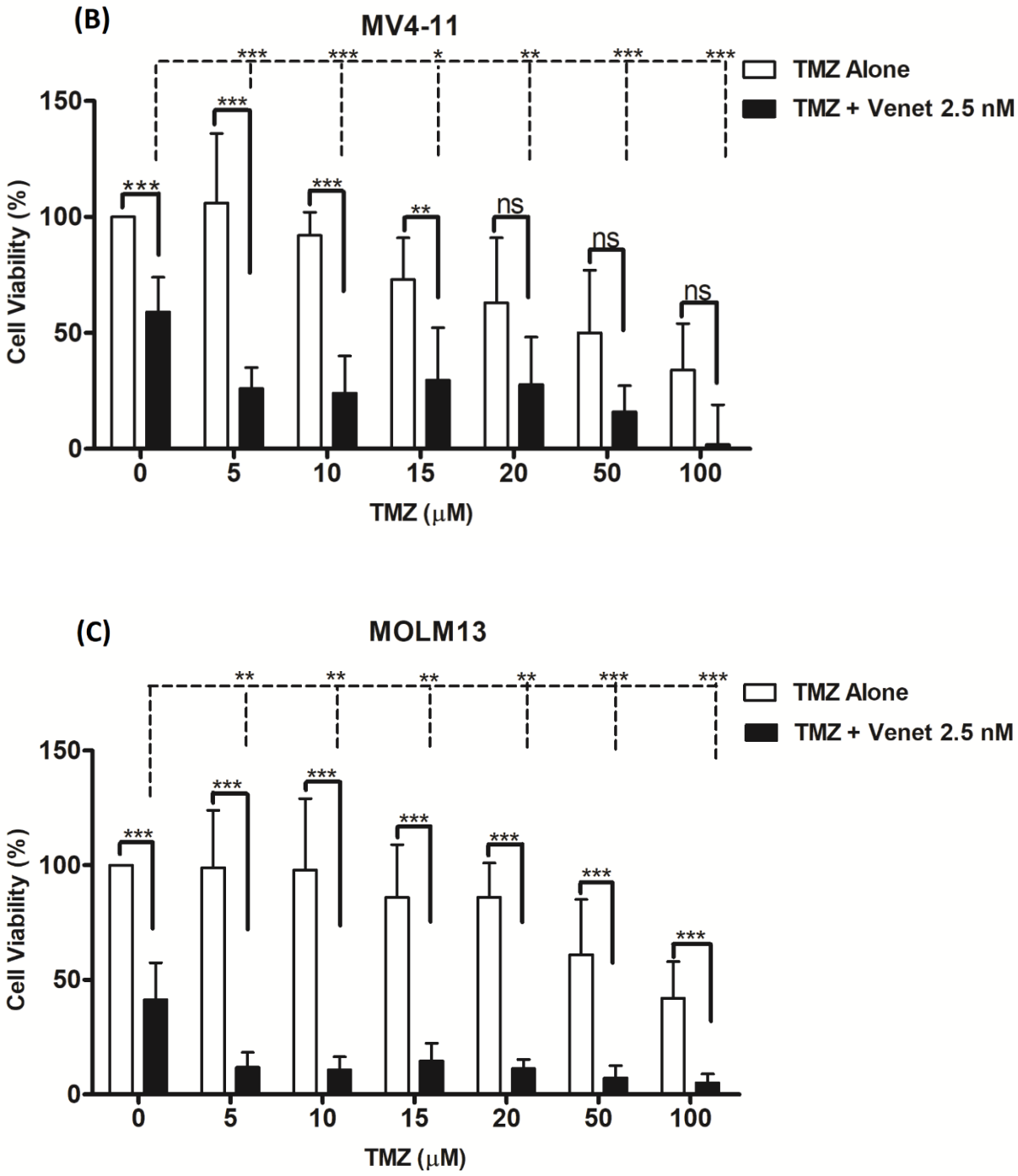

Figure 2.3: Cell lines viability after treated for 48 hours with TMZ alone (□) and combination with IC50 concentrations of VEN. (■) 1000 nM **(A)** KG1 (n= 10), 2.5 nM **(B)** MV4-11 (n= 7), and **(C)** MOLM13 (n= 6). Graphs represent as mean ± standard deviation. The

paired *t*-test was used to compare the mean of TMZ and VEN alone versus the combination. The annotated: * P < 0.05, ** P < 0.005, *** P < 0.001, and < 0.0001 and ns as not significant.

2.3.1.3 Cell Apoptosis

There was a significant additive effect (P ≤ 0.05) seen in early apoptosis between TMZ alone and the TMZ+VEN combination in KG1 at 5, 10, and 15 μM concentrations. No difference was observed between VEN and TMZ alone or in combination. In MV4-11 and MOLM13, no additive effect was observed, as both cell lines were highly susceptible to VEN alone. Late apoptosis in combination MV4-11 and MOLM13 treated cells at 10 and 15 μM, respectively, was significantly increased compared to TMZ alone (Figs. 2.4 A-C).

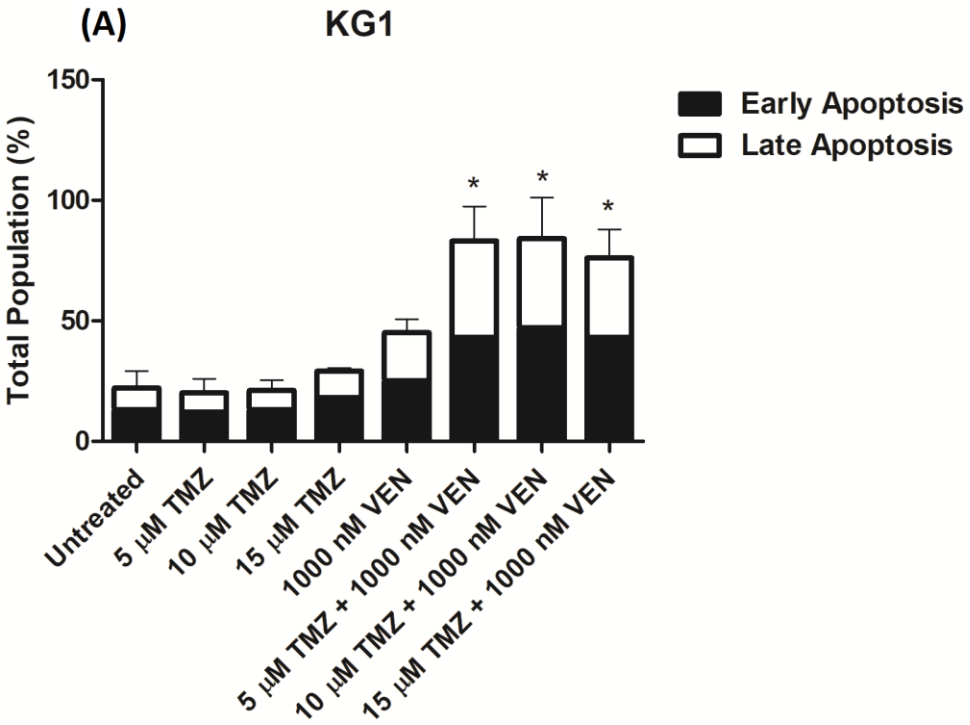

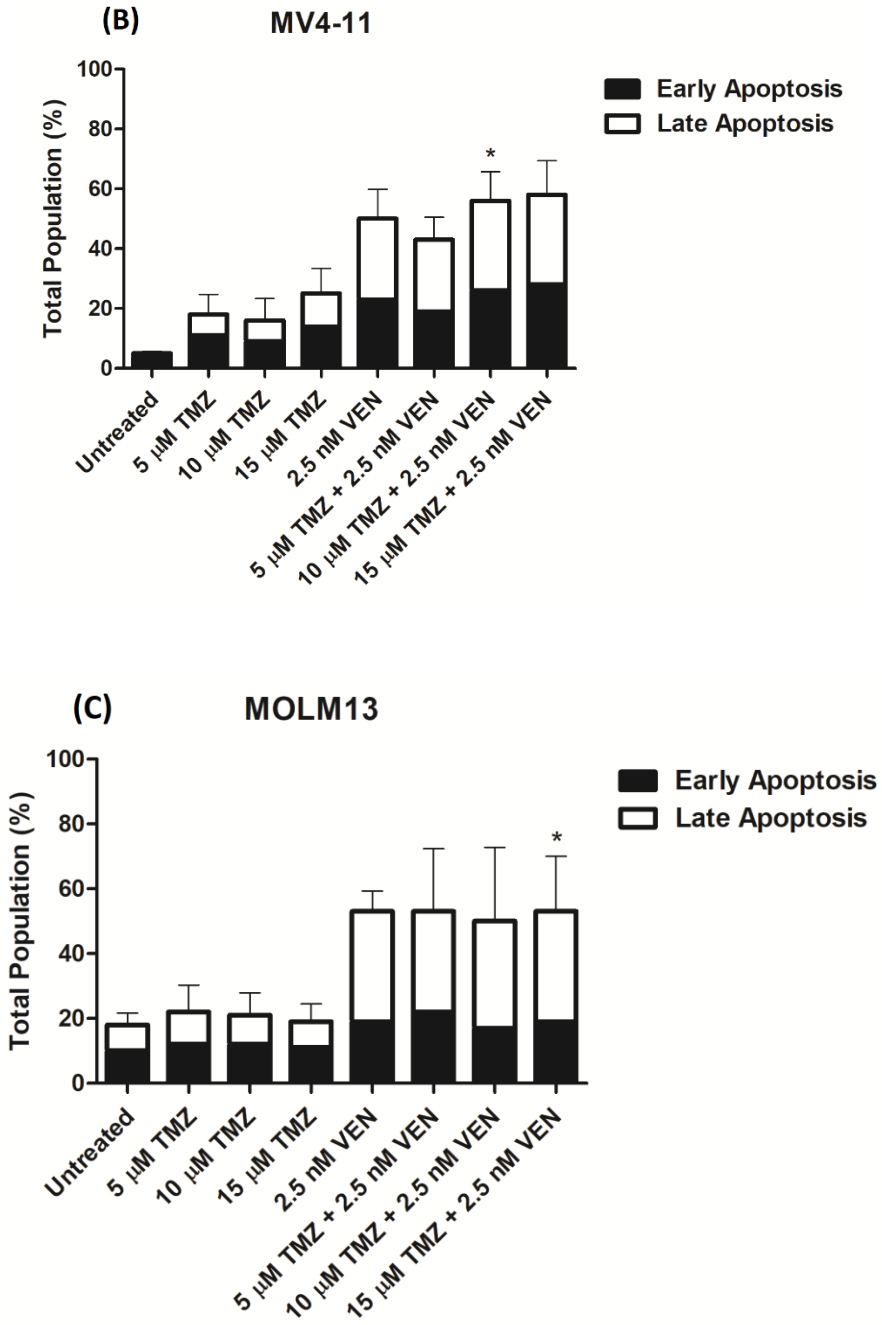

Figure 2.4: 48 Hours of early (■) and late (□) cells apoptosis of TMZ alone and combination with VEN IC50 concentrations treated cells. 1000 nM **(A)** KG1 (n= 3), 2.5 nM **(B)** MV4-11 (n= 5), and **(C)** MOLM13 (n= 6). Graphs represent as mean ± standard deviation. Paired *t*-test, was used to compare TMZ alone to the combination at the same concentration. The annotated: * $P < 0.05$.

Cleaved-poly (ADP-ribose) polymerases 1 (C-PARP 1) expression was evaluated using Western blot at three hours' time point and selected drugs concentrations. KG1 cells were treated with 250 and 500 nM VEN separately and combined with 10 μM TMZ. PARP 1 was intact in TMZ alone treated cells as well as untreated ($P = 0.699$). On the other hand, PARP 1 was strongly cleaved to 89 kDa fragment with VEN alone at both concentrations and when combined with TMZ (Figs. 2.5 A and B). A statistically significant difference was observed between TMZ combined with VEN at 250 nM ($P = 0.003$) and 500 nM ($P = 0.000$) and TMZ alone. However, C-PARP 1 expression was not significantly different ($P > 0.05$) between VEN concentrations alone and the TMZ-VEN combination. For MV4-11 and MOLM13, cells were treated for three hours with 10 μM TMZ and 2.5 nM VEN separately and combined. PARP 1 was intact and no significant increase in C-PARP 1 was found in any of the treated cells (Figs. 2.5 C- F).

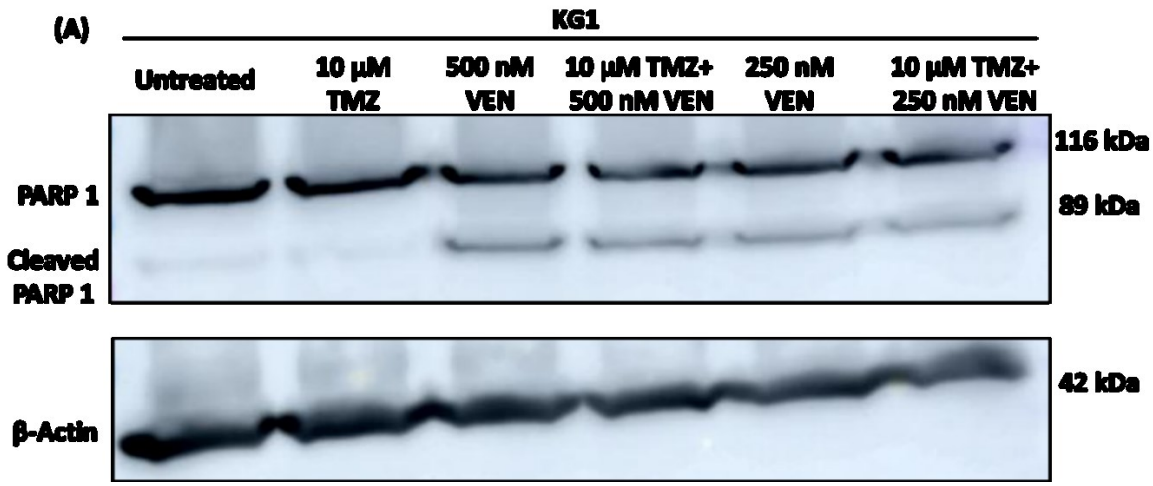
(A)
KG1
Untreated
10 µM TMZ
500 nM VEN
10 µM TMZ+ 500 nM VEN
250 nM VEN
10 µM TMZ+ 250 nM VEN
PARP 1
Cleaved PARP 1
116 kDa
89 kDa
β-Actin
42 kDa

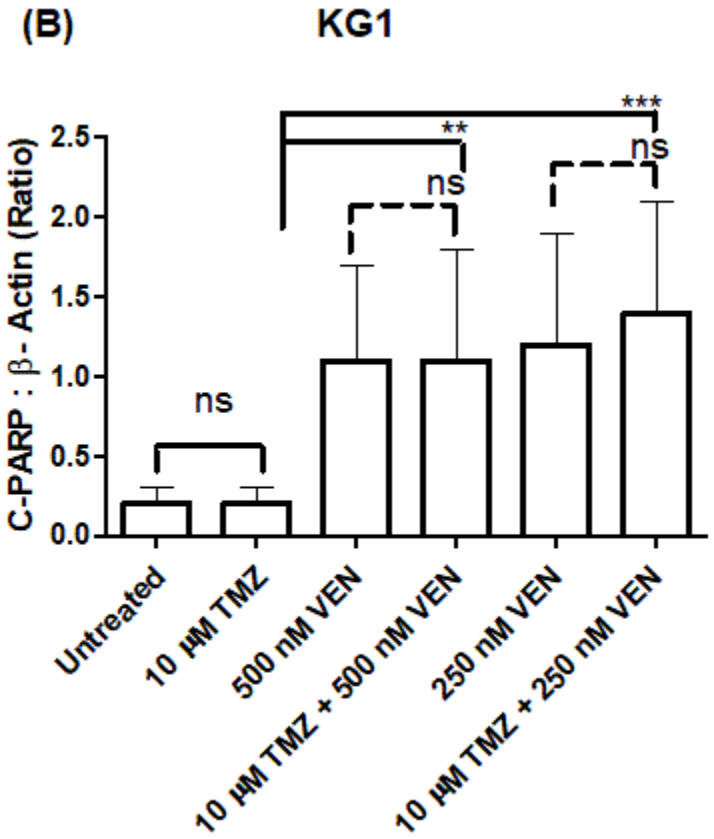
(B)
KG1
C-PARP : β- Actin (Ratio)
2.5
2.0
1.5
1.0
0.5
0.0
ns
**
***
ns
ns
Untreated
10 µM TMZ
500 nM VEN
10 µM TMZ + 500 nM VEN
250 nM VEN
10 µM TMZ + 250 nM VEN

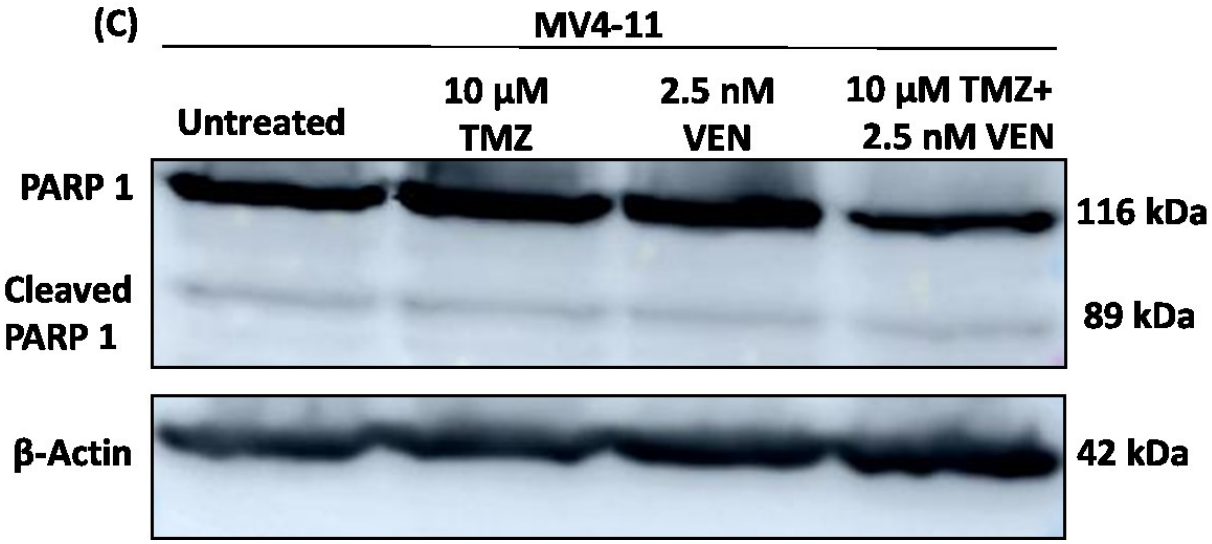
(C)
MV4-11
Untreated
10 µM TMZ
2.5 nM VEN
10 µM TMZ+ 2.5 nM VEN
PARP 1
Cleaved PARP 1
β-Actin
116 kDa
89 kDa
42 kDa

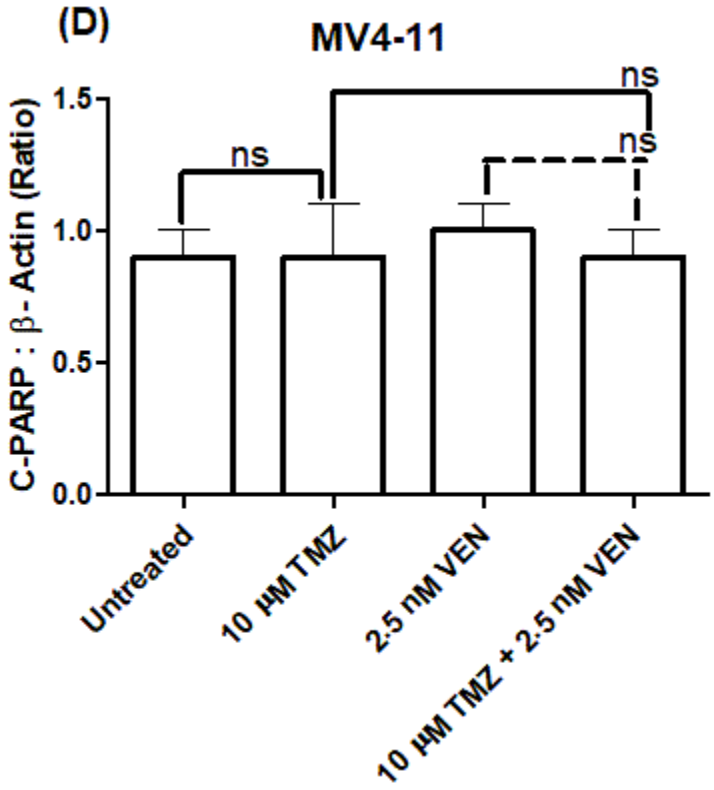
(D)
MV4-11
C-PARP : β- Actin (Ratio)
1.5
1.0
0.5
0.0
ns
ns
ns
Untreated
10 µM TMZ
2.5 nM VEN
10 µM TMZ + 2.5 nM VEN

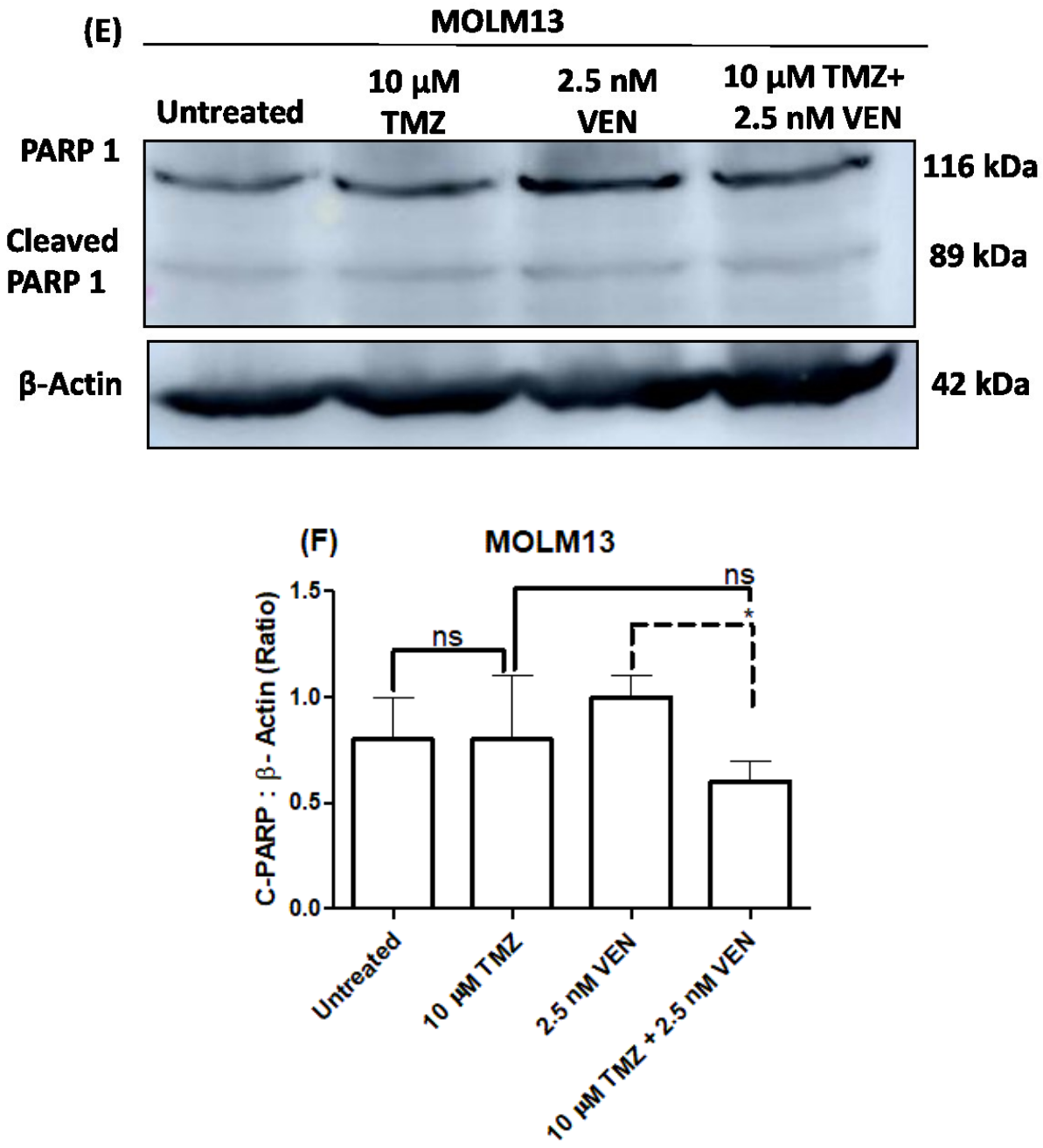

Figure 2.5: Immunoblotting of AML cell lines of total (116 kDa) **and C-PARP 1** (89 kDa) **treated with TMZ alone and combination with VEN. (A, B)** KG1 (n= 4), **(C, D)** MV4-11 (n= 2), and **(E, F)** MOLM13 (n= 2). A β-actin (42 kDa) was used as loading control. Cells were treated with selected doses of TMZ and VEN combined and separately for 3 hours before protein was extracted using the RIPA method to perform a Western blot. Paired *t*-test was used to

compare the protein expression ratio between TMZ and VEN alone versus the combination. The annotated: ** $P < 0.005$, *** $P < 0.001$ and ns as not significant.

2.3.1.4 DNA Damage

In KG1, there was no difference seen in the DNA tail percentage between untreated cells and either TMZ or VEN alone ($P > 0.05$). A significantly ($P = 0.001$) greater degree of DNA damage occurred with the combination when compared with each drug alone (Figs. 2.6 A and B). In MV4-11, the TMZ+VEN combination also induced increased DNA damage, but this difference was only significant when compared with untreated and VEN treated cells (Figs. 2.6 C and D). The MOLM13 cells treated with the TMZ+VEN combination demonstrated significantly increased DNA damage compared to untreated cells and to each drug alone ($P < 0.005$) (Figs. 2.6 E and F).

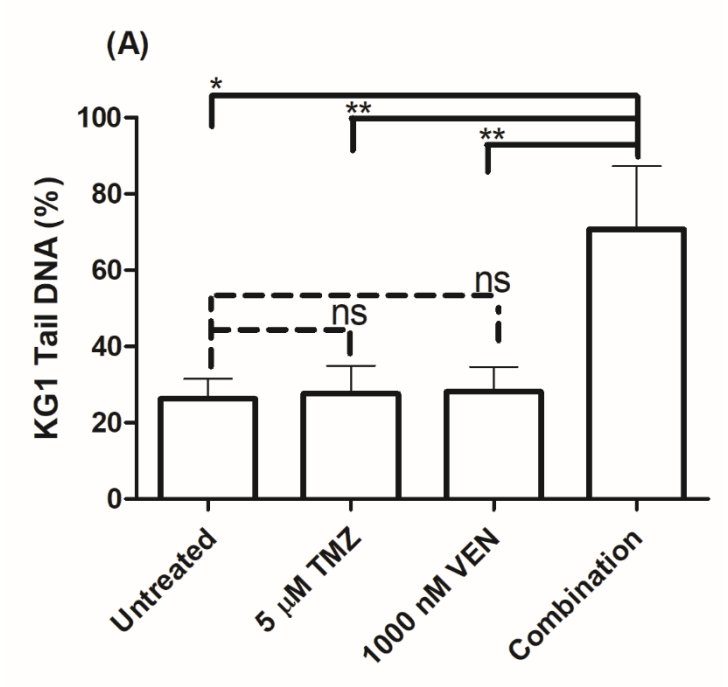
(A)
KG1 Tail DNA (%)
100
80
60
40
20
0
*
**
**
ns
ns
Untreated
5 μM TMZ
1000 nM VEN
Combination

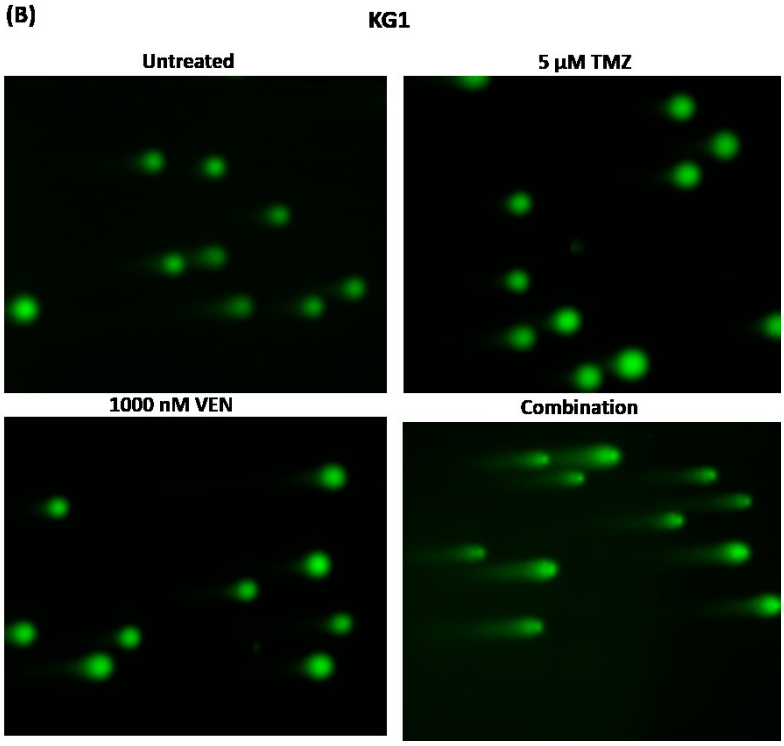
(B)
KG1
Untreated
5 μM TMZ
1000 nM VEN
Combination

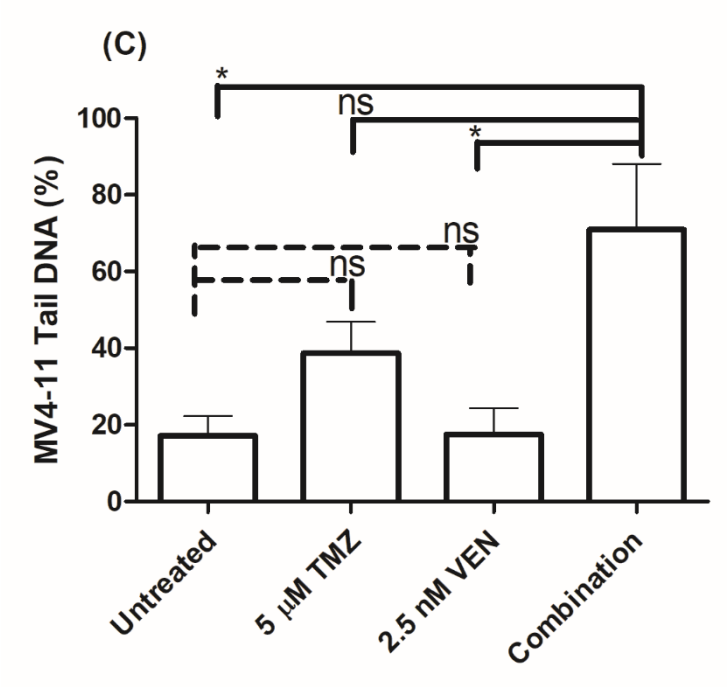
(C)
MV4-11 Tail DNA (%)
100
80
60
40
20
0
*
ns
*
ns
ns
Untreated
5 μM TMZ
2.5 nM VEN
Combination

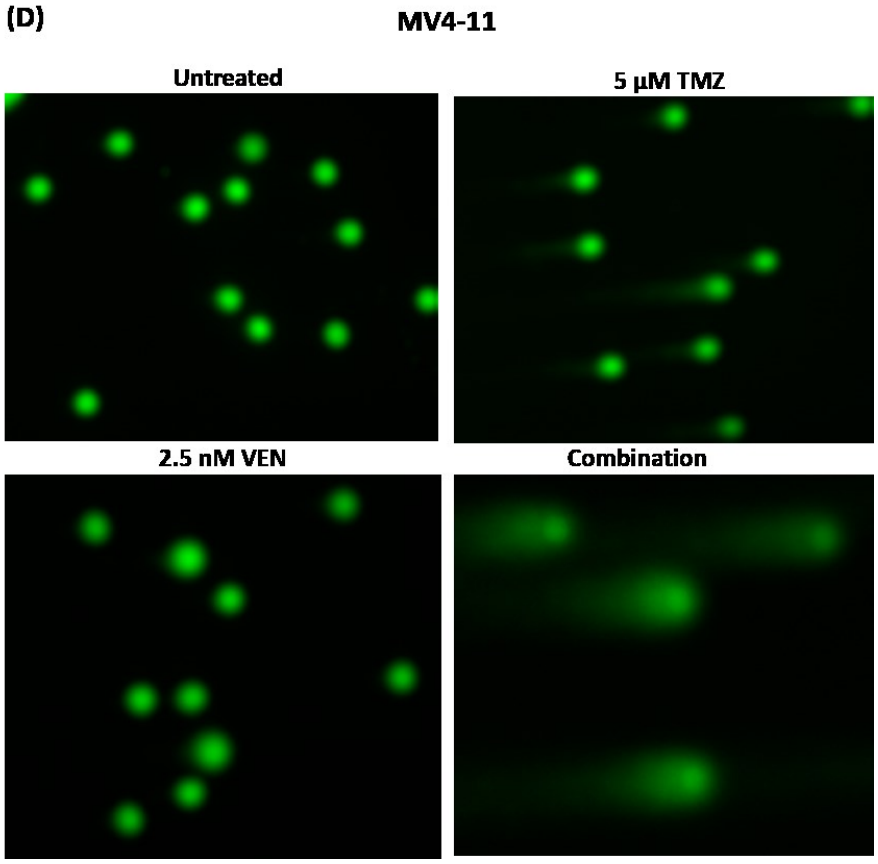
(D)
MV4-11
Untreated
5 μM TMZ
2.5 nM VEN
Combination

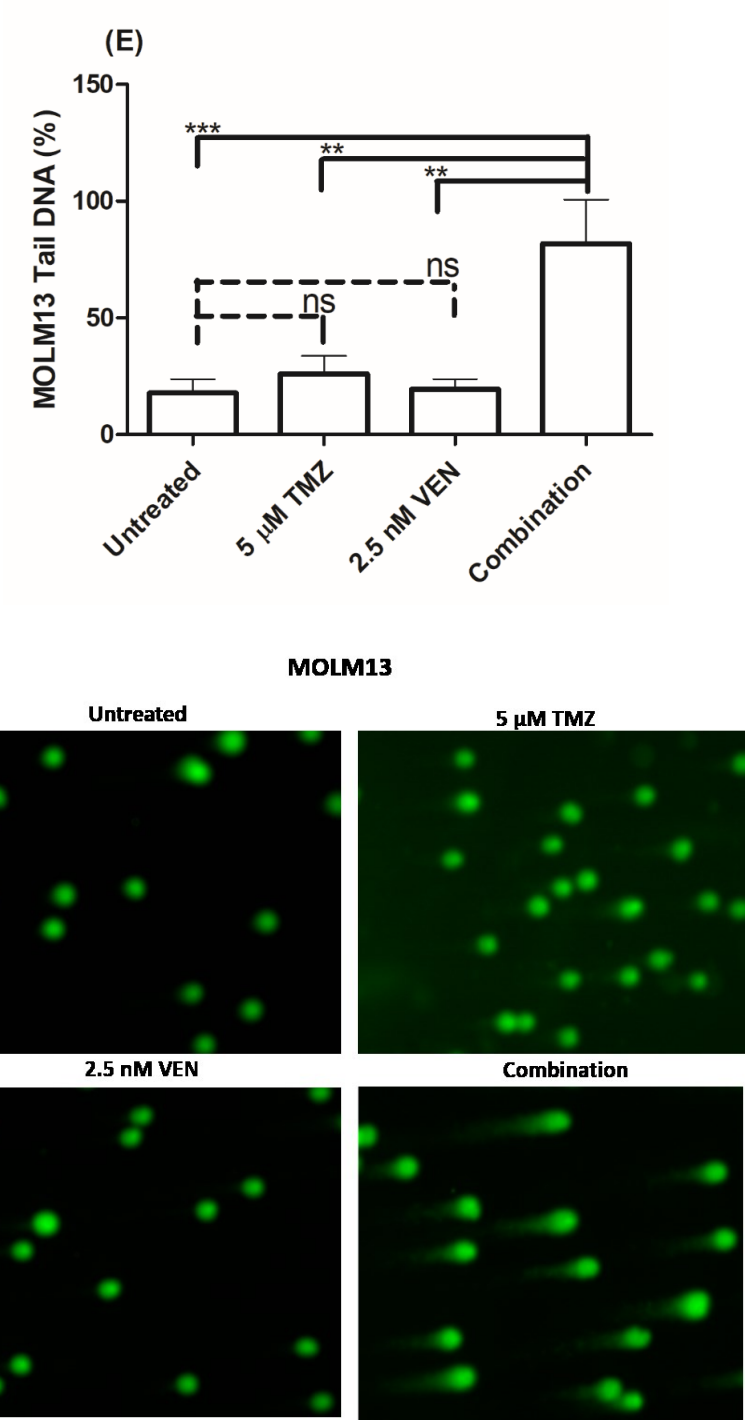

Figure 2.6: Leukemia cell lines tail DNA percentage after 6 hours of treatment with 5 µM TMZ and IC50 concentrations of VEN. 1000 nM **(A, B)** KG1 (n= 2), 2.5 nM **(C, D)** MV4-11 (n= 2), and **(E, F)** MOLM13 (n= 2). Graphs represent the mean of 100 cells performed in duplicate at different time point ± standard division. The paired *t*-test was used to compare the

mean of untreated and the combination versus TMZ and VEN alone. The annotated: * $P < 0.05$, ** $P < 0.005$, *** $P < 0.001$ and ns as not significant.

2.3.2 AML Patient Samples

2.3.2.1 Protein Expression

All patients' samples selected had at least 70% blast cells and all were obtained from previously untreated patients. The baseline BM cytogenetics and nucleophosmin *(NPM1)* and FMS-like tyrosine kinase 3 – internal tandem duplication *(FLT3 – ITD)* mutational status are summarized in Table 2.1. The MGMT protein expression by Western blot varied, with 8 exhibiting strong expression (MGMT: β-actin ratios > 0.4), and two with low expression (ratios ≤ 0.2). BCL-2: β-actin ratios were ≥ 0.2 in all tested samples. Please refer to the Appendix for each patient Western blot.

Table 2.1: AML patient samples - baseline characteristics, proteins expression of MGMT and BCL-2, and TMZ and VEN drug sensitivity

	AML #	199	191	120	119	112	97	90	82	79	48
	Blasts (%)	71	96	90	84	80	74	76	79	76	90
	Cytogenetics	der(X)	Normal	Normal	Complex	Normal	Complex	Normal	Inv(16)	+8	UK
Molecular	FLT3-ITD	Wild-type	Wild-type	Mutated	Wild-type	Wild-type	UK	Wild-type	Wild-type	UK	UK
Molecular	NPM1	Wild-type	Wild-type	Mutated	Wild-type	Wild-type	UK	Wild-type	Wild-type	UK	UK
Protein: β- Actin (Ratio)†	MGMT	0.7	0.7	0.2	1.3	0.9	0.9	0.8	0.7	0.1	0.8
Protein: β- Actin (Ratio)†	BCL-2	0.6	1.7	1.2	0.7	1.6	0.5	3.9	0.2	2.1	1.4
Sensitivity*	TMZ	-	-	-	-	-	-	-	-	-	-
Sensitivity*	VEN	++	++	++	-	-	+	++	-	++	-
Sensitivity*	Combination	++	++	++	++	++	+	++	++	++	++

† Protein: β-actin ratio < 0.2 negative, 0.2-0.4 weak + and > 0.4 strong +, the MGMT protein and BCL-2 expressions were determined using patient's whole-cell lysate that was subjected to Western blot and probed with specific antibodies. * Sensitivity determined at 5 μM TMZ and 1000 nM VEN separately and combined: (-): ≥ 60%, (+): ≤ 50%, (++): ≤ 20%.
BCL-2, B-cell lymphoma gene-2; der(X), derivative (X); FLT3-ITD, FMS like tyrosine kinase 3-internal tandem duplication; Inv(16), Inversion 16; MGMT, O^6-methylguanine methyltransferase; NPM1, Nucleophosmin 1; TMZ, Temozolomide; UK, Unknown; VEN, Venetoclax.

2.3.2.2 Cell Viability

Correlating with high MGMT expression in most of the patient samples, all samples demonstrated relative resistance to TMZ alone at usual therapeutic drug concentrations (5 – 20 μM), with an average of 90% viability compared to baseline; some responded at supra-therapeutic concentrations (50 –100 μM) (Fig. 2.7 A and Table 2.1).

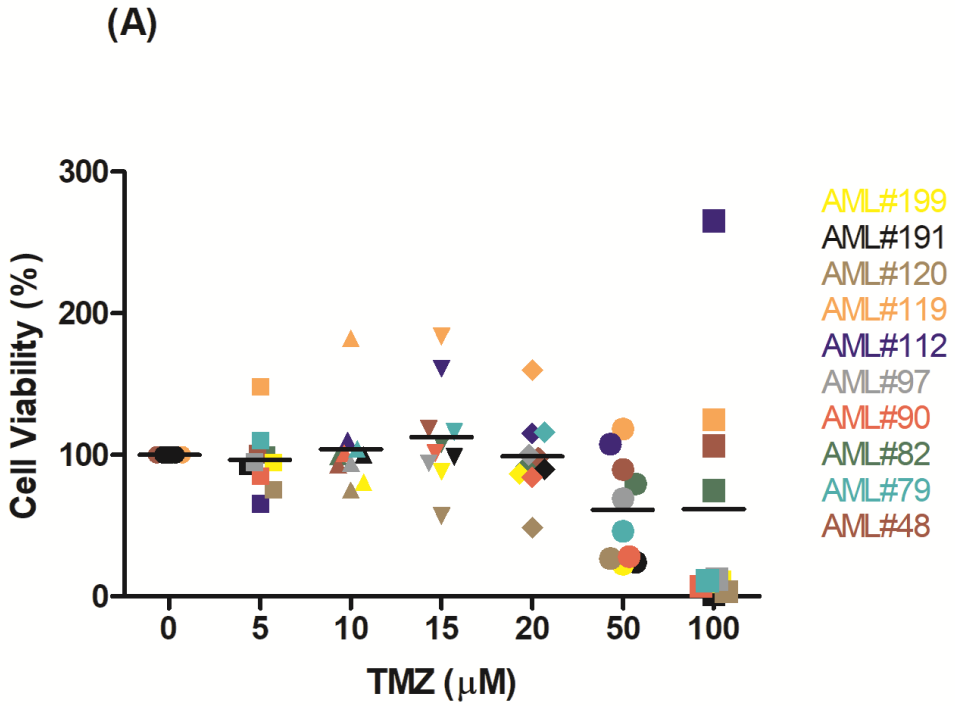

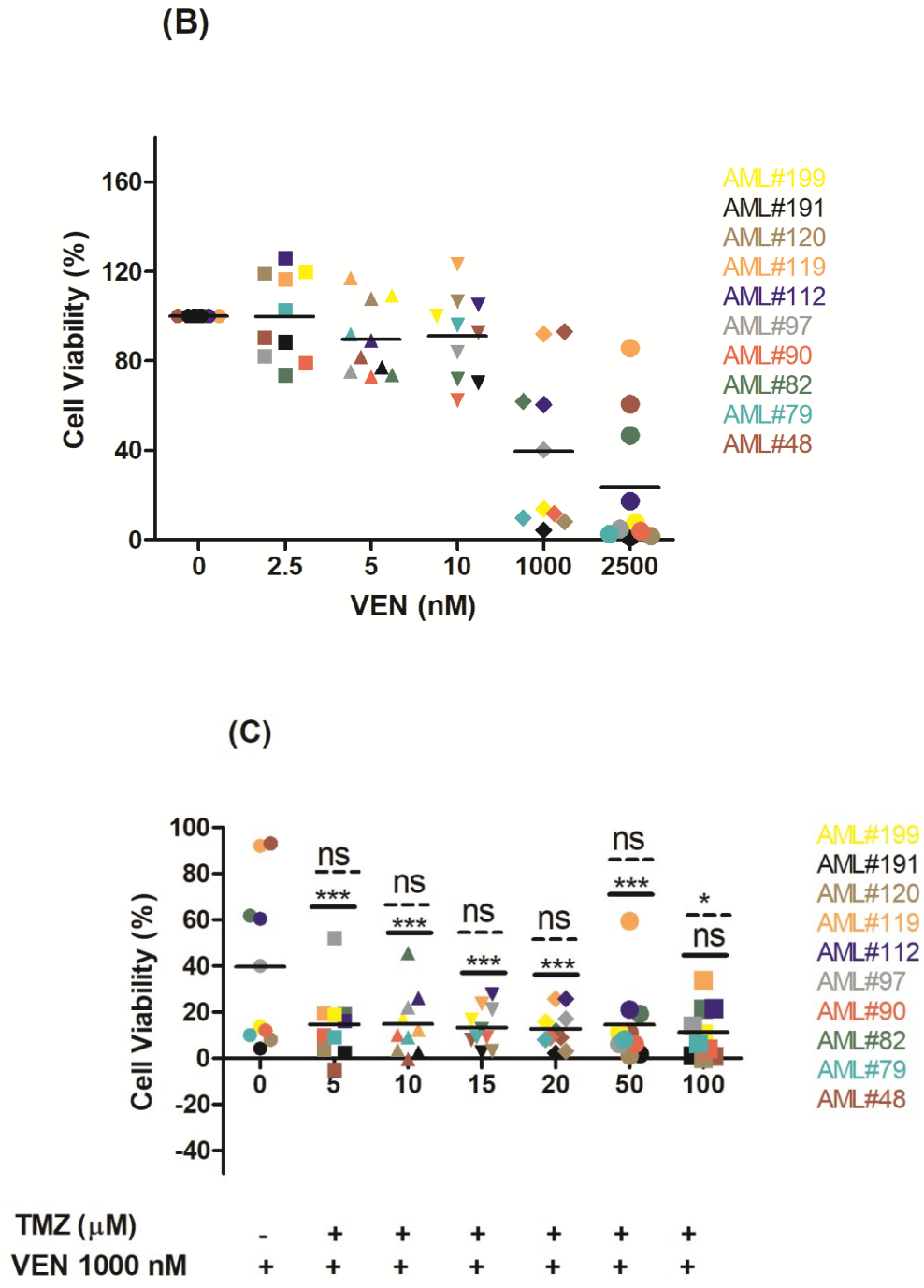

Figure 2.7: AML patients' cell viability after 48 hours of treatment with TMZ and VEN separately and combined. (A) TMZ, **(B)** VEN, and **(C)** TMZ combined with 1000 nM of VEN. Ten patients' samples were selected and treated for 48 hours with TMZ and VEN separately and

combined. Each mark represents the mean ± standard division of cell viability performed once in triplicate, due to sample limited availability per patient. Mann-Whitney test was used to compare the mean of (−) TMZ alone (Figure A) versus the combination at corresponding TMZ concentration. The (---) represents comparing the mean of 1000 nM VEN alone versus the combination. The annotated: * $P \leq 0.05$, *** $P < 0.001$ and ns as insignificant.

Five of the patient samples demonstrated sensitivity to VEN at 1000 nM, with viability reduced to less than 20% (Table 2.1 and Fig. 2.7 B). However, adding this concentration of VEN to TMZ resulted in a reduction in viability to < 50% of baseline at 5 μM TMZ in all AML tested samples, including those with high MGMT expression; 9/10 had ≤ 20% residual viability at 5 μM TMZ (Table 2.1 and Fig. 2.7 C). In the Appendix, each patient viability result is displayed individually.

2.3.2.3 DNA Damage

The DNA damage was also assessed by alkaline comet assay in two fresh AML patient samples. The isolated blast-containing MNC demonstrated DNA damage in cells treated with each drug alone compared to untreated in both samples, although was only statistically significant in one. However, significantly more severe DNA damage was observed, with the longest tail, ($P \leq 0.05$) with the TMZ+VEN combination, compared to each treatment alone in both patient samples (Figs. 2.8 A- D).

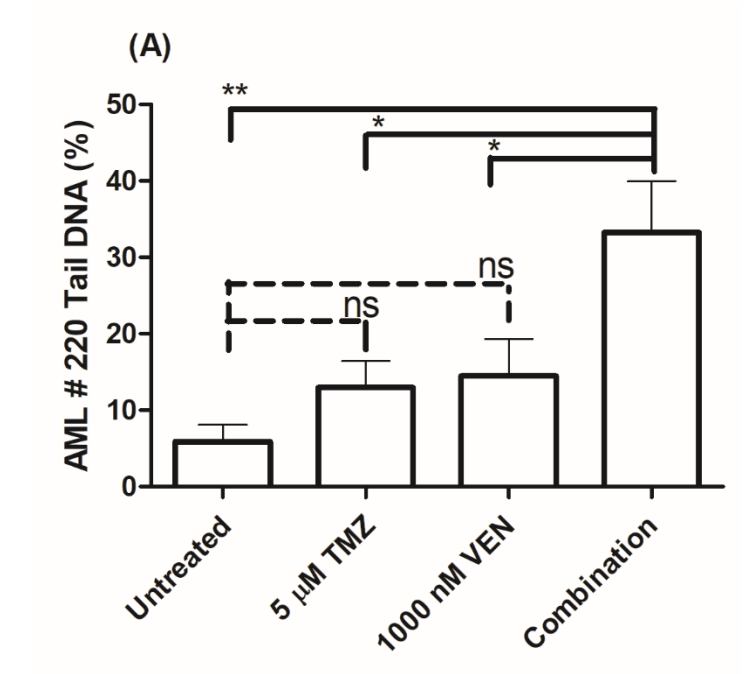
(A)
AML # 220 Tail DNA (%)
50
40
30
20
10
0
**
*
*
ns
ns
Untreated
5 μM TMZ
1000 nM VEN
Combination

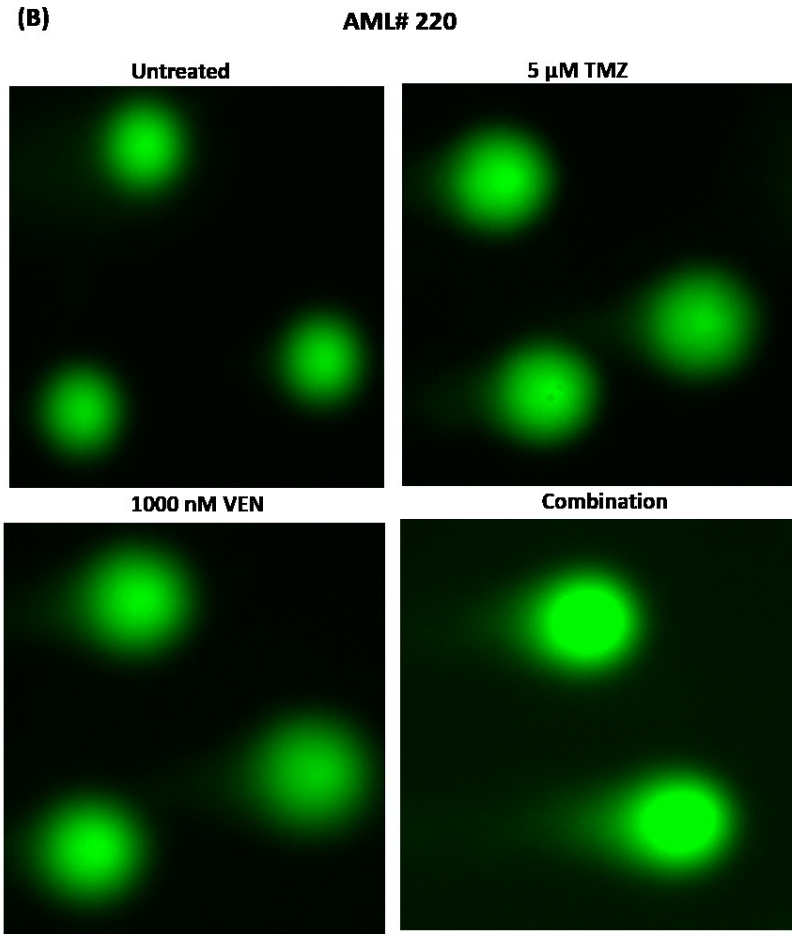
(B)
AML# 220
Untreated
5 μM TMZ
1000 nM VEN
Combination

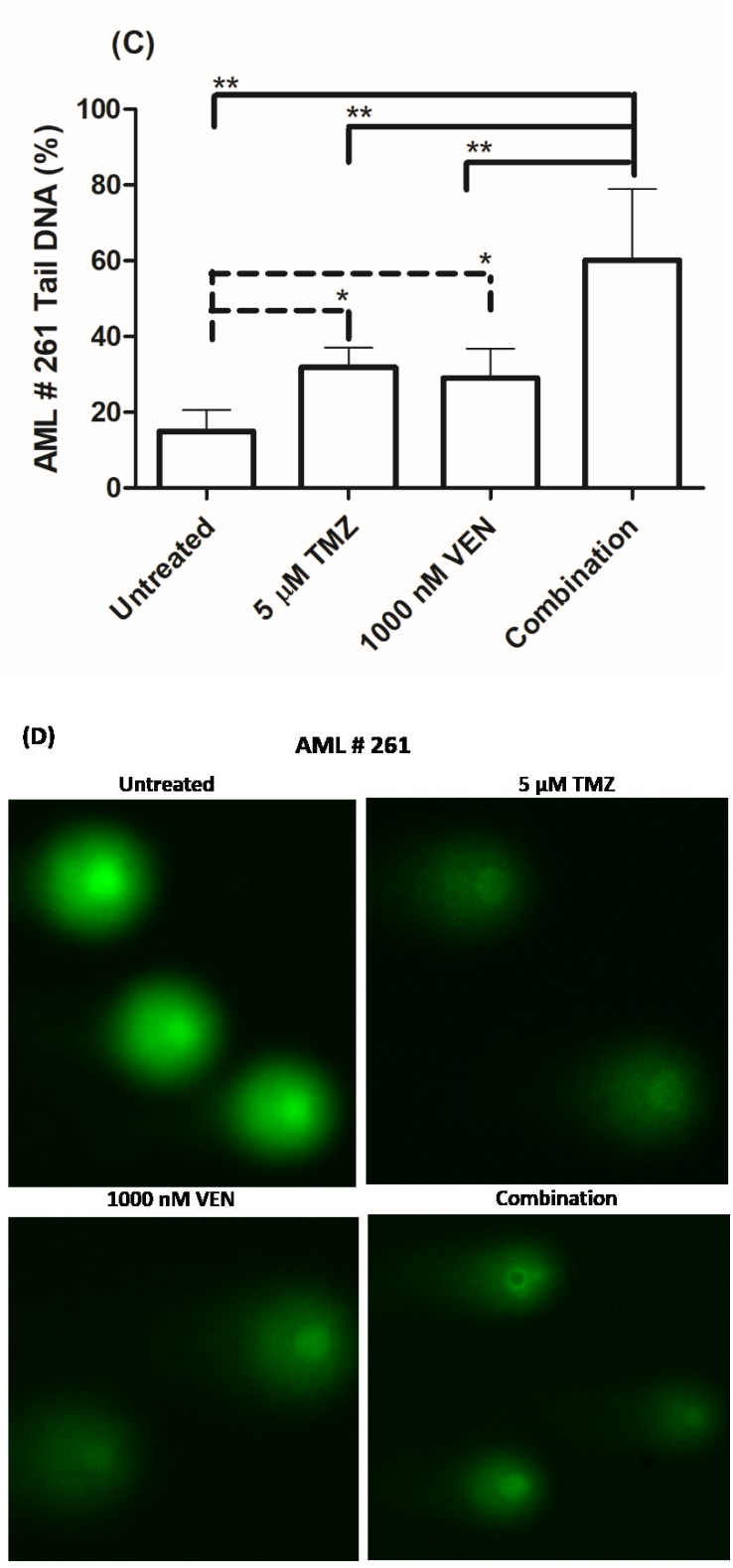

Figure 2.8: Tail DNA percentage of AML patient cells after 6 hours of treatment with 5 μM TMZ and 1000 nM VEN. (A, B) 220, and **(C, D)** 261. Graphs represent as mean of 50 cells

performed once in duplicate ± standard deviation. The paired *t*-test was used to compare the mean of untreated and the combination versus TMZ and VEN alone. The annotated: * $P < 0.05$, ** $P < 0.005$, and ns as not significant. AML# 220 expressed MGMT and BCL-2 proteins: β-actin ratio of 0.9 and 1, respectively. AML # 261 expressed MGMT and BCL-2 proteins with protein: β-actin ratio of 0.7 and 0.5, respectively. Please refer to the Appendix for each patient's Western blot.

2.3.3 Animal Model

2.3.3.1 Temozolomide

In TMZ alone experiment three different doses were evaluated; 25, 50 and 100 mg/kg. All mice injected with MOLM13 had successful leukemia engraftment based on $CD45^+$ expression in the marrow (Fig. 2.9 A).

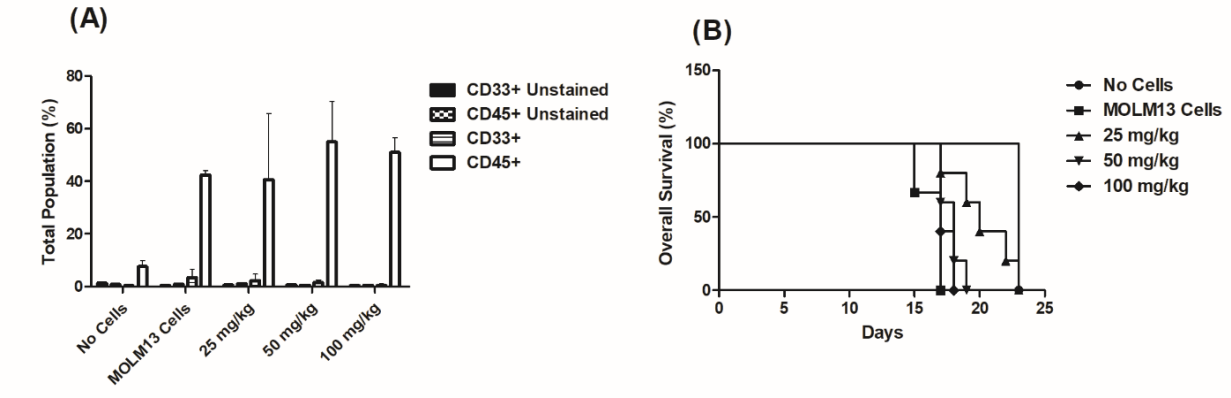

Figure 2.9: Engrafted mice treated with TMZ alone. (A) $CD33^+$, and $CD45^+$ populations (%), **(B)** overall survival (%). NOD/scid $IL2Rg^{null}$ mice were injected with 10×10^6 MOLM13 cells intravenously. On day 8, treated mice were administered TMZ intraperitoneally once daily for five days with: 25, 50, and 100 mg/kg. No cells and MOLM13 cell cohorts were administered with PBS. Any mouse that lost ≥ 15% of their body weight was euthanized. Flushed femur BM was used to evaluate the $CD33^+$ and $CD45^+$ expression by flow cytometry. The number of days each mouse survived from cell injection was counted to determine the overall survival.

The 25 mg/kg cohort showed better survival ($P < 0.05$) with median OS 20 days compared to the other 2 concentrations (18 days at 50 mg/kg and 17 days at 100 mg/kg) (Fig. 2.9 B). There was no significant ($P > 0.05$) difference observed in OS between 50 and 100 mg/kg cohorts, and $CD45^+$ expression in the marrow was not significantly different between any of the 3 dosing cohorts.

Post-mortem examination was done in two subjects from each TMZ concentration group. The histopathological of the spleen revealed leukemia engraftment in all MOLM13 injected mice, while investigation of other organs revealed no evidence of drug toxicity. The engrafted groups in the different TMZ dosing cohorts had varying degrees of spleen enlargement, mild to moderate at 25 and 50 mg/kg and severe at 100 mg/kg. The control no-cells injected mice had normal spleens (Post-mortem report page 95).

2.3.3.2 Venetoclax

In the VEN alone experiment two different doses were evaluated; 50 and 100 mg/kg. Successful MOLM13 engraftment again occurred in all injected mice, based on $CD45^+$ expression (Fig. 2.10 A), with no difference in OS observed between the 50 and 100 mg/kg treated cohorts ($P = 0.118$) (Fig. 2.10 B).

Treated mice with 100 mg/kg showed a significant ($P = 0.05$) reduction in $CD45^+$ cells with 29% expression compared to MOLM13 cells. No mice were sent for post-mortem examination since the veterinary pathologist was unavailable at the time of the experiment.

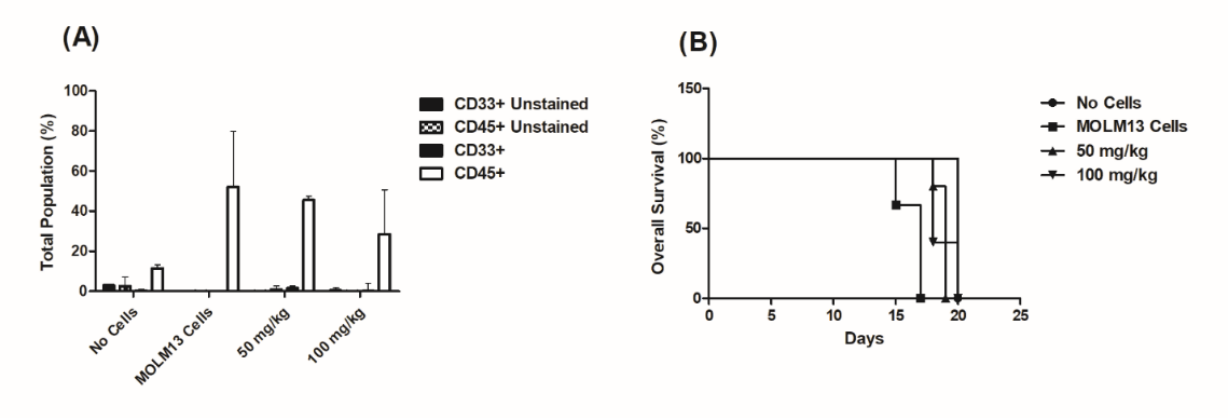

Figure 2.10: Engrafted mice treated with VEN alone. (A) $CD33^+$, and $CD45^+$ populations (%), **(B)** overall survival (%). NOD/scid $IL2Rg^{null}$ mice were injected with 10×10^6 MOLM13 cells intravenously. On day 8, treated mice were given VEN orally once daily for five days with: 50 and 100 mg/kg. No cells and MOLM13 cell cohorts were administered with vehicle CMC-Na. Any mouse that lost ≥ 15% of their body weight was euthanized. Flushed femur BM was used to evaluate the $CD33^+$ and $CD45^+$ expression by flow cytometry. The number of days each mouse survived from cell injection was counted to determine the overall survival.

2.3.3.3 Temozolomide and Venetoclax Combination

In the combination experiment 25 mg/kg TMZ and 100 mg/kg VEN were chosen based on the single agent experiments. Successful leukemia engraftment was again demonstrated in all cohorts based on post-mortem $CD45^+$ marrow expression (Fig. 2.11 A) and histologic examination of the spleen.

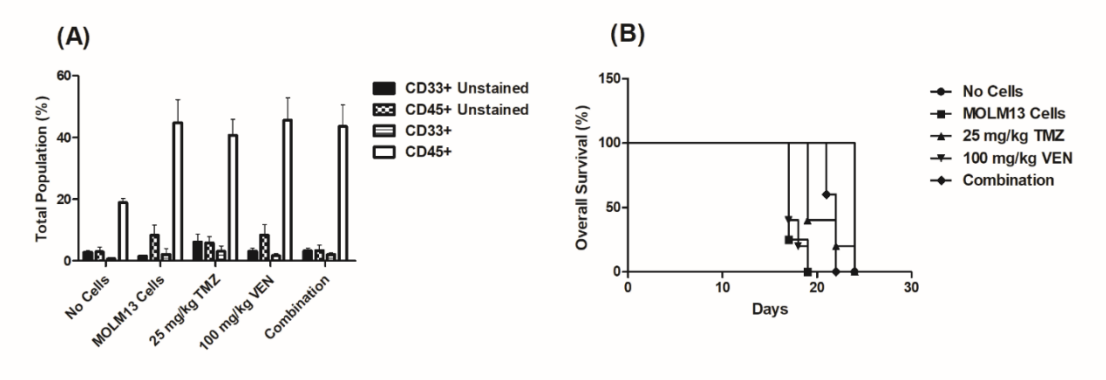

Figure 2.11: Engrafted mice treated with TMZ and VEN separately and combined. (A) $CD33^+$, and $CD45^+$ populations (%), **(B)** overall survival (%). NOD/scid $IL2Rg^{null}$ mice were injected with 10×10^6 MOLM13 cells intravenously. On day 8, treated mice were administered 25 mg/kg of TMZ intraperitonially and 100 mg/kg of VEN orally once daily for five days. No cells and MOLM13 cell cohorts were administered with both vehicles, which were PBS and CMC-Na. Any mouse that lost ≥ 15% of their body weight was euthanized. Flushed femur BM was used to evaluate the $CD33^+$ and $CD45^+$ expression by flow cytometry. The number of days each mouse survived from cell injection was counted to determine the overall survival.

The VEN treated cohort did not demonstrate any survival difference compared to the MOLM13 cell cohort. Both the TMZ-alone and the TMZ+VEN combination cohorts demonstrated significantly longer survival than the MOLM13 no drug cohort, with the combination being much more significant (median OS 22 days vs 17 days, $P < 0.01$). However, although the median OS was somewhat longer in the TMZ+VEN cohort compared with the TMZ alone group (22 vs 19 days), the OS difference was not statistically significant ($P = 0.264$) (Fig. 2.11 B). Following the completion of the drug course, the mice's body weight was monitored on a daily basis. There was no noticeable difference in the body weight between the combination and each drug alone treated mice, Fig. 2.12.

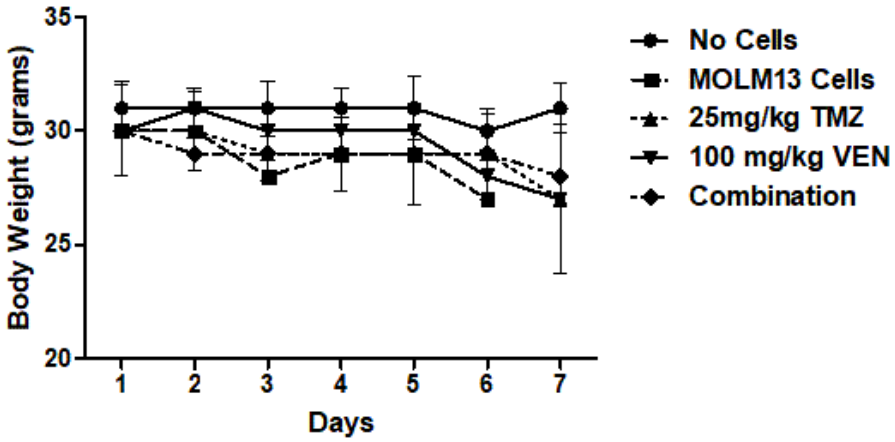

Figure 2.12: Cohorts mice body weight over time. Mice were weighted every other day until they were euthanized.

There was again no histologic evidence of drug toxicity in liver, small intestine and colon. The post-mortem toxicity revealed various degrees of spleen enlargement with mild in VEN, moderate in TMZ and severe in the combination (Post-mortem report page 99).

2.4 Discussion

The antileukemic activity of TMZ in AML is limited due to a high frequency of high expression of the DNA repair enzyme MGMT in blasts, but is also limited in patients whose blasts cells demonstrate low MGMT expression [10]. The reasons for the latter are unclear, but could be related to other drug resistance mechanisms, including high expression of anti-apoptotic proteins such as BCL-2.

Our studies demonstrate that the BCL-2 inhibitor VEN is capable of significantly enhancing the sensitivity of AML cell to TMZ at therapeutically achievable concentrations. This enhancement was seen in both low and high MGMT expressing cell lines. In KG1, a high MGMT expressing

cell line, the combination of TMZ and VEN resulted in increased apoptosis and DNA damage compared to TMZ alone, with a trend toward reduced cell viability. The effect was seen more dramatically in the patient-derived samples, 8 of whom exhibited high MGMT expression. Four of AML patients were resistant *in vitro* to both TMZ and VEN alone. However, all of them were demonstrated high sensitivity to the combination.

In the low MGMT expressing cell lines MV4-11 and MOLM13, the combination resulted in significantly lower cell viability than with either drug alone, at clinically achievable concentrations. This was accompanied by an increase in DNA strand breaks. Although there was increased apoptosis, based on Annexin V/ PI staining, with the combination compared with TMZ alone, we were not able to demonstrate an increase compared with VEN alone, largely due to the high degree of apoptosis seen with the latter drug in these cell lines.

A death substrate, PARP 1 was assessed after treating the cells with specific VEN and TMZ concentrations alone and combined. In KG1, PARP 1 was cleaved to produce an 89 kDa fragment after three hours of treatment in VEN alone and combination. This fragment is translocated from the nucleus to the cytoplasm after cleaved by caspase-3, a product of intrinsic apoptotic pathway activation [16]. The resulting ATP and NAD^+ depletion causes cell necrosis [17].

In MV4-11 and MOLM13, C-PARP 1 was not detected in any of the treated samples. The reason why this was not detected, despite a reduction in cell viability and high apoptosis, is unclear. It is possible that it could be related to activation by VEN of caspase-independent pathway. It has been found overexpression of BCL-2 prevents the release of apoptotic-inducing factor (AIF). Consequently, inhibiting BCL-2 through VEN increases MOMP, which promotes AIF cleavage. In Rosenberg's study [18] VEN was able to activate the caspase-independent pathway when

combined with FTY720, an MCL-1 inhibitor, to treat multiple myeloma cells. The cells treated with FTY720 alone have sequestered mitochondrial AIF. Conversely, when combined with VEN, the AIF translocates from mitochondria to the cytosol and further to the nucleus to cause DNA damage through phosphorylated histone H2AX. H2AX is formed a complex with the cyclophilin A, developing an abundance of DNA fragments leads to cell necrosis [19]. VEN also showed metabolic target effects independent of BCL-2 inhibitory function through impairing the tricarboxylic acid (TCA) cycle, which knows as Krebs cycle, and caused activation of reductive carboxylation. VEN also inhibited mitochondrial respiration by decreasing the oxygen consumption rate. The cells integrated stress response activated through increasing the level of activating transcription factor 4, which is an important regulator in mitochondrial stress. The dysfunction in mitochondrial respiration caused by VEN leads to a change in mitochondrial morphology, which inhibits the activity of all electron transport chains function (complexes I, II and IV)[20], resulting in cell death.

The mechanism of the marked increase in the severity of DNA damage with the TMZ+VEN combination in both high and low MGMT cell lines is also unclear. TMZ functions as a DNA methylating agent which changes the DNA's integrity and stability, leading to DNA strand breaks. In contrast, VEN is not involved in the DNA damage response. Adding VEN to TMZ significantly induced DNA damage in both high and low-MGMT cell lines. It is possible that this increased DNA damage in low-MGMT cells may have been mediated by increased translocation of AIF to the nucleus as described above. PARP 1 plays a role in the DNA damage response via base excision repair following TMZ exposure [21, 22]. In the case of KG1 cells, it is possible that PARP 1 cleavage and the corresponding reduction in intact PARP 1 availability in the nucleus may have resulted in reduced DNA repair and increased DNA stand breaks. It has been

observed that VEN impaired the repair of DNA strand breaks induced by vosaroxin, a topoisomerase II inhibitor and DNA intercalating agent, in AML cells [22], accompanied by inhibition RAD51/BRCA1-dependent DNA repair and induction of caspase-3 and PARP 1 activation [23, 24]. This observation requires further study, but may at least partially explain the sensitization of TMZ by VEN in high MGMT expressing cells. However, this would not explain the enhanced DNA damage seen with the TMZ-VEN combination in MV4-11 and MOLM13, as there was no significant increase in C-PARP 1 demonstrated.

The majority of AML patients have significant MGMT expression. Studies reported that only 10– 25% of leukemia cells had low levels of MGMT [8, 9]. Consequently, the samples demonstrated resistance to TMZ alone, except at a super-therapeutic concentration (50 and 100 μM).

The AML patient samples # 48, 82, 112 and 119 did not respond to VEN alone despite BCL-2 expression. It could be a result of overexpression other anti-apoptotic proteins such as MCL-1 and BCL-XL. These proteins found to cause VEN treatment resistance [25]. However, these patients' samples showed cell viability inhibition after TMZ+VEN combination treatment.

AML patient sample # 79 was resistant to TMZ alone, despite low MGMT expression. The cytogenetic profiling of this patient displays trisomy 8 (+8), which is most common in AML. The +8 is related to the RUNX1 mutation, with a frequency of 32% in AML [26]. Upregulation of RUNX1 in glioblastoma patients causes TMZ resistance through multidrug resistance-associated protein 1 [27]. However, the sample responded well when combined with VEN.

The TMZ and VEN doses selected to be used *in vivo* were established in two sets of experiments. For TMZ, 25 mg/kg was selected for superior OS than 50 and 100 mg/kg. For VEN, 100 mg/kg

was chosen because it significantly inhibited $CD45^+$ cells compared to MOLM13 cells. Applying the TMZ+VEN combination *in vivo* improved the OS but did not prevent leukemic engraftment. Furthermore, the OS was not significantly greater than TMZ alone. The combination-treated mice did not demonstrate any evidence of non-leukemic toxicity (Fig. 2.12), so it may be possible to increase the drug dosages and/or durations, and this could potentially produce a more effective antileukemic effect. However, this would require further study.

To conclude, the VEN and TMZ combination decreased cell viability, increased cytotoxicity, and induced DNA damage in high and low MGMT expressing cells, as compared to TMZ alone. This would support investigating the therapeutic use of this combination in AML patients, regardless of MGMT expression. As each drug is well tolerated, even in older frail patients, with non-overlapping toxicities, the combination should be well-tolerated as well but would need to be confirmed in a clinical trial.

ANIMAL PATHOLOGY SERVICES (APS) LTD.

POSTMORTEM REPORT (TMZ ALONE)

CASE NUMBER: 22-001 **DATE EXAMINED:** 19 October 2021

PRINCIPAL INVESTIGATOR: Dr. Brandwein

SUBMITTED BY: Teresa Fong

VETERINARIAN: Dr. D. Domahidi
HSLAS,
1-132 La K i Shing Centre
U of A T6G 2E1

SPECIES/STRAIN: Mouse/NOD.Cg-Prkdc<scid>l 12rg<tmlW;l>/SzJ X 8

AGE: 3 months **SEX:** M

HISTORY: We have another batch of 8 mice that we would like to send for PM. These mice are from a different experiment, with a different drug (Temozolomide) but the overall process is similar (inject with AML cells then treat with the drug for 5 days). It seems that these mice progressed way faster after developing even the mildest of symptoms. In previous batches we would see a gradual weight loss and they would slowly get less and less active until we had to euthanize them from 15% weight loss or hind leg paralysis. These ones however, seem to appear perfectly healthy and then in a matter of a couple hours would be moribund. The most surprising thing I found was that most of the mice I've had to euthanize or that were found dead had almost no weight loss at all whereas in previous experiments, weight loss was one of the primary indicators of engraftment. I was wondering if we could see if the drug had any toxic effect on the mice. I think that engraftment is still why they died but was wondering if the toxicity of the drug made mice sicker which is why they died so suddenly.

DIAGNOSIS: Diffuse leukemic engraftment, all animals except mouse 8.

COMMENTS: Postmortem findings are of successful engraftment in all animals but number 8 which I expect is the saline control (I am blinded as to individual treatments). As you noted in your history, all mice are in good body condition and show no signs of weight loss. The

microscopic findings are of a rapidly developing and aggressive tumor and not drug toxicity. Just as a special note: my designation of mild, moderate and severe enlargement of the spleen is relative to the various affected mice in your ongoing experiments. With respect to the saline control in this group and other normal mice, all of the affected experimental mice would be considered to have severely enlarged spleens.

GROSS POSTMORTEM FINDINGS:

All mice are in good body condition with good fat reserves. Unless mentioned below, all internal organs are normal in appearance on gross examination.

Mouse #1 (CC#551 406 L L notch) 50 mg/kg TMZ: This mouse has a moderately enlarged, grey spleen. The left lateral and middle lobes of the liver each have an extensive area of pale parenchyma.

Mouse #2 (CC# 551 407 L notch) MOLM13 CELLS: This mouse has a pale, mildly enlarged spleen.

Mouse #3 (CC# 551 406 L notch) 50 mg/kg TMZ: The spleen of this mouse is slightly pale and very large. The last 1 cm of the cecum is dark red.

Mouse #4 (CC# 551 404 R ear notch) 25 mg/kg TMZ: This mouse has a moderately enlarged, grey spleen. The left lateral and middle lobes of the liver each have an extensive area of pale parenchyma.

Mouse #5: (CC# 551 404 L /R notch) 25 mg/kg TMZ: The spleen is moderately enlarged and pale.

Mouse # 6: (CC# 551 405 R notch) 100 mg/kg TMZ: The spleen is severely enlarged and pale.

Mouse # 7: (CC# 551 408 R notch) 100 mg/kg TMZ: The spleen is severely enlarged and pale.

Mouse # 8: (CC#552 314 N mouse) COTROL NO DRUG/NO CELLS: The spleen and all other internal organs of this mouse is grossly normal.

HISTOPATHOLOGY:

Animals 1 - 7 had similar microscopic findings which consisted of severe enlargement of the spleen due to a generalized infiltrate of the injected tumor cells overrunning and replacing all of the normal cell population and much of the stroma. There are only a few isolated megakaryocytes in the sinuses and some very small areas of erythropoiesis that are compressed against the smooth muscle trabeculae. All the rest of the spleen is occupied by a uniform sheet of tumor cells. The kidneys all had multifocal areas of tumor infiltration in the cortices. These

varied in severity from animal to animal. The sinusoids of the liver and alveolar walls of the lungs also had infiltrates of tumor cells within them. In the lungs many of these cells were in the capillaries and were probably circulating through and settling out in the alveolar septae. The hearts were free of tumor cells in the myocardium, but tumor was present in the circulating blood. The organs of animal 8 were microscopically normal. Individual differences in quality or degree from the common microscopic pattern described above are as follows:

Mouse #1 (CC#551 406 L L notch) 50 mg/kg TMZ: There are degenerative changes and loss of hepatocytes in the centrilobular areas of the liver of this mouse. These are most likely hypoxic in nature.

Mouse #2 (CC# 551 407 L notch) MOLM13 CELLS: The lungs of this mouse are very severely infiltrated

by tumor cells. There is also a large infiltrate in the perirenal fat near the renal pelvis. Degenerative changes and loss of hepatocytes as described for mouse 1 are present but not as severe in this mouse.

Mouse #3 (CC# 551 406 L notch) 50 mg/kg TMZ: This mouse has a greater degree of infiltration of the lungs and sinusoids of the liver than the average described above.

Mouse #4 (CC# 551 404 R ear notch) 25 mg/kg TMZ: There is a lesser degree of infiltration of the kidney of this animal.

Mouse #5: (CC# 551 404 L /R notch) 25 mg/kg TMZ: Degenerative changes are present in some of the renal tubules, especially in areas of cortical tumor infiltrates. This mouse has a focal area of dystrophic bone formation in the spleen. This is a finding unrelated to the tumor or experimental procedure which I have seen very occasionally in mice on a random basis.

Mouse # 6: (CC# 551 405 R notch) 100 mg/kg TMZ: There is a large mass of tumor cells in the blood circulating through the left atrium of the heart. The lungs have more severe tumor infiltration than in the general description above.

Mouse # 7: (CC# 551 408 R notch) 100 mg/kg TMZ: The lungs of this mouse are more heavily infiltrated by tumor than in the general description above. In addition, there is a very large mass of tumor cells in the renal pelvic fat. Degenerative changes are present in some of the renal tubules, especially in areas of cortical tumor infiltrates.

Mouse # 8: (CC#552 314 N mouse) COTROL NO DRUG/NO CELLS: All internal organs examined are microscopically normal.

P. N. Nation, DVM, PhD, Diplomate ACVP.

per Animal Pathology Services APS Ltd.

ANIMAL PATHOLOGY SERVICES (APS) LTD.

POSTMORTEM REPORT COMBINATION

CASE NUMBER: 23-008 **DATE EXAMINED:** 18 March 2023

PRINCIPAL INVESTIGATOR: Dr. Brandwein

SUBMITTED BY: Teresa Fong

VETERINARIAN: Dr. N. Bosvik
HSLAS,
1-132 La Ki Shing Centre
U of A T6G 2E1

SPECIES/STRAIN: Mouse/NOD.Cg-Prkdc<scid>112rg<tm1W;l>/SzJ X 4

AGE: 3 months **SEX:** M

HISTORY: We are primarily looking for any indications of drug toxicity, especially since this is the first time we gave them our drug combination. Please indicate how much tumor engraftment each mouse has. Our groups were control, untreated, venetoclax, temozolomide and then a combination cocktail. We expected the combination to have a stronger effect than the separate treatments and all 3 treated to have lower engraftment than the untreated. Our flow cytometry experiments didn't work as well as we wanted due to our endpoints so it'd be great if the slides showed it.

DIAGNOSIS/COMMENT: There is leukemic engraftment with varying degrees of severity in the spleens and livers of all mice. The sections of intestine and colon were microscopically normal in all mice. The degree of engraftment in each case is indicated in Table 1. There were no changes of toxicity in any of the tissues examined. All microscopic findings are attributable to minor autolytic change and infiltration by tumor cells.

HISTOPATHOLOGY

Mouse 591 001 RN: 25 mg/kg TMZ ALONE

Spleen: there is diffuse infiltration of the sinuses by tumor cells with crowding out of the normal cellular population and enlargement of the spleen. More than 90% of the splenic volume consists of malignant cells.

Liver: tumor cells are infiltrating the perivenous spaces forming cuffs 3-5 cells deep. There are individual malignant cells throughout the sinusoids and occasional widely scattered clusters of malignant cells in the parenchyma.

Intestine: microscopically normal

Mouse 591 002 RN: 25 mg/kg TMZ ALONE

Spleen: there is diffuse infiltration of the sinuses by tumor cells with crowding out of the normal cellular population and some enlargement, however, this is less in extent than in mouse 591 001 RN.

Liver: Tumor cells are infiltrating the perivenous parenchyma but are present in clusters and not forming complete cuffs. Individual malignant cells are present in the sinusoids

Intestine: microscopically normal

Mouse 591 001 LL: COMBINATION (25 mg/kg TMZ + 100 mg/kg VEN)

Spleen: there is diffuse infiltration of the sinuses by tumor cells with crowding out of the normal cellular population and enlargement of the spleen. More than 90% of the splenic volume consists of malignant cells.

Liver: microscopically similar to Mouse 591 001 RN but without clusters of malignant cells in the parenchyma.

Intestine: mildly autolytic but microscopically normal

Mouse 591 003 LL: COMBINATION (25 mg/kg TMZ + 100 mg/kg VEN)

Spleen: there is severe sinus tumor cell infiltration in this animal with enlargement and greater than 90% of the volume occupied by malignant cells.

Liver: tumor cells are infiltrating the perivenous spaces forming cuffs greater than 5 cells deep. Malignant cells are present throughout the sinusoids and there are areas of necrosis of the parenchyma.

Intestine: microscopically normal

Mouse 591 000 LR: 100 mg/kg VEN ALONE

Spleen: microscopically qualitatively similar but quantitatively much milder infiltration than the other animals in this study. Only approximately 10% of the volume of the spleen is infiltrated and there is no apparent enlargement.

Liver: tumor cells are infiltrating the perivenous spaces forming cuffs greater than 5 cells deep. Malignant cells are present throughout the sinusoids and there are multiple foci of suppurative inflammation in the parenchyma.

Intestine: mildly autolytic but microscopically normal

Mouse 591 002 LR: 100 mg/kg VEN ALONE

There is moderate autolysis of the tissues of this mouse

Spleen: there is diffuse infiltration of the sinuses by tumor cells with crowding out of the normal cellular population and some enlargement similar to that in mouse 591 002 RN.

Liver: mild sinusoidal infiltration

Intestine: mildly autolytic but microscopically normal

Mouse number	Spleen	Liver	Intestine
591 001 RN 25 mg/kg TMZ alone	3	2	Normal
591 002 RN 25 mg/kg TMZ alone	2	1	Normal
591 001 LL COMBINATION (25 mg/kg TMZ + 100 mg/kg VEN)	3	2	Normal
591 003 LL COMBINATION (25 mg/kg TMZ + 100 mg/kg VEN)	3	3	Normal
591 000 LR 100 mg/kg VEN ALONE	1	3	Normal
591 002 LR 100 mg/kg VEN ALONE	2	1	Normal

SCORING KEY

1. **Spleen**

   0 = microscopically normal

   1 = infiltration of the sinuses by tumor cells, some enlargement of the spleen, and less than 75% of volume occupied by malignant cells.

   2 = diffuse infiltration of the sinuses by tumor cells with enlargement and 75 - 90% of the volume occupied by malignant cells.

   3 = diffuse infiltration of the sinuses by tumor cells with severe enlargement and more than 90% of the volume occupied by malignant cells.

2. **Liver**

   0 = microscopically normal

   1 = Tumor cells are infiltrating the perivenous parenchyma but are present in clusters and not forming complete cuffs. Individual malignant cells are present in the sinusoids

   2 = sheets of tumor cells are infiltrating the perivenous parenchyma forming cuffs 2 – 5 cells deep and individual malignant cells are diffusely infiltrative throughout the sinusoids

   3 = tumor cells are infiltrating the perivenous spaces forming cuffs greater than 5 cells deep. Malignant cells are present throughout the sinusoids and there are areas of necrosis or inflammation of the parenchyma.

P. N. Nation, DVM, PhD, Diplomate ACVP.

per Animal Pathology Services APS Ltd.

2.5 References

1. Hoffbrand AV, Moss PAH, Pettit JE. Essential Haematology. 5th ed. Massachustts, USA: Blackwell; 2006.

2. Ossenkoppele G, Löwenberg B. How I treat the older patient with acute myeloid leukemia. Blood. 2015;125(5):767-74.

3. Bhansali RS, Pratz KW, Lai C. Recent advances in targeted therapies in acute myeloid leukemia. J Hematol Oncol. 2023;16(1).

4. Wei AH, Montesinos P, Ivanov V, DiNardo CD, Novak J, Laribi K, et al. Venetoclax plus LDAC for newly diagnosed AML ineligible for intensive chemotherapy: a phase 3 randomized placebo-controlled trial. Blood. 2020;135(24):2137-45.

5. Jiapaer S, Furuta T, Tanaka S, Kitabayashi T, Nakada M. Potential strategies overcoming the temozolomide resistance for glioblastoma. Neurol Med Chir (Tokyo). 2018;58(10):405-21.

6. Wesolowski JR, Rajdev P, Mukherji SK. Temozolomide (Temodar). AJNR Am J Neuroradiol. 2010;31(8):1383-4.

7. Verbeek B, Southgate TD, Gilham DE, Margison GP. O6-Methylguanine-DNA methyltransferase inactivation and chemotherapy. Br Med Bull. 2008;85:17-33.

8. Brandwein JM, Yang L, Schimmer AD, Schuh AC, Gupta V, Wells RA, et al. A phase II study of temozolomide therapy for poor-risk patients aged >or=60 years with acute myeloid leukemia: low levels of MGMT predict for response. Leukemia. 2007;21(4):821-4.

9. D'Atri S, Piccioni D, Castellano A, Tuorto V, Franchi A, Lu K, et al. Chemosensitivity to triazene compounds and O6-alkylguanine-DNA alkyltransferase levels: studies with blasts of leukaemic patients. Ann Oncol. 1995;6(4):389-93.

10. Brandwein JM, Kassis J, Leber B, Hogge D, Howson-Jan K, Minden MD, et al. Phase II study of targeted therapy with temozolomide in acute myeloid leukaemia and high-risk myelodysplastic syndrome patients pre-screened for low O(6) -methylguanine DNA methyltransferase expression. Br J Haematol. 2014;167(5):664-70.

11. Konopleva M, Pollyea DA, Potluri J, Chyla B, Hogdal L, Busman T, et al. Efficacy and biological correlates of response in a phase II study of venetoclax monotherapy in patients with acute Myelogenous Leukemia. Cancer Discov. 2016;6(10):1106-17.

12. Zhu H, Almasan A. Development of venetoclax for therapy of lymphoid malignancies. Drug Des Devel Ther. 2017;11:685-94.

13. Korycka-Wolowiec A, Wolowiec D, Kubiak-Mlonka A, Robak T. Venetoclax in the treatment of chronic lymphocytic leukemia. Expert Opin Drug Metab Toxicol. 2019;15(5):353-66.

14. Campos EDV, Pinto R. Targeted therapy with a selective BCL-2 inhibitor in older patients with acute myeloid leukemia. Hematol Transfus Cell Ther. 2019;41(2):169-77.

15. Comet Assay Kit (3-well slides) (ab238544): Abcam; 2018 [Available from: https://www.abcam.com/ps/products/238/ab238544/documents/Comet-Assay-protocol-book-v2b-ab238544%20(website).pdf.

16. Jagtap P, Szabó C. Poly(ADP-ribose) polymerase and the therapeutic effects of its inhibitors. Nat Rev Drug Discov. 2005;4(5):421-40.

17. Chaitanya GV, Steven AJ, Babu PP. PARP-1 cleavage fragments: signatures of cell-death proteases in neurodegeneration. Cell Commun Signal. 2010;8:31.

18. Rosenberg E, Voevoda V, Magen H, Ostrovsky O, Shimoni A, Peled A, et al. Venetoclax Reverses Metabolic Reprogramming Induced By S1P Modulator FTY720, Suppresses Oxidative

Phosphorylation and Synergistically Targets Multiple Myeloma. Blood. 2021;138(Supplement 1):1195-95.

19. Sosna J, Voigt S, Mathieu S, Lange A, Thon L, Davarnia P, et al. TNF-induced necroptosis and PARP-1-mediated necrosis represent distinct routes to programmed necrotic cell death. Cell Mol Life Sci. 2014;71(2):331-48.

20. Roca-Portoles A, Rodriguez-Blanco G, Sumpton D, Cloix C, Mullin M, Mackay GM, et al. Venetoclax causes metabolic reprogramming independent of BCL-2 inhibition. Cell Death Dis. 2020;11(8):616.

21. Trivedi RN, Almeida KH, Fornsaglio JL, Schamus S, Sobol RW. The role of base excision repair in the sensitivity and resistance to temozolomide-mediated cell death. Cancer Res. 2005;65(14):6394-400.

22. Horton TM, Jenkins G, Pati D, Zhang L, Dolan ME, Ribes-Zamora A, et al. Poly(ADP-ribose) polymerase inhibitor ABT-888 potentiates the cytotoxic activity of temozolomide in leukemia cells: influence of mismatch repair status and O6-methylguanine-DNA methyltransferase activity. Mol Cancer Ther. 2009;8(8):2232-42.

23. Liu F, Knight T, Su Y, Edwards H, Wang G, Wang Y, et al. Venetoclax Synergistically Enhances the Anti-leukemic Activity of Vosaroxin Against Acute Myeloid Leukemia Cells Ex Vivo. Target Oncol. 2019;14(3):351-64.

24. Xiufeng Z, Haijun Z, Silei B, Manman D, Yong Z, Lian Y, et al. Co-operation of ABT-199 and gemcitabine in impeding DNA damage repair and inducing cell apoptosis for synergistic therapy of T-cell acute lymphoblastic leukemia. Anti-Cancer Drugs. 2019;30(2):138-48.

25. Liu J, Chen Y, Yu L, Yang L. Mechanisms of venetoclax resistance and solutions. Front Oncol. 2022;12:1005659.

26. Becker H, Maharry K, Mrózek K, Volinia S, Eisfeld AK, Radmacher MD, et al. Prognostic gene mutations and distinct gene- and microRNA-expression signatures in acute myeloid leukemia with a sole trisomy 8. Leukemia. 2014;28(8):1754-8.

27. Xu J, Song J, Xiao M, Wang C, Zhang Q, Yuan X, Tian S. RUNX1 (RUNX family transcription factor 1), a target of microRNA miR-128-3p, promotes temozolomide resistance in glioblastoma multiform by upregulating multidrug resistance-associated protein 1 (MRP1). Bioengineered. 2021;12(2):11768-81.

CHAPTER 3

The Effect of MDM2 Target Inhibitor Idasanutlin on Temozolomide Sensitivity

3 The Effect of MDM2 Target Inhibitor Idasanutlin on Temozolomide Sensitivity

3.1 Introduction

Acute myeloid leukemia (AML) is a blood cancer characterized by highly proliferative myeloid progenitors known as myeloblasts. These myeloblasts accumulate in the bone marrow (BM), resulting in impaired hematopoiesis [1]. They are poorly differentiated, have a long lifespan, and can pass into the peripheral blood (PB), leading to organ infiltration. A circulating myeloblast percentage of ≥ 20% in the PB is one of the diagnostic features of AML [2]. The production of both red blood cells and platelets is impacted by imbalanced hematopoiesis, and their insufficiency causes anemia and bleeding, respectively.

AML is a highly aggressive disease that mostly affects older individuals with a median age of 65 years. The five-year overall survival (OS) is only 28%, reducing to 5% in patients ≥ 70 years old [3]. In this age group, around 30% of patients have primary refractory disease, and 74% experience a disease relapse [4].

Temozolomide (TMZ) is a cytotoxic alkylating agent used as a standard of chemotherapeutic care along with radiation for patients with glioblastoma and melanoma. It causes DNA methylation at the O^6 and N^7 guanine and N^3 adenine nucleobases. The methylated adducts formed are highest at 70% in N^7 guanine, followed by 9% in N^3 adenine and 8% in O^6 guanine [5].

O^6 methylguanine (O^6-MeG) has the most potential to initiate cell apoptosis when mispaired with thymine (T) instead of cytosine (C); this generates O^6-MeG:T in the presence of active

mismatch repair , which leads to DNA double-strand breaks and apoptosis [5]. However, the DNA repair enzyme methylguanine methyltransferase (MGMT) can normalize the O^6 guanine nucleotide by removing the methyl group added by TMZ [6].

A strong correlation has been observed between MGMT expression and the TMZ response in older AML patients with a poor prognosis. Patients whose marrows expressed MGMT were significantly less likely (P= 0.003) to respond to TMZ compared to MGMT-negative patients, with an overall response rate (ORR) of 6% and 60%, respectively [7]. Further, a selective study on low-MGMT leukemia patients was specifically performed before TMZ administration. Only 22% of these patients achieved complete response (CR) and CR with incomplete platelet recovery. The majority (67%) had either partial, minor response or were non-responsive to treatment [8].

The tumour suppressor p53 gene (*TP53*) is involved in cell cycle arrest, DNA damage and apoptosis [9]. Phosphorylated p53 causes cell cycle arrest by inducing p21, which inhibits the cyclin E/cyclin-dependent kinase (CDK) 2 and cyclin D/CDK4 complexes to arrest cells in the G1 phase [10, 11]. P21 also arrests the cell in the G2/M phases by targeting cyclin A/ CDK 1 and cyclin B/CDK 2 to block the transition between the G2 and M phases [10].

The activated p53 protein regulates the intrinsic apoptotic pathway by inducing pro-apoptotic proteins with BH3 only; p53-upregulated modulator of apoptosis (PUMA), NOXA or (phorbol-12-myristate-13-acetate-induced protein 1 (PMAIP1)) and BCL-2 antagonist of cell death (BAD) and pro-apoptotic effectors BCL-2-associated X protein (BAX) and BCL-2-antagonist/killer (BAK) to enhance mitochondrial outer membrane permeabilization and release cytochrome *c* [10]. In the presence of ATP, cytochrome *c* interacts with apoptotic protease activating factor-1

(APAF-1) and pro-caspase-9 to form an apoptosome [12, 13]. The apoptosome activates caspases- 9, 3, and 7, resulting in cell apoptosis [1].

p53 plays a role in the extrinsic apoptotic pathway (EAP) by inducing the death receptors associated death domain (Fas) and TNF-related apoptosis-inducing ligand (TRAIL) R1 and R2, also known as DR4 and DR5, respectively [10, 14]. Fas and DR5 initiate the EAP through dimerization and the recruitment of death receptors. Activation of pro-caspase 8, followed by caspases 3 and 7, causes cell apoptosis [10].

In cases of significant DNA damage, a high level of p53 is produced to activate the cell apoptosis pathways as mentioned previously. If the damage is fixable, a low level of p53 is induced to cause cell cycle arrest to repair the DNA damage [10]. Regarding DNA repair, the DNA damage sensors ataxia telangiectasia mutated (ATM) and ATM and Rad3-related protein (ATR) are activated and recruited at the site of damage [15]. Then, p53 is phosphorylated and induces p21, which inhibits the cyclin E/CDK2 complex to cause cell cycle arrest [10]. Alternatively, the cyclin complex inactivates the retinoblastoma protein (pRb) through phosphorylation. Therefore, Rb binds to the E2F transcription factor, which prevents cell cycle progression to upregulate a specific DNA repair pathway [11].

The *TP53* gene is mutated in most cancers; however, these mutations are less common in hematological malignancies [1]. The mutations account for 5–10% of de novo AML and increase to 25% in adult with aged 60–67 years [16]. Luckily, over 80% of AML cases have wild-type p53, even in relapsed/refractory (R/R) AML [4, 17]. Although, the p53 functions are disabled because of the overexpression of double minute 2 homolog (MDM2), a negative regulator of p53[18]. MDM2 has a hydrophobic pocket to which p53 can bind and is shaped as an alpha helix. MDM2 binds to p53's Trp23, Leu26 and Phe19 amino acids [19]. MDM2 degrades p53

through the ubiquitin-proteasomal pathway [20]. MDM2 overexpression inhibits p53 functions such as cell apoptosis and cell cycle arrest, which results in chemotherapeutic resistance and cell survival.

Idasanutlin (IDA) is a highly potent and selective to MDM2 that disrupts the p53:MDM2 interaction to reactivate p53 functions [21]. It has a pyrrolidine derivative that causes cell cycle arrest and/or apoptosis through p53 activation in wild-type p53 cell lines and inhibits osteosarcoma in xenograft mice [19]. It has no activity in mutated p53 cells.

IDA is administered orally to AML patients. It has been found to decrease leukemic cell counts and produce responses in AML patients with R/R p53 wild-type with minimal myelosuppressive effects on the BM [1, 22]. It also has shown encouraging activity in R/R AML when combined with venetoclax (VEN), with a 38% ORR [23]. The MIRROS study, a large Phase III clinical trial in patients with R/R AML, randomized patients to receive cytarabine plus either IDA or placebo. Although the ORR was higher in the IDA arm (39% vs 22%), there was no significant difference in CR rate or overall survival (OS) [4].

Reactivating the cell guardian p53 through the disruption of p53:MDM2 binding using IDA in the presence of TMZ promotes cell apoptosis and suppresses proliferation. We hypothesized that combining the MDM2 inhibitor IDA with TMZ treatment would enhance TMZ sensitivity in AML cells with high and low levels of MGMT expression, in p53 wild-type AML.

3.2 Materials and Methods

3.2.1 Cell Lines

Human leukemia cell lines; KG1, MV4-11, MOLM13 and OCI-AML3 were purchased from American Type Tissue Collection (ATCC). These cells were previously stored at liquid nitrogen

in 10% dimethyl sulfoxide (DMSO) and 90% fetal bovine serum (FBS). KG1, MV4-11, MOLM13 were cultured in Roswell Park Memorial Institute (RPMI) 1640 (Gibco Life Technology) and OCI-AML3 in Minimum Essential Medium Alpha (MEM α) (Gibco Life Technology) after reconstituting with 10% FBS and 1% penicillin–streptomycin. When needed the cells were thawed at 37 ºC water bath then washed with desired media as mentioned previously. The cells growth was maintained at 37 ºC and 5% CO_2.

3.2.2 AML Patients Samples

Prior ethics approval was obtained from the University of Alberta Health Research Ethics Board (HREB). After obtaining consent, PB or BM samples were obtained from newly diagnosed AML patients who were being managed at the University of Alberta Hospital. Samples were drawn in sodium heparin anti-coagulant tubes. The blast-containing mononuclear cells (MNC) were isolated using the Ficoll–Paque (GE Healthcare) method (refer to 2.2.2 for details). Samples were then stored in 10% DMSO and 90% FBS in liquid nitrogen at the Canadian Biosample Repository at the University of Alberta until needed. Sorting for blast cells was not performed; however, only samples with a minimum 70% blast cells were chosen for analysis. Thawed cells were washed with RPMI 1640 and 2% DNase I solution (Stem Cell Technologies) to reduce cell clumping after thawing high-concentrated cryopreserved cells prior to performing the desired experiment.

3.2.3 Treatments

The TMZ was purchased from Enzo and IDA (RG-7388) from Selleckchem. Both drugs were dissolved in DMSO then stored as recommended temperature. A serial dilution of each treatment was prepared freshly in sterile PBS to minimize the cytotoxicity effect may cause by the DMSO.

3.2.4 Protein Expression

A total of 10×10^6 cells were collected for protein extraction to be used for Wester blot. Radioimmunoprecipitation (RIPA) lysis buffer, in presence of phosphatase and protease inhibitors, was used to quantify the extracted protein using bicinchoninic acid (BCA) assay (Thermo Scientific). The protocol was followed as per manufacturer recommendation. A total of 50 µg extracted protein was separated on an acrylamide sodium dodecyl sulphate (SDS) gel, 12% for MGMT detection and 8% for p53 and MDM2 detection. Nitrocellulose blotting membrane was used for wet-transfer and blocked with Tris-buffer saline in 5% skimmed milk and 0.1% Tween for one hour.

The MGMT (# 2739), p53 (# 48818) and MDM2 (**#** 76794**)** antibodies (Cell Signaling Technology) concentration (1:1,000) were incubated overnight at 4˚C. Horse radish peroxidase conjugated secondary antibody (1:5,000) was chosen to match the primary antibody species used. Housekeeping gene β-actin (**#** 5125) (Cell Signaling Technology) was used as loading control.

ImageQuant LAS 500 (GE Healthcare) was used to develop the membrane. The protein of interest and housekeeping gene were quantified using ImageJ. The protein ratio was normalized to the housekeeping gene; a ratio of protein: housekeeping gene < 0.2 was considered negative, between 0.2-0.4 weakly positive and > 0.4 strongly positive [7]. The expression ratio was the average of the protein's expression in multiple blots at various times after normalizing to the housekeeping gene. For p53 mutation status in AML patients' samples, next generation sequencing (NGS) technique was used and assessed by Alberta Precision Laboratories at the University of Alberta Hospital.

3.2.5 Cell Viability

Cells were treated with escalating doses of TMZ; 5, 10, 15, 20, 50 and 100 μM. For IDA, concentrations 2.5, 5, 10, 1000 and 2500 nM were used. The treated cells were incubated at 37°C and 5% CO_2 with a single drug for 48 hours for drug sensitivity screening and determining the 50% inhibitory concentrations (IC50).

For cell line, 0.2×10^6 cells/mL of KG1, MV4-11 and MOLM13 cells were incubated in RPMI 1640 and OCI-AML3 in MEM α at 37°C with 5% CO_2. The KG1 a p53 mutated cell line, was used a negative control, while MV4-11, MOLM13 and OCI-AML3 are p53 wild-type and were used as positive test samples. After 48 hours, the cell viability was evaluated using PrestoBlue assay. For the test principle, refer to Section 2.2.5.

For AML patients' samples viability, 2×10^6 cells were plated in serum-free expansion medium (SFEM), containing $CD34^+$ expansion supplement, StemRegenin1 (SR1) and UM729 (pyrimido-[4,5-b]-indole derivative) supplements (Stem Cell Technologies). The CellTiter-Fluor (Promega) was used to determine the patients' cell viability. For the test principle, refer to Section 2.2.5.

Both experimental protocols were followed as per manufacturer's recommendation. All samples were read in a black well plate with a clear bottom to reduce the background noise and improve specificity. The results were normalised to untreated cells to calculate the viability percentage. Low viability percentage indicates the drug efficacy to inhibit the cell proliferation and promote cell death.

3.2.6 DNA Damage

A total of 0.1×10^6 cells for leukemia cell lines and between $0.1 – 0.3 \times 10^6$ of fresh isolated patient cells were treated with selected doses of TMZ and IDA separately and combined. The

cell lines were incubated in designated media and patient cells in SFEM for six hours. The Alkaline Comet Assay was used to assess the DNA damage that may occur after treatment. The damaged DNA migrates out of the nucleoid under the influence of an electric current, whereas intact DNA does not. Trevigen kit (Catalog # 4250-050-K**)** was used with minor modifications. After six hours incubation, the cells were washed and suspended in PBS. A 1:10 ratio of treated cell suspension and 1% low-melting agarose was applied on comet microscopic slide. The coated slides were incubated in the dark for 10 min at room temperature then 30 min at 4 °C to solidify the gel. Slides were immersed in lysis solution, cooling for 20 min, and then incubated at 4 °C overnight. The next day, the slides were incubated for one hour in freshly prepared alkaline unwinding solution (pH > 13) at 4 °C.

Slides were subjected to electrophoresis at 25 V using fresh alkaline solution (pH > 13) for 90 min; the slides were washed with dH_2O, then incubated for 5 min in 70% ethanol. Dried slides were stained with 1x Syber DNA gel stain for 30 min. A fluorescence microscope (Invitrogen EVOS M5000 Imaging System) was used to detect 100 cells per sample. For analysis, CometScore software was used to quantify the comet tail DNA percentage, which is 100 × tail DNA intensity/ cell DNA intensity [24]. High tails DNA percentage is displayed long comet tails microscopically and indicates DNA damaged caused by the treatment.

3.2.7 Statistical Test

Graphs were represented as means $\pm$ standard deviation. Paired *t*- test and Mann-Whitney were used to calculate the P value for AML cell lines and patient samples, respectively. The test compared the mean of TMZ and IDA alone verses the combination at each concentration. P values ≤ 0.05 were considered statistically significant; these were annotated in the figures as: * $P \leq 0.05$, ** $P < 0.005$, *** $P < 0.001$, $P < 0.0001$ and ns as not significant.

3.3 Results

3.3.1 AML Cell Lines

3.3.1.1 Protein Expression

MGMT protein was highly expressed in both KG1 and OCI-AML3, and absent in MV4-11 and MOLM13 (Fig. 3.1 A). MV4-11, MOLM13 and OCI-AML3 had strong p53 expression, while; KG1 (p53 mutated cell line) did not. Acordingly, MDM2 level was strongly expressed in MV4-11, MOLM13 and OCI-AML3, and it was absent in KG1, as shown in Figs. 3.1 B and C.

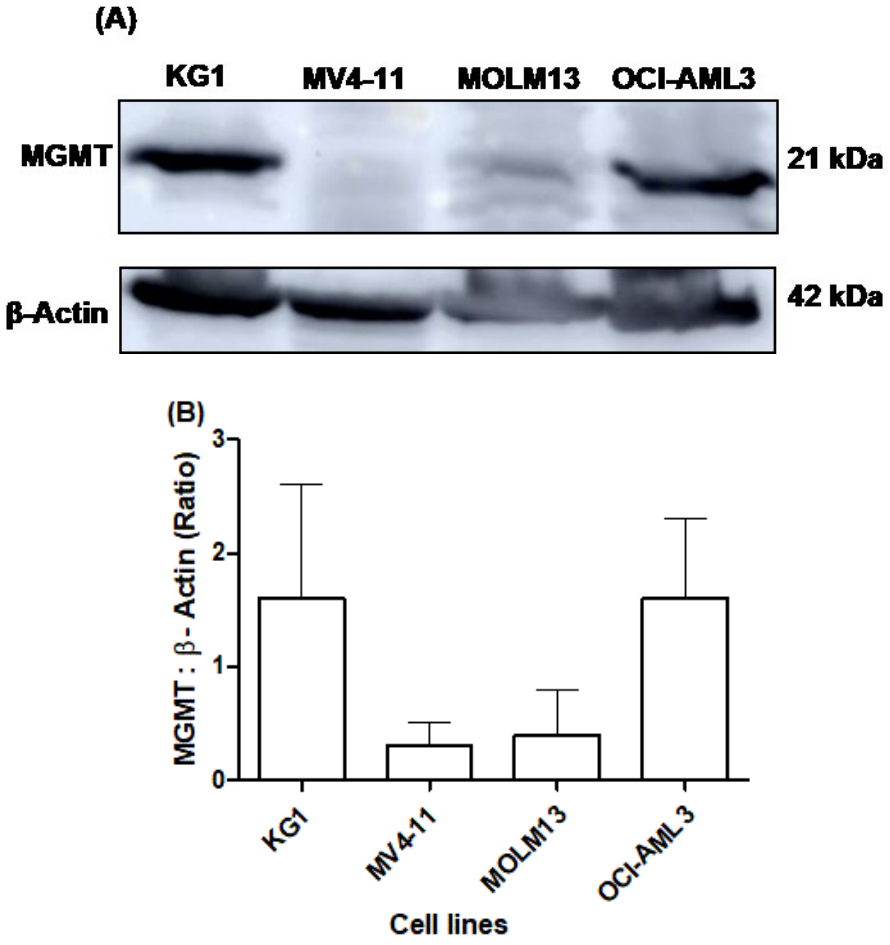

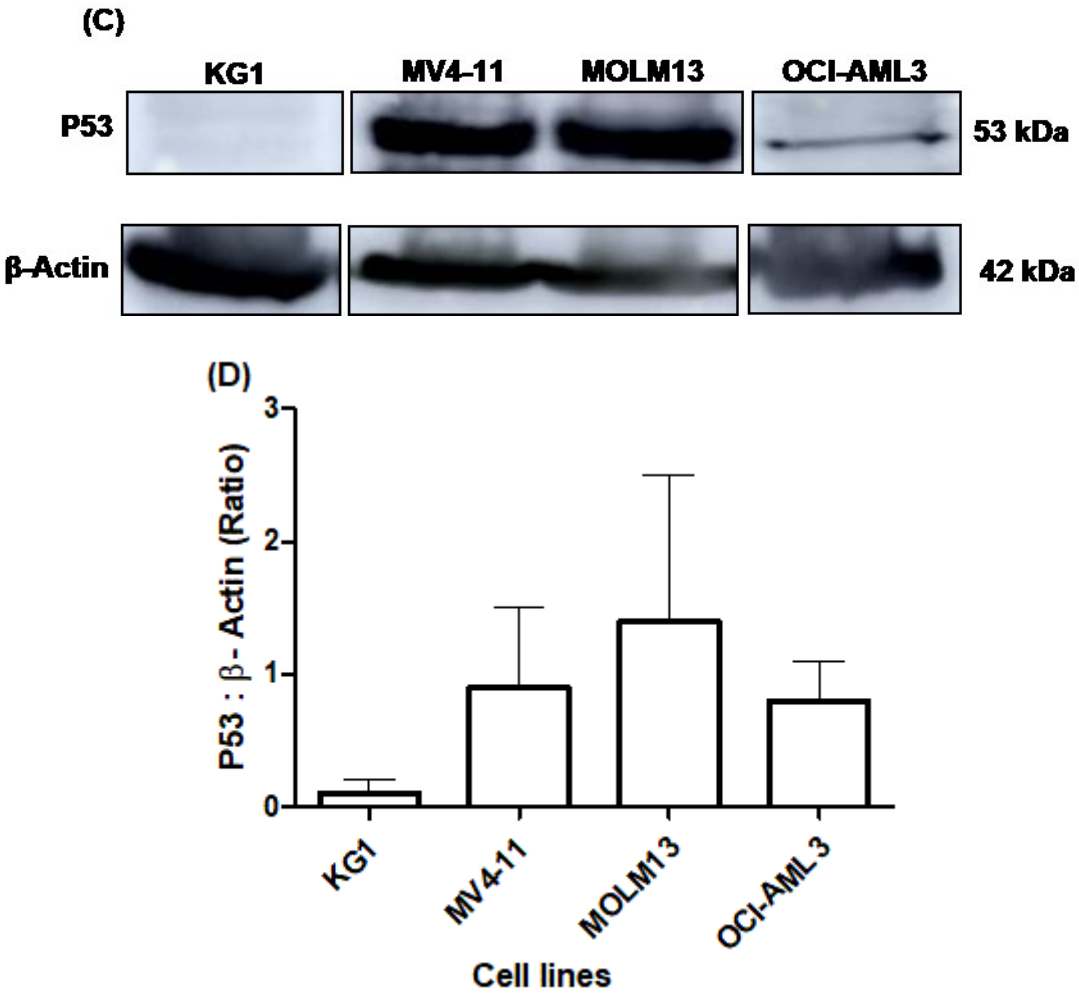
(C)
KG1
MV4-11
MOLM13
OCI-AML3
P53
53 kDa
β-Actin
42 kDa
(D)
P53 : β- Actin (Ratio)
3
2
1
0
KG1
MV4-11
MOLM13
OCI-AML3
Cell lines

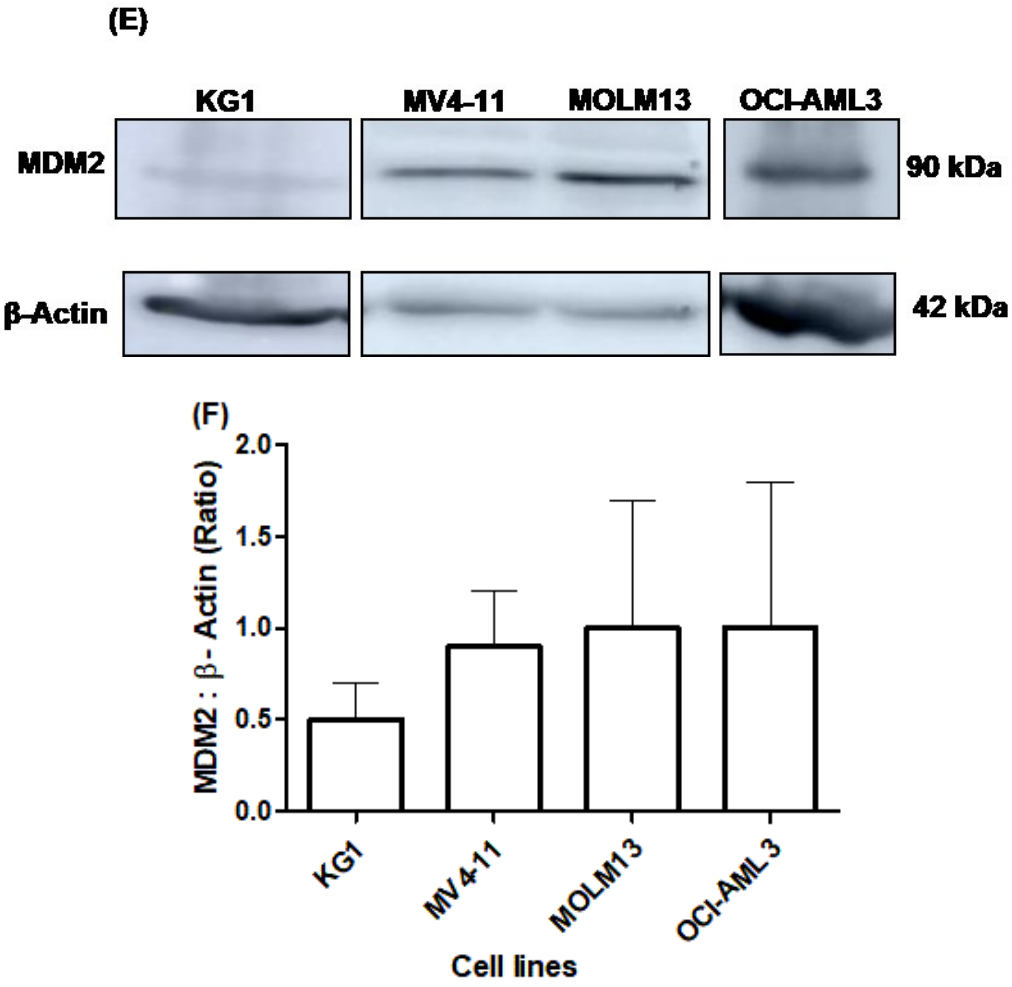

Figure 3.1: Immunoblotting of MGMT, p53 and MDM2 in AML cell lines. (A, B) MGMT (21 kDa), **(C, D)** p53 (53 kDa), and **(E, F)** MDM2 (90 kDa). A β-Actin (42 kDa) was used as loading control. The indicated protein expression was determined using whole-cell lysate that was subjected to Western blot and probed with specific antibodies. MGMT: KG1 (n= 18), MV4-11 (n= 16), MOLM13 (n= 16) and OCI-AML3 (n= 3); p53: KG1 (n= 8), MV4-11 (n= 6), MOLM13 (n= 7) and OCI-AML3 (n= 3); MDM2: KG1 (n= 8), MV4-11 (n= 6), MOLM13 (n= 7) and OCI-AML3 (n= 2).

3.3.1.2 Cell Viability

The leukemia cell lines' viability was evaluated after treating with pre-selected concentrations of the TMZ and IDA inhibitor for 48 hours. In term of TMZ, both KG1 and OCI-AML3 showed resistance by maintaining a high cell viability. However, MV4-11 and MOLM13 were more sensitive, with cell viability reduced to around 50% at 20 and 50 µM, respectively (Fig. 3.2 A).

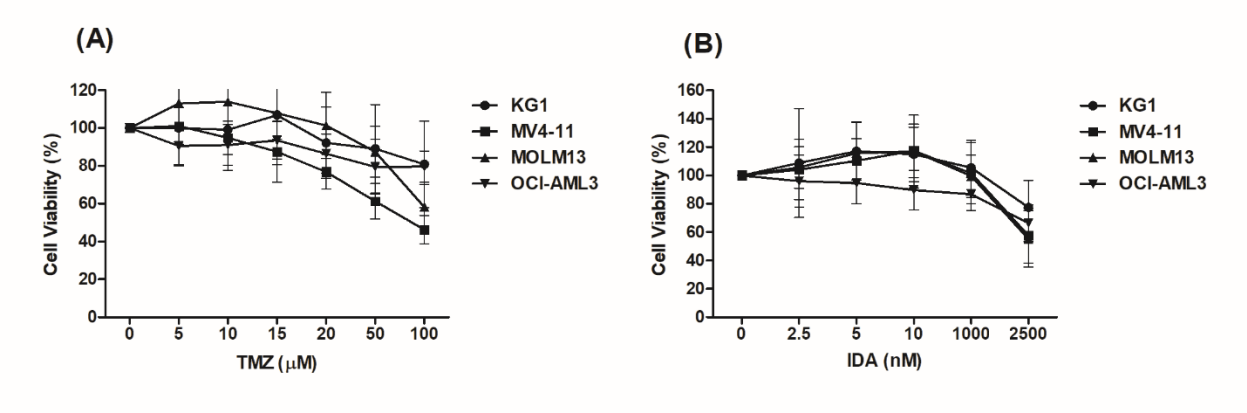

Figure 3.2: Cell line viability after treatment for 48 hours with TMZ and IDA separately. **(A)** TMZ, and **(B)** IDA. (●) KG1, (■) MV4-11, (▲) MOLM13, and (▼) OCI-AML3. Graphs represent as mean ± standard deviation. TMZ: KG1 (n= 8), MV4-11 (n= 8), MOLM13 (n= 9) and OCI-AML3 (n= 4); IDA: KG1 (n= 8), MV4-11 (n= 7), MOLM13 (n= 7) and OCI-AML3 (n= 4).

In terms of IDA inhibitor, KG1 and OCI-AML3 demonstrated resistance at all concentration, except at 2500 nM. At this concentration the residual cell viability was 78 and 67%, respectively. The same effect was noted in MV4-11 and MOLM13, however the vitality was inhibited to 58 and 55% respectively at the same concentration (Fig. 3.2 B).

In the KG1 and OCI-AML3 cell lines, adding 2500 nM IDA to TMZ did not change (P > 0.05) the sensitivity despite the difference in p53 expression and mutation status; the cell viability persisted in combination after 48 hours (Figs. 3.3 A and B).

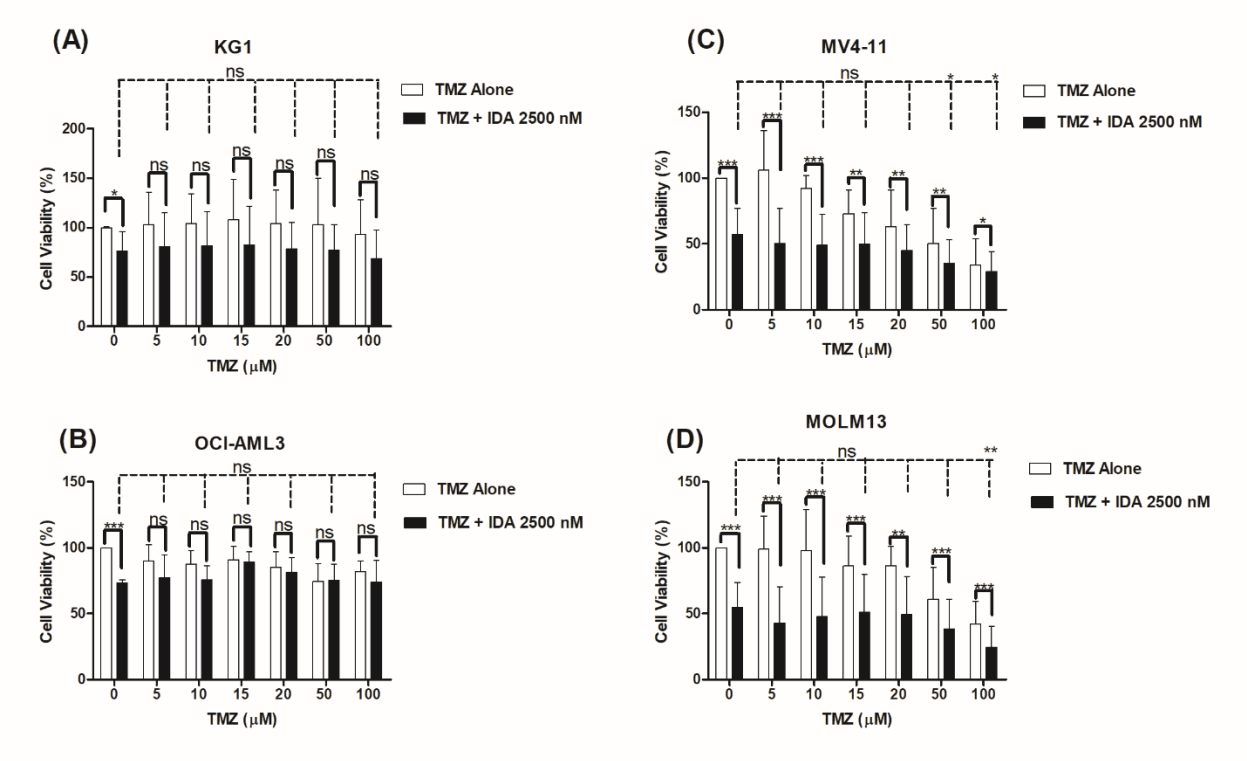

Figure 3.3: Cell lines viability after treatment for 48 hours with TMZ alone (□) and combination with 2500 nM IDA (■). (A) KG1 (n= 7), **(B)** OCI-AML3 (n= 3), **(C)** MV4-11 (n= 7), and **(D)** MOLM13 (n= 7). Graphs represent the mean ± standard deviation. The paired *t*-test was used to compare the mean of TMZ and IDA alone versus the combination. The annotated: * P < 0.05, ** P < 0.005, *** P < 0.001, and < 0.0001 and ns as not significant.

In contrast to the resistance observed in KG1 and OCI-AML3 cells, the combination of TMZ and IDA significantly (P < 0.0005) reduced the cell viability of MV4-11 and MOLM13 cells to ≤ 50% compared to TMZ alone. However, the viability was not significantly different between 2500 nM IDA alone and IDA combined with TMZ at TMZ concentrations up to 20 μM (P >

0.05) (Figs. 3.3 C and D). There was an additive effect of the combination seen in MV4-11 at 50 and 100 μM and in MOLM13 at 100 μM.

3.3.1.3 DNA Damage

In KG1 and OCI-AML3, a similar DNA percentage in comet tails was obtained when treated with TMZ alone or combined with 2500 nM IDA ($P > 0.05$). There was also no significant increase in the number of DNA strand breaks in KG1 and OCI-AML3 treated with IDA alone compared to the combination ($P > 0.05$) (Figs. 3.4 A- D).

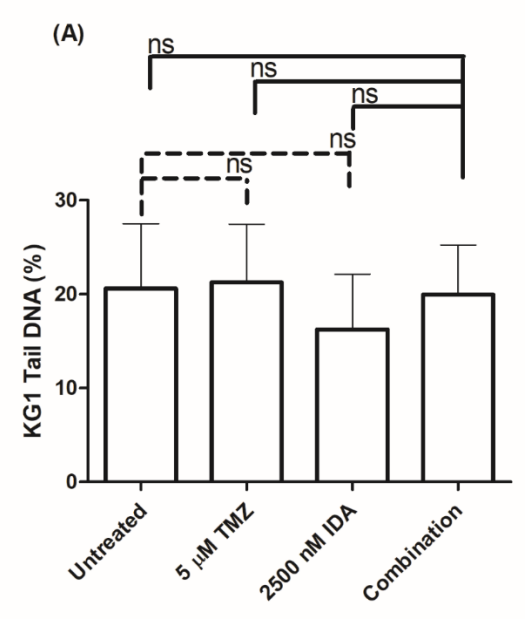
(A)
ns
ns
ns
ns
ns
KG1 Tail DNA (%)
30
20
10
0
Untreated
5 μM TMZ
2500 nM IDA
Combination

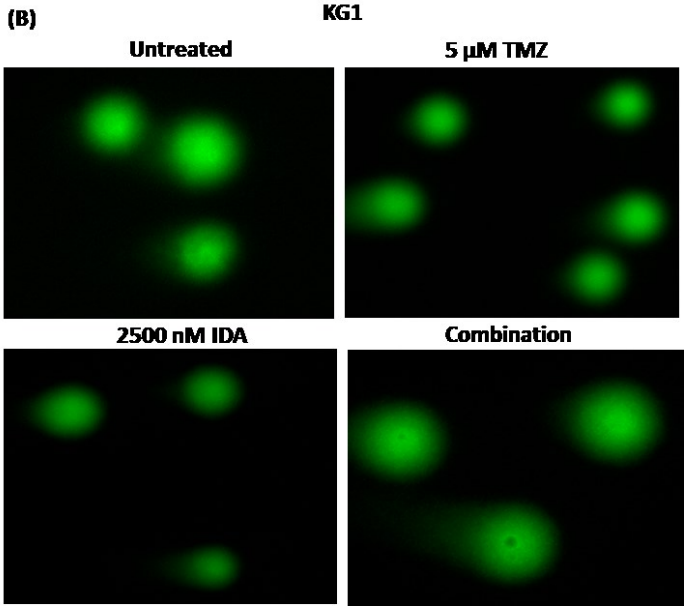
(B)
KG1
Untreated
5 μM TMZ
2500 nM IDA
Combination

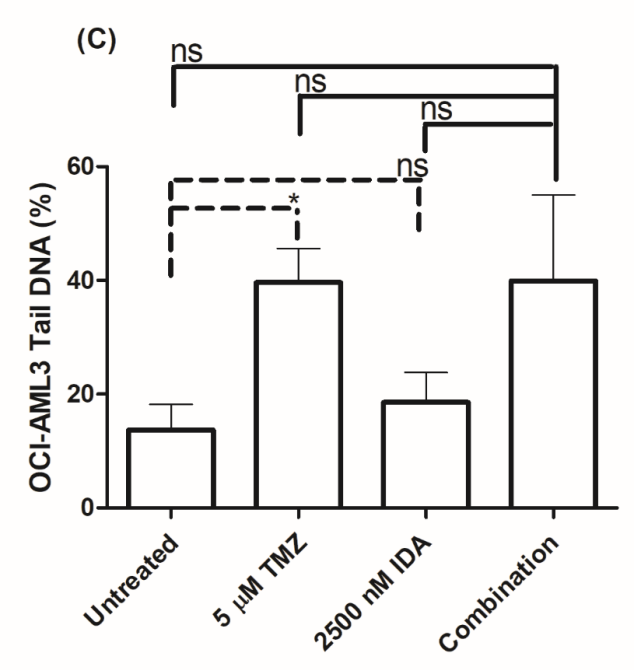
(C)
ns
ns
ns
ns
*
60
40
20
0
OCI-AML3 Tail DNA (%)
Untreated
5 μM TMZ
2500 nM IDA
Combination

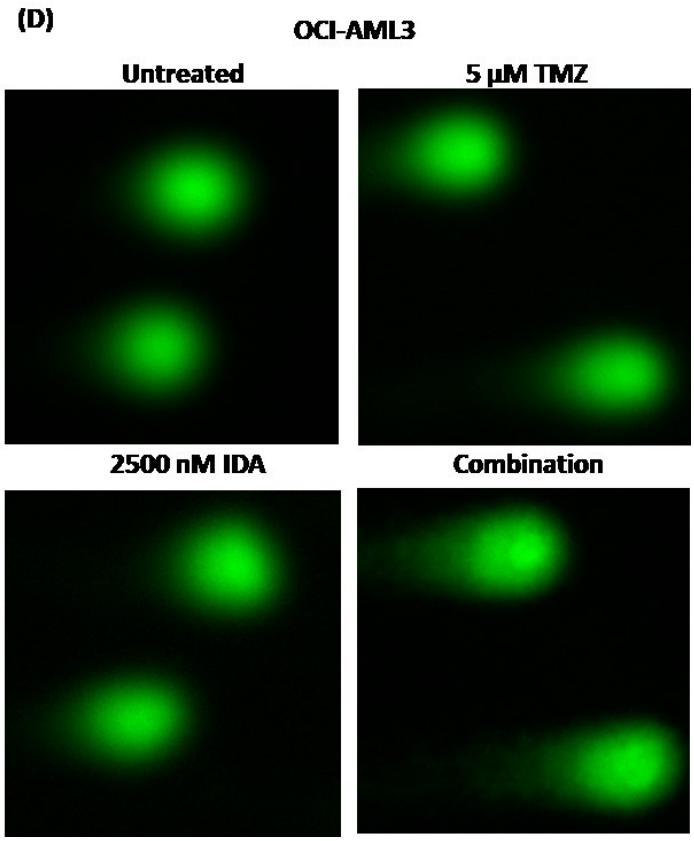
(D)
OCI-AML3
Untreated
5 μM TMZ
2500 nM IDA
Combination

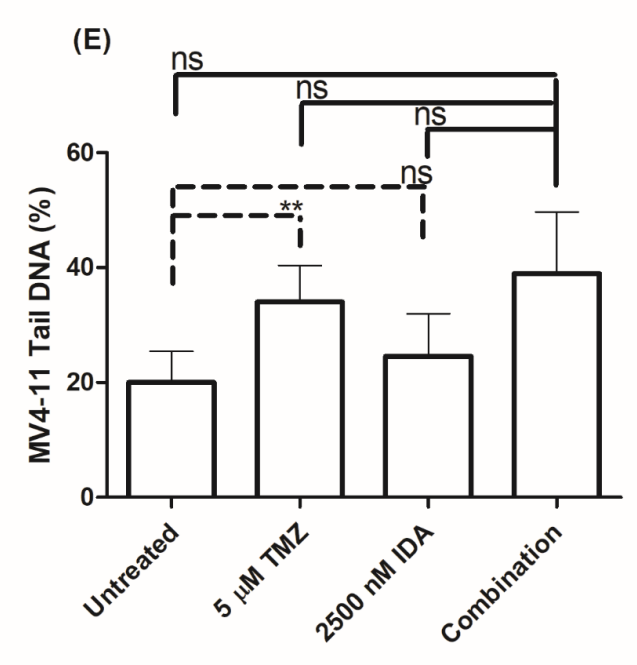
(E)
ns
ns
ns
ns
**
60
40
20
0
MV4-11 Tail DNA (%)
Untreated
5 μM TMZ
2500 nM IDA
Combination

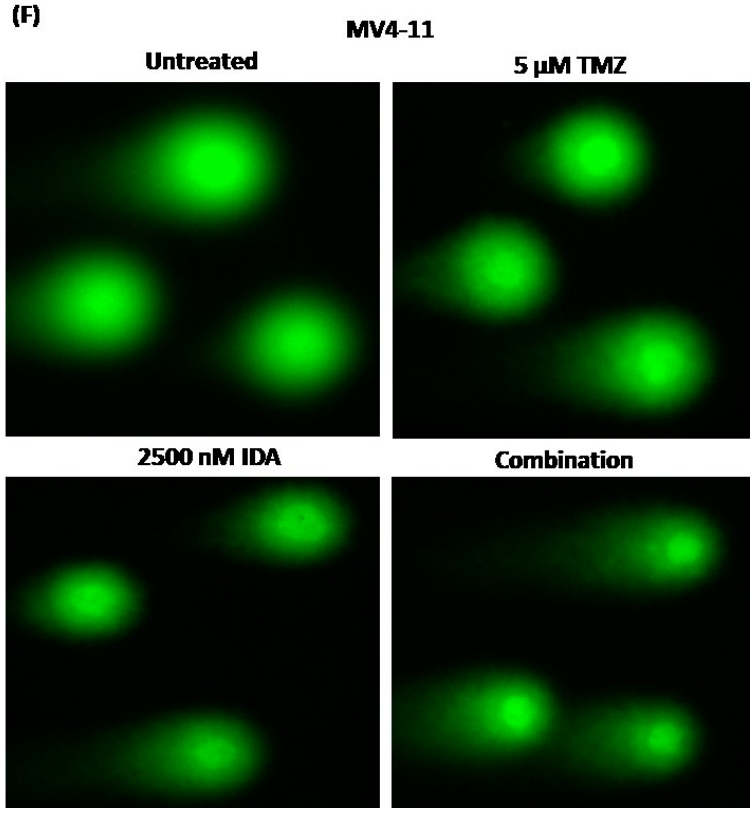
(F)
MV4-11
Untreated
5 μM TMZ
2500 nM IDA
Combination

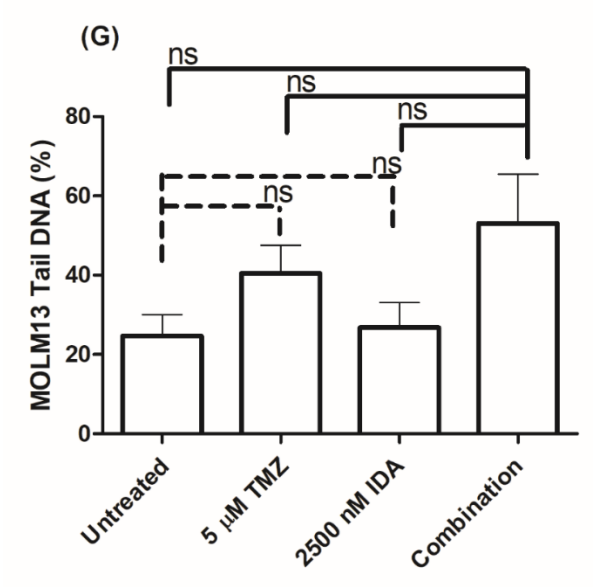

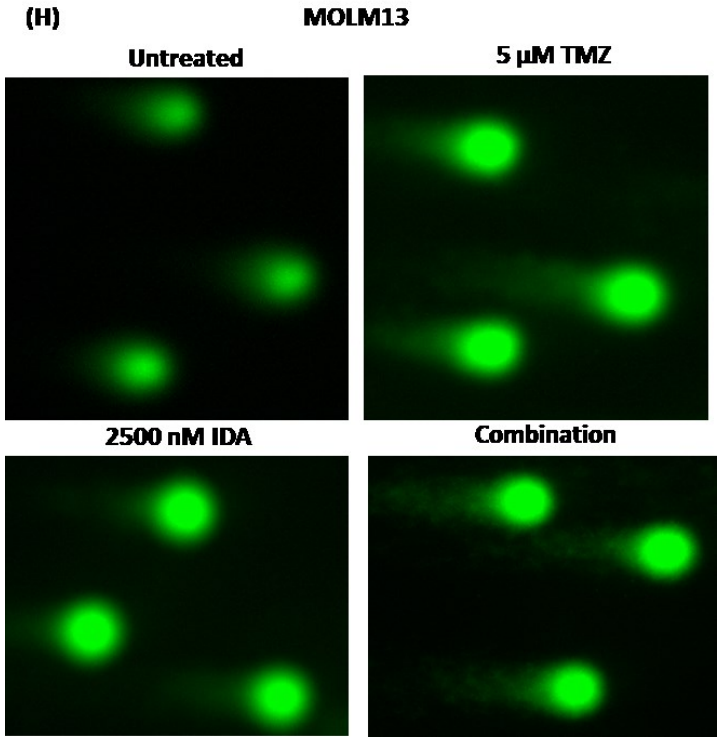

Figure 3.4: Leukemia cell lines tail DNA percentage after 6 hours of treatment with 5 μM TMZ and 2500 nM IDA. (A, B) KG1 (n= 2), **(C, D)** OCI-AML3 (n= 2), **(E, F)** MV4-11 (n= 2), and **(G, H)** MOLM13 (n= 2). Graphs represent the mean of 100 cells performed in duplicate at different time points ± standard deviation. The paired *t*-test was used to compare the mean of

untreated and the combination versus TMZ and IDA alone. The annotated: * $P < 0.05$, ** $P < 0.005$, and ns as not significant.

Similar results were obtained in MV4-11 and MOLM13 (Figs. 3.4 E-H). The DNA strand breaks in the comet tails were not significantly different in the combination compared to each drug alone ($P > 0.05$). As previously determined, TMZ caused significant DNA strand breaks in MV4-11 compared to untreated cells.

3.3.2 Acute Myeloid Leukemia Patient Samples

3.3.2.1 Protein Expression

Nine leukemia patients' samples were recruited for the IDA combination study, whose high levels of MGMT expression were detected by Western blot except for one sample (AML # 174); please refer to the Appendix for each patient Western blot. The NGS for p53 status demonstrated wild-type in all selected patients except one (AML # 188) (Table 3.1). The majority of samples had wild-type *FLT3-ITD* and *NPM1* mutation status; three had the NPM1 mutation and two had both.

Table 3.1: AML patient samples - baseline characteristics, MGMT, p53 and MDM2 proteins expression and TMZ and IDA drug sensitivity

	AML #	206	191	188	174	129	67	61	44	32
	Blasts (%)	92	96	89	92	76	80	88	78	89
	Cytogenetics	del7q	Normal	Complex	t(9;11)	11q23/ MLL rearrangement	Normal	UK	Normal	del3q
Molecular	FLT3-ITD	Wild type	Wild type	Wild type	Mutated	Wild type	Wild type	Mutated	Mutated	Wild type
Molecular	NPM1	Wild type	Wild type	Wild type	Wild type	Wild type	Mutated	Mutated	Mutated	Wild type
	MGMT: β-Actin (Ratio) †	0.7	0.4	0.4	0	0.6	0.4	0.8	0.9	0.5
	P53 (NGS)	Wild type	Wild-type	Mutant	Wild-type	Wild-type	Wild-type	Wild-type	Wild-type	Wild-type
*Sensitivity	TMZ	-	-	-	-	-	-	-	-	-
*Sensitivity	IDA	++	++	-	++	++	++	++	++	++
*Sensitivity	Combination	++	++	-	++	++	++	++	++	++

†Protein: β-actin ratio < 0.2 negative, 0.2-0.4 weak + and > 0.4 strong +, the MGMT protein expression was determined using patient's whole-cell lysate that was subjected to Western blot and probed with specific antibodies. P53 status was determined using NGS. * Viability

sensitivity determined at 5 µM TMZ and 2500 nM IDA separately and combined: (-): ≥ 60%, (+): ≤ 50%, (++): ≤ 20%.

del, deletion; FLT3-ITD, FMS-like tyrosine kinase3-internal tandem duplication; IDA, Idasanutlin; MGMT, O^6-methylguanine methyltransferase; MLL, mixed-lineage leukemia; NPM1, Nucleophosmin; NSG, next generation sequence; t, translocation; TMZ, Temozolomide; UK: Unknown.

3.3.2.2 Cell Viability

Figure 3.5 A depicts the viability of the AML patient samples after 48 hours of TMZ treatment alone. Viability was maintained with an average of 90% up to 20 µM and reduced at higher concentrations.

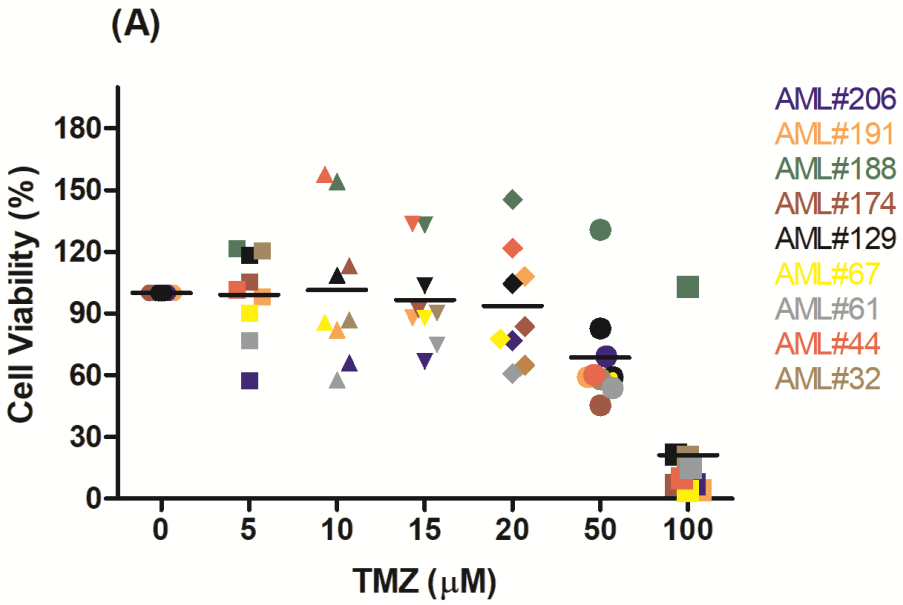

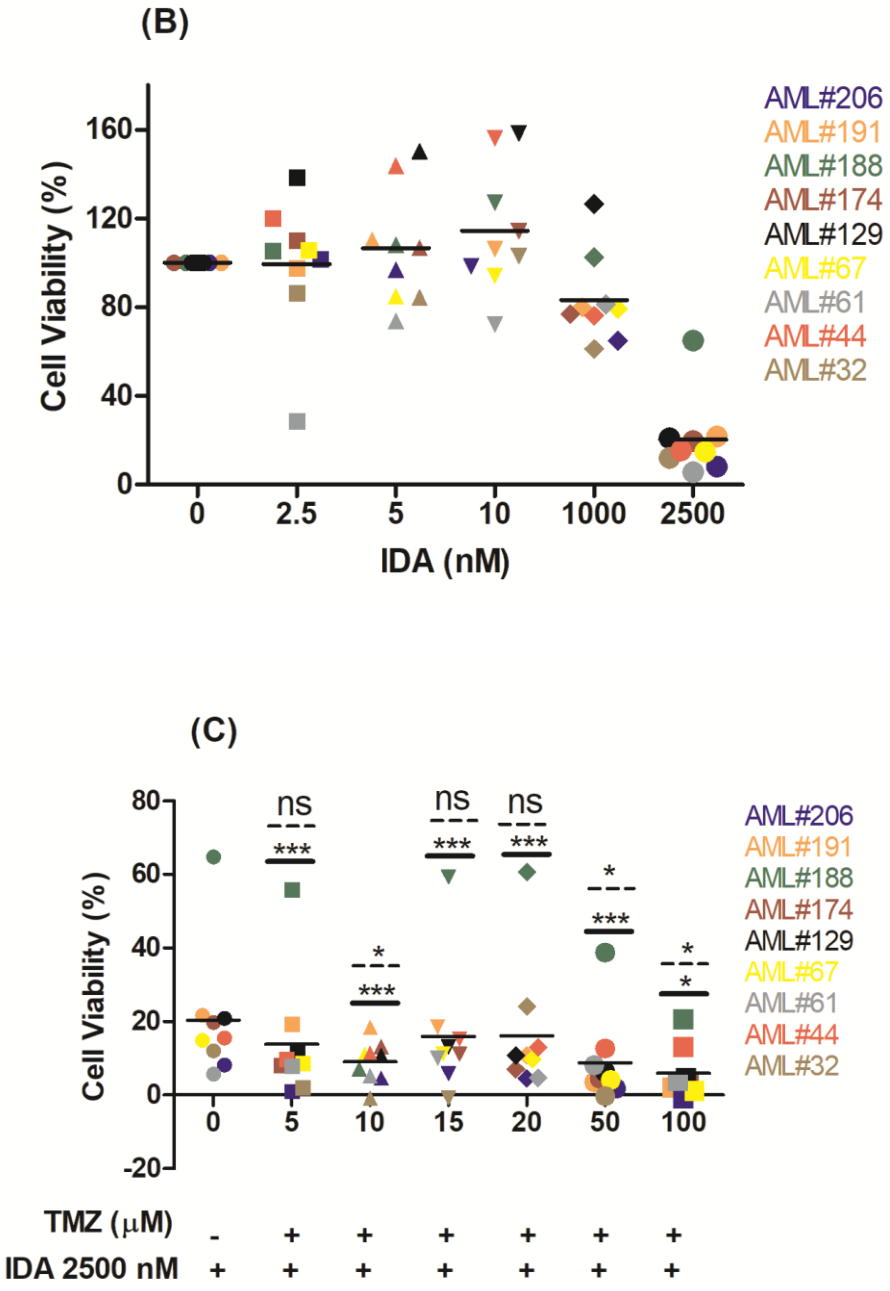

Figure 3.5: AML patient's cell viability after 48 hours of treatment with TMZ and IDA separately and combined. (A) TMZ, **(B)** IDA, and **(C)** TMZ combined with 2500 nM of IDA. Nine patients' samples were selected and treated for 48 hours with TMZ and IDA separately and combined. Each mark represents the mean ± standard division of cell viability performed once in triplicate, due to sample limited availability per patient. Mann-Whitney test was used to compare

the mean of (−) TMZ alone (Figure A) versus the combination at corresponding TMZ concentration. The (---) represents comparing the mean of 2500 nM IDA alone versus the combination. The annotated: * $P \leq 0.05$, *** $P < 0.001$ and ns as insignificant.

The IDA alone inhibited the cells' growth at 1000 and 2500 nM concentrations (Fig. 3.5 B). At 2500 nM concentration the cell viability dramatically decreased to ≤ 20% (Table 3.2). This concentration was chosen for the combination experiment based on the IC50 of cell line (OCI-AML3) high-MGMT expressing and wild-type p53 as most of our patients. Since only 20% of the cell viability was remaining at 2500 nM alone, adding this concentration to the TMZ did not cause a further decrease in viability, as demonstrated in Fig. 3.5 C. In the Appendix, each patient viability result is displayed individually.

3.3.2.3 DNA Damage

DNA damage was assessed in two fresh patient samples by alkaline comet assay. There was a significant increase ($P < 0.05$) in damage using the combination compared to each one alone in AML# 206 sample, but not in AML# 266. In both samples, no difference was observed between untreated cells and TMZ alone (Figs. 3.6 A and B).

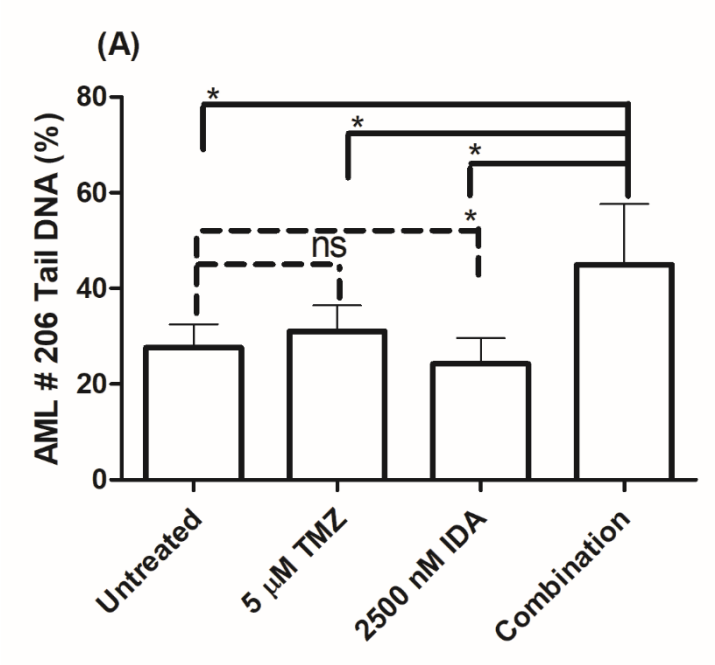
(A)
AML # 206 Tail DNA (%)
80
60
40
20
0
*
*
*
*
ns
Untreated
5 µM TMZ
2500 nM IDA
Combination

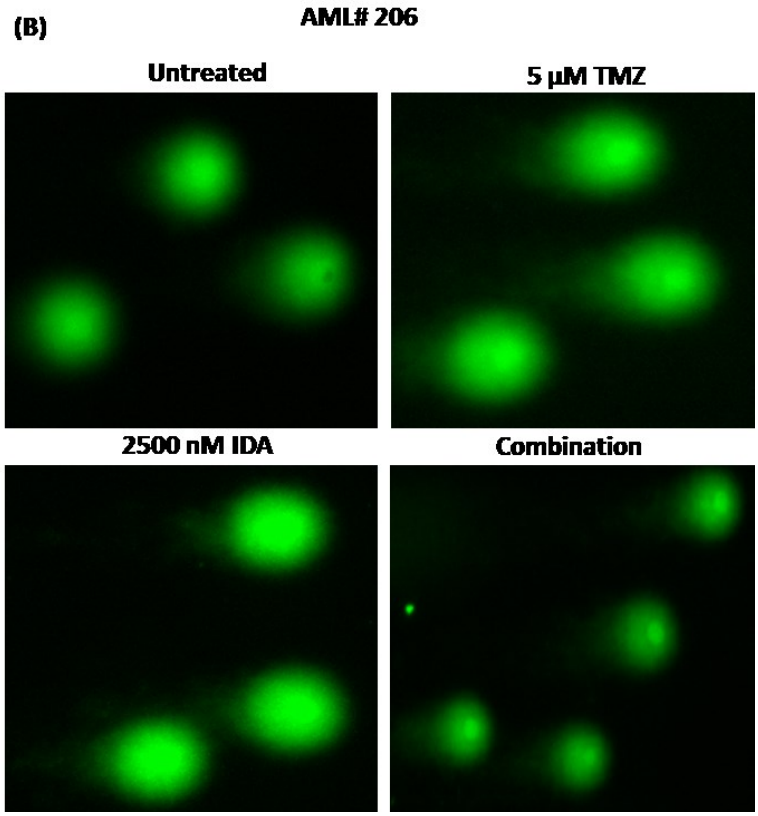
(B)
AML# 206
Untreated
5 µM TMZ
2500 nM IDA
Combination

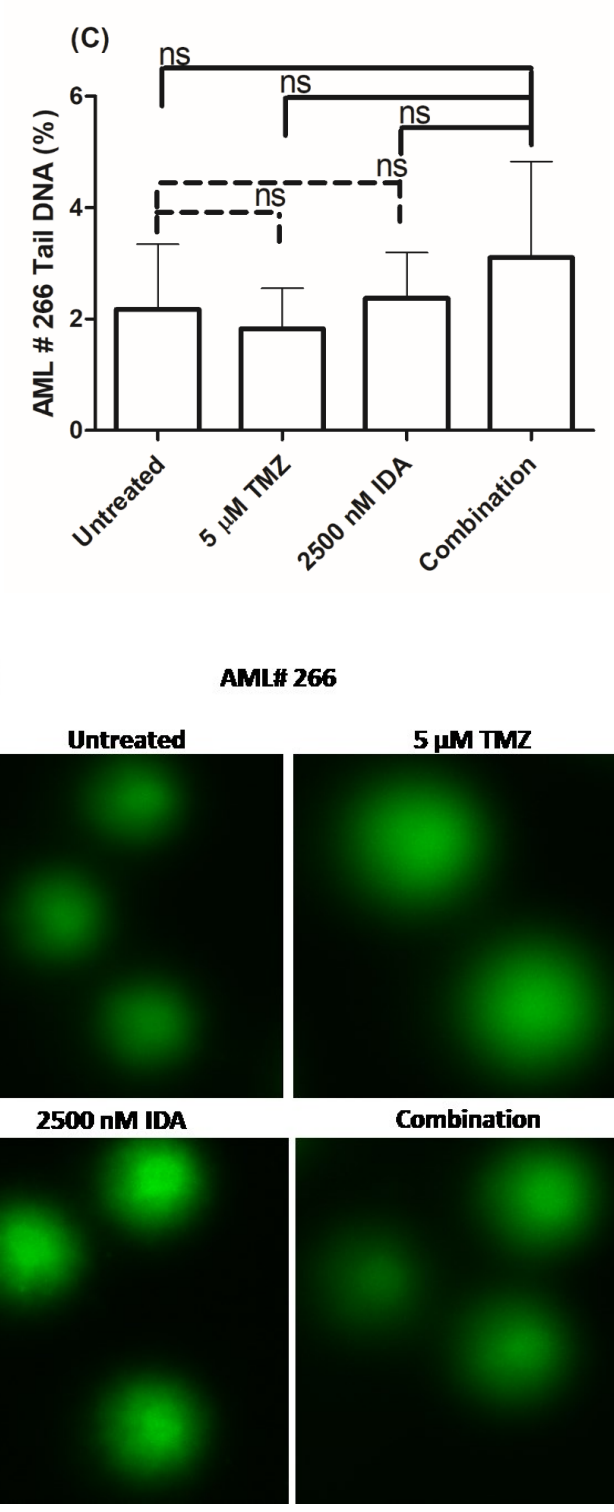

Figure 3.6: Tails DNA percentage of AML patient's cells after 6 hours of treatment with 5 μM TMZ and 2500 nM IDA. (A, B) 206, and **(C, D)** 266. Graphs represent the mean of 50 cells performed in duplicate ± standard deviation. The paired *t*-test was used to compare the mean of

untreated and the combination versus TMZ and IDA alone. The annotated: * $P < 0.05$, and ns as not significant. AML# 206 MGMT ratio 0.7 and wild-type p53; AML# 266 MGMT ratio 2.4 and wild-type p53. Please refer to the Appendix for each patient's Western blot MGMT expression.

3.4 Discussion

This study was conducted to determine whether TMZ sensitivity in AML cells could be enhanced by incorporating a specific targeted MDM2 inhibitor, IDA, into the treatment regimen. The KG1, OCI-AML3, MV4-11 and MOLM13 cell lines were chosen as our models. The level of the DNA repair protein MGMT was assessed before treating the cells with TMZ. KG1 and OCI-AML3 expressed high levels of MGMT. Consequently, these two cell lines demonstrated a strong resistance to TMZ alone. This effect is mediated by MGMT, which can reverse the DNA methylation induced by TMZ, as mentioned earlier. Conversely, MV4-11 and MOLM13 had low MGMT expression, resulting in an adequate sensitivity to TMZ. Thus, the DNA methylation induced by TMZ is able to cause cell death in low-MGMT expressing cells. However, TMZ sensitivity needs to be enhanced to promote cell death at low concentrations.

Regarding the MDM2 inhibitor, IDA was selected as the most clinically available and highly potent agent. P53 and MDM2 levels were evaluated in the same selected cell lines. Both proteins were evaluated as they strongly correlated under the autoregulatory feedback loop. OCI-AML3, MV4-11 and MOLM13 had wild-type p53 and consequently expressed high levels of MDM2. On the other hand, KG1 had mutant p53 and low MDM2 expression.

The relationship between p53 and MGMT expression is unclear. Wild-type p53 cells have variable levels of MGMT expression. Wild-type p53 MV4-11 and MOLM13 demonstrated low MGMT expression. It is possible that p53 may impact MGMT expression, as it can downregulate

MGMT through sequestration of the SP1 transcription factor. Overexpression of SP1 prevents it from binding the cognate *cis*-elements in the MGMT promoter [25]. Conversely, in some cell types wild-type p53 has been correlated with a high MGMT level. When cells are exposed to ionizing radiation or alkylating agents, p53 is necessary to upregulate MGMT for DNA repair mechanisms [25]. *MGMT* mRNA and protein were detected in murine wild-type p53 astrocytes. Knockdown of wild-type p53 by RNA interference significantly inhibited MGMT expression (> 90%) [26]. This is representative of the OCI-AML3 cell line, which has both p53 and MGMT proteins. In mutant p53 cell such as KG1 the MGMT is high, which facilitates DNA repair and causes cell survival [27].

Treating the cells with IDA alone revealed resistance at all concentrations, except at 2500 nM, which is clinically achievable to use in patients. MV4-11 and MOLM13 were more responsive at this concentration compared to KG1 and OCI-AML3. Interestingly, OCI-AML3 demonstrated resistance to TMZ and IDA. This cell line can survive TMZ through two DNA-repairing pathways, directly through MGMT in a one-step reaction that removes the methyl group added by TMZ or indirectly through the p53 repair mechanism, which also indirectly induces MGMT transcription, as mentioned earlier.

Regarding IDA resistance, a similar result was obtained in the study by Lehmann *et al*. [17] when treating OCI-AML3 with IDA alone. Cell viability was maintained, and cell apoptosis was minimal at the tested concentrations, which ranged from 1 to 1000 nM.

We added IDA to the TMZ treated cells in order to increase TMZ sensitivity. This was done at the 48-hour time-point for TMZ to enable the determination of the baseline sensitivity before the addition of IDA. While for IDA's 48-hour was also chose to identify the IC50 dosage that will be

combined with TMZ for each cell line. The 2500 nM concentration of IDA was preferred over 1000 nM due to the significant inhibition caused in all tested cell lines.

KG1 and OCI-AML3 viability was maintained after adding IDA to TMZ at all concentration; therefore, this combination provided no advantage in these cells. This is likely related to the p53 mutated status in KG1 and high MGMT expression in OCI-AML3. In contrast, more inhibition was observed in MV4-11 and MOLM13 cells treated with the combination compared to those treated with TMZ alone. However, upon closer evaluation, the IDA was found to be responsible for the inhibition, as evidenced by the non-significant difference between the use of 2500 nM IDA alone and in combination with TMZ concentrations. These findings indicate that TMZ sensitivity was not improved by adding IDA.

The TMZ and IDA combination did not cause increased DNA damage in any of the tested cell lines. In contrast to the combination and TMZ alone, cells treated with IDA alone had the lowest tail DNA %. A similar result was observed after treating melanoma cells with 100 μM TMZ and 10 μM of the MDM2 inhibitor nutlin-3a for 3 days. Nutlin-3a protected the cells from DNA damage caused by TMZ by inhibiting the DNA damage marker γH2AX. In the same study, IDA was used alone and in combination with a senescence-inducing inhibitor of the mitotic kinase Aurora A (AURKA). γH2AX was seen in AURKA inhibitor-treated cells only, in contrast to those treated with IDA alone or the combination of the two agents. MDM2 antagonists were concluded to protect the DNA from damage [28].

Most of the AML patients selected had weak to strongly positive MGMT expression (≥ 0.4). Consequently, the cells showed resistance when treated with TMZ alone. However, despite the wild-type p53 status in most samples (except AML# 188), the response to IDA alone was minimal at low concentrations (2.5, 5, 10 and 1000 nM) but they were sensitive to the 2500 nM

concentration, with only around 20% residual viability. At this concentration, in combination with 5 μM TMZ, the viability percentage was maintained across TMZ concentrations with no additive effect seen. The residual surviving cells were very resistant to both treatments and could possibly be leukemia stem-like cells that have a quiescent phenotype and are highly drug-resistant [29]. However, this would require further evaluation.

Three of our patient samples have FLT3 – ITD mutations. FLT3 activates tyrosine kinase, which activates phosphatidylinositol 3 kinase (PI3K)/RAS/ signal transducer and activator of transcription (STAT) pathways, which are correlated with low sensitivity to MDM2 inhibition [30]. However, we did not detect any differences in drug sensitivity between FLT3-ITD mutated and wild-type samples.

The DNA damage that may be caused by TMZ and IDA in AML patient blast cells was evaluated. AML# 206 showed increased damage in combination-treated cells compared to cells treated with each agent alone; however, AML# 266 was not affected. The differences in cell response to the treatment could be related to the MGMT level. AML# 206 had a lower MGMT level compared with AML # 266 (Ratio 0.7 and 2.4, respectively). IDA exerts an anti-tumour effect by limiting cell viability but does not affect DNA integration.

As mentioned earlier, IDA has been used in combination with cytarabine to treat R/R AML patients. Although this combination improved the ORR, there was no difference in OS between patients treated with cytarabine alone and those treated with IDA+cytarabine (median OS 8.3 vs. 9.1 months). The results were not considered promising enough to move forward with treating R/R AML patients; therefore, further development was not pursued [4]. As we found in this study, not much difference was seen when adding IDA to TMZ, regardless of p53 expression in

AML cell lines. Consequently, we do not feel that this combination warrants further evaluation in the mouse model or in humans.

The MDM2 antagonist theory is based on disrupting p53 and MDM2 binding to reactivate p53 functions, which range from cell cycle arrest to apoptosis. As mentioned earlier, most of our AML patients had wild-type p53, although their cells were still resistant to IDA, except at 2500 nM concentration. Additionally, DNA integrity was unaffected. Although MDM2 is overexpressed in AML, the effectiveness of the IDA was not as expected. This indicates that could be other mechanism interfere with IDA function and cause resistance.

3.5 References

1. Cassier PA, Castets M, Belhabri A, Vey N. Targeting apoptosis in acute myeloid leukaemia. Br J Cancer. 2017;117(8):1089-98.

2. Döhner H, Wei AH, Appelbaum FR, Craddock C, DiNardo CD, Dombret H, et al. Diagnosis and management of AML in adults: 2022 recommendations from an international expert panel on behalf of the ELN. Blood. 2022;140(12):1345-77.

3. Sasaki K, Ravandi F, Kadia TM, DiNardo CD, Short NJ, Borthakur G, et al. De novo acute myeloid leukemia: A population-based study of outcome in the United States based on the Surveillance, Epidemiology, and End Results (SEER) database, 1980 to 2017. Cancer. 2021;127(12):2049-61.

4. Konopleva MY, Röllig C, Cavenagh J, Deeren D, Girshova L, Krauter J, et al. Idasanutlin plus cytarabine in relapsed or refractory acute myeloid leukemia: results of the MIRROS trial. Blood Adv. 2022;6(14):4147-56.

5. Shinji K, Shinya T. Chemotherapeutic Agent for Glioma: IntechOpen; 2013. Available from: https://doi.org/10.5772/54353.

6. Verbeek B, Southgate TD, Gilham DE, Margison GP. O6-Methylguanine-DNA methyltransferase inactivation and chemotherapy. Br Med Bull. 2008;85:17-33.

7. Brandwein JM, Yang L, Schimmer AD, Schuh AC, Gupta V, Wells RA, et al. A phase II study of temozolomide therapy for poor-risk patients aged >or=60 years with acute myeloid leukemia: low levels of MGMT predict for response. Leukemia. 2007;21(4):821-4.

8. Brandwein JM, Kassis J, Leber B, Hogge D, Howson-Jan K, Minden MD, et al. Phase II study of targeted therapy with temozolomide in acute myeloid leukaemia and high-risk

myelodysplastic syndrome patients pre-screened for low O(6) -methylguanine DNA methyltransferase expression. Br J Haematol. 2014;167(5):664-70.

9. Hernández Borrero LJ, El-Deiry WS. Tumor suppressor p53: Biology, signaling pathways, and therapeutic targeting. Biochim Biophys Acta Rev Cancer. 2021;1876(1):188556.

10. Chen J. The Cell-Cycle Arrest and Apoptotic Functions of p53 in Tumor Initiation and Progression. Cold Spring Harb Perspect Med. 2016;6(3):a026104.

11. Weinberg RA. The Biology of Cancer. 1st ed. New York: Garland Science; 2007.

12. Zhu H, Almasan A. Development of venetoclax for therapy of lymphoid malignancies. Drug Des Devel Ther. 2017;11:685-94.

13. Korycka-Wolowiec A, Wolowiec D, Kubiak-Mlonka A, Robak T. Venetoclax in the treatment of chronic lymphocytic leukemia. Expert Opin Drug Metab Toxicol. 2019;15(5):353-66.

14. Jan R, Chaudhry GE. Understanding Apoptosis and Apoptotic Pathways Targeted Cancer Therapeutics. Adv Pharm Bull. 2019;9(2):205-18.

15. Abeloff's clinical oncology. 6th ed. Niederhuber JE, Armitage JO, Doroshow JH, Kastan MB, Tepper JE, Abeloff MD, editors: Elsevier; 2020.

16. George B, Kantarjian H, Baran N, Krocker JD, Rios A. TP53 in Acute Myeloid Leukemia: Molecular Aspects and Patterns of Mutation. Int J Mol Sci. 2021;22(19).

17. Lehmann C, Friess T, Birzele F, Kiialainen A, Dangl M. Superior anti-tumor activity of the MDM2 antagonist idasanutlin and the Bcl-2 inhibitor venetoclax in p53 wild-type acute myeloid leukemia models. J Hematol Oncol. 2016;9(1).

18. Quintás-Cardama A, Hu C, Qutub A, Qiu YH, Zhang X, Post SM, et al. P53 pathway dysfunction is highly prevalent in acute myeloid leukemia independent of TP53 mutational status. Leukemia. 2017;31(6):1296-305.

19. Neochoritis C, Estrada-Ortiz N, Khoury K, Dömling A. P53–MDM2 and MDMX Antagonists. In: Desai MC, editor. Annual Reports in Medicinal Chemistry. 49: Academic Press; 2014. p. 167-87.

20. Brooks CL, Gu W. Dynamics in the p53-Mdm2 ubiquitination pathway. Cell Cycle. 2004;3(7):895-9.

21. Reis B, Jukofsky L, Chen G, Martinelli G, Zhong H, So WV, et al. Acute myeloid leukemia patients' clinical response to idasanutlin (RG7388) is associated with pre-treatment MDM2 protein expression in leukemic blasts. Haematologica. 2016;101(5):e185-e8.

22. Yee K, Martinelli G, Vey N, Dickinson MJ, Seiter K, Assouline S, et al. Phase 1/1b Study of RG7388, a Potent MDM2 Antagonist, in Acute Myelogenous Leukemia (AML) Patients (Pts). Blood. 2014.

23. Daver NG, Dail M, Garcia JS, Jonas BA, Yee KWL, Kelly KR, et al. Venetoclax and idasanutlin in relapsed/refractory AML: a nonrandomized, open-label phase 1b trial. Blood. 2023;141(11):1265-76.

24. Comet Assay Kit (3-well slides) (ab238544): Abcam; 2018 [Available from: https://www.abcam.com/ps/products/238/ab238544/documents/Comet-Assay-protocol-book-v2b-ab238544%20(website).pdf.

25. Bocangel D, Sengupta S, Mitra S, Bhakat KK. p53-Mediated down-regulation of the human DNA repair gene O6-methylguanine-DNA methyltransferase (MGMT) via interaction with Sp1 transcription factor. Anticancer Res. 2009;29(10):3741-50.

26. Blough MD, Zlatescu MC, Cairncross JG. O6-methylguanine-DNA methyltransferase regulation by p53 in astrocytic cells. Cancer Res. 2007;67(2):580-4.

27. Baran K, Yang M, Dillon CP, Samson LL, Green DR. The proline rich domain of p53 is dispensable for MGMT-dependent DNA repair and cell survival following alkylation damage. Cell Death Differ. 2017;24(11):1925-36.

28. Vilgelm AE, Cobb P, Malikayil K, Flaherty D, Andrew Johnson C, Raman D, et al. MDM2 Antagonists Counteract Drug-Induced DNA Damage. EBioMedicine. 2017;24:43-55.

29. Long NA, Golla U, Sharma A, Claxton DF. Acute Myeloid Leukemia Stem Cells: Origin, Characteristics, and Clinical Implications. Stem Cell Rev and Rep. 2022;18(4):1211-26.

30. Haronikova L, Bonczek O, Zatloukalova P, Kokas-Zavadil F, Kucerikova M, Coates PJ, et al. Resistance mechanisms to inhibitors of p53-MDM2 interactions in cancer therapy: can we overcome them? Cell Mol Biol Lett. 2021;26(1):53.

CHAPTER 4

Discussion, Conclusion and Future Directions

4 Discussion, Conclusion and Future Directions

4.1 Discussion and Conclusion

Temozolomide (TMZ) is an alkylating agent that efficiently targets DNA by causing cell cycle arrest at the G2/M phase; it is well-tolerated and has demonstrated antileukemic activity in patients with acute myeloid leukemia (AML). However, antileukemic responses are limited to cells exhibiting very low or absent expression of the DNA repair protein methyl guanine methyl transferase (MGMT). Even in patients pre-selected for low/absent MGMT expression, most AML patients treated with TMZ did not respond. Only 28% had complete clearance of blasts in the marrow, with 22% having complete responses [1], indicating that other mechanisms mediating drug resistance must be circumvented.

This research focuses on exploring ways to enhance cytotoxicity to TMZ in both high and low-MGMT expressing AML cells by incorporating small molecule inhibitors targeting apoptotic pathways. We selected venetoclax (VEN) and idasanutlin (IDA), two potent and clinically available selective inhibitor drugs VEN inhibits the anti-apoptotic protein B-cell lymphoma-2 (BCL-2) to promote cell apoptosis, while IDA inhibits mouse double minute 2 homolog (MDM2) to disrupt the interaction with tumor suppressor p53 (p53) and restore its functions. As discussed, both agents have been used and shown to be well-tolerated when combined with conventional chemotherapy agents.

VEN was demonstrated to increase remission rates and overall survival (OS) in newly diagnosed AML patients (≥75 years) who were ineligible for intensive chemotherapy when given in combination with azacitidine [2] or low-dose cytarabine [3]. IDA also has increased response rates when given in combination with cytarabine to older AML patients [4].

As described in Chapter 2, TMZ was tested *in vitro* alone and in combination with VEN using AML cell lines and isolated blast-containing mononuclear cells (MNCs) obtained from patients. Furthermore, this combination was explored *in vivo* using a mouse model engrafted with an AML cell line. VEN enhanced TMZ sensitivity by decreasing cell viability, increasing apoptosis, and inducing DNA damage compared to TMZ alone in both high and low-MGMT expressing AML cells *in vitro*.

In KG1 and patients' samples highly expressing MGMT and BCL-2, the VEN+TMZ combination tended to inhibit cell viability and increase apoptosis. Inhibiting BCL-2 through VEN promotes cell death through intrinsic apoptotic pathway (IAP) activation, regardless of MGMT. As shown, this combination demonstrated an encouraging result in AML patients, which would strongly benefit them as they mainly show high MGMT and BCL-2 protein expression. VEN enhanced TMZ and significantly induced early and late apoptosis in KG1 compared to TMZ alone. This enhancement was observed in the apoptotic assay using flow cytometry due to KG1 resistance to TMZ alone. However, it was not achieved in the viability assay due to the large number of cell deaths obtained at a 1000 nM concentration of VEN alone, which made no difference when TMZ was added. Due to cell apoptosis, the signature death marker Cleaved-poly-(ADP ribose) polymerase 1 (C-PARP 1) was detected in VEN alone and in combination. PARP 1 can be cleaved through caspase-3 due to IAP activation, which occurs after BCL-2 inhibition by VEN (Fig. 4.1).

The VEN+TMZ induced extensive DNA damage in high-MGMT cells. The high quantities of DNA strand breaks observed could result from VEN inhibiting the base excision repair pathway mediated by PARP 1 after TMZ exposure (Fig. 4.1). Overall, PARP 1 was cleaved in KG1

treated with the combination to inhibit DNA repair and increase DNA strand breaks, resulting in cell apoptosis.

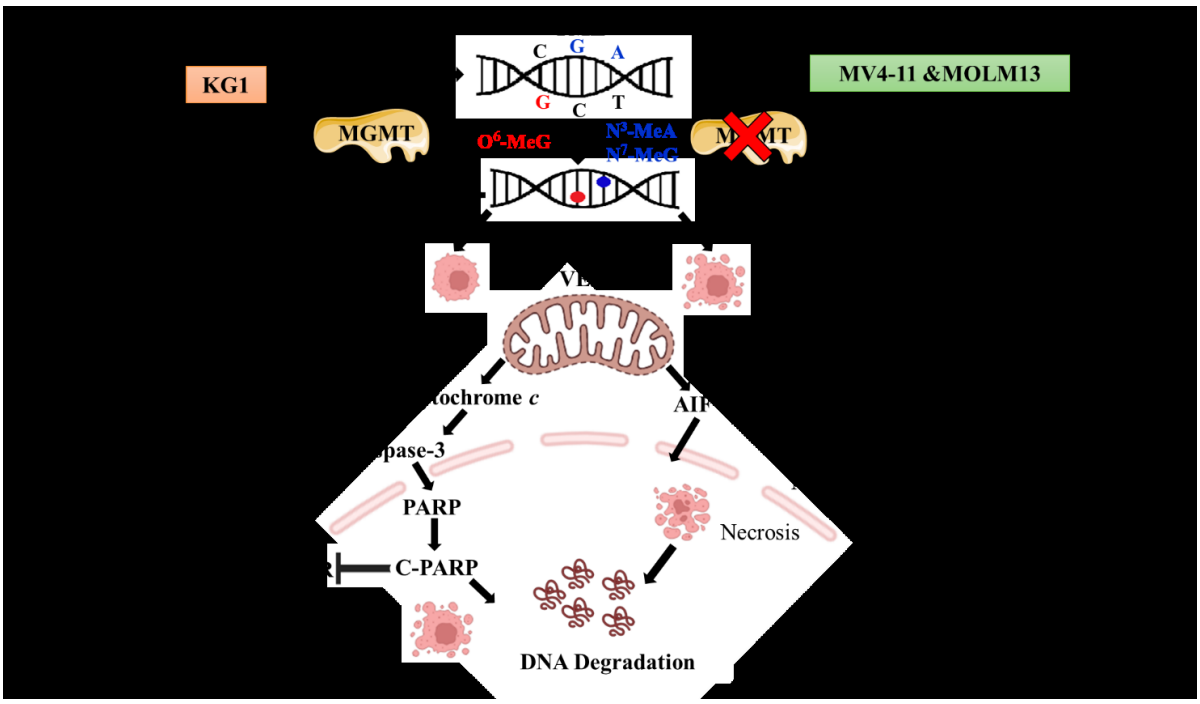

Figure 4.1: The proposed TMZ and VEN combination mechanism in high and low-MGMT cells. Temozolomide (TMZ) causes DNA methylation at O^6 and N^7 positions of guanine and the N^3 position of adenine. In KG1 cells, with high methylguanine methyltransferase (MGMT) protein, MGMT removes the methyl group added to O^6 guanine causing cell resistance. However, adding Venetoclax (VEN) activated the caspase dependent mitochondrial apoptotic pathway, resulting in release of cytochrome *c* and formation of cleaved caspase-3. The latter then translocates from mitochondria to the cytoplasm, then to the nucleus to cleave PARP. PARP may also be cleaved as a result of VEN inhibiting the base excision repair (BER) pathway following TMZ exposure. Both pathways would result in increased DNA stand breaks, DNA degradation, and cell death. MV4-11 and MOLM13 cells, with low-MGMT protein expression, are sensitive to TMZ alone with reasonable cell apoptosis obtained. However, adding VEN activates the mitochondrial caspase independent pathway and translocates apoptotic inducing factor (AIF) from mitochondria to the cytoplasm and further to the nucleus to enhance cell necrosis, resulting in a high amount of DNA degradation.

With MV4-11 and MOLM13, with low MGMT and high BCL-2 expression, the TMZ+VEN combination inhibited cell viability and caused cell apoptosis. A significant enhancement was observed in viability inhibition with the combination compared to each drug alone. Unfortunately, this enhancement was not observed in apoptosis assessed by flow cytometry since these two cell lines were highly sensitive to VEN. The low inhibitory concentration (IC50) VEN concentration used may cause a minor inhibition in the cell's metabolic activity, resulting in a difference between VEN alone and the combination. Enhancement of DNA strand breaks is also observed in cells with absent MGMT expression. The DNA damage caused by TMZ alone was modest; however, it became severe after adding VEN, suggesting that cell death may occur through a caspase-independent pathway by releasing the apoptosis-inducing factor (AIF) (Fig. 4.1). Cell death through this pathway could be possible as AIF function is increasing the exposure of phosphatidyl serine (Annexin V) [5], which explains the high apoptosis seen with no difference between VEN alone and combination.

The TMZ and VEN combination *in vivo* improved the OS compared with controls and VEN alone. However, it did not prevent the emergence of leukemia; furthermore, although a trend existed toward longer survival compared with TMZ alone, this difference was modest and not statistically significant.

As described in Chapter 3, we evaluated the TMZ sensitivity after adding the MDM2 inhibitor IDA *in vitro* using AML cell lines and patients' isolated blast-MNCs. Regardless of p53 expression, IDA did not enhance TMZ sensitivity. The cell viability inhibition caused by TMZ+IDA was limited in MV4-11 and MOLM13 with low-MGMT and wild-type p53 cells. The limited viability inhibition observed in MV4-11 and MOLM13 may result from p53 activation, which may cause cell cycle arrest after inducing p21 (Fig. 4.2). As previously shown

after treating melanoma cells with Nutlin-3a, the cells were arrested at the transition of G1/S phases, and p21 levels were elevated [6]. Inducing p21 also inactivates the retinoblastoma protein (pRb), which inhibits E2F transcription factor, preventing cell cycle progression [7].

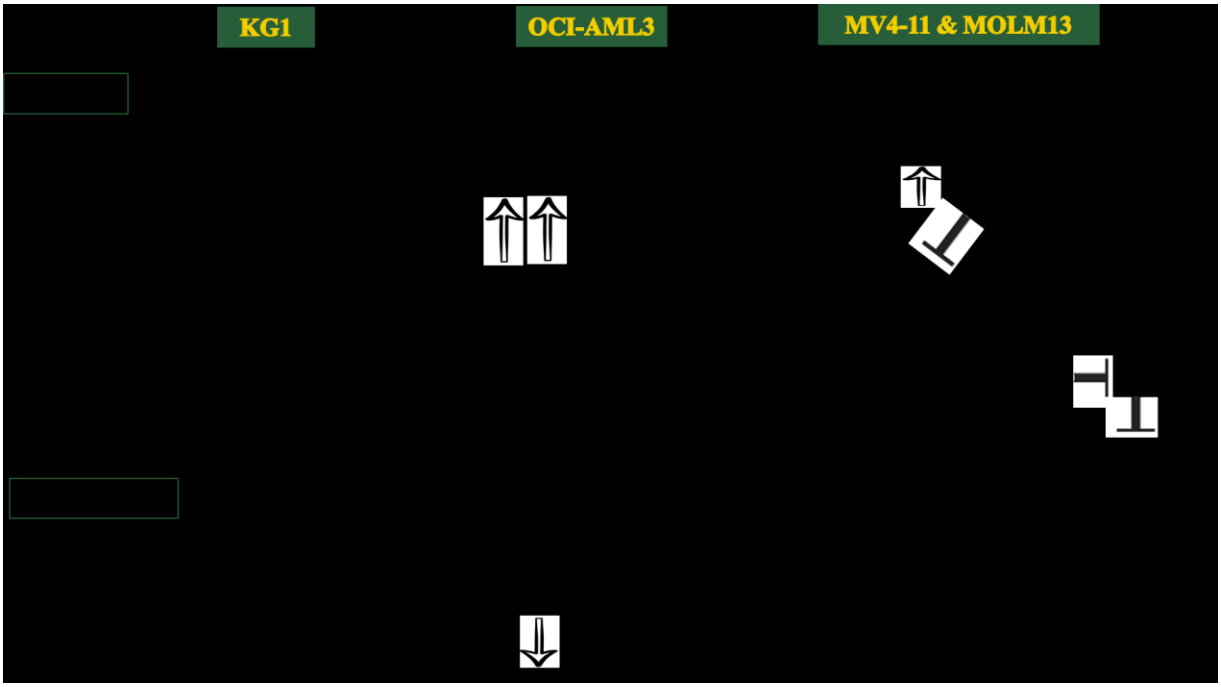

Figure 4.2: A schematic summary of TMZ and IDA combination outcomes in viability and DNA damage in high and low-MGMT cells. KG1 was resistant to the Temozolomide (TMZ) and Idasanutlin (IDA) combination after being treated for 48 hours as a result of p53 mutated status. Although p53 wild-type cell OCI-AML3 demonstrated resistance as well, it could be due to MGMT protein expression, as p53 can upregulate the MGMT level [8] to repair the DNA damage after TMZ exposure. MV4-11 and MOLM13 displayed inhibition as a result of p53 activation, which induces p21. The p21 protein inhibits the cyclin-dependent kinase (CDK)/cyclin E complex to arrest the cell in the G1 phase. Cell-cycle arrest at G1 phase results in hypophosphorylation of retinoblastoma protein (pRb), which tightly binds to E2F1 to prevent cell-cycle progression to the S phase. The insignificant effect seen on DNA damage in all cell lines may be related to the ability of IDA to protect the DNA from damage through inhibiting γH2AX.

However, the effect of the combination was minimal in damaging the DNA of MV4-11 and MOLM13. The IDA was demonstrated to have a protective effect against the senescence-inducing inhibitor of the mitotic kinase Aurora A (AURKA) as seen previously in the Vilgelm *et al.* study, through inhibiting γH2AX after treating melanoma cells with IDA alone or in combination [6].

The viability was maintained with high MGMT in both wild-type and mutant p53 cells, OCI-AML3 and KG1, respectively (Fig. 4.2). The result in KG1 is expected, as this is a p53 mutated cell line, and mutant p53 does not interact with MDM2, rendering the cells resistant to MDM2 inhibition. Conversely, OCI-AML3 has p53 that may activate after MDM2 inhibition by IDA, but the presence of MGMT halts the IDA function and causes cell resistance. Both MGMT and p53 are activated following exposure to DNA-damaging agents, including alkylating agents, to repair the DNA damage. It was discovered that p53 induces MGMT to maintain its function [9].

Similarly, most of the AML patients' samples exhibited weak to strong positive MGMT expression with wild-type p53. Applying IC50 IDA dosage to TMZ caused cell death, with ≤20% residual cells remaining. Those patient samples were frozen, which could be fragile and effortless to death. KG1 cells demonstrated resistance to both treatments due to p53 mutations and high MGMT expression. The DNA integrity remained stable after treatment exposure, as TMZ resistance and IDA's protective effect against DNA damage, as mentioned earlier.

A promising outcome was obtained at the beginning of IDA used *in vitro* and in phase I and II clinical studies. However, the phase III study demonstrated limited improvement in complete response (CR) and OS rates in relapsed/refractory (R/R) AML patients [10]. Consequently, no further studies were conducted using IDA on AML. Additionally, the toxicity adverse events observed on the gastrointestinal tract when used orally raised safety concerns about IDA

use [11]. Our studies provide further evidence that IDA is not a promising agent to study further in *in vivo* experiments. It is unclear whether other MDM2 inhibitors would be more effective; however, this appears unlikely as even supratherapeutic doses did not produce additive effects.

In conclusion, the VEN and TMZ combination increased cytotoxicity, decreased cell viability, and induced DNA damage in AML cell lines and AML patient samples with high and low-MGMT expression compared to TMZ alone. Further testing of this combination in mouse models showed promising outcomes. This is encouraging for a potential human clinical trial. Unfortunately, the IDA and TMZ combination did not produce similar outcomes. Regardless of the p53 wild-type status, cell viability was maintained and DNA integrity stabilized in AML cell lines and AML patient samples with high and low-MGMT expression. A mechanism should be involved that prevents p53 reactivation. These factors must be addressed to improve IDA sensitivity and activate p53 functions, which include cell cycle arrest and apoptosis.

4.2 Limitations and Future Directions

A 48-hour time point was selected to assess cell viability and apoptosis after drug combination. In low-MGMT cell lines MV4-11 and MOLM13, the results obtained demonstrated a viability enhancement compared to TMZ alone and no additive effect on apoptosis. However, no difference was detected in apoptosis between VEN and TMZ+VEN in these two cell lines by flow cytometry, as they were highly sensitive to VEN treatment. Evaluating these cells at shorter incubation times may demonstrate differences in apoptosis that were not apparent at 48 hours, and this should be assessed.

Cleaved caspase-3 must be evaluated to investigate caspase apoptotic pathway further and confirm the PARP 1 cleavage caused by VEN in KG1. The caspase-3 activity (Cell Signaling Kit

#5723) resulting from apoptosis can be evaluated in apoptotic cell lysate after incubation with fluorogenic substrate N-Acetyl-Asp-Glu-Val-Asp-7-amino-4-methylcoumarin (Ac-DEVD-AMC). Activated caspase-3 cleaves this substrate between DEVD and AMC, which can be detected using a fluorescent reader at excitation (Ex) 380 nm/emission (Em) 420 nm [12]. Cleaved caspase-3 can also be detected by Western blot. We are expecting high caspase-3 activity in the combination treated cells compared to VEN alone.

The lack of demonstrable generation of C-PARP 1 in MV4-11 and MOLM13 with VEN or TMZ-VEN must also be investigated further. AIF must be assessed to demonstrate that VEN activates the caspase-independent pathway in these cells. In apoptosis, AIF is translocated from the mitochondria to the cytosol then to the nuclease. It is detectable by Western blot or confocal fluorescence microscopy after labelling the cells with an anti-AIF antibody (ab 32516) and a FITC-conjugated secondary IgG antibody [13]. This could explain the lack of C-PARP 1 generation in MV4-11 and MOLM13 and the markedly enhanced DNA damage in the combination treated cells. Consequently, would expect a high level of AIF in the combination treated cells compared to VEN alone.

Overall, the mitochondrial membrane potential should be investigated after using the VEN+TMZ combination to observe its influence. The mitochondrial membrane potential assay (ab Kit # 113850) principle is that active mitochondria (hyperpolarized) have high membrane potential that can aggregate fluorescently labelled tetraethylbenzimidazolylcarbocyanine iodide (JC-1) and emit a red to orange colour detected at Em 590 nm. Conversely, inactive mitochondria (depolarized) have a low membrane potential and leave JC-1 as a monomer, which can be detected as a green colour at Em 530 nm. The fluorescence signal ratio of red/green is calculated to determine depolarized versus hyperpolarized mitochondria [14]. We would anticipate that the

drug combination may inhibit the mitochondrial membrane potential, causing depolarization, to a great extent, compared to VEN alone. We would not expect TMZ alone to have this effect.

An interesting result was obtained when assessing the DNA damage in fresh samples from AML patients in VEN+TMZ, although our sample size is small. It is difficult to obtain fresh samples frequently, although more samples must be recruited to optimize our observations. Additionally, the DNA damage response marker γH2AX may be measured using Western blot to observe the difference in the combination compared to TMZ alone. We may see high γH2AX expression in the combination compared to each drug alone.

Recent studies found the anti-apoptotic protein myeloid cell leukemia sequence-1 (MCL-1) mediates resistance to VEN [15]. This occurs through the activation 'substitution mechanism', maintaining the binding between anti-apoptotic and BH3-only proteins, which results in the inactivation of mitochondrial outer membrane permeabilization and cell survival. Some of our tested patients showed resistance to VEN alone at 1000 nM while exhibiting positive BCL-2 expression. MCL-1 is involved in VEN resistance as it can bind to BCL-2 interacting mediator of cell death (BIM) preventing cell apoptosis, which cannot be targeted by VEN. Therefore, MCL-1 protein evaluation must be included to determine the reason for the lack of VEN sensitivity.

Promising results were obtained from the mouse experiment after VEN and TMZ combination treatments. Although several limitations must be addressed, the small number of mice treated in each cohort is an important factor. Increasing the sample size to ten mice per group to obtain precise statistical evidence. Another possible factor is inadequate TMZ and VEN drug exposure in the combination experiment. The concentrations may be considered low and could not inhibit the leukemic cells in the engrafted mice. The short treatment duration of only 5 days may be insufficient to suppress the leukemic cell proliferation. As observed, the combination group had

the longest survival among the groups; however, by the time of death, no difference was observed in the leukemic cells compared to the MOLM13 group. Keeping the mice for a long time without cycling the treatment may enable these leukemic cells to re-proliferate as they do in the living host. Since no toxicity was observed in the combination experiment, this would support retesting the mice using higher drug concentrations or longer exposure durations.

Additionally, we only used MOLM13, a low-MGMT expressing cell line. A high-MGMT expressing cell line, such as KG1, should be tested in the mouse model to determine whether the *in vitro* effects of combination therapy in these cells are also observed *in vivo*. Using an *in vivo* imaging system with bioluminescent cells would also be helpful in monitoring leukemic cells after treatment; unfortunately, this was not available to us during the experiments. Furthermore, a xenograft mouse model may be used to evaluate the combination's efficacy on primary patient leukemic cells. If the results are encouraging, a pilot human clinical trial may be considered.

The IC50 of IDA was determined with a viability assay after 48 hours. A significantly greater inhibition effect was seen in TMZ+ IDA combination in low-MGMT cells compared to TMZ alone. It could be a result of cell cycle arrest or cell apoptosis. P21 and BIM need to be evaluated to determine the p53 activation pathway.

An IDA concentration of 2500 nM resulted in 67% residual cell viability in OCI-AML3. This cell line is highly representative of AML patients with high-MGMT and wild-type p53. Unfortunately, combining 2500 nM IDA with TMZ did not change the cell viability in the OCI-AML3 cell line. There should be a mechanism of resistance to prevent cell death that needs to be investigated.

Although 2500 nM IDA only produced partial inhibition in viability using our cell lines, this concentration produced almost a complete loss of viability in AML patients' samples. This impeded our ability to test for any additive effects of the combination in patient cells. The patients' cells are delicate and derived from heterogeneous and complex environments. Using frozen samples may impact the result as well; therefore, a fresh sample is better to use. Reducing the IDA concentration to 1000 nM to observe an enhancement effect would be preferable; unfortunately, we did not have sufficient patient material to repeat the experiment using this concentration. Overall, the p53 protein status must still be evaluated before IDA administration, as p53 mutated cells will not respond.

The DNA was maintained after IDA+TMZ combination treatment, therefore γH2AX needs to be assessed to prove the IDA DNA protective effect in high and low-MGMT cell lines. We are expecting low γH2AX in IDA and the combination compared TMZ alone.

4.3 References

1. Brandwein JM, Kassis J, Leber B, Hogge D, Howson-Jan K, Minden MD, et al. Phase II study of targeted therapy with temozolomide in acute myeloid leukaemia and high-risk myelodysplastic syndrome patients pre-screened for low O(6) -methylguanine DNA methyltransferase expression. Br J Haematol. 2014;167(5):664-70.

2. DiNardo CD, Jonas BA, Pullarkat V, Thirman MJ, Garcia JS, Wei AH, et al. Azacitidine and Venetoclax in Previously Untreated Acute Myeloid Leukemia. N Engl J Med. 2020;383(7):617-29.

3. Wei AH, Montesinos P, Ivanov V, DiNardo CD, Novak J, Laribi K, et al. Venetoclax plus LDAC for newly diagnosed AML ineligible for intensive chemotherapy: a phase 3 randomized placebo-controlled trial. Blood. 2020;135(24):2137-45.

4. Yee K, Martinelli G, Vey N, Dickinson MJ, Seiter K, Assouline S, et al. Phase 1/1b Study of RG7388, a Potent MDM2 Antagonist, in Acute Myelogenous Leukemia (AML) Patients (Pts). Blood. 2014.

5. Cregan SP, Dawson VL, Slack RS. Role of AIF in caspase-dependent and caspase-independent cell death. Oncogene. 2004;23(16):2785-96.

6. Vilgelm AE, Cobb P, Malikayil K, Flaherty D, Andrew Johnson C, Raman D, et al. MDM2 Antagonists Counteract Drug-Induced DNA Damage. EBioMedicine. 2017;24:43-55.

7. Weinberg RA. The Biology of Cancer. 1st ed. New York: Garland Science; 2007.

8. Blough MD, Zlatescu MC, Cairncross JG. O6-methylguanine-DNA methyltransferase regulation by p53 in astrocytic cells. Cancer Res. 2007;67(2):580-4.

9. Grombacher T, Eichhorn U, Kaina B. p53 is involved in regulation of the DNA repair gene O6-methylguanine-DNA methyltransferase (MGMT) by DNA damaging agents. Oncogene. 1998;17(7):845-51.

10. Konopleva MY, Röllig C, Cavenagh J, Deeren D, Girshova L, Krauter J, et al. Idasanutlin plus cytarabine in relapsed or refractory acute myeloid leukemia: results of the MIRROS trial. Blood Adv. 2022;6(14):4147-56.

11. Cassier PA, Castets M, Belhabri A, Vey N. Targeting apoptosis in acute myeloid leukaemia. Br J Cancer. 2017;117(8):1089-98.

12. Caspase-3 Activity Assay Kit #5723: Cell Signaling [Available from: https://www.cellsignal.com/products/cellular-assay-kits/caspase-3-activity-assay-kit/5723?_requestid=1114846.

13. Skyrlas A, Hantschke M, Passa V, Gaitanis G, Malamou-Mitsi V, Bassukas ID. Expression of apoptosis-inducing factor (AIF) in keratoacanthomas and squamous cell carcinomas of the skin. Exp Dermatol. 2011;20(8):674-6.

14. JC-1 - Mitochondrial Membrane Potential Assay Kit (ab113850): abcam; [Available from: https://www.abcam.com/products/assay-kits/jc-1-mitochondrial-membrane-potential-assay-kit-ab113850.html.

15. Liu J, Chen Y, Yu L, Yang L. Mechanisms of venetoclax resistance and solutions. Front Oncol. 2022;12:1005659.

Bibliography

Abeloff's clinical oncology. 6th ed. Niederhuber JE, Armitage JO, Doroshow JH, Kastan MB, Tepper JE, Abeloff MD, editors: Elsevier; 2020.

Acute myeloid leukemia : methods and protocols: Humana Press; 2017. Available from: https://link-springer-com.login.ezproxy.library.ualberta.ca/book/10.1007/978-1-4939-7142-8.

Apoptosis: Biology dictionary; [updated 2017. Available from: https://biologydictionary.net/apoptosis/.

Arber DA, Orazi A, Hasserjian RP, Borowitz MJ, Calvo KR, Kvasnicka H-M, et al. International Consensus Classification of Myeloid Neoplasms and Acute Leukemias: integrating morphologic, clinical, and genomic data. Blood. 2022;140(11):1200-28.

Baran K, Yang M, Dillon CP, Samson LL, Green DR. The proline rich domain of p53 is dispensable for MGMT-dependent DNA repair and cell survival following alkylation damage. Cell Death Differ. 2017;24(11):1925-36.

Bates I. Chapter 6 - Bone marrow biopsy. In: Lewis SM, Bain BJ, Bates I, editors. Dacie and Lewis Practical Haematology. 10th ed. Philadelphia: Churchill Livingstone; 2006. p. 115-30.

Becker H, Maharry K, Mrózek K, Volinia S, Eisfeld AK, Radmacher MD, et al. Prognostic gene mutations and distinct gene- and microRNA-expression signatures in acute myeloid leukemia with a sole trisomy 8. Leukemia. 2014;28(8):1754-8.

Bhansali RS, Pratz KW, Lai C. Recent advances in targeted therapies in acute myeloid leukemia. J Hematol Oncol. 2023;16(1).

Bocangel D, Sengupta S, Mitra S, Bhakat KK. p53-Mediated down-regulation of the human DNA repair gene O6-methylguanine-DNA methyltransferase (MGMT) via interaction with Sp1 transcription factor. Anticancer Res. 2009;29(10):3741-50.

Bolufer P, Barragan E, Collado M, Cervera J, López JA, Sanz MA. Influence of genetic polymorphisms on the risk of developing leukemia and on disease progression. Leuk Res. 2006;30(12):1471-91.

Blough MD, Zlatescu MC, Cairncross JG. O6-methylguanine-DNA methyltransferase regulation by p53 in astrocytic cells. Cancer Res. 2007;67(2):580-4.

Brandwein JM, Yang L, Schimmer AD, Schuh AC, Gupta V, Wells RA, et al. A phase II study of temozolomide therapy for poor-risk patients aged >or=60 years with acute myeloid leukemia: low levels of MGMT predict for response. Leukemia. 2007;21(4):821-4.

Brandwein JM, Kassis J, Leber B, Hogge D, Howson-Jan K, Minden MD, et al. Phase II study of targeted therapy with temozolomide in acute myeloid leukaemia and high-risk myelodysplastic syndrome patients pre-screened for low O(6) -methylguanine DNA methyltransferase expression. Br J Haematol. 2014;167(5):664-70.

Brandwein JM, Saini L, Geddes MN, Yusuf D, Liu F, Schwann K, et al. Outcomes of patients with relapsed or refractory acute myeloid leukemia: a population-based real-world study. Am J Blood Res. 2020;10(4):124-33.

Brandwein JM, Hallett D, Karkhaneh M, Zhu N, Liew E, Bolster L, et al. An evaluation of no-treatment decisions in patients with newly diagnosed acute myeloid leukemia. Am J Hematol. 2021;96(1): E17-e20.

Brooks CL, Gu W. Dynamics in the p53-Mdm2 ubiquitination pathway. Cell Cycle. 2004;3(7):895-9.

Campos EDV, Pinto R. Targeted therapy with a selective BCL-2 inhibitor in older patients with acute myeloid leukemia. Hematol Transfus Cell Ther. 2019;41(2):169-77.

Caspase-3 Activity Assay Kit #5723: Cell Signaling [Available from: https://www.cellsignal.com/products/cellular-assay-kits/caspase-3-activity-assay-kit/5723?_requestid=1114846.

Cassier PA, Castets M, Belhabri A, Vey N. Targeting apoptosis in acute myeloid leukaemia. Br J Cancer. 2017;117(8):1089-98.

Chaitanya GV, Steven AJ, Babu PP. PARP-1 cleavage fragments: signatures of cell-death proteases in neurodegeneration. Cell Commun Signal. 2010; 8:31.

Chen J. The Cell-Cycle Arrest and Apoptotic Functions of p53 in Tumor Initiation and Progression. Cold Spring Harb Perspect Med. 2016;6(3): a026104.

Comet Assay Kit (3-well slides) (ab238544): Abcam; 2018 [Available from: https://www.abcam.com/ps/products/238/ab238544/documents/Comet-Assay-protocol-book-v2b-ab238544%20(website).pdf.

Cregan SP, Dawson VL, Slack RS. Role of AIF in caspase-dependent and caspase-independent cell death. Oncogene. 2004;23(16):2785-96.

Croce CM, Reed JC. Finally, An Apoptosis-Targeting Therapeutic for Cancer. Cancer Res. 2016;76(20):5914-20.

D'Atri S, Piccioni D, Castellano A, Tuorto V, Franchi A, Lu K, et al. Chemosensitivity to triazene compounds and O6-alkylguanine-DNA alkyltransferase levels: studies with blasts of leukaemic patients. Ann Oncol. 1995;6(4):389-93.

Daver NG, Dail M, Garcia JS, Jonas BA, Yee KWL, Kelly KR, et al. Venetoclax and idasanutlin in relapsed/refractory AML: a nonrandomized, open-label phase 1b trial. Blood. 2023;141(11):1265-76.

Diepstraten ST, Marca JEL, Huang DCS, Kelly GL. Principles for understanding mechanisms of cell death and their role in cancer biology. Precision Cancer Therapies2023. p. 133-50.

DiNardo CD, Stein EM, de Botton S, Roboz GJ, Altman JK, Mims AS, et al. Durable Remissions with Ivosidenib in IDH1-Mutated Relapsed or Refractory AML. N Engl J Med. 2018;378(25):2386-98.

DiNardo CD, Jonas BA, Pullarkat V, Thirman MJ, Garcia JS, Wei AH, et al. Azacitidine and Venetoclax in Previously Untreated Acute Myeloid Leukemia. N Engl J Med. 2020;383(7):617-29.

Döhner H, Weisdorf DJ, Bloomfield CD. Acute Myeloid Leukemia. N Engl J Med. 2015;373(12):1136-52.

Döhner H, Wei AH, Appelbaum FR, Craddock C, DiNardo CD, Dombret H, et al. Diagnosis and management of AML in adults: 2022 recommendations from an international expert panel on behalf of the ELN. Blood. 2022;140(12):1345-77.

Dombret H, Seymour JF, Butrym A, Wierzbowska A, Selleslag D, Jang JH, et al. International phase 3 study of azacitidine vs conventional care regimens in older patients with newly diagnosed AML with >30% blasts. Blood. 2015;126(3):291-9.

Du X, Hu H. The Roles of 2-Hydroxyglutarate. Front Cell Dev Biol. 2021;9: 651317.

Dutto I, Tillhon M, Cazzalini O, Stivala LA, Prosperi E. Biology of the cell cycle inhibitor p21CDKN1A: molecular mechanisms and relevance in chemical toxicology. Archives of Toxicology. 2015;89(2):155-78.

Fan CH, Liu WL, Cao H, Wen C, Chen L, Jiang G. O6-methylguanine DNA methyltransferase as a promising target for the treatment of temozolomide-resistant gliomas. Cell Death Dis. 2013;4(10): e876-e.

George B, Kantarjian H, Baran N, Krocker JD, Rios A. TP53 in Acute Myeloid Leukemia: Molecular Aspects and Patterns of Mutation. Int J Mol Sci. 2021;22(19).

Gewirtz DA. A critical evaluation of the mechanisms of action proposed for the antitumor effects of the anthracycline antibiotics adriamycin and daunorubicin. Biochem Pharmacol. 1999;57(7):727-41.

Grombacher T, Eichhorn U, Kaina B. p53 is involved in regulation of the DNA repair gene O6-methylguanine-DNA methyltransferase (MGMT) by DNA damaging agents. Oncogene. 1998;17(7):845-51.

Haferlach T, Schmidts I. The power and potential of integrated diagnostics in acute myeloid leukaemia. Br J Haematol. 2020;188(1):36-48.

Haronikova L, Bonczek O, Zatloukalova P, Kokas-Zavadil F, Kucerikova M, Coates PJ, et al. Resistance mechanisms to inhibitors of p53-MDM2 interactions in cancer therapy: can we overcome them? Cell Mol Biol Lett. 2021;26(1):53.

Hernández Borrero LJ, El-Deiry WS. Tumor suppressor p53: Biology, signaling pathways, and therapeutic targeting. Biochim Biophys Acta Rev Cancer. 2021;1876(1):188556.

Hoffbrand AV, Moss PAH, Pettit JE. Essential Haematology. 5th ed. Massachustts, USA: Blackwell; 2006.

Horton TM, Jenkins G, Pati D, Zhang L, Dolan ME, Ribes-Zamora A, et al. Poly(ADP-ribose) polymerase inhibitor ABT-888 potentiates the cytotoxic activity of temozolomide in leukemia cells: influence of mismatch repair status and O6-methylguanine-DNA methyltransferase activity. Mol Cancer Ther. 2009;8(8):2232-42.

Hou H, Sun D, Zhang X. The role of MDM2 amplification and overexpression in therapeutic resistance of malignant tumors. Cancer Cell Int. 2019;19: 216.

Italiano A, Miller WH, Jr., Blay JY, Gietema JA, Bang YJ, Mileshkin LR, et al. Phase I study of daily and weekly regimens of the orally administered MDM2 antagonist idasanutlin in patients with advanced tumors. Invest New Drugs. 2021;39(6):1587-97.

Jagtap P, Szabó C. Poly(ADP-ribose) polymerase and the therapeutic effects of its inhibitors. Nat Rev Drug Discov. 2005;4(5):421-40.

Jan R, Chaudhry GE. Understanding Apoptosis and Apoptotic Pathways Targeted Cancer Therapeutics. Adv Pharm Bull. 2019;9(2):205-18.

JC-1 - Mitochondrial Membrane Potential Assay Kit (ab113850): abcam; [Available from: https://www.abcam.com/products/assay-kits/jc-1-mitochondrial-membrane-potential-assay-kit-ab113850.html.

Jiapaer S, Furuta T, Tanaka S, Kitabayashi T, Nakada M. Potential strategies overcoming the temozolomide resistance for glioblastoma. Neurol Med Chir (Tokyo). 2018;58(10):405-21.

Kaina B, Christmann M. DNA repair in personalized brain cancer therapy with temozolomide and nitrosoureas. DNA Repair. 2019;78:128-41.

Kala SG, Chinni S. Development and Characterization of Venetoclax Nanocrystals for Oral Bioavailability Enhancement. AAPS PharmSciTech. 2021;22(3):92.

Kelley MR, Fishel ML. DNA Repair in Cancer Therapy: Molecular Targets and Clinical Applications. 2nd ed: Elsevier Inc.; 2016. 1-444 p.

Khoury JD, Solary E, Abla O, Akkari Y, Alaggio R, Apperley JF, et al. The 5th edition of the World Health Organization Classification of Haematolymphoid Tumours: Myeloid and Histiocytic/Dendritic Neoplasms. Leukemia. 2022;36(7):1703-19.

Khurana A, Shafer DA. MDM2 antagonists as a novel treatment option for acute myeloid leukemia: perspectives on the therapeutic potential of idasanutlin (RG7388). Onco Targets Ther. 2019;12:2903-10.

Konopleva M, Pollyea DA, Potluri J, Chyla B, Hogdal L, Busman T, et al. Efficacy and biological correlates of response in a phase II study of venetoclax monotherapy in patients with acute Myelogenous Leukemia. Cancer Discov. 2016;6(10):1106-17.

Konopleva MY, Röllig C, Cavenagh J, Deeren D, Girshova L, Krauter J, et al. Idasanutlin plus cytarabine in relapsed or refractory acute myeloid leukemia: results of the MIRROS trial. Blood Adv. 2022;6(14):4147-56.

Korycka-Wolowiec A, Wolowiec D, Kubiak-Mlonka A, Robak T. Venetoclax in the treatment of chronic lymphocytic leukemia. Expert Opin Drug Metab Toxicol. 2019;15(5):353-66.

Kumar CC. Genetic abnormalities and challenges in the treatment of acute myeloid Leukemia. Genes Cancer. 2011;2(2):95-107.

Lambert J, Pautas C, Terré C, Raffoux E, Turlure P, Caillot D, et al. Gemtuzumab ozogamicin for de novo acute myeloid leukemia: final efficacy and safety updates from the open-label, phase III ALFA-0701 trial. Haematologica. 2019;104(1):113-9.

Lancet JE, Uy GL, Newell LF, Lin TL, Ritchie EK, Stuart RK, et al. Five-year final results of a phase III study of CPX-351 versus 7+3 in older adults with newly diagnosed high-risk/secondary AML. J Clin Oncol. 2020;38(15_suppl):7510-10.

Lee KE. Immunohistochemical Assessment of O(6)-Methylguanine-DNA Methyltransferase (MGMT) and Its Relationship with p53 Expression in Endometrial Cancers. J Cancer Prev. 2013;18(4):351-4.

Lehmann C, Friess T, Birzele F, Kiialainen A, Dangl M. Superior anti-tumor activity of the MDM2 antagonist idasanutlin and the Bcl-2 inhibitor venetoclax in p53 wild-type acute myeloid leukemia models. J Hematol Oncol. 2016;9(1).

Lewis SM. Chapter 2 - Reference ranges and normal values. In: Lewis SM, Bain BJ, Bates I, editors. Dacie and Lewis Practical Haematology. 10th ed. Philadelphia: Churchill Livingstone; 2006. p. 11-24.

Liu F, Knight T, Su Y, Edwards H, Wang G, Wang Y, et al. Venetoclax Synergistically Enhances the Anti-leukemic Activity of Vosaroxin Against Acute Myeloid Leukemia Cells Ex Vivo. Target Oncol. 2019;14(3):351-64.

Liu H, Michmerhuizen MJ, Lao Y, Wan K, Salem AH, Sawicki J, et al. Metabolism and Disposition of a Novel Bcl-2 Inhibitor Venetoclax in Humans and Characterization of its Unusual Metabolites. Drug Metab Dispos. 2016;45(3):294-305.

Liu J, Chen Y, Yu L, Yang L. Mechanisms of venetoclax resistance and solutions. Front Oncol. 2022;12: 1005659.

Long NA, Golla U, Sharma A, Claxton DF. Acute Myeloid Leukemia Stem Cells: Origin, Characteristics, and Clinical Implications. Stem Cell Rev and Rep. 2022;18(4):1211-26.

Matutes E, Morilla R, Catovsky D. Chapter 14 - Immunophenotyping. In: Lewis SM, Bain BJ, Bates I, editors. Dacie and Lewis Practical Haematology. 10th ed. Philadelphia: Churchill Livingstone; 2006. p. 335-55.

Megías-Vericat JE, Solana-Altabella A, Ballesta-López O, Martínez-Cuadrón D, Montesinos P. Drug-drug interactions of newly approved small molecule inhibitors for acute myeloid leukemia. Ann Hematol. 2020;99(9):1989-2007.

Merchant SL, Culos K, Wyatt H. Ivosidenib: IDH1 Inhibitor for the Treatment of Acute Myeloid Leukemia. J Adv Pract Oncol. 2019;10(5):494-500.

Meshinchi S, Appelbaum FR. Structural and functional alterations of FLT3 in acute myeloid leukemia. Clin Cancer Res. 2009;15(13):4263-9.

Mihalyova J, Jelinek T, Growkova K, Hrdinka M, Simicek M, Hajek R. Venetoclax: A new wave in hematooncology. Exp Hematol. 2018;61: 10-25.

Moll UM, Petrenko O. The MDM2-p53 interaction. Mol Cancer Res. 2003;1(14):1001-8.

Momparler RL. Optimization of cytarabine (ARA-C) therapy for acute myeloid leukemia. Exp Hematol Oncol. 2013; 2:20.

Nagasubramanian R, Dolan ME. Temozolomide: Realizing the promise and potential. Curr Opin Oncol. 2003;15(6):412-8.

Nakano K, Vousden KH. PUMA, a Novel Proapoptotic Gene, Is Induced by p53. Molecular Cell. 2001;7(3):683-94.

Neochoritis C, Estrada-Ortiz N, Khoury K, Dömling A. P53–MDM2 and MDMX Antagonists. In: Desai MC, editor. Annual Reports in Medicinal Chemistry. 49: Academic Press; 2014. p. 167-87.

Ochs K, Kaina B. Apoptosis induced by DNA damage O6-methylguanine is Bcl-2 and caspase-9/3 regulated and Fas/caspase-8 independent. Cancer Res. 2000;60(20):5815-24.

Ortiz R, Perazzoli G, Cabeza L, Jiménez-Luna C, Luque R, Prados J, Melguizo C. Temozolomide: An updated overview of resistance mechanisms, nanotechnology advances and clinical applications. Curr Neuropharmacol. 2021;19(4):513-37.

Ossenkoppele G, Löwenberg B. How I treat the older patient with acute myeloid leukemia. Blood. 2015;125(5):767-74.

Padmakumar D, Chandraprabha VR, Gopinath P, Vimala Devi ART, Anitha GRJ, Sreelatha MM, et al. A concise review on the molecular genetics of acute myeloid leukemia. Leuk Res. 2021;111: 106727.

Pan R, Hogdal LJ, Benito JM, Bucci D, Han L, Borthakur G, et al. Selective BCL-2 inhibition by ABT-199 causes on-target cell death in acute myeloid Leukemia. Cancer Discov. 2014;4(3):362-675.

Pápai Z, Chen LC, Da Costa D, Blotner S, Vazvaei F, Gleave M, et al. A single-center, open-label study investigating the excretion balance, pharmacokinetics, metabolism, and absolute bioavailability of a single oral dose of [(14)C]-labeled idasanutlin and an intravenous tracer dose of [(13)C]-labeled idasanutlin in a single cohort of patients with solid tumors. Cancer Chemother Pharmacol. 2019;84(1):93-103.

Pelcovits A, Niroula R. Acute Myeloid Leukemia: A Review. R I Med J (2013). 2020;103(3):38-40.

Perl AE, Martinelli G, Cortes JE, Neubauer A, Berman E, Paolini S, et al. Gilteritinib or Chemotherapy for Relapsed or Refractory FLT3-Mutated AML. N Engl J Med. 2019;381(18):1728-40.

Pollyea DA, Jordan CT. Why are hypomethylating agents or low-dose cytarabine and venetoclax so effective? Curr Opin Hematol. 2019;26(2):71-6.

PubChem. Compound Summary for CID 53358942, Idasanutlin: National Center for Biotechnology Information; [Available from: https://pubchem.ncbi.nlm.nih.gov/compound/Idasanutlin.

Qin D. Molecular testing for acute myeloid leukemia. Cancer Biol Med. 2021;19(1):4-13.

Quintás-Cardama A, Hu C, Qutub A, Qiu YH, Zhang X, Post SM, et al. P53 pathway dysfunction is highly prevalent in acute myeloid leukemia independent of TP53 mutational status. Leukemia. 2017;31(6):1296-305.

Rao A, Ramani N, Stoppacher R, Coyle T. Complete response to temozolomide in chronic lymphocytic leukemia. Clin Case Rep. 2017;5(7):1130-1.

Reis B, Jukofsky L, Chen G, Martinelli G, Zhong H, So WV, et al. Acute myeloid leukemia patients' clinical response to idasanutlin (RG7388) is associated with pre-treatment MDM2 protein expression in leukemic blasts. Haematologica. 2016;101(5):e185-e8.

Reitman ZJ, Yan H. Isocitrate dehydrogenase 1 and 2 mutations in cancer: alterations at a crossroads of cellular metabolism. J Natl Cancer Inst. 2010;102(13):932-41.

Roca-Portoles A, Rodriguez-Blanco G, Sumpton D, Cloix C, Mullin M, Mackay GM, et al. Venetoclax causes metabolic reprogramming independent of BCL-2 inhibition. Cell Death Dis. 2020;11(8):616.

Rosenberg E, Voevoda V, Magen H, Ostrovsky O, Shimoni A, Peled A, et al. Venetoclax Reverses Metabolic Reprogramming Induced By S1P Modulator FTY720, Suppresses Oxidative Phosphorylation and Synergistically Targets Multiple Myeloma. Blood. 2021;138(Supplement 1):1195-95.

Salem AH, Agarwal SK, Dunbar M, Nuthalapati S, Chien D, Freise KJ, Wong SL. Effect of Low- and High-Fat Meals on the Pharmacokinetics of Venetoclax, a Selective First-in-Class BCL-2 Inhibitor. J Clin Pharmacol. 2016;56(11):1355-61.

Sasaki K, Ravandi F, Kadia TM, DiNardo CD, Short NJ, Borthakur G, et al. De novo acute myeloid leukemia: A population-based study of outcome in the United States based on the Surveillance, Epidemiology, and End Results (SEER) database, 1980 to 2017. Cancer. 2021;127(12):2049-61.

Saxena R, Pati HP. Hematopathology: Advances in Understanding. Singapore: Springer 2019. 1-502 p.

Seiter K, Liu D, Loughran T, Siddiqui A, Baskind P, Ahmed T. Phase I study of temozolomide in relapsed/refractory acute leukemia. J Clin Oncol. 2002;20(15):3249-53.

Seiter K, Katragadda S, Ponce D, Rasul M, Ahmed N. Temozolomide and cisplatin in relapsed/refractory acute leukemia. J Hematol Oncol. 2009; 2:21.

Sharma S, Salehi F, Scheithauer BW, Rotondo F, Syro LV, Kovacs K. Role of MGMT in tumor development, progression, diagnosis, treatment and prognosis. Anticancer Res. 2009;29(10):3759-68.

Shen W, Hu JA, Zheng JS. Mechanism of temozolomide-induced antitumour effects on glioma cells. J Int Med Res. 2014;42(1):164-72.

Shimony S, Stahl M, Stone RM. Acute myeloid leukemia: 2023 update on diagnosis, risk-stratification, and management. Am J Hematol. 2023;98(3):502-26.

Shinji K, Shinya T. Chemotherapeutic Agent for Glioma: IntechOpen; 2013. Available from: https://doi.org/10.5772/54353.

Singh RK, Kumar S, Prasad DN, Bhardwaj TR. Therapeutic journery of nitrogen mustard as alkylating anticancer agents: Historic to future perspectives. Eur J Med Chem. 2018;151: 401-33.

Singh R, Mehrotra S, Gopalakrishnan M, Gojo I, Karp JE, Greer JM, et al. Population pharmacokinetics and exposure-response assessment of veliparib co-administered with temozolomide in patients with myeloid leukemias. Cancer Chemother Pharmacol. 2019;83(2):319-28.

Singh N, Miner A, Hennis L, Mittal S. Mechanisms of temozolomide resistance in glioblastoma - a comprehensive review. Cancer Drug Resist. 2021;4(1):17-43.

Stein EM, DiNardo CD, Pollyea DA, Fathi AT, Roboz GJ, Altman JK, et al. Enasidenib in mutant IDH2 relapsed or refractory acute myeloid leukemia. Blood. 2017;130(6):722-31.

Skyrlas A, Hantschke M, Passa V, Gaitanis G, Malamou-Mitsi V, Bassukas ID. Expression of apoptosis-inducing factor (AIF) in keratoacanthomas and squamous cell carcinomas of the skin. Exp Dermatol. 2011;20(8):674-6.

Sosna J, Voigt S, Mathieu S, Lange A, Thon L, Davarnia P, et al. TNF-induced necroptosis and PARP-1-mediated necrosis represent distinct routes to programmed necrotic cell death. Cell Mol Life Sci. 2014;71(2):331-48.

Stone RM, Mandrekar SJ, Sanford BL, Laumann K, Geyer S, Bloomfield CD, et al. Midostaurin plus Chemotherapy for Acute Myeloid Leukemia with a FLT3 Mutation. N Engl J Med. 2017;377(5):454-64.

Tomar MS, Kumar A, Srivastava C, Shrivastava A. Elucidating the mechanisms of Temozolomide resistance in gliomas and the strategies to overcome the resistance. Biochim Biophys Acta Rev Cancer. 2021;1876(2):188616.

Trivedi RN, Almeida KH, Fornsaglio JL, Schamus S, Sobol RW. The role of base excision repair in the sensitivity and resistance to temozolomide-mediated cell death. Cancer Res. 2005;65(14):6394-400.

Vakiti A, Mewawalla P. Acute Myeloid Leukemia. StatPearls [Internet]. Treasure Island (FL): StatPearls; 2022. Available from: www.ncbi.nlm.nih.gov/books/NBK507875/.

Venetoclax: Ontario Health (Cancer Care Ontario); [updated 2022. Available from: https://www.cancercareontario.ca/en/drugformulary/drugs/monograph/44476.

Verbeek B, Southgate TD, Gilham DE, Margison GP. O6-Methylguanine-DNA methyltransferase inactivation and chemotherapy. Br Med Bull. 2008;85: 17-33.

Vicente ATS, Salvador JAR. MDM2-Based Proteolysis-Targeting Chimeras (PROTACs): An Innovative Drug Strategy for Cancer Treatment. Int J Mol Sci. 2022;23(19):11068.

Vilgelm AE, Cobb P, Malikayil K, Flaherty D, Andrew Johnson C, Raman D, et al. MDM2 Antagonists Counteract Drug-Induced DNA Damage. EBioMedicine. 2017;24: 43-55.

Vogt KC. Untersuchungen über die Entwicklungsgeschichte der Geburtshelferkrte (Alytes obstetricans): Solothurn: Jent & Gassmann; 1842. Available from: http://hdl.handle.net/10111/UIUCOCA:untersuchungen00vogt.

Vulliamy T, Kaeda J. Chapter 21 - Molecular and cytogenetic analysis. In: Lewis SM, Bain BJ, Bates I, editors. Dacie and Lewis Practical Haematology. 10th ed. Philadelphia: Churchill Livingstone; 2006. p. 555-94.

Wade M, Li YC, Wahl GM. MDM2, MDMX and p53 in oncogenesis and cancer therapy. Nat Rev Cancer. 2013;13(2):83-96.

Waldron M, Winter A, Hill BT. Pharmacokinetic and Pharmacodynamic Considerations in the Treatment of Chronic Lymphocytic Leukemia: Ibrutinib, Idelalisib, and Venetoclax. Clin Pharmacokinet. 2017;56(11):1255-66.

Wang K, Kievit FM, Chiarelli PA, Stephen ZR, Lin G, Silber JR, et al. siRNA nanoparticle suppresses drug-resistant gene and prolongs survival in an orthotopic glioblastoma xenograft mouse model. Adv Funct Mater. 2021;31(6).

Wei AH, Montesinos P, Ivanov V, DiNardo CD, Novak J, Laribi K, et al. Venetoclax plus LDAC for newly diagnosed AML ineligible for intensive chemotherapy: a phase 3 randomized placebo-controlled trial. Blood. 2020;135(24):2137-45.

Wei Y, Cao Y, Sun R, Cheng L, Xiong X, Jin X, et al. Targeting Bcl-2 Proteins in Acute Myeloid Leukemia. Front Oncol. 2020;10.

Weinberg RA. The Biology of Cancer. 1st ed. New York: Garland Science; 2007.

Wesolowski JR, Rajdev P, Mukherji SK. Temozolomide (Temodar). AJNR Am J Neuroradiol. 2010;31(8):1383-4.

Westhus J, Noppeney R, Dührsen U, Hanoun M. FLAG salvage therapy combined with idarubicin in relapsed/refractory acute myeloid leukemia. Leuk Lymphoma. 2019;60(4):1014-22.

Xiufeng Z, Haijun Z, Silei B, Manman D, Yong Z, Lian Y, et al. Co-operation of ABT-199 and gemcitabine in impeding DNA damage repair and inducing cell apoptosis for synergistic therapy of T-cell acute lymphoblastic leukemia. Anti-Cancer Drugs. 2019;30(2):138-48.

Xu J, Song J, Xiao M, Wang C, Zhang Q, Yuan X, Tian S. RUNX1 (RUNX family transcription factor 1), a target of microRNA miR-128-3p, promotes temozolomide resistance in glioblastoma multiform by upregulating multidrug resistance-associated protein 1 (MRP1). Bioengineered. 2021;12(2):11768-81.

Yang Y, Shu Y, Chen G, Yin Y, Li F, Li J. A real-world pharmacovigilance study of FDA Adverse Event Reporting System (FAERS) events for venetoclax. PLOS ONE. 2022;17(12):e0278725.

Yee K, Martinelli G, Vey N, Dickinson MJ, Seiter K, Assouline S, et al. Phase 1/1b Study of RG7388, a Potent MDM2 Antagonist, in Acute Myelogenous Leukemia (AML) Patients (Pts). Blood. 2014.

Zhai Y, Shang J, Yao W, Wu D, Fu C, Yan L. Successful eradication of central nervous system infiltration of primary plasma cell leukemia by temozolomide. Ann Hematol. 2022;101(11):2555-7.

Zheng G, Li P, Zhang X, Pan Z. The fifth edition of the World Health Organization Classification and the International Consensus Classification of myeloid neoplasms: evolving guidelines in the molecular era with practical implications. Curr Opin Hematol. 2023;30(2):53-63.

Zhu H, Almasan A. Development of venetoclax for therapy of lymphoid malignancies. Drug Des Devel Ther. 2017;11: 685-94.

Appendix

Table 1: 2022 International Consensus Classification (ICC) of Myeloid Neoplasms and Acute Leukemia [1]

MPNs o Chronic myeloid leukemia o Polycythemia vera o Essential thrombocythemia o Primary myelofibrosis o Early/prefibrotic primary myelofibrosis o Overt primary myelofibrosis o Chronic neutrophilic leukemia o Chronic eosinophilic leukemia, not otherwise specified o MPN, unclassifiable
Myeloid/lymphoid neoplasms with eosinophilia and tyrosine kinase gene fusions o Myeloid/lymphoid neoplasm with *PDGFRA* rearrangement o Myeloid/lymphoid neoplasm with *PDGFRB* rearrangement o Myeloid/lymphoid neoplasm with *FGFR1* rearrangement o Myeloid/lymphoid neoplasm with *JAK2* rearrangement o Myeloid/lymphoid neoplasm with *FLT3* rearrangement o Myeloid/lymphoid neoplasm with *ETV6::ABL1*
Mastocytosis
Myelodysplastic/myeloproliferative neoplasms o Chronic myelomonocytic leukemia o Clonal cytopenia with monocytosis of undetermined significance o Clonal monocytosis of undetermined significance o Atypical chronic myeloid leukemia o Myelodysplastic/myeloproliferative neoplasm with thrombocytosis and *SF3B1* mutation o Myelodysplastic/myeloproliferative neoplasm with ring sideroblasts and thrombocytosis, not otherwise specified o Myelodysplastic/myeloproliferative neoplasm, not otherwise specified
Premalignant clonal cytopenias and myelodysplastic syndromes o Clonal cytopenia of undetermined significance o Myelodysplastic syndrome with mutated *SF3B1* o Myelodysplastic syndrome with del(5q) o Myelodysplastic syndrome with mutated *TP53* o Myelodysplastic syndrome, not otherwise specified (MDS, NOS) o MDS, NOS without dysplasia o MDS, NOS with single lineage dysplasia o MDS, NOS with multilineage dysplasia o Myelodysplastic syndrome with excess blasts o Myelodysplastic syndrome/acute myeloid leukemia (MDS/AML) o MDS/AML with mutated *TP53* o MDS/AML with myelodysplasia-related gene mutations o MDS/AML with myelodysplasia-related cytogenetic abnormalities o MDS/AML, not otherwise specified
Pediatric and/or germline mutation-associated disorders o Juvenile myelomonocytic leukemia o Juvenile myelomonocytic leukemia-like neoplasms

- Noonan syndrome-associated myeloproliferative disorder
- Refractory cytopenia of childhood
- Hematologic neoplasms with germline predisposition

Acute myeloid leukemias (Introduction Table 1.1)

Myeloid proliferations associated with Down syndrome

Blastic plasmacytoid dendritic cell neoplasm

Acute leukemia of ambiguous lineage

- Acute undifferentiated leukemia
- Mixed phenotype acute leukemia (MPAL) with t(9;22)(q34.1;q11.2);
- *BCR::ABL1*
- MPAL, with t(v;11q23.3); *KMT2A* rearranged
- MPAL, B/myeloid, NOS
- MPAL, T/myeloid, NOS

B-lymphoblastic leukemia/lymphoma

- B-ALL with recurrent genetic abnormalities
- B-ALLwith t(9;22)(q34.1;q11.2)/*BCR::ABL1*
- with lymphoid only involvement
- with multilineage involvement
- B-ALLwith t(v;11q23.3)/*KMT2A* rearranged
- B-ALL with t(12;21)(p13.2;q22.1)/*ETV6::RUNX1*
- B-ALL, hyperdiploid
- B-ALL, low hypodiploid
- B-ALL, near haploid
- B-ALL with t(5;14)(q31.1;q32.3)/*IL3::IGH*
- B-ALL with t(1;19)(q23.3;p13.3)/*TCF3::PBX1*
- B-ALL, *BCR::ABL1*–like, ABL-1 class rearranged
- B-ALL, *BCR::ABL1*–like, JAK-STAT activated
- B-ALL, *BCR::ABL1*–like, NOS
- B-ALL with iAMP21
- B-ALL with *MYC* rearrangement
- B-ALL with *DUX4* rearrangement
- B-ALL with *MEF2D* rearrangement
- B-ALL with *ZNF384(362)* rearrangement
- B-ALL with *NUTM1* rearrangement
- B-ALL with *HLF* rearrangement
- B-ALL with *UBTF::ATXN7L3/PAN3,CDX2* (“CDX2/UBTF”)
- B-ALL with mutated *IKZF1* N159Y
- B-ALLwith mutated *PAX5* P80R
- Provisional entity: B-ALL, *ETV6::RUNX1*-like
- Provisional entity: B-ALL, with *PAX5* alteration
- Provisional entity: B-ALL, with mutated *ZEB2* (p.H1038R)/ *IGH::CEBPE*
- Provisional entity: B-ALL, *ZNF384* rearranged-like
- Provisional entity: B-ALL, *KMT2A* rearranged-like
- B-ALL, NOS

T-lymphoblastic leukemia/lymphoma

- Early T-cell precursor ALL with *BCL11B* rearrangement
- Early T-cell precursor ALL, NOS
- T-ALL, NOS

Table 2: Differentiation markers and criteria for AML types defined by differentiation [2]

Type	Diagnostic Criteria
AML with minimal differentiation	o Blasts are negative (<3%) for MPO and SBB by cytochemistry o Expression of two or more myeloid-associated antigens, such as CD13, CD33, and CD117
AML without maturation	o ≥3% blasts positive for MPO (by immunophenotyping or cytochemistry) or SBB and negative for NSE by cytochemistry o Maturing cells of the granulocytic lineage constitute <10% of the nucleated bone marrow cells o Expression of two or more myeloid-associated antigens, such as MPO, CD13, CD33, and CD117
AML with maturation	o ≥3% blasts positive for MPO (by immunophenotyping or cytochemistry) or SBB by cytochemistry o Maturing cells of the granulocytic lineage constitute ≥10% of the nucleated bone marrow cells o • Monocyte lineage cells constitute < 20% of bone marrow cells o Expression of two or more myeloid-associated antigens, such as MPO, CD13, CD33, and CD117
Acute basophilic leukemia	o Blasts & immature/mature basophils with metachromasia on toluidine blue staining o Blasts are negative for cytochemical MPO, SBB, and NSE o No expression of strong CD117 equivalent (to exclude mast cell leukemia)
Acute myelomonocytic leukemia	o ≥20% monocytes and their precursors o ≥20% maturing granulocytic cells o ≥3% of blasts positive for MPO (by immunophenotyping or cytochemistry)
Acute monocytic leukemia	o ≥80% monocytes and/or their precursors (monoblasts and/or promonocytes) o <20% maturing granulocytic cells o Blasts and promonocytes expressing at least two monocytic markers including CD11c, CD14, CD36 and CD64, or NSE positivity on cytochemistry
Acute erythroid leukemia	o ≥30% immature erythroid cells (proerythroblasts) o Bone marrow with erythroid predominance, usually ≥80% of cellularity
Acute megakaryoblastic leukemia	o Blasts express at least one or more of the platelet glycoproteins: CD41 (glycoprotein llb), CD61 (glycoprotein IIIa), or CD42b (glycoprotein lb)b

MOP, Myeloperoxidase; NSE, Nonspecific esterase; SSB, Sudan Black B.

Chapter 2 and 3 AML patients' Western blots. Patients' cells used ranged from 2–10 × 10^6 cells, depending on sample availability, to target between 20 and 50 μg of protein. For cell lines, a total of 10 × 10^6 cells were used to obtain 50 μg of protein. The protein was extracted using radioimmunoprecipitation (RIPA) lysis buffer in the presence of phosphatase and protease inhibitors. The protein was quantified using a bicinchoninic acid (BCA) assay. The whole-cell lysate was subjected to Western blot and probed with the indicated antibodies: MGMT (21 kDa), BCL-2 (26 kDa), p53 (53 kDa), and MDM2 (90 kDa). A β-Actin (42 kDa) was used as a loading control.

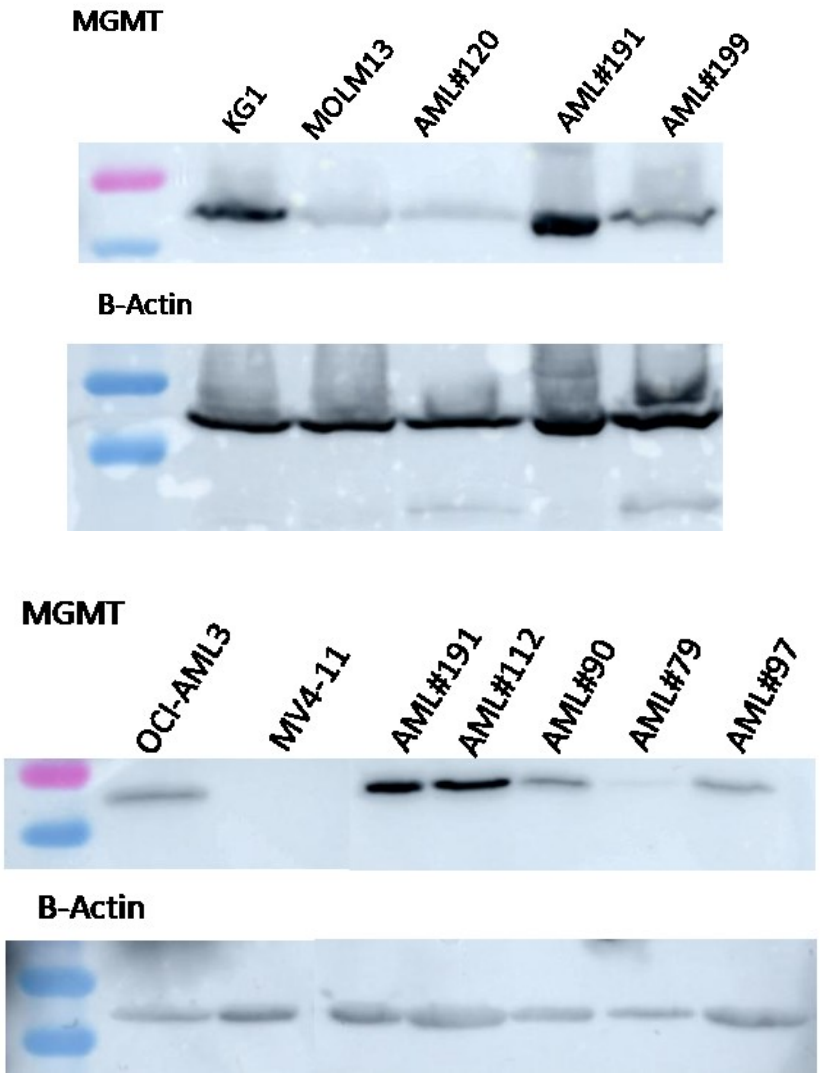

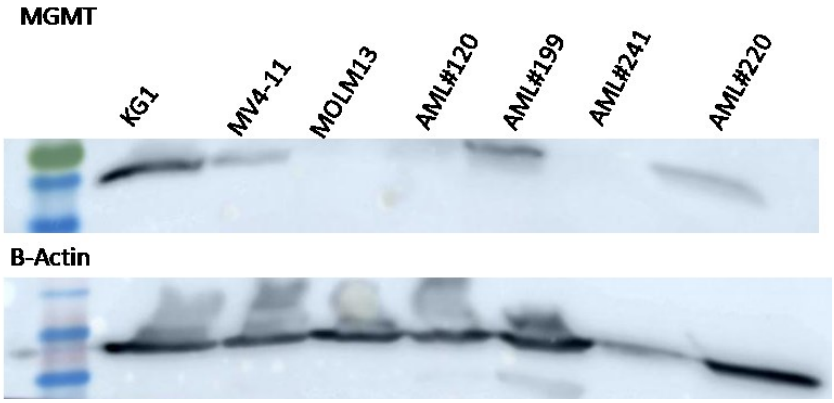

AML#241 was excluded from the study

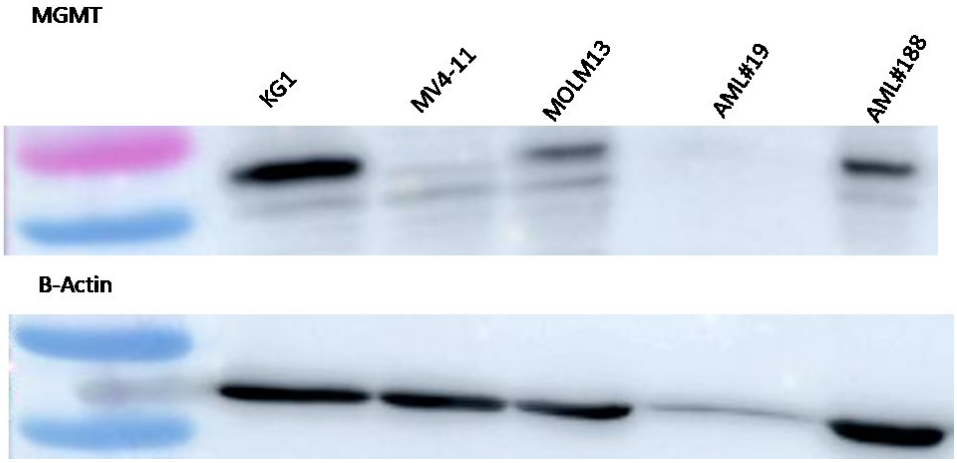

AML#19 was excluded from the study. A 20 µg/ul protein was used in all samples

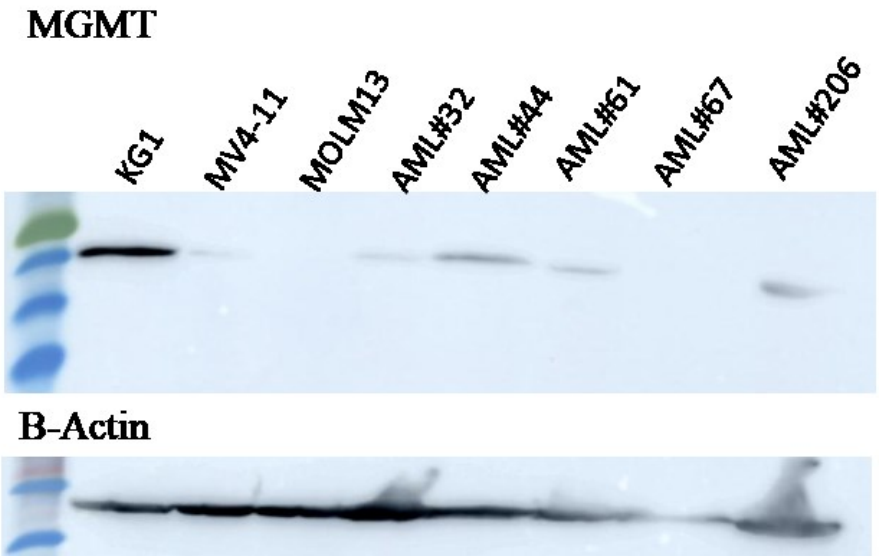

A 50 µg/ul protein was used in all samples except AML#44 and AML#67 was 35 and 15 µg/ul, respectively.

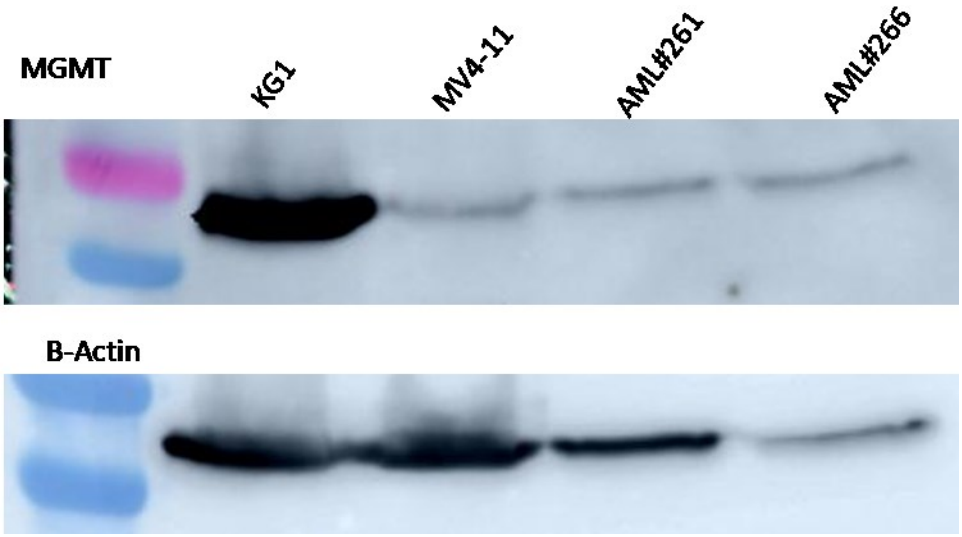

A 50 µg/ul protein was used in all samples except AML#266 was 7 µg/ul.

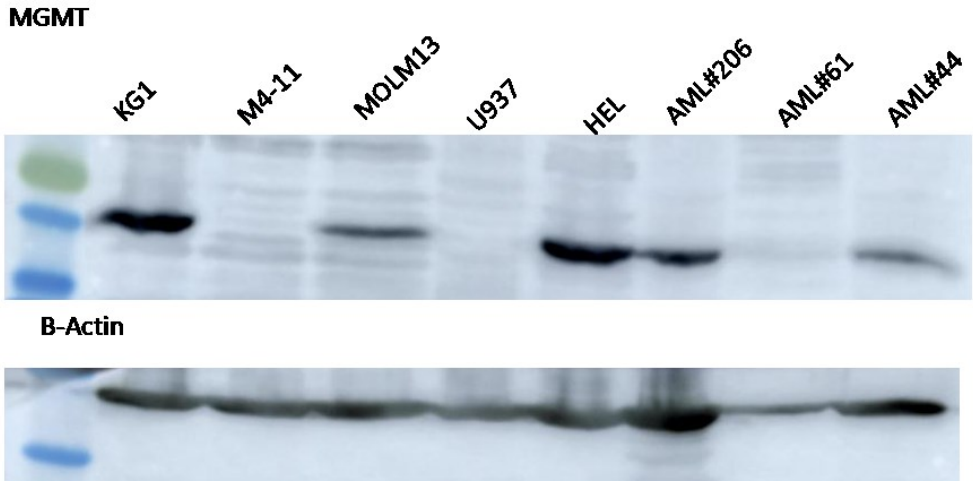

MOLM13 quantification was excluded from this blot.

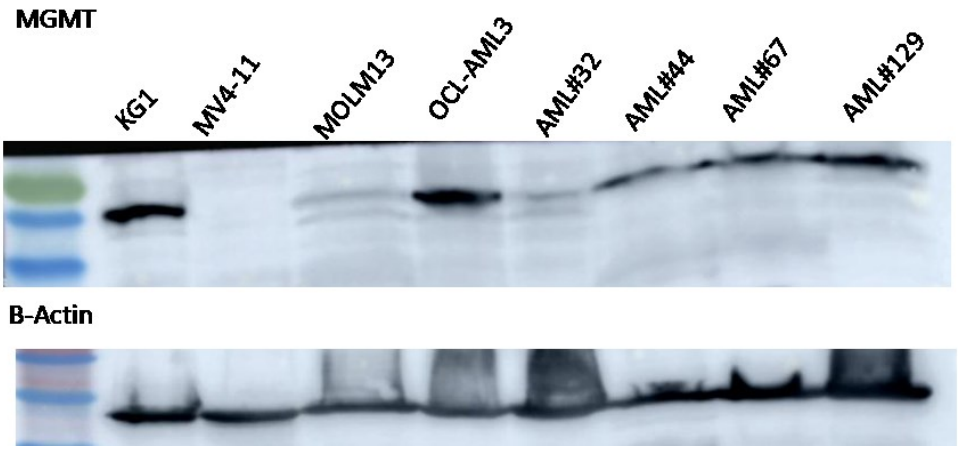

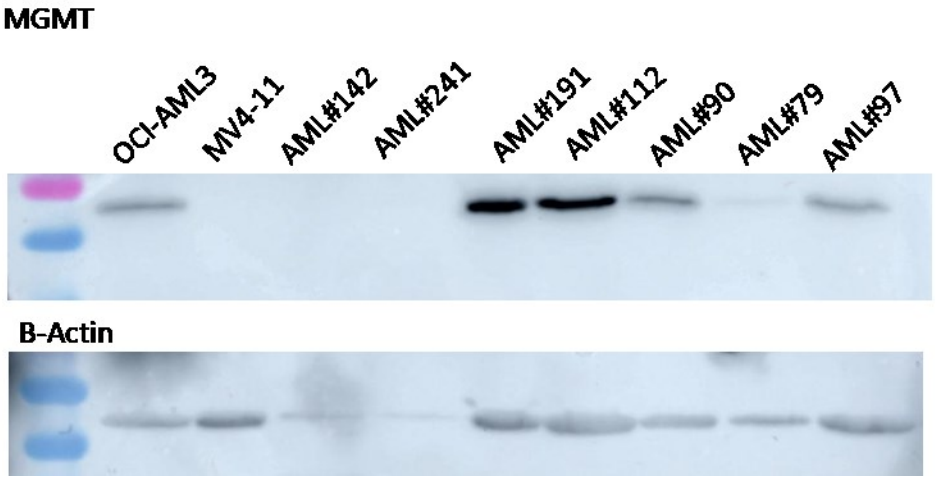

AML#142 and 241 were excluded from the study

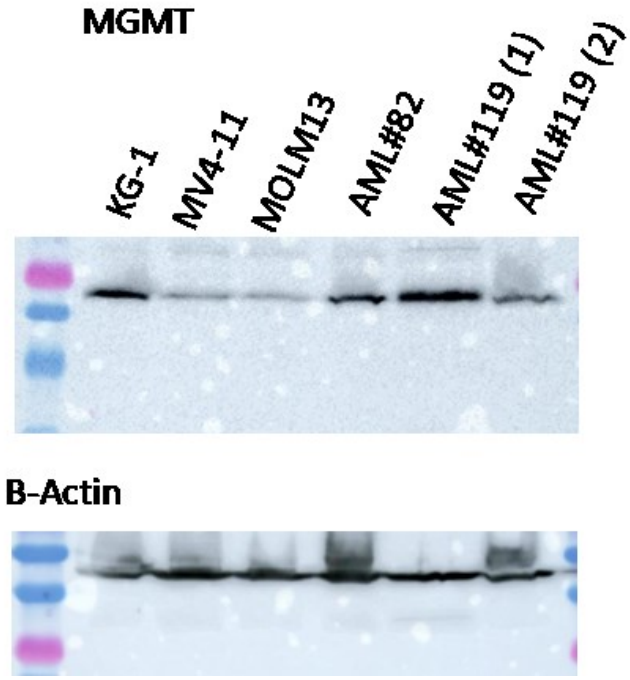

AML#119 (1) and (2) were two separate vials from the same patient

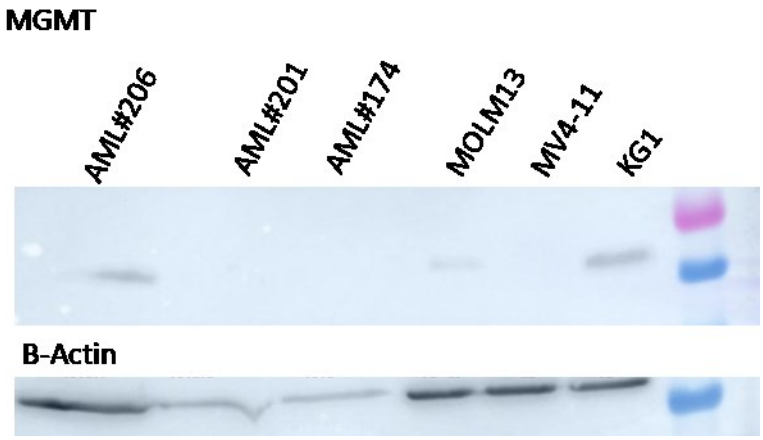

AML#201 were excluded from the study

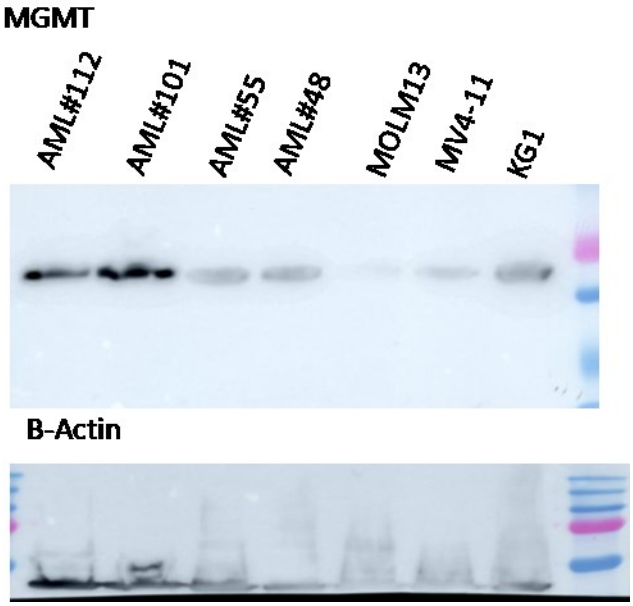

AML#55 and 101 were excluded from the study

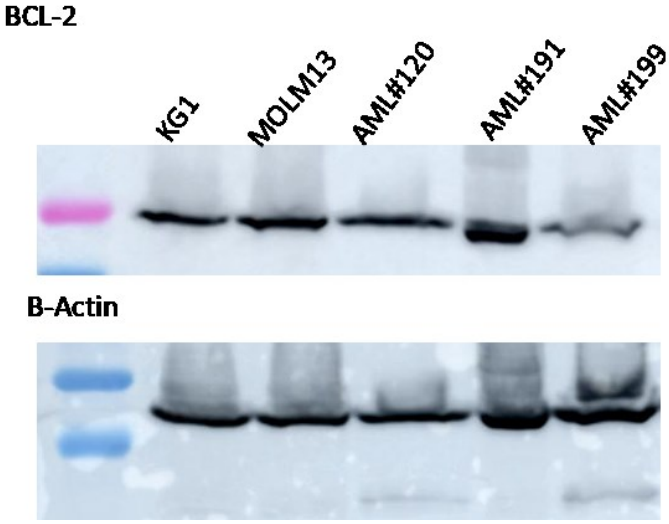

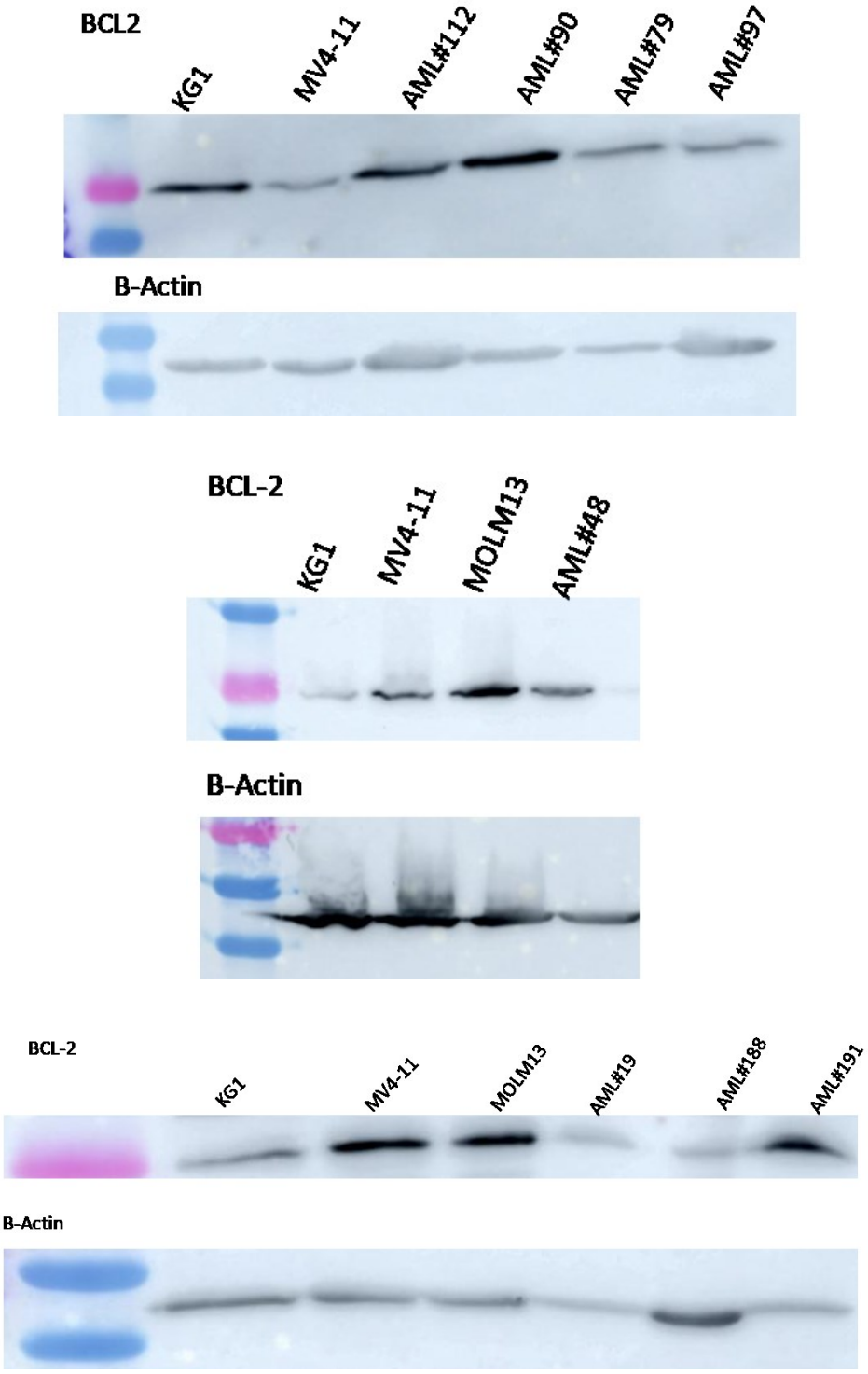

AML#19 was excluded from the study. AML#188 was included in IDA study.

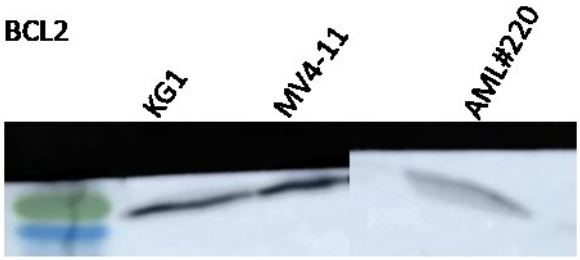
BCL2
KG1
MV4-11
AML#220


B-actin

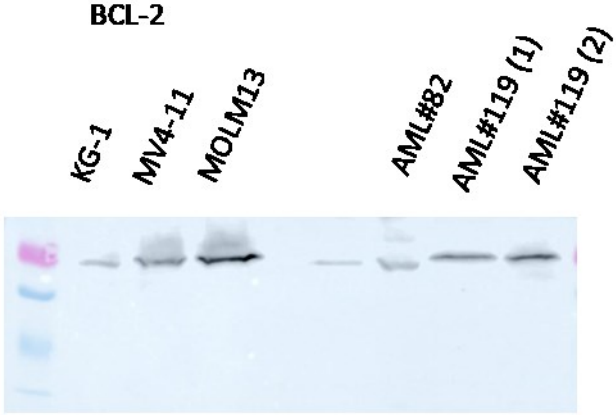
BCL-2
KG-1
MV4-11
MOLM13
AML#82
AML#119 (1)
AML#119 (2)

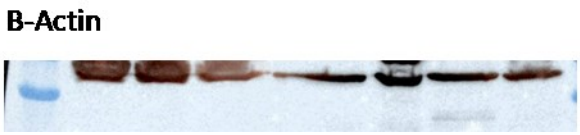
B-Actin

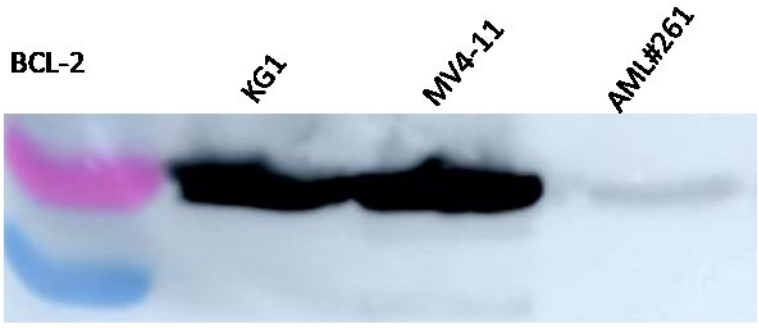
BCL-2
KG1
MV4-11
AML#261


B-Actin

Chapter 2: Cell viability of AML patient samples treated with TMZ and VEN separately and combined. 2×10^6 cells/mL patient's cells were plated in serum-free expansion medium (SFEM), containing $CD34^+$ expansion supplement, StemRegenin1 (SR1), and UM729 (pyrimido-[4,5-b]-indole derivative) supplements for 48 hours with the indicated treatment. The CellTiter-Fluor was used to determine the cell viability.

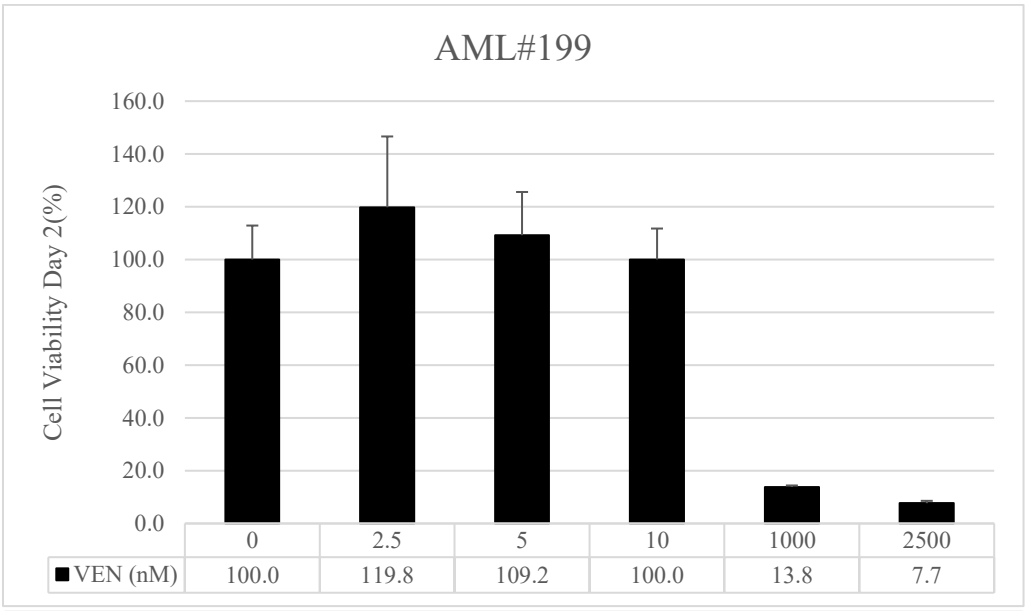

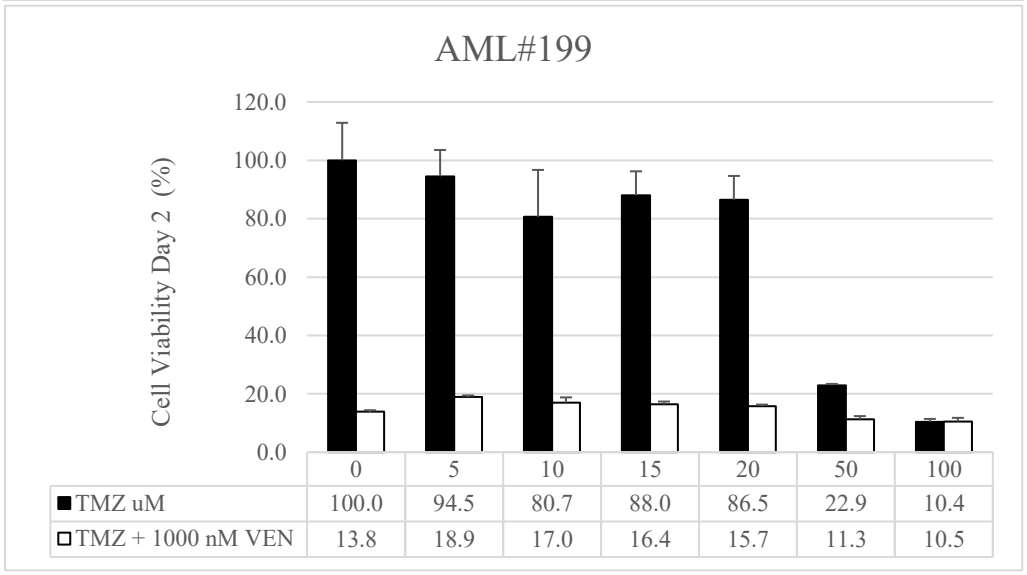

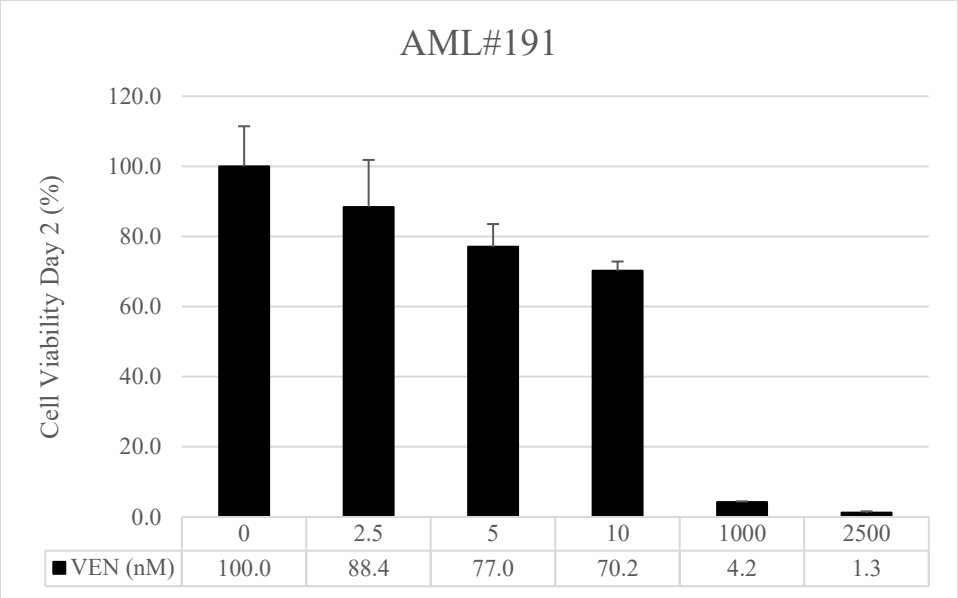
AML#191
Cell Viability Day 2 (%)
120.0
100.0
80.0
60.0
40.0
20.0
0.0
0
2.5
5
10
1000
2500
VEN (nM)
100.0
88.4
77.0
70.2
4.2
1.3

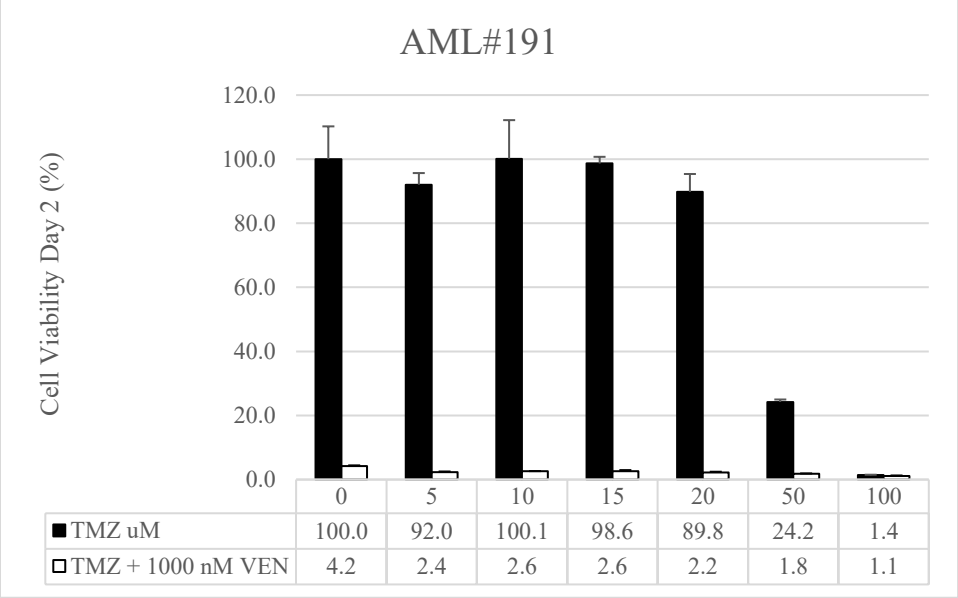
AML#191
Cell Viability Day 2 (%)
120.0
100.0
80.0
60.0
40.0
20.0
0.0
0
5
10
15
20
50
100
TMZ uM
100.0
92.0
100.1
98.6
89.8
24.2
1.4
TMZ + 1000 nM VEN
4.2
2.4
2.6
2.6
2.2
1.8
1.1

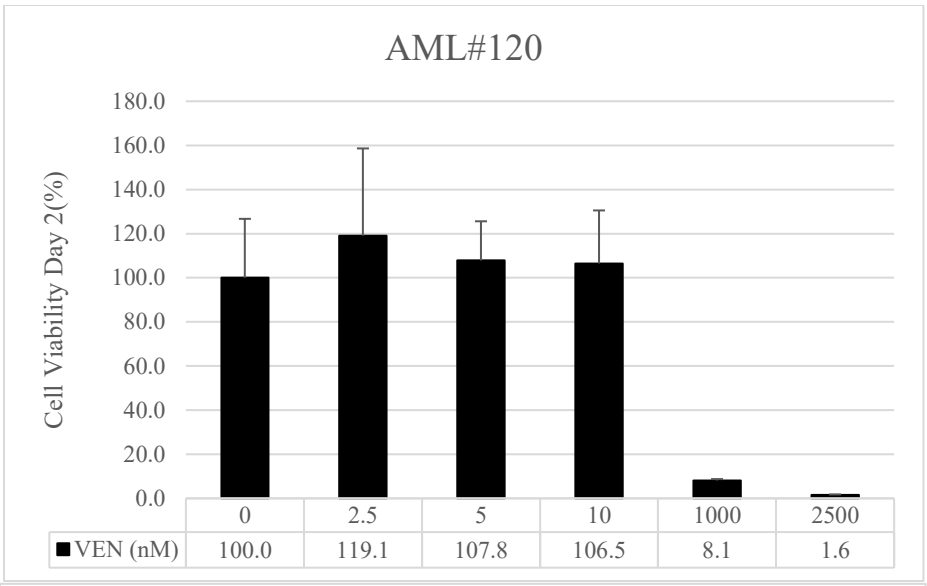
AML#120
Cell Viability Day 2(%)
180.0
160.0
140.0
120.0
100.0
80.0
60.0
40.0
20.0
0.0
0
2.5
5
10
1000
2500
VEN (nM)
100.0
119.1
107.8
106.5
8.1
1.6

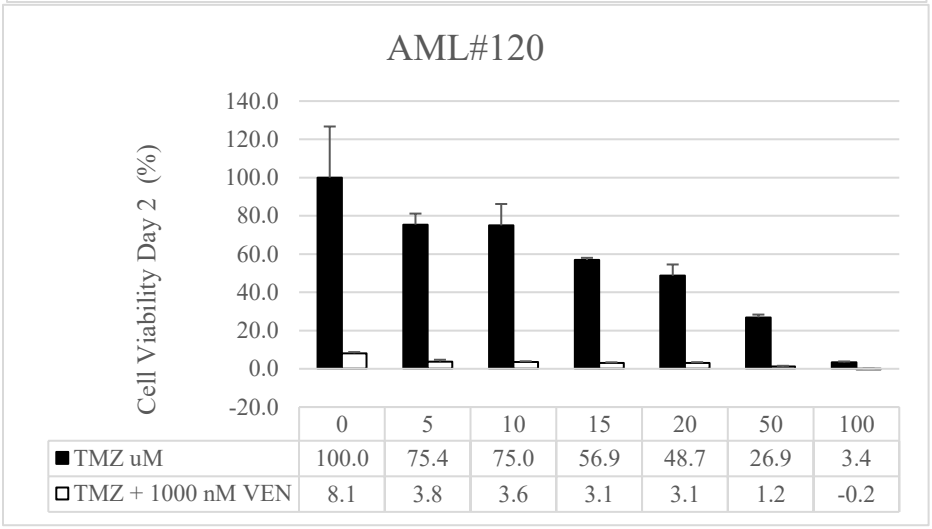
AML#120
Cell Viability Day 2 (%)
140.0
120.0
100.0
80.0
60.0
40.0
20.0
0.0
-20.0
0
5
10
15
20
50
100
TMZ uM
100.0
75.4
75.0
56.9
48.7
26.9
3.4
TMZ + 1000 nM VEN
8.1
3.8
3.6
3.1
3.1
1.2
-0.2

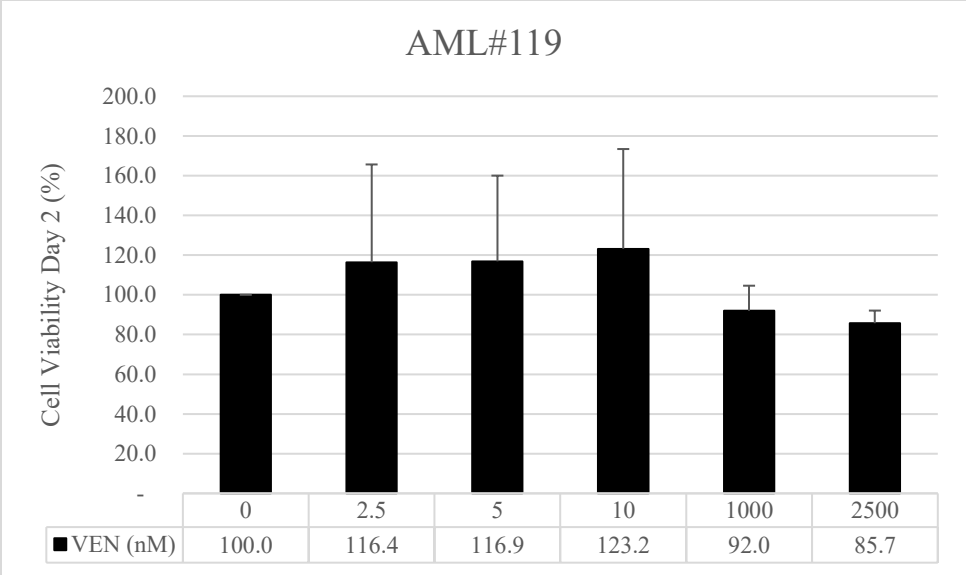
AML#119
Cell Viability Day 2 (%)
200.0
180.0
160.0
140.0
120.0
100.0
80.0
60.0
40.0
20.0
-
0 2.5 5 10 1000 2500
VEN (nM) 100.0 116.4 116.9 123.2 92.0 85.7

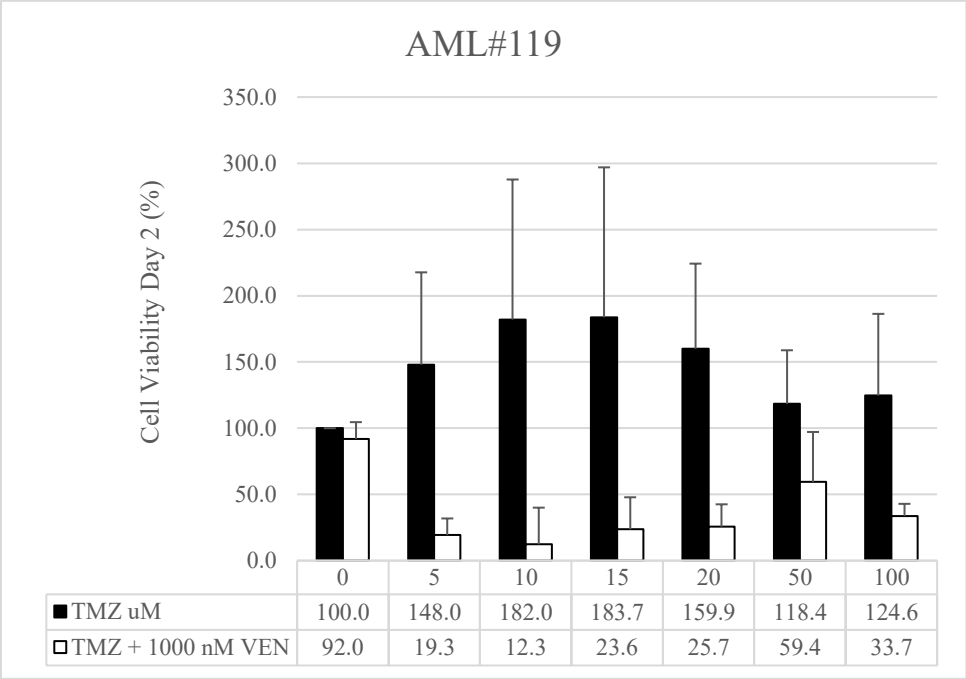
AML#119
Cell Viability Day 2 (%)
350.0
300.0
250.0
200.0
150.0
100.0
50.0
0.0
0 5 10 15 20 50 100
TMZ uM 100.0 148.0 182.0 183.7 159.9 118.4 124.6
TMZ + 1000 nM VEN 92.0 19.3 12.3 23.6 25.7 59.4 33.7

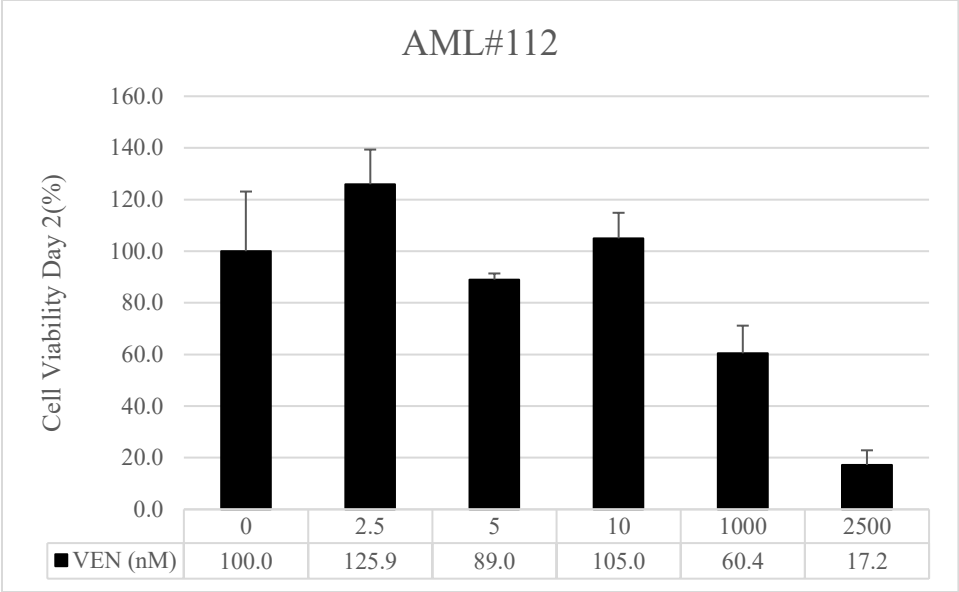
AML#112
Cell Viability Day 2(%)
160.0
140.0
120.0
100.0
80.0
60.0
40.0
20.0
0.0
0 2.5 5 10 1000 2500
VEN (nM) 100.0 125.9 89.0 105.0 60.4 17.2

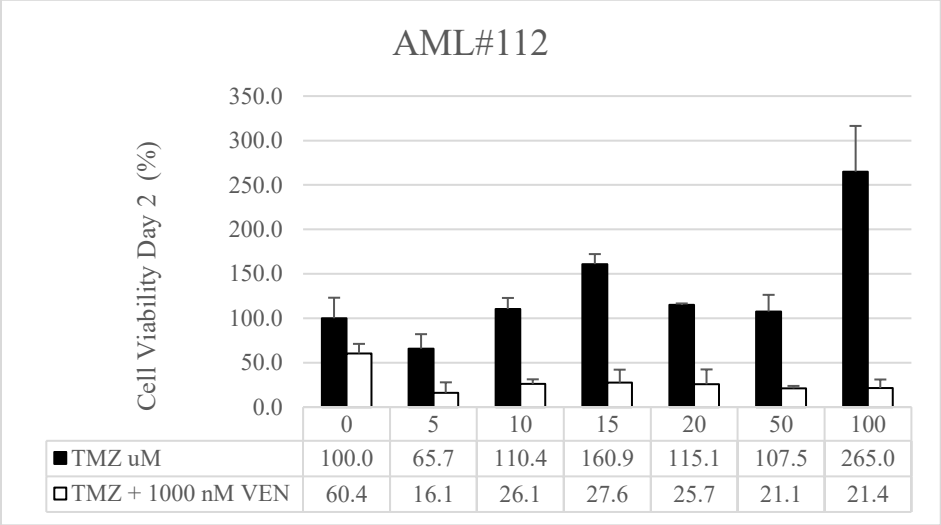
AML#112
Cell Viability Day 2 (%)
350.0
300.0
250.0
200.0
150.0
100.0
50.0
0.0
0 5 10 15 20 50 100
TMZ uM 100.0 65.7 110.4 160.9 115.1 107.5 265.0
TMZ + 1000 nM VEN 60.4 16.1 26.1 27.6 25.7 21.1 21.4

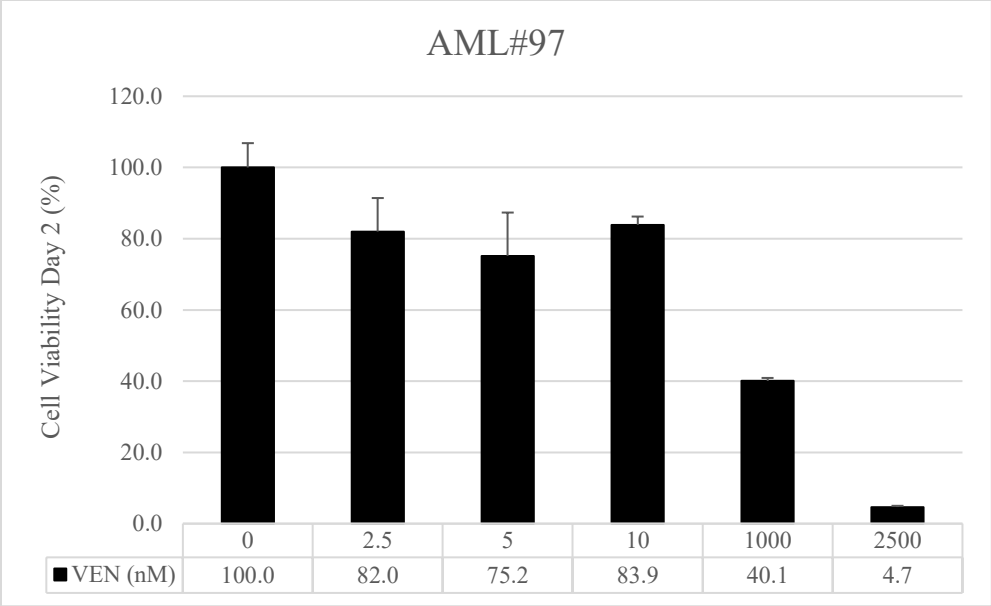
AML#97
Cell Viability Day 2 (%)
120.0
100.0
80.0
60.0
40.0
20.0
0.0
0
2.5
5
10
1000
2500
VEN (nM)
100.0
82.0
75.2
83.9
40.1
4.7

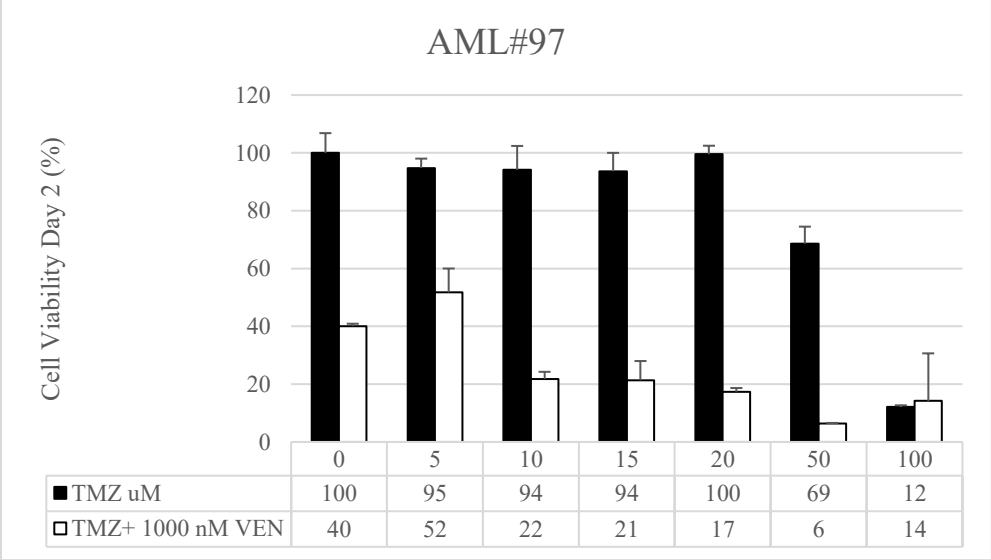
AML#97
Cell Viability Day 2 (%)
120
100
80
60
40
20
0
0
5
10
15
20
50
100
TMZ uM
100
95
94
94
100
69
12
TMZ+ 1000 nM VEN
40
52
22
21
17
6
14

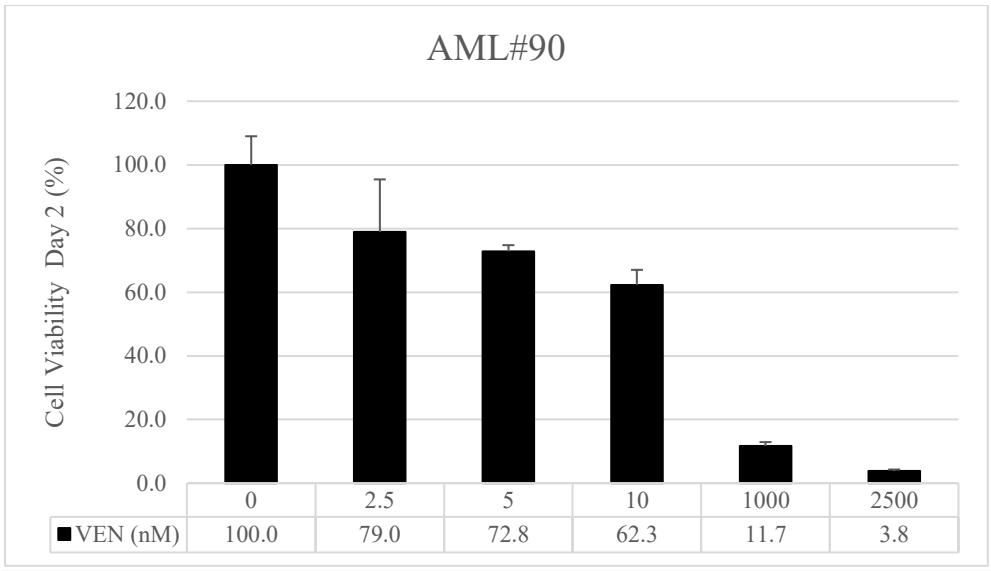
AML#90
Cell Viability Day 2 (%)
120.0
100.0
80.0
60.0
40.0
20.0
0.0
0
2.5
5
10
1000
2500
VEN (nM)
100.0
79.0
72.8
62.3
11.7
3.8

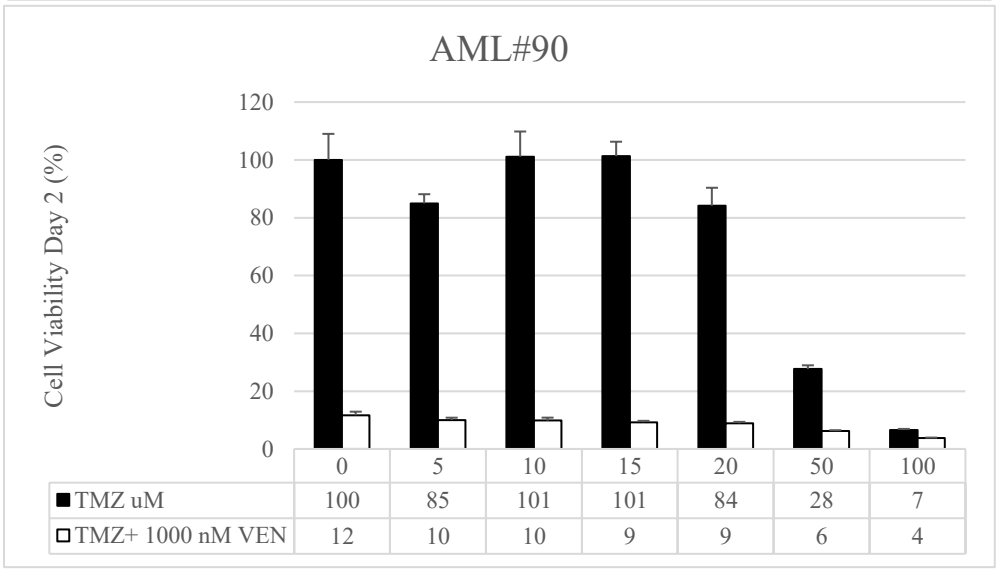
AML#90
Cell Viability Day 2 (%)
120
100
80
60
40
20
0
0
5
10
15
20
50
100
TMZ uM
100
85
101
101
84
28
7
TMZ+ 1000 nM VEN
12
10
10
9
9
6
4

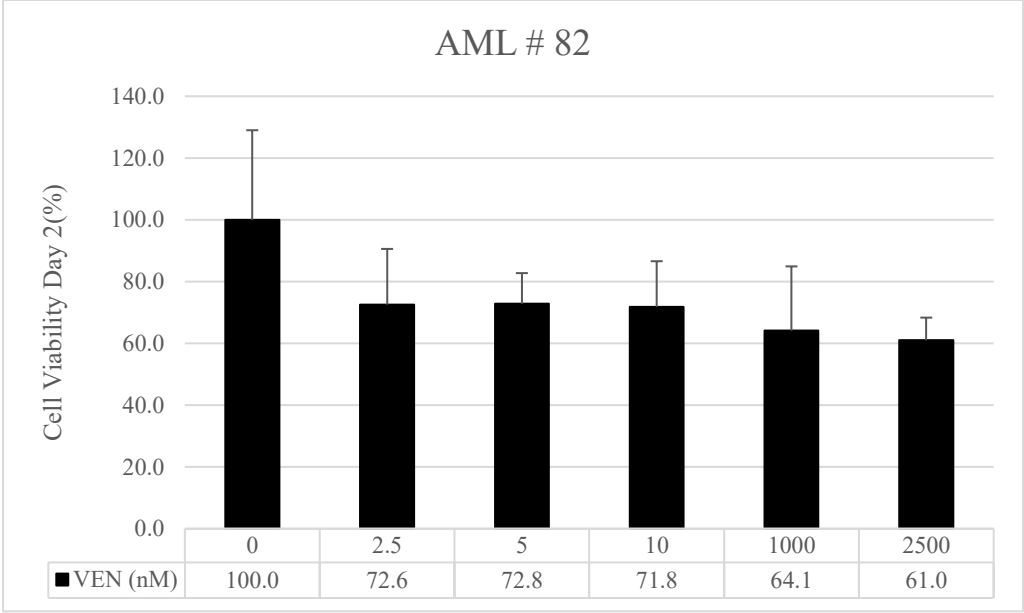
AML # 82
Cell Viability Day 2(%)
140.0
120.0
100.0
80.0
60.0
40.0
20.0
0.0
0 2.5 5 10 1000 2500
VEN (nM) 100.0 72.6 72.8 71.8 64.1 61.0

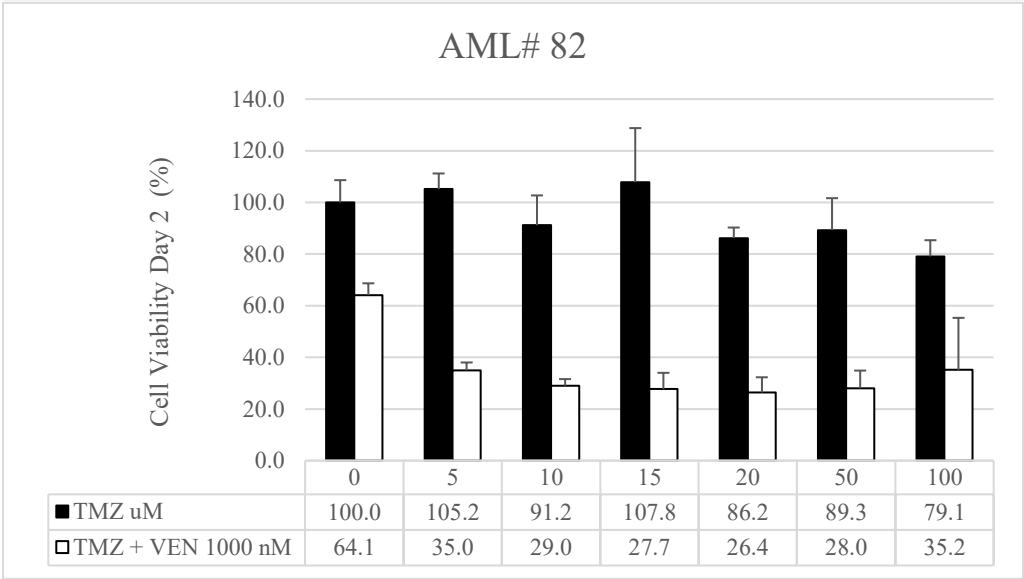
AML# 82
Cell Viability Day 2 (%)
140.0
120.0
100.0
80.0
60.0
40.0
20.0
0.0
0 5 10 15 20 50 100
TMZ uM 100.0 105.2 91.2 107.8 86.2 89.3 79.1
TMZ + VEN 1000 nM 64.1 35.0 29.0 27.7 26.4 28.0 35.2

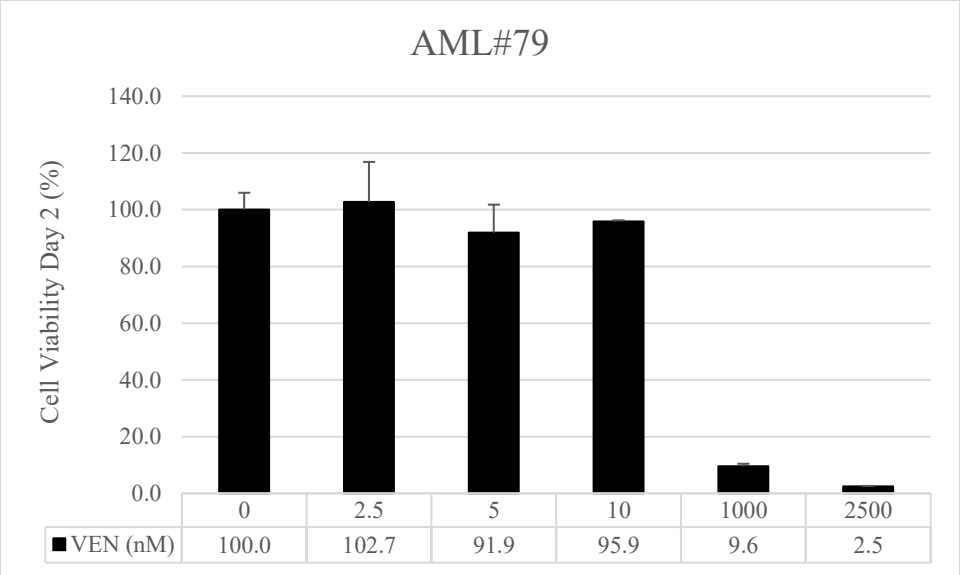
AML#79
Cell Viability Day 2 (%)
140.0
120.0
100.0
80.0
60.0
40.0
20.0
0.0
0
2.5
5
10
1000
2500
VEN (nM)
100.0
102.7
91.9
95.9
9.6
2.5

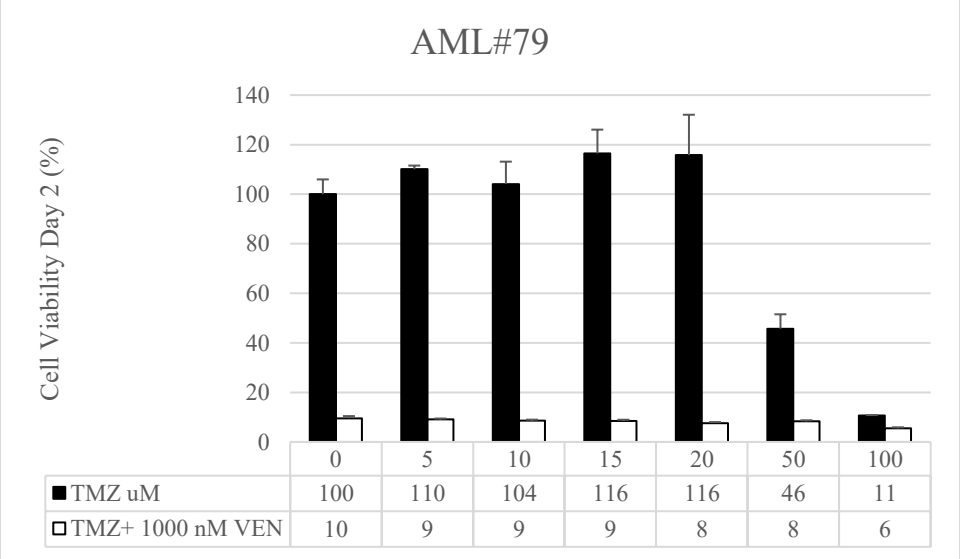
AML#79
Cell Viability Day 2 (%)
140
120
100
80
60
40
20
0
0
5
10
15
20
50
100
TMZ uM
100
110
104
116
116
46
11
TMZ+ 1000 nM VEN
10
9
9
9
8
8
6

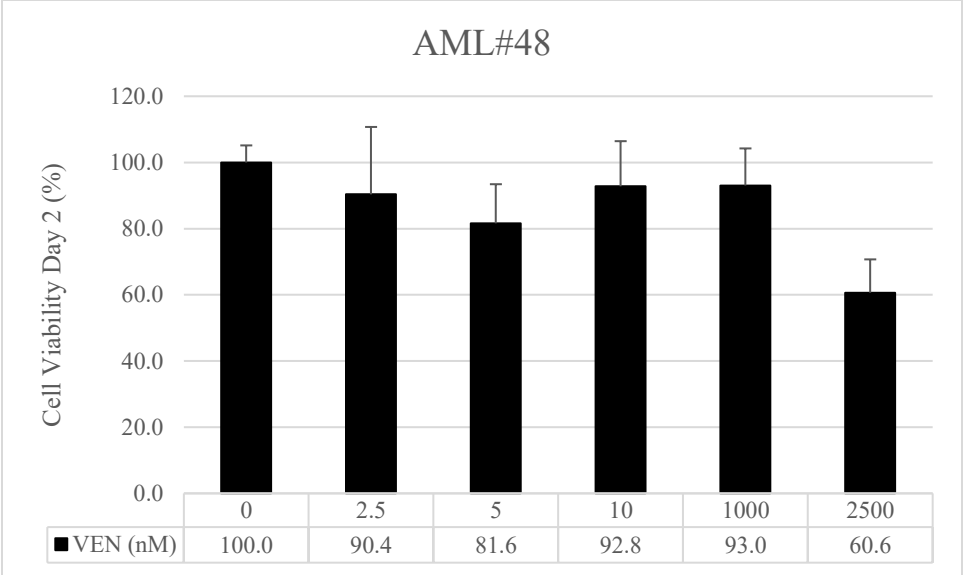
AML#48
Cell Viability Day 2 (%)
120.0
100.0
80.0
60.0
40.0
20.0
0.0
0
2.5
5
10
1000
2500
VEN (nM)
100.0
90.4
81.6
92.8
93.0
60.6

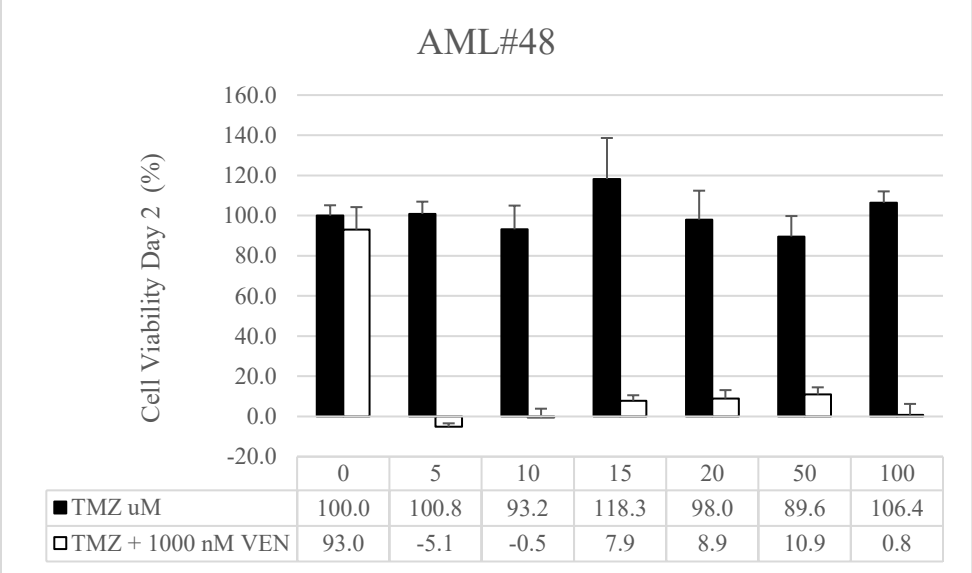
AML#48
Cell Viability Day 2 (%)
160.0
140.0
120.0
100.0
80.0
60.0
40.0
20.0
0.0
-20.0
0
5
10
15
20
50
100
TMZ uM
100.0
100.8
93.2
118.3
98.0
89.6
106.4
TMZ + 1000 nM VEN
93.0
-5.1
-0.5
7.9
8.9
10.9
0.8

Chapter 3: Cell viability of AML patient samples treated with TMZ and IDA separately and combined. 2×10^6 cells/mL patient's cells were plated in serum-free expansion medium (SFEM), containing $CD34^+$ expansion supplement, StemRegenin1 (SR1), and UM729 (pyrimido-[4,5-b]-indole derivative) supplements for 48 hours with the indicated treatment. The CellTiter-Fluor was used to determine the cell viability.

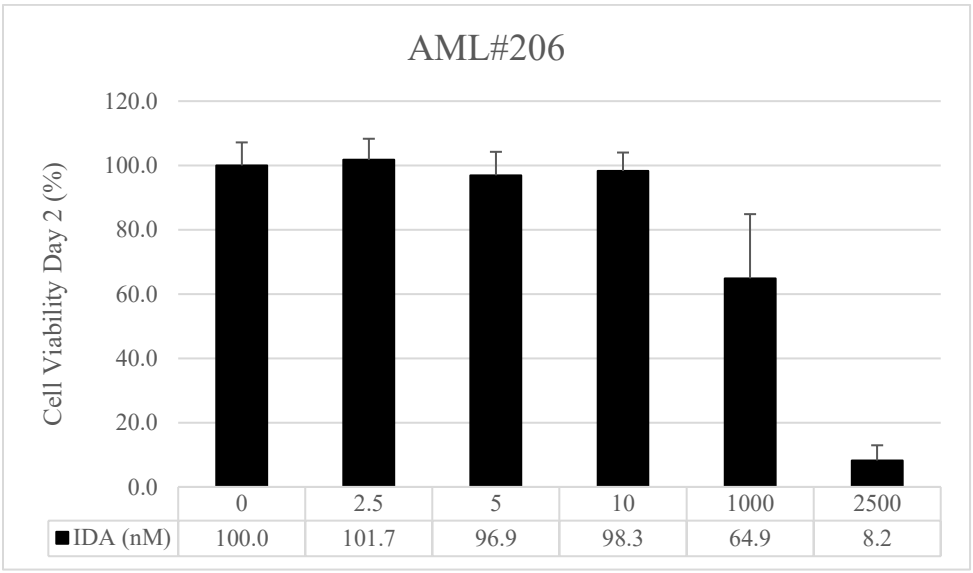

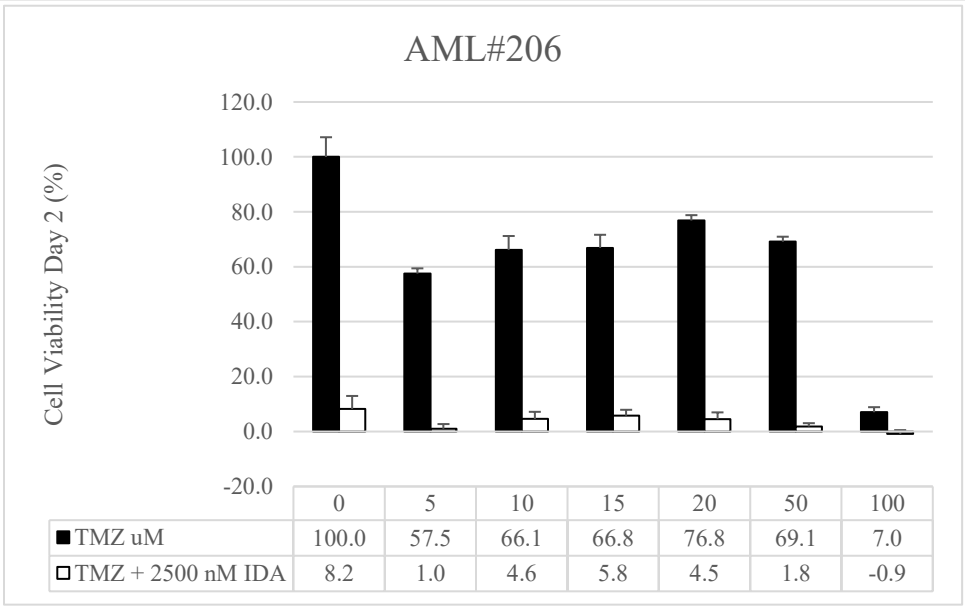

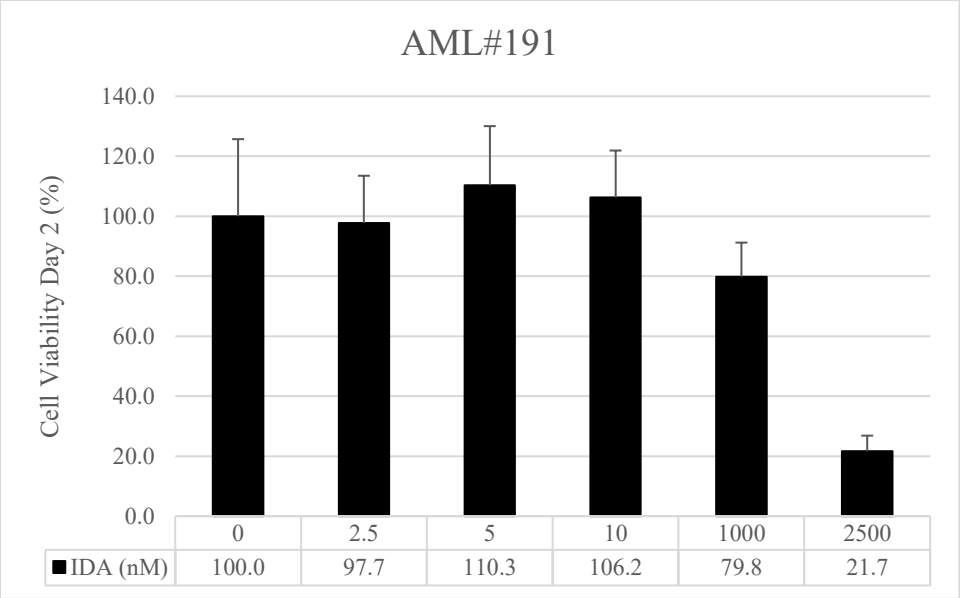
AML#191
Cell Viability Day 2 (%)
140.0
120.0
100.0
80.0
60.0
40.0
20.0
0.0
0 2.5 5 10 1000 2500
IDA (nM) 100.0 97.7 110.3 106.2 79.8 21.7

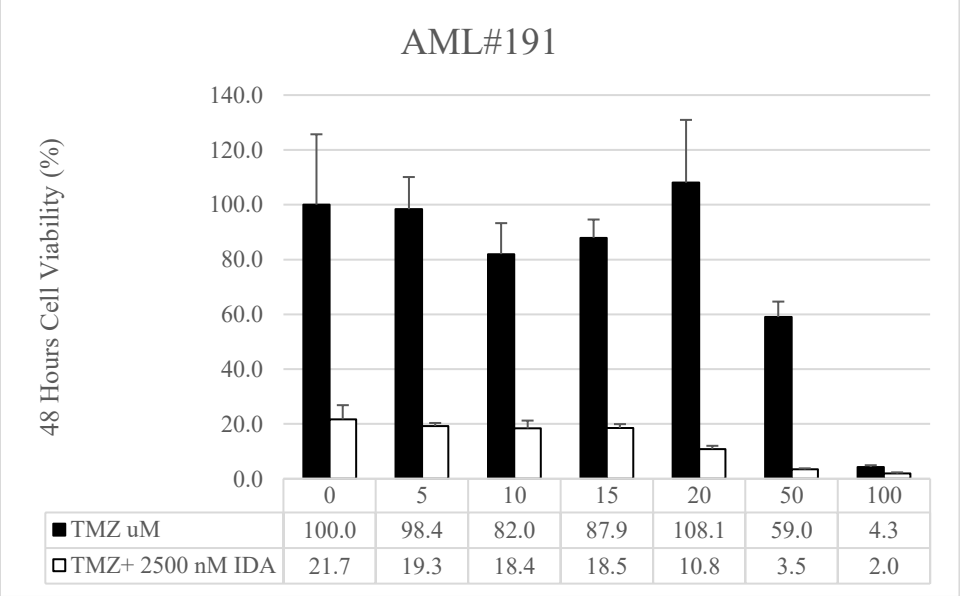
AML#191
48 Hours Cell Viability (%)
140.0
120.0
100.0
80.0
60.0
40.0
20.0
0.0
0 5 10 15 20 50 100
TMZ uM 100.0 98.4 82.0 87.9 108.1 59.0 4.3
TMZ+ 2500 nM IDA 21.7 19.3 18.4 18.5 10.8 3.5 2.0

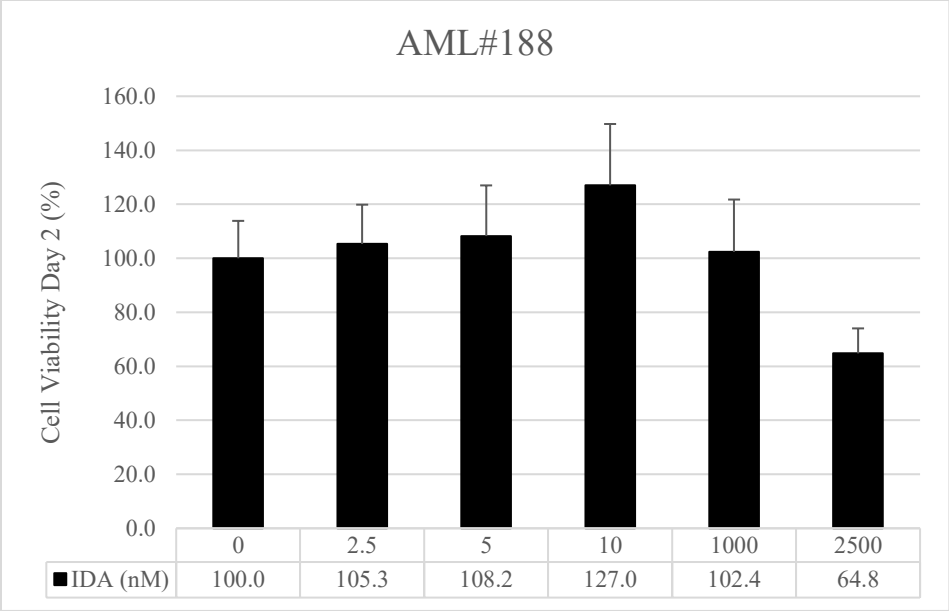
AML#188
Cell Viability Day 2 (%)
160.0
140.0
120.0
100.0
80.0
60.0
40.0
20.0
0.0
0 2.5 5 10 1000 2500
IDA (nM) 100.0 105.3 108.2 127.0 102.4 64.8

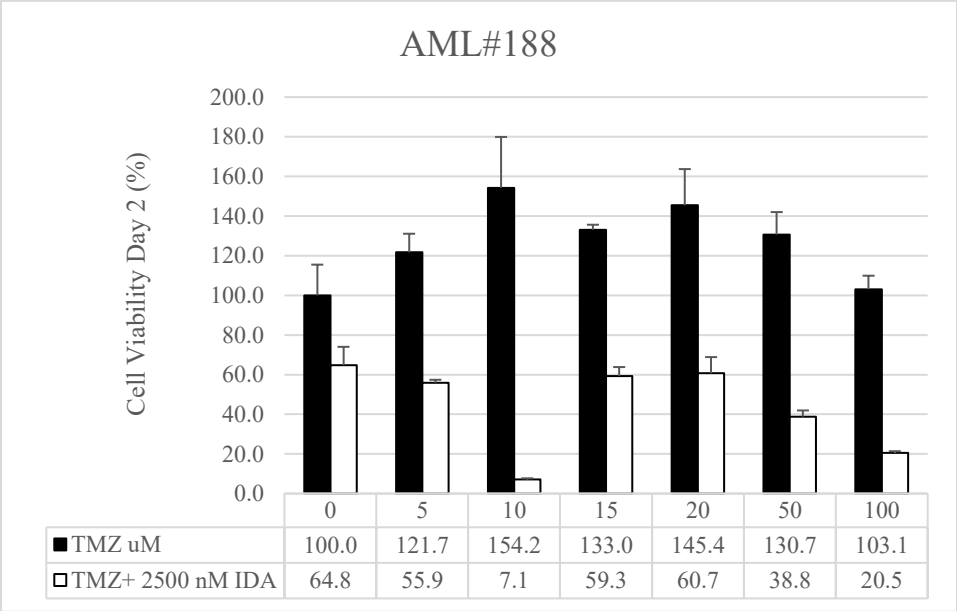
AML#188
Cell Viability Day 2 (%)
200.0
180.0
160.0
140.0
120.0
100.0
80.0
60.0
40.0
20.0
0.0
0 5 10 15 20 50 100
TMZ uM 100.0 121.7 154.2 133.0 145.4 130.7 103.1
TMZ+ 2500 nM IDA 64.8 55.9 7.1 59.3 60.7 38.8 20.5

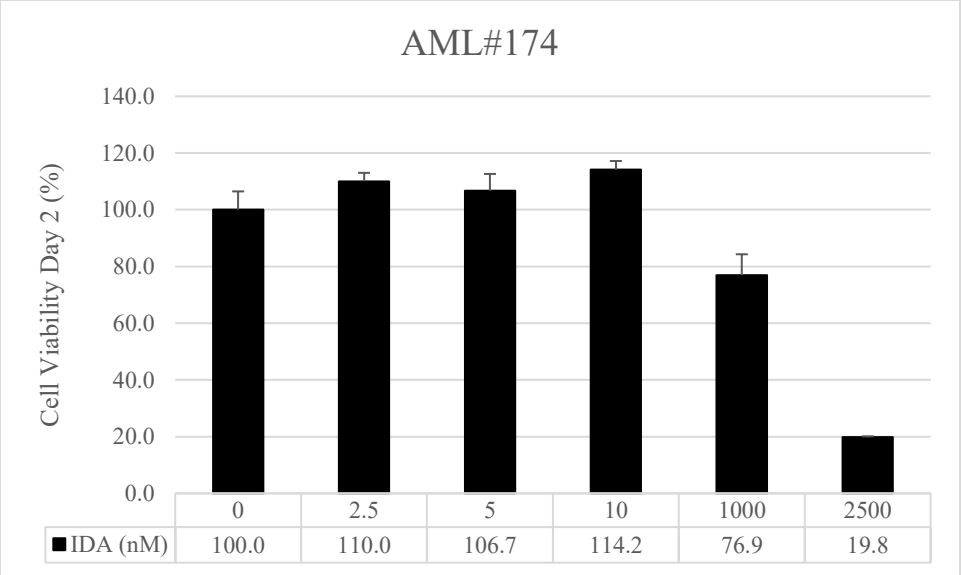
AML#174
Cell Viability Day 2 (%)
140.0
120.0
100.0
80.0
60.0
40.0
20.0
0.0
0
2.5
5
10
1000
2500
IDA (nM)
100.0
110.0
106.7
114.2
76.9
19.8

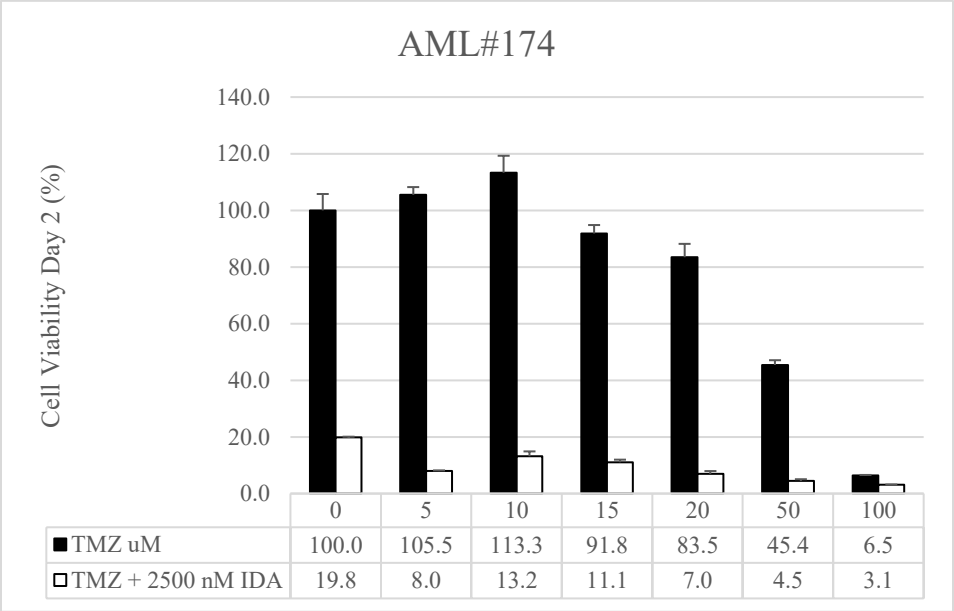
AML#174
Cell Viability Day 2 (%)
140.0
120.0
100.0
80.0
60.0
40.0
20.0
0.0
0
5
10
15
20
50
100
TMZ uM
100.0
105.5
113.3
91.8
83.5
45.4
6.5
TMZ + 2500 nM IDA
19.8
8.0
13.2
11.1
7.0
4.5
3.1

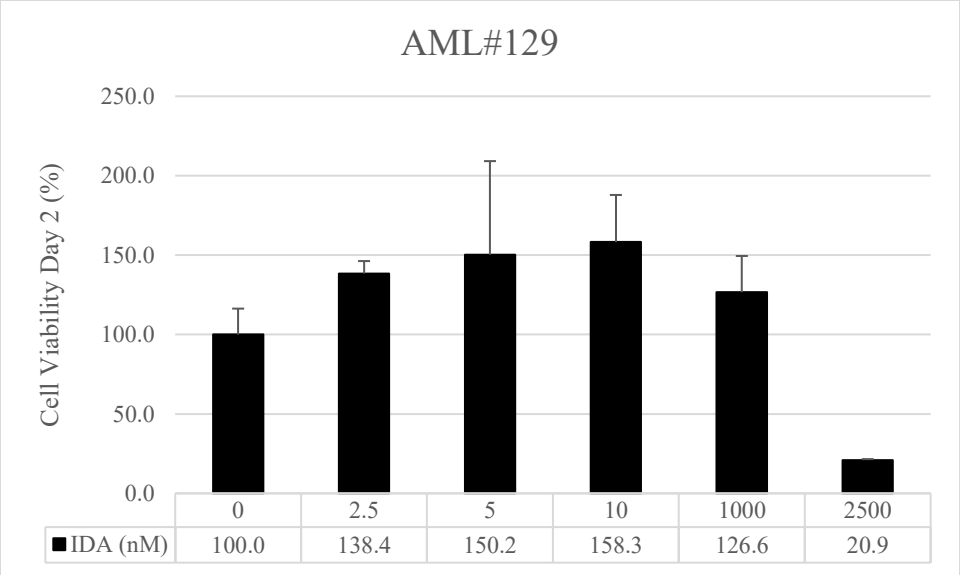
AML#129
Cell Viability Day 2 (%)
250.0
200.0
150.0
100.0
50.0
0.0
0 2.5 5 10 1000 2500
IDA (nM) 100.0 138.4 150.2 158.3 126.6 20.9

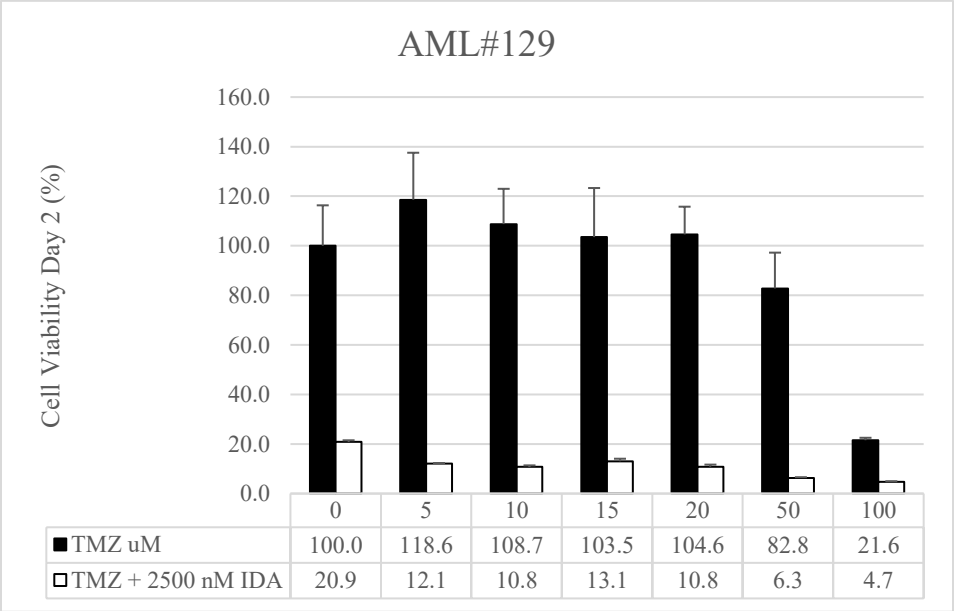
AML#129
Cell Viability Day 2 (%)
160.0
140.0
120.0
100.0
80.0
60.0
40.0
20.0
0.0
0 5 10 15 20 50 100
TMZ uM 100.0 118.6 108.7 103.5 104.6 82.8 21.6
TMZ + 2500 nM IDA 20.9 12.1 10.8 13.1 10.8 6.3 4.7

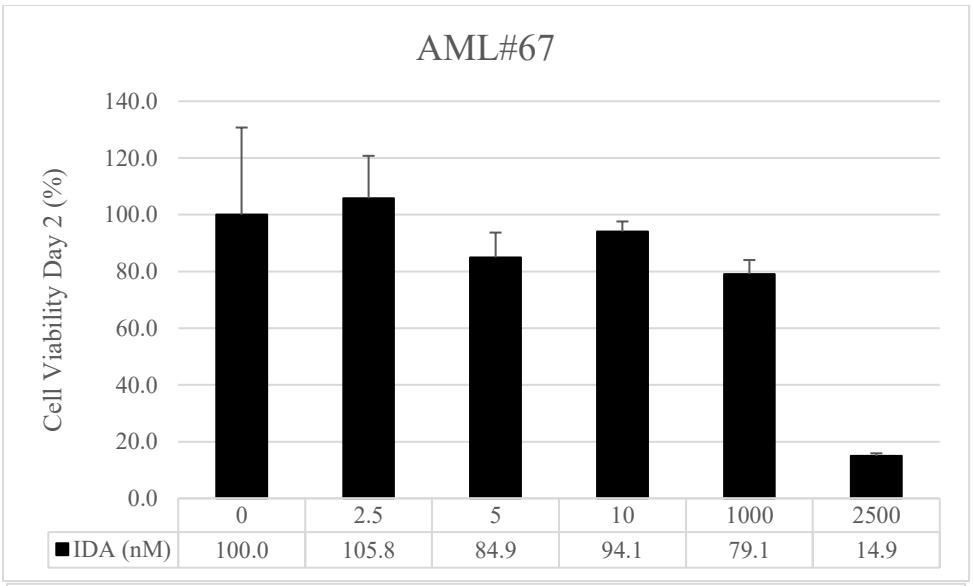
AML#67
Cell Viability Day 2 (%)
140.0
120.0
100.0
80.0
60.0
40.0
20.0
0.0
0
2.5
5
10
1000
2500
IDA (nM)
100.0
105.8
84.9
94.1
79.1
14.9

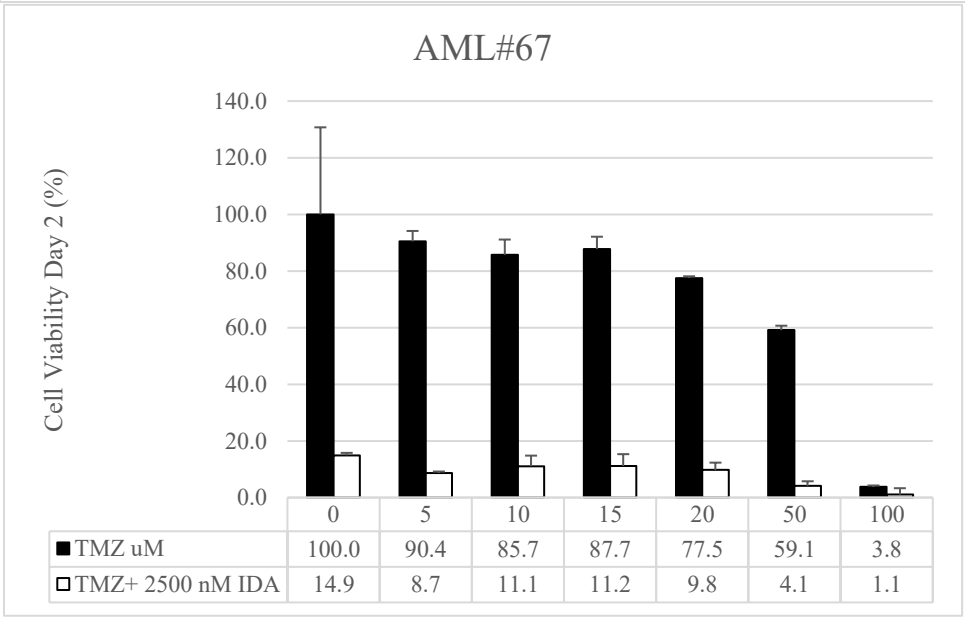
AML#67
Cell Viability Day 2 (%)
140.0
120.0
100.0
80.0
60.0
40.0
20.0
0.0
0
5
10
15
20
50
100
TMZ uM
100.0
90.4
85.7
87.7
77.5
59.1
3.8
TMZ+ 2500 nM IDA
14.9
8.7
11.1
11.2
9.8
4.1
1.1

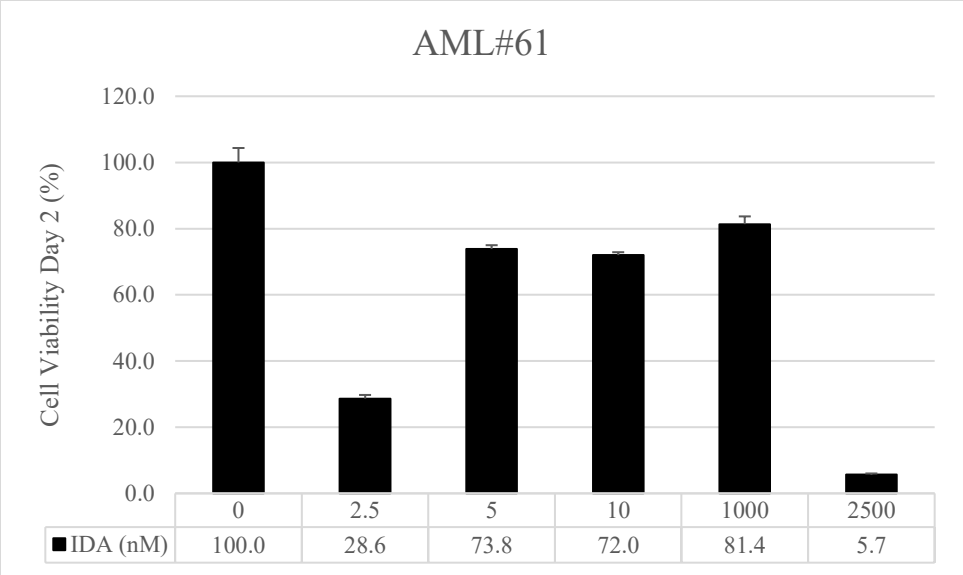
AML#61
Cell Viability Day 2 (%)
120.0
100.0
80.0
60.0
40.0
20.0
0.0
0 2.5 5 10 1000 2500
IDA (nM) 100.0 28.6 73.8 72.0 81.4 5.7

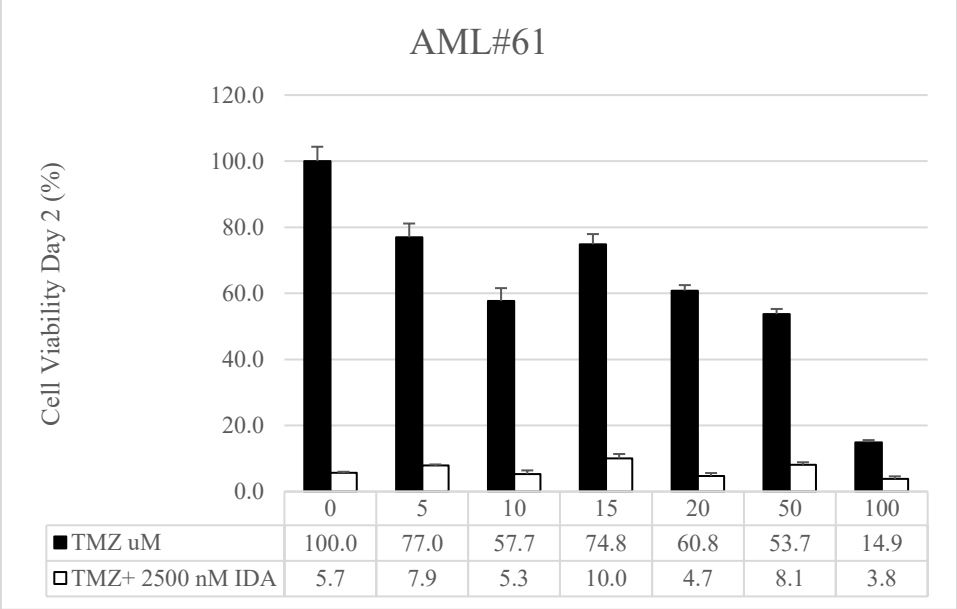
AML#61
Cell Viability Day 2 (%)
120.0
100.0
80.0
60.0
40.0
20.0
0.0
0 5 10 15 20 50 100
TMZ uM 100.0 77.0 57.7 74.8 60.8 53.7 14.9
TMZ+ 2500 nM IDA 5.7 7.9 5.3 10.0 4.7 8.1 3.8

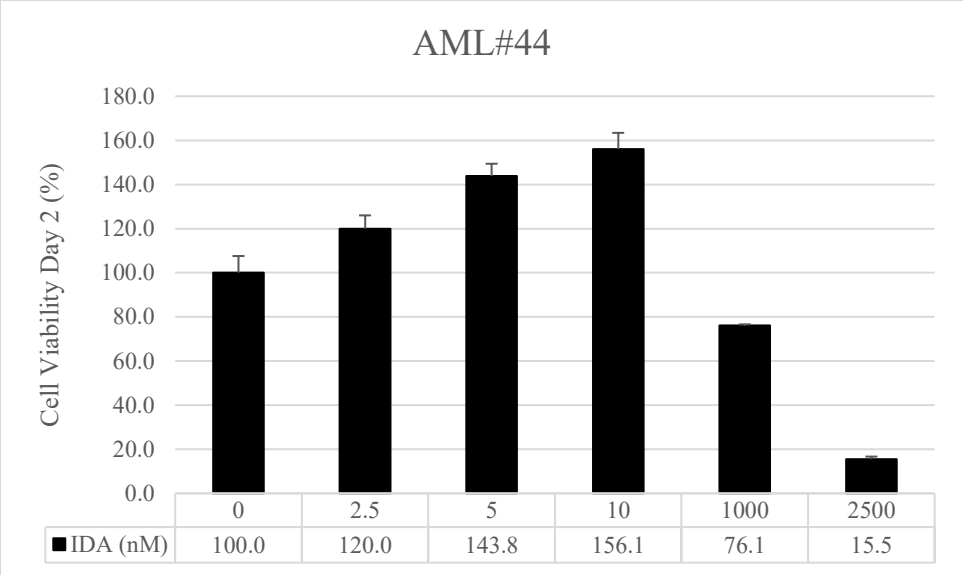
AML#44
Cell Viability Day 2 (%)
180.0
160.0
140.0
120.0
100.0
80.0
60.0
40.0
20.0
0.0
0
2.5
5
10
1000
2500
IDA (nM)
100.0
120.0
143.8
156.1
76.1
15.5

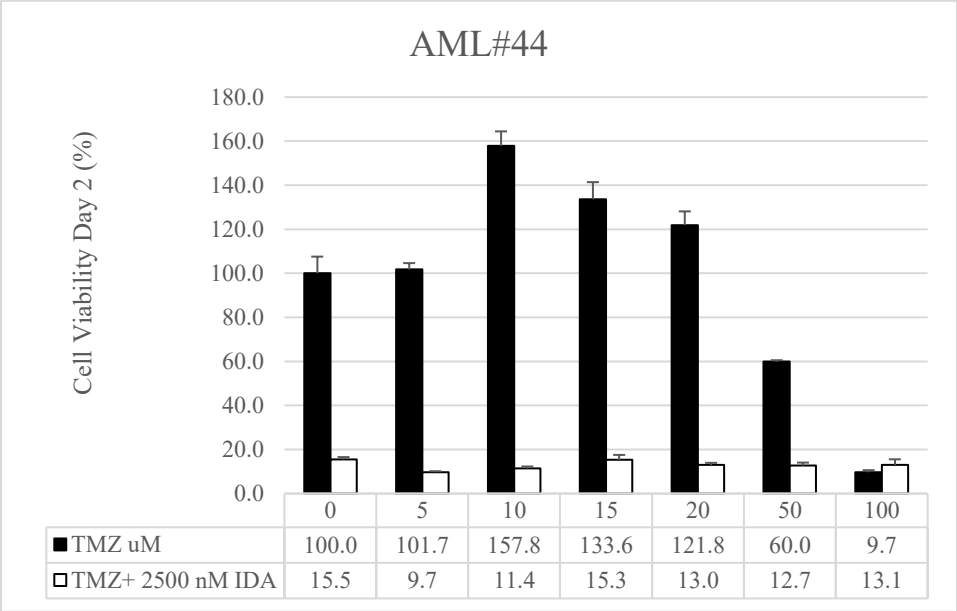
AML#44
Cell Viability Day 2 (%)
180.0
160.0
140.0
120.0
100.0
80.0
60.0
40.0
20.0
0.0
0
5
10
15
20
50
100
TMZ uM
100.0
101.7
157.8
133.6
121.8
60.0
9.7
TMZ+ 2500 nM IDA
15.5
9.7
11.4
15.3
13.0
12.7
13.1

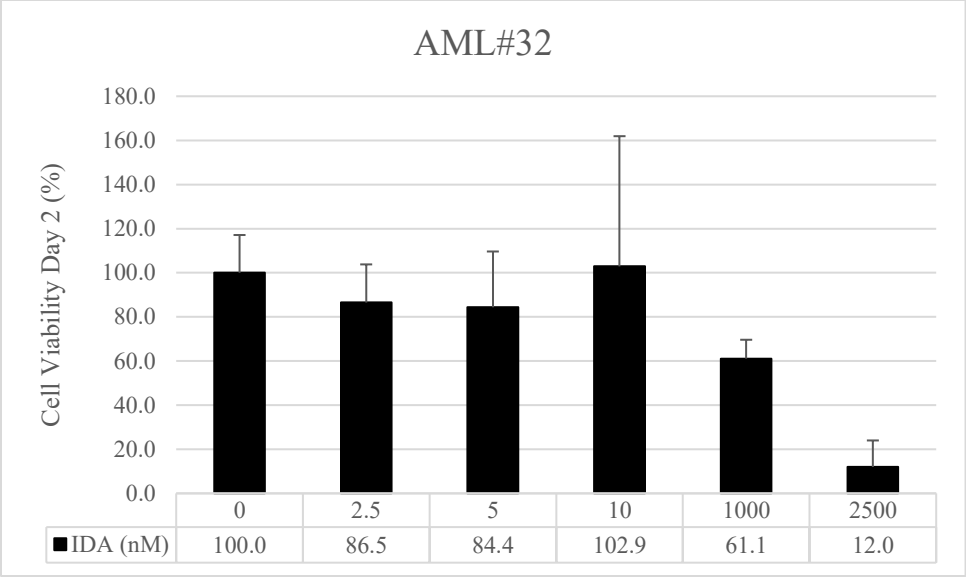
AML#32
Cell Viability Day 2 (%)
180.0
160.0
140.0
120.0
100.0
80.0
60.0
40.0
20.0
0.0
0
2.5
5
10
1000
2500
IDA (nM)
100.0
86.5
84.4
102.9
61.1
12.0

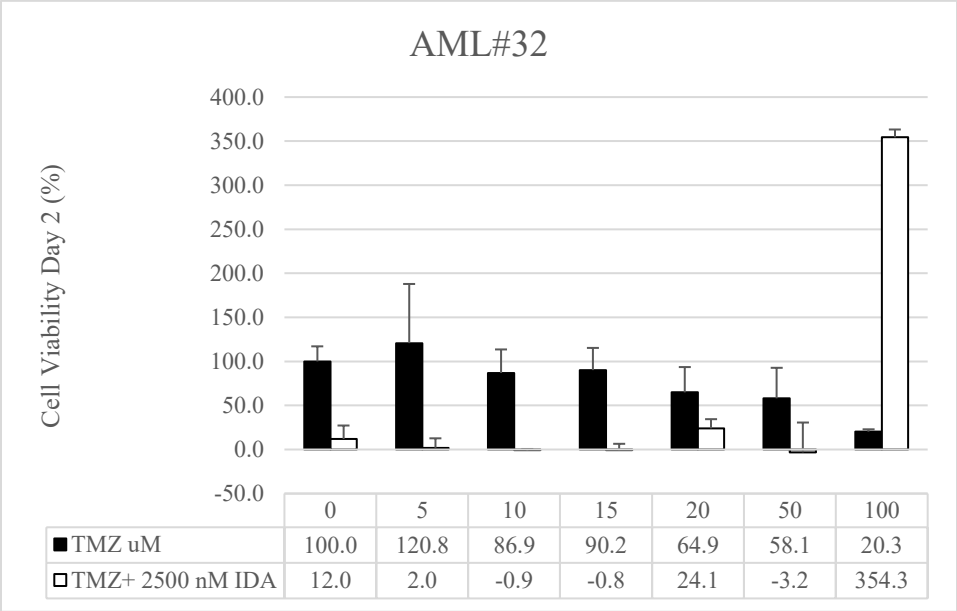
AML#32
Cell Viability Day 2 (%)
400.0
350.0
300.0
250.0
200.0
150.0
100.0
50.0
0.0
-50.0
0
5
10
15
20
50
100
TMZ uM
100.0
120.8
86.9
90.2
64.9
58.1
20.3
TMZ+ 2500 nM IDA
12.0
2.0
-0.9
-0.8
24.1
-3.2
354.3

References

1. Arber DA, Orazi A, Hasserjian RP, Borowitz MJ, Calvo KR, Kvasnicka H-M, et al. International Consensus Classification of Myeloid Neoplasms and Acute Leukemias: integrating morphologic, clinical, and genomic data. Blood. 2022;140(11):1200-28.

2. Khoury JD, Solary E, Abla O, Akkari Y, Alaggio R, Apperley JF, et al. The 5th edition of the World Health Organization Classification of Haematolymphoid Tumours: Myeloid and Histiocytic/Dendritic Neoplasms. Leukemia. 2022;36(7):1703-19.